RADIOLABELLED PEPTIDES AND AMINO ACIDS FOR PET IMAGING OF CANCER

Ashleigh Lilian Farnsworth

ORCID ID: 0000-0001-6938-4370

Submitted in total fulfilment of the requirements of the Degree of Doctor of Philosophy

September 2019

School of Chemistry

Bio21 Molecular Science and Biotechnology Institute

Peter MacCallum Cancer Institute

The University of Melbourne

ABBREVIATIONS

5Av	5-aminovaleric acid
A	alanine
AA	amino acid
AAT	amino acid transporter
Aib	aminoisobutyric acid
Ala	alanine
βAla	beta alanine
Alloc	allyloxycarbonyl
$AMBF_3$	aminomethyltrifluoroborate
Arg	arginine
ASCT	alanine-serine-cysteine transporter
Asp	aspartic acid
BAA	boramino acid
Boc	*tert*-butoxycarbonyl
Bq	becquerel
C	cysteine
C18	octadecyl carbon chain

CBz	benzyloxycarbonyl
CD4	cluster of differentiation 4
Ci	curie
CXCR4	chemokine receptor 4
CXCR7	chemokine receptor 7
Cys	cysteine
D	aspartic acid
DBN	1,5-diazabicyclo[4.3.0]non-5-ene
DBU	1,8-diazabicyclo[5.4.0]undec-7-ene
d.c	decay corrected
DEAD	diethylazidocarboxylate
DFT	density functional theory
DIAD	diisopropylazodicarboxylate
DIC	N,N'-diisopropylcarbodiimide
DOTA	1,4,7,10-tetraazacyclododecane-1,4,7,10-tetraacetic acid
dr	diastereomeric ratio
DTPA	diethylenetriaminepentaacetic acid
ee	enantiomeric excess

ESF	ethane sulfonyl fluoride
tBuOH	*tert*-butanol
ESI	electrospray ionisation
F	phenylalanine
FACBC	*anti*-1-amino-3-[^{18}F]-fluorocyclobutane-1-carboxylic acid
FAMT	L-3-[^{8}F]-fluoro-α-methyl tyrosine
FB	fluorobenzoate
FBA	fluorobenzoic acid
FDG	fluorodeoxyglucose
FET	[^{18}F]-fluoroethyltyrosine
FMA	3-(1-[^{18}F]-fluoromethyl)-L-alanine
Fmoc	fluorenylmethoxycarbonyl
FOV	field of view
FPhPA	2-amino-5-(4-[^{18}F]-fluorophenyl)pent-4-ynoic acid
FP	fluoropropionate
FPy	fluoropyridine
FSPG	(4S)-4-(3-[^{18}F]-fluoropropyl)-l-glutamate
G	glycine

GABA	γ-aminobutyric acid
Gly	glycine
GMP	good manufacturing practice
HATU	hexafluorophosphate azabenzotriazole tetramethyl uronium
HFIP	hexafluoro-2-propanol
HIF	hypoxia induced factor
HIV-1	human immunodeficiency virus 1
HRMS	high resolution mass spectrometry
HOBt	N-hydroxylbenzotriazole
IC_{50}	half maximal inhibitory concentration
IEX	isotope exchange
K	lysine
K_{222}	4,7,13,16,21,24-Hexaoxa-1,10-diazabicyclo[8.8.8]hexacosane
K_d	dissociation constant
K_i	inhibitory constant
L	leucine
LAT	large neutral amino acid transporter
Leu	leucine

Lys	lysine
M	methionine
mCPBA	*meta*-chloroperoxybenzoic acid
Met	methionine
MS	mass spectrometry
MTBE	methyl *tert*-butyl ether
mTOR	mammalian target of rapamycin
MV4-11	acute myeloid leukemia cell line
Nal	napthylalanine
NBSCl	nitrobenzene sulfonyl chloride
n.d.c	non-decay corrected
NFP	4-nitrophenyl-2-fluoropropionate
NHS	N-hydroxysuccinimide
NHPI	N-hydroxyphthalimide
NMR	nuclear magnetic resonance
Orn	ornithine
P	proline
Pbf	2,2,4,6,7-pentamethyldihydrobenzofuran-5-sulfonyl

PBS	phosphate buffered saline
PET	positron emission tomography
Phe	phenylalanine
Pin	pinacolato
PMB	*para*-methoxybenzyl
PNP	*para*-nitrophenyl
Pro	proline
PTC	phase transfer catalyst
QMA	quaternary methyl ammonium
R	arginine
RAE	redox active ester
RAMLA	row action maximum likelihood algorithm
RGD	arginine-glycine-aspartic acid
ROI	region of interest
RP-HPLC	reverse phase high performance liquid chromatography
rt	room temperature
Salen	N,N'-bis(salicylidene)ethylenediamine
SAR	structure activity relationship

SCID	severe combined immunodeficiency
SDF-1	stromal cell derived factor 1
SFB	N-succinimidyl-4-fluorobenzoate
SOS	start of synthesis
SPE	solid phase extraction
SPECT	single photon emission computed tomography
SPPS	solid phase peptide synthesis
T	threonine
t-AmOH	*tert*-amyl alcohol
TBAF	tetra-n-butyl ammonium fluoride
tBu	*tert*-butyl
TFA	trifluoroacetic acid
TFE	2,2,2-trifluoroethanol
TFP	tetrafluorophenyl
Thr	threonine
TIPS	triisopropylsilane
TMA	trimethylammonium
TNSB	trinitrosulfonylbenzene

TOF	time of flight
Trp	tryptophan
TSTU	N,N,N′,N′-tetramethyl-*O*-(*N*-succinimidyl)uronium tetrafluoroborate
Tyr	tyrosine
V	valine
Val	valine
W	tryptophan
Y	tyrosine
Z138	mantle cell lymphoma cell line

ABSTRACT

Cell surface receptors, which are overexpressed in cancerous tumours, are feasible molecular targets for tumour imaging. The transmembrane G-protein coupled receptor CXCR4 is overexpressed in tumours and has a crucial role in organ-specific metastasis of tumour cells. Cyclic pentapeptides such as FC131 and analogues have been developed to bind with high affinity and specificity to CXCR4. Unfortunately, when FC131 is radiolabelled and evaluated as a PET imaging agent, it demonstrates high retention in the liver due to its lipophilic character. Sulfonation of aromatic groups, such as the phenolic group in tyrosine, results in a significant reduction of a peptide's lipophilic character. Evaluation of sulfonated FC131 peptide analogues as PET imaging agents has been undertaken. In addition to radiolabelled peptides, PET imaging using amino acids has shown promise for tumour detection. ^{18}F containing radiolabelled amino acids are transported across the cell membranes by amino acid transporter proteins. As such, several approaches to synthesise fluorothreonine, fluoroaspartic acid and fluorotyrosine analogues have been examined.

DECLARATION

I certify that the thesis comprises of my original work towards the PhD and that due acknowledgment has been made in the text to all other material used. The thesis is less than 100,000 words in length.

Ashleigh Lilian Farnsworth

September 2019

ACKNOWLEDGMENTS

First and foremost, thanks to Associate Professor Craig Hutton for putting up with me for 6 years! Thank you for your consistent encouragement and belief in me. Thank you for your patience when I perhaps didn't know things about chemistry when I probably should have! I found my PhD to be quite challenging, but your unwavering support certainly helped me through. To my dear friend and mentor Dr Carlie Charron, I cannot thank you enough for your advice particularly in relation to my project's direction. You identified and formulated some great ideas and it has been a pleasure working alongside you. Dr Peter Roselt, thank you for your guidance throughout my Master's and PhD. Your kindness and words of wisdom were certainly needed at times.

Thank you to Dr Mohammad Haskali, who is the busiest man I know but who went above and beyond regardless to support and guide me. The radiochemistry aspect of my PhD was certainly a highlight and I feel very privileged to have been working alongside a great radiochemist and scientist. Thank you to Francisco Bravo for your contribution to the amino acid section of this project – your hard work was invaluable. Similarly, to third year students Yu Qing Yap and Matthew Bell, thank you for your contribution to this section.

To my panel, Professor Paul Donnelly and Professor Jonathan White, I have found your guidance to be most helpful. Thank you both for helping me stay on track. Thank you to Dr Hamish Grant and Dr Sunnia Rajput for all your assistance with NMR of my very small amounts of (sometimes dirty) peptides. To Associate Professor Nick Williamson, Dr Ching-Seng Ang and Dr Shuai Nie, many apologies for my constant use of the mass spectrometry and HPLC facilities. There will certainly be more time for others to use those instruments now! To Dr Troy Attard, thank you for your company and great chats in the peptide lab! Oh, and thank you for managing it too!

Thank you especially to Associate Professor Len Luyt, Dr Carlie Charron and Emily Murrell at The University of Western Ontario, Canada for kindly offering your assistance with binding assays.

Thank you to Marija, Sadegh, Mo, Varsha, Ria, Manisha, Luke, Nick, Alex and Biana who have given me such helpful feedback on my thesis! To Hutton group members past and present, thanks for all the fun times, shared stressful times and support over the years. Thank you to the Williams group who has accepted me as one of your own. It has been a pleasure having an occasional coffee with you at 10 am. To the Donnelley group and Rizzacasa group, thank you for your company and resources…but mostly your resources!

To those that have lived with me while I have been a nervous wreck – my former housemate JJ, my partner Ria, and my three-legged cat friend Fagin – I could not have done it without you! Ria, you could not have been more supportive even when I had long hours and came home grumpy. Thank you for your patience above all. To my friends who have seen me suffer during this journey - don't worry - it's over now! To my Mum, Dad and brother- I am glad to have made you proud! Thank you for your incredible support of me over the years.

Finally, thank you to The University of Melbourne, The Bio21 Molecular Science and Biotechnology Institute and The Centre for Molecular Imaging and Translational Research Laboratory at The Peter MacCallum Cancer Centre. It has been an absolute privilege to be involved with research at such world-class institutions.

TABLE OF CONTENTS

ABBREVIATIONS 2

ABSTRACT 10

DECLARATION 11

ACKNOWLEDGMENTS 12

TABLE OF CONTENTS 14

LIST OF FIGURES 17

LIST OF TABLES 19

LIST OF SCHEMES 20

CHAPTER 1: INTRODUCTION 24

1.1 Cancer diagnosis 24

1.2 PET imaging 25

1.3 FDG imaging of cancer 26

1.4 Amino acid transporters in cancer 27

1.5 Amino acid transporters in tumour imaging 30

1.6 Overexpressed receptors and their targeting peptides 32

$\alpha_v\beta_3$ integrin and RGD 32

Chemokine receptor 4 (CXCR4) and the targeting peptide FC131 34

1.7 Radiolabelled peptides for PET imaging of cancer 37

1.8 Synthesis of radiolabelled peptides 38

Automation in radiolabelling 39

DOTA peptides 40

Indirect $^{18}F^-$ fluorine labelling of peptides 41

1.9 Radiolabelled peptides and problems with lipophilicity 47

Increasing hydrophilicity of radiolabelled peptides by sulfonation 48

1.10 Aims 50

Aim 1: Apply sulfonation method to CXCR4-targeting peptides 50

Aim 2: Expand direct ^{18}F fluorination of nitrophenyl ester prosthetic groups and radiolabelling of CXCR4 targeting-peptides 50

Aim 3: Investigate synthesis of ^{18}F-labelled threonine 51

RESULTS AND DISCUSSION 52

CHAPTER 2: SULFONATION OF CXCR4-TARGETING PEPTIDES 52

2.1 Sulfonation of FC131-type peptides 52

Synthesis of FC131-type peptide 53

RP-HPLC analysis of FC131-type sulfonated analogues 59

2.2 Radiolabelling and biodistribution of sulfonated FC131-type peptide 61

Automated radiosynthesis module TRACERlab FXFN 61

[^{18}F]NFP synthesis and conjugation 62

Biological evaluation of [^{18}F]FP sulfonated FC131-type peptide 64

2.3 Small library of CXCR4 targeting cyclic pentapeptides 65

General SPPS pathway for CXCR4-targeting peptide analogues before side chain modification 66

Synthesis of CXCR4 targeting peptide pentixafor and sulfonated analogue 68

Synthesis of CXCR4-targeting peptide cyclo(D-Tyr(SO_3H)-N(Me)-D-Orn(FB)-Arg-Nal-Gly) 69

Synthesis of CXCR4-targeting peptide cyclo(D-Tyr(SO_3H)-N(Me)-D-Orn(FPy)-Arg-Nal-Gly) 70

Synthesis of CXCR4-targeting peptide cyclo(D-Tyr(SO_3H)-N(Me)-D-Orn(ESF)-Arg-Nal-Gly) 72

Alternative synthetic strategy 73

Synthesis of CXCR4-targeting peptides prior to solution phase side chain modification 74

2.4 Competitive binding assays on CXCR4- targeting peptide analogues 80

CHAPTER 3: DIRECT ^{18}F-FLUORINATION OF NITROPHENYL ESTER PROSTHETIC GROUPS AND RADIOLABELLING OF CXCR4 TARGETING-PEPTIDES 83

3.1 Synthesis of [^{18}F]-fluoronicotinic esters 83

3.2 Synthesis of [^{18}F]-fluorobenzoates 87

3.3 Relative efficiencies of acylation: PNP versus TFP ester 91

3.4 Automated radiolabelling of CXCR4 peptide with [^{18}F]4-nitrophenyl 4-fluorobenzoate 92

3.5 Radiolabelling of sulfonated pentixafor precursor with [^{68}Ga] 94

CHAPTER 4: SYNTHESIS OF ^{18}F-LABELLED THREONINE ANALOGUES 96

4.1 Fluorine-18 labelling of amino acids 96

4.2 [^{18}F]-fluorothreonine via cobalt mediated epoxide ring opening 97

4.3 Organotrifluoroborates for ^{18}F-labeling 100

Boramino acid as a marker for amino acid transporters 102

Radiolabelling of threonine trifluoroborate 107

CONCLUSIONS AND FUTURE WORK 109

CHAPTER 5: EXPERIMENTAL 111

REFERENCES 185

LIST OF FIGURES

Figure 1: Diagram of PET imaging.[6]

Figure 2: Structures of D-glucose and [^{18}F]-FDG.

Figure 3: The amino acid transporters that are upregulated in cancer coupling.[14]

Figure 4: ^{11}C-methyl-L-methionine (MET) and O-(2-[^{18}F]fluoroethyl)-L-tyrosine (FET).

Figure 5: Fluorine-18 labelled FACBC and FMA.

Figure 6: Cilengitide.

Figure 7: T22 ([Tyr^{5,12},Lys^{7}]-polyphemusin.

Figure 8: T140 **9** and its analogue FC131 **10**.

Figure 9: Somatostatin and ^{111}In-DTPA-Octreotide.

Figure 10: Methods of incorporating radionuclides onto peptides.[47]

Figure 11: iPHASE MultiSyn module for automated radiosynthesis.[49]

Figure 12: [^{68}Ga]DOTA-Tyr-Octreotide.

Figure 13: [^{124}I]-FC131.

Figure 14: [^{68}Ga]-Pentixafor.

Figure 15: [^{18}F]-fluoropropionate sulfonated “RGD” peptide.

Figure 16: ^{1}H NMR of aromatic region of **51**.

Figure 17: Aromatic region of ^{1}H NMR spectrum of **52**.

Figure 18: RP-HPLC traces of non-sulfonated and sulfonated FC131-type peptides.

Figure 19: TRACERlab FXFN.

Figure 20: RP-HPLC radiotrace of [^{18}F]NFP.

Figure 21: RP-HPLC trace of cold standard **63** (blue) (UV=254 nm) and radiotrace of reaction mixture containing product **64** (red).

Figure 22: Micro PET typical biodistribution of sulfonated FC131-type peptide **64** in an MV4-11 cell line.

Figure 23: Proposed CXCR4-targeting peptide analogues.

Figure 24: IC_{50} plot of FC131 with 96 well plate method.

Figure 25: iPHASE FlexLAB module.[59]

Figure 26: Proposed design of precursor.

Figure 27: Acylation of esters with benzyl amine to afford amidated products. Yield calculated as an average over 3 runs.

Figure 28: RadioTLC showing "free" $^{68}Ga^{3+}$ (left) and chelated $^{68}Ga^{3+}$ (right).

Figure 29: Amino acid and boramino acid.

Figure 30: Phenylalanine, boronic acid and trifluoroborate analogues and their molecular electrostatic potential (MEP) prediction.[100]

Figure 31: RadioTLC plate of $^{19}F/^{18}F$ IEX of Thr-BF_3.

Figure 32: Yields, stability and reactvity of PNP's vs TFP nicotinates and benzoates.

LIST OF TABLES

Table 1: Comparison of PET radionuclides.

Table 2: Amino acid transporters that are upregulated in cancer.[14]

Table 3: Comparison of overall yields.

Table 4: Comparison of binding affinities of CXCR4 targeting peptide analogues at 10^{-5} M and 10^{-8} M concentrations.

Table 5: Lewis acid promoted fluorination of epoxide with a range of catalysts/fluoride sources.

Table 6: Automation details of [^{18}F]NFP.

Table 7: Automation details of [^{18}F]NFB, [^{18}F]NFN, [^{18}F]TFN or [^{18}F]TFB.

Table 8: Automation details for labelling CXCR4 peptides with [^{18}F]NFB on iPHASE Flexlab.

LIST OF SCHEMES

Scheme 1: Synthesis of [^{18}F]-labelled peptide via [^{18}F]SFB.

Scheme 2: Guhlke et al. synthesis of [^{18}F]NFP.

Scheme 3: Chen et al. synthesis of [^{18}F]NFP.

Scheme 4: One-step radiosynthesis of [^{18}F]NFP and acylation of peptide.[59]

Scheme 5: [^{18}F]FP -Galacto RGD synthesis with [^{18}F]NFP.

Scheme 6: Radiosynthesis of TFP ligation to RGD peptide.[61]

Scheme 7: Sulfonation of FC131 analogue with chlorosulfonic acid.

Scheme 8: Radiofluorination of 4-nitrophenyl esters containing appropriate leaving groups.

Scheme 9: Methods to achieve radiolabelled “threonine” analogues via an epoxide or trifluoroborate.

Scheme 10: Proposed retrosynthesis of sulfonated FC131-type peptide.

Scheme 11: SPPS, macrocylisation and global deprotection of FC131-type peptide.

Scheme 12: Sulfonation of FC131 with excess chlorosulfonic acid.

Scheme 13: Sulfonation of FC131 with 1 equiv. chlorosulfonic acid.

Scheme 14: Sulfonation of Fmoc-D-Tyr(tBu)-OH.

Scheme 15: Sulfonation and Fmoc protection of D-tyrosine.

Scheme 16: Synthesis of sulfonated FC131-type peptide.

Scheme 17: ^{19}F cold standard synthesis.

Scheme 18: Synthesis of ^{18}F radiolabelled FC131-type peptide.

Scheme 19: General SPPS pathway for CXCR4 targeting peptides before side chain modification.

Scheme 20: Synthesis of pentixafor and sulfonated pentixafor.

Scheme 21: Synthesis of CXCR4 targeting peptide containing fluorobenzamide.

Scheme 22: Synthesis of CXCR4 targeting peptide containing fluoronicotinamide.

Scheme 23: Synthesis of CXCR4 targeting peptide containing ethane sulfonyl fluoride.

Scheme 24: Proposed retrosynthesis of CXCR4 targeting peptides.

Scheme 25: Synthesis of cyclo(DTyr^{1}-NMe-DOrn^{2}-Arg^{3}-Nal^{4}-Gly^{5}) 106 and sulfonated analogue 107.

Scheme 26: Alternative synthesis of CXCR4 targeting peptides.

Scheme 27: Olberg et al. method of synthesis of [^{18}F]TFP active ester.

Scheme 28: Synthesis of bromide salt.

Scheme 29: The synthesis of TFP [^{18}F]-fluoronicotinic ester.

Scheme 30: Synthesis of trimethyl ammonium nicotinic 4-nitrophenyl ester.

Scheme 31: Radiolabelling of fluoronicotinic 4-nitrophenyl ester.

Scheme 32: Synthesis of trimethyl ammonium benzoic acid 4-nitrophenyl ester.

Scheme 33: Unsuccessful radiolabelling of ester.

Scheme 34: Synthesis of diaryliodonium salt PNP ester.

Scheme 35: Manual optimization of [^{18}F]-fluorobenzoic ester via iodonium salt.

Scheme 36: Synthesis of TFP iodonium salt.

Scheme 37: Synthesis of TFP [^{18}F]-fluorobenzoate.

Scheme 38: Relative efficiencies of acylation of TFP versus PNP with benzylamine as a substrate.

Scheme 39: Fully automated synthesis of CXCR4-targting peptides with [^{18}F]-fluorobenzoate 4-nitrophenyl ester

Scheme 40: Radiolabelling of sulfonated pentixafor with $^{68}Ga^{3+}$.

Scheme 41: [^{18}F]-FET radiofluorination described by Siddiq et al.

Scheme 42: [^{18}F]-FACBC radiofluorination as described by McConathy.

Scheme 43: [^{18}F]-L-fluorothreonine synthesis via cobalt mediated epoxide ring opening.

Scheme 44: Synthesis of protected epoxide precursor.

Scheme 45: [^{18}F]-fluorination and deprotection of epoxide precursor.

Scheme 46: Synthesis of azidoethyl-AMBF_3.

Scheme 47: Facile labelling of rhodamine B by ^{18}F-^{19}F isotope exchange (IEX).

Scheme 48: ^{18}F-BAAs radiosynthesised via one-step ^{18}F-^{19}F isotope exchange reaction.

Scheme 49: General synthetic routes of α-amino trifluoroborates.

Scheme 50: Nickel catalysed decarboxylative borylation of amino acid.

Scheme 51: Proposed synthesis of α amino trifluoroborates via nickel catalysed decarboxylation.

Scheme 52: Nickel catalysed decarboxylation, borylation and trifluoroborate synthesis from N-Boc-L-Thr-OtBu-OH.

Scheme 53: Nickel catalysed decarboxylation, borylation and trifluoroborate synthesis from N-Boc-L-Tyr-OtBu-OH.

Scheme 54: Nickel catalysed decarboxylation, borylation and trifluoroborate synthesis from N-Boc-L-Asp-OtBu-OH.

Scheme 55: Radiolabelling of Thr-BF_3 via IEX.

Scheme 56: Synthesis of amino acid trifluoroborates from protected amino acids.

Scheme 57: Synthetic strategy to afford library of sulfonated CXCR4-targeting peptides.

CHAPTER 1: INTRODUCTION

1.1 Cancer diagnosis

Cancer is the leading cause of death in Australia. In 2010, it was estimated that more than 43,000 deaths were caused by cancer. In the same year, 114,000 new cancer cases were reported. "Cancer" is a generic term for various diseases in which abnormal cells divide uncontrollably and may spread to other parts of the body. There are over 100 reported types of cancer, all differing in malignancy, rate of growth, diagnosis and response to therapy.[1,2]

Accurate cancer diagnosis involves locating and identifying tumours, staging the disease, and determining the most suitable treatment. Anatomical and structural imaging techniques are the most common diagnostic tools for the detection of cancer. Common structural imaging techniques include Computed Tomography (CT) and Magnetic Resonance Imaging (MRI). Such techniques have the ability to provide detailed images of structural abnormalities at high resolution. However, structural imaging techniques have significant drawbacks, including their inability to differentiate tumour types, or malignant from benign growths.[2,3]

Molecular imaging in the form of positron emission tomography (PET) or single photon emission computed tomography (SPECT) provides real time visualisation of underlying biochemical processes distinct to tumour growth. This insight into the functional and metabolic nature of a tumour allows for the detection of functional abnormalities prior to the appearance of morphological changes visualised by CT or MRI.[4]

1.2 PET imaging

Positron Emission Tomography (PET) is a sophisticated nuclear imaging technique that produces three-dimensional images of functional processes in the body (Figure 1). PET proceeds by spontaneous positron emission from the nuclei of unstable ultra-short-lived radionuclides.[5] After emission, the positron loses energy though interactions with the surrounding tissue and annihilates with an electron, releasing two gamma photons of the same energy (511 keV) in opposing directions, which can be captured in coincidence by opposing detectors.[6] Single photon emission computed tomography (SPECT) is similar to PET, but differs in image resolution, as it uses radionuclides that decay to generate a single gamma photon. In addition, photons in SPECT are captured in multiple directions, similar to X-ray imaging. Poorer image quality can be attributed to the requirement of a collimator in SPECT to evaluate the origin of each photon.[7]

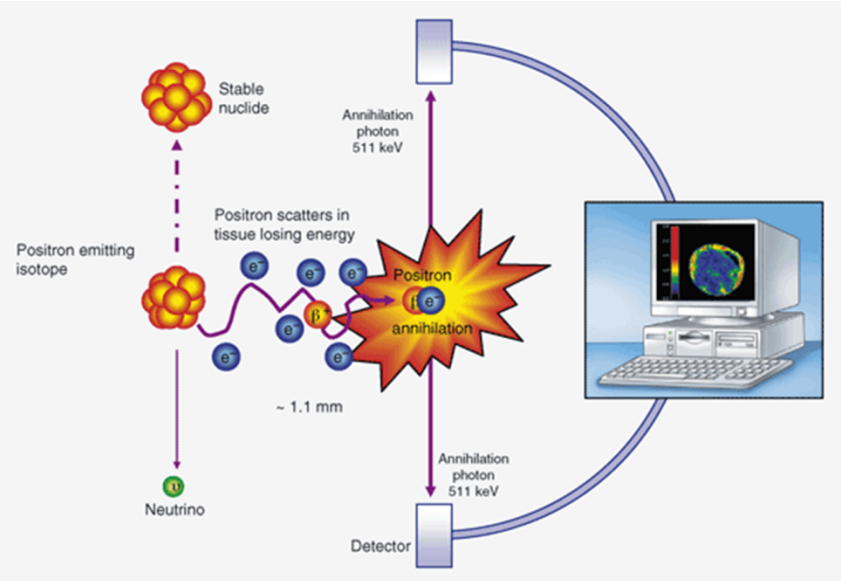

Figure 1: Diagram of PET imaging[6]

Flourine-18 is the most common radionuclide used in PET imaging. Fluorine-18 is an ideal radionuclide with a low energy of emission, allowing for increased dosage, and nearly 100%

positron decay, limiting unwanted radiation such as beta-decay, electron capture and alpha-decay (Table 1). The half-life of 110 min is ample time for complex radiosynthesis, yet limits prolonged patient exposure to ionising radiation.[8]

Gallium-68 is also a favourable radioisotope as it does not require the use of a cyclotron for its production. It can be easily accessed from a $^{68}Ge/^{68}Ga$ generator, which also results in significant cost reduction. $^{68}Ga^{3+}$ has an obvious advantage of rich coordination chemistry, which enables relatively straightforward labelling with a chelator. Despite the high energy of emission, in some applications, the images produced from gallium-68 are comparable to fluorine-18.[8]

Radionuclide	Half-life (min)	E_{max} β^+(KeV)	% β^+ Decay
^{15}O	2.1	1732	100
^{13}N	9.97	1190	100
^{11}C	20.3	961	100
^{68}Ga	67.6	1899	89
^{18}F	110	634	97
^{64}Cu	762	653	18

Table 1: Comparison of PET radionuclides

1.3 FDG imaging of cancer

PET first became recognised as a critical technique for imaging cancer in the 1990s through mapping of glucose consumption within the body, using the glucose analogue [^{18}F]-fluorodeoxyglucose (FDG) (Figure 2, **2**). Glucose metabolism is elevated in malignant cells and the high uptake of [^{18}F]-FDG can correspond to cancerous tissue even without anatomic correlation. [^{18}F]-FDG is the most widely used positron-emitting radiopharmaceutical in PET

imaging. The estimated number of PET studies in the United States grew from 69,000 to 155,000 from 1998 to 2000.[9] [^{18}F]-FDG has high sensitivity in detecting multiple malignancies, and is routinely applied in clinics for staging, restaging and monitoring treatment. Despite its widespread use, [^{18}F]-FDG has shortcomings including limited sensitivity to early stage tumours and an inability to distinguish between cancer and inflammation. In addition, [^{18}F]-FDG cannot detect tumours that do not exhibit increased glucose metabolism, such as prostate cancer.[9]

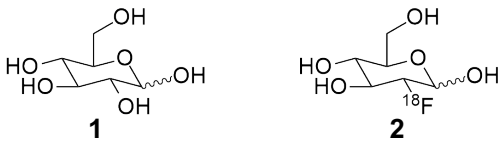

Figure 2: Structures of D-glucose and [^{18}F]-FDG

Accordingly, the development of novel radioimaging agents for the detection of cancer is ongoing. Other 'targets' that have been used for radiochemical diagnostic agents include amino acid transporters, which visualise cells with upregulated metabolism in a similar manner to [^{18}F]FDG, and extracellular receptors, which are over-expressed in cancer cells and have the advantage of being specific to the imaging of cancer cells. In addition, receptors are typically involved with processes essential for cancer growth and survival, such as angiogenesis and cell migration/invasion.[10]

1.4 Amino acid transporters in cancer

All mammalian cells require the following essential amino acids: Thr, His, Met, Phe, Trp, Val, Ile, Leu and Lys. These amino acids must be obtained through diet and cannot be synthesised de novo. The primary function of amino acids is to act as building blocks for protein synthesis; however, some amino acids have additional specific biological functions. Glutamine, glycine and aspartate are required for nucleotide biosynthesis, a critical process for tumour cell proliferation.

Serine plays an important role as a one carbon source, essential for nucleotide synthesis and DNA methylation. Leucine, glutamine and arginine act as signalling molecules and activate mTOR, a central regulator for tumour formation and angiogenesis (Figure 3). [11-13]

Amino acids are internalised via membrane transporter proteins. There are approximately two dozen amino acid transporters in humans, and tumour cells must upregulate one or more of these transporters to supply their demand for amino acids.[14] These amino acid transporters include systems L (leucine-preferring, LAT), A (alanine-preferring), ASCT (alanine-serine-cysteine-preferring), and X_c–(cystine/glutamate exchange transporter). Increased expression of LAT1, ASCT2 and X_c, in particular, have been associated with cancer metastasis and poor diagnosis in gliomas, lung, prostate and colon carcinomas. Research over the previous decades has focused mainly on LAT1 substrates (Figure 3). [15-17]

LAT1 (L-Amino acid Transporter 1) shows high affinity for the transport of branched chain amino acids (Val, Ile and Leu) and also bulky amino acids (Phe, Tyr, Trp, Gln, Asn, and Met). LAT-1 is highly expressed in most cancers.[11] Recent studies have shown that the hypoxia inducible factor HIF2α upregulates LAT-1.[14] As hypoxia plays a critical role in cancer growth and progression, the control of LAT-1 expression by HIF2α presents a possible molecular mechanism for the high expression of this transporter in cancer.[19,20]

The role of LAT-1 in controlling the cellular uptake of leucine with high selectivity has further stimulated interest in LAT-1's involvement in cancer. In addition, LAT-1 is also functionally coupled to ASCT2 to activate mTOR in cancer. The loss of ASCT2 leads to the inability of LAT-1 to activate mTOR (Figure 3).[21] As such, there has been increased interest in ASCT2, which also has an important role in nucleotide synthesis (essential for DNA production in cancer cells), glutaminolysis (an important energy source in cancer cells) and one carbon

metabolism (associated with disturbances in nucleotide synthesis and repair in several types of cancers). Previous studies have shown that ASCT2 function is important for cancer cell growth in melanoma, acute myeloid leukaemia, lung cancer, neuroblastoma and pancreatic ductal carcinoma. [14, 17, 22]

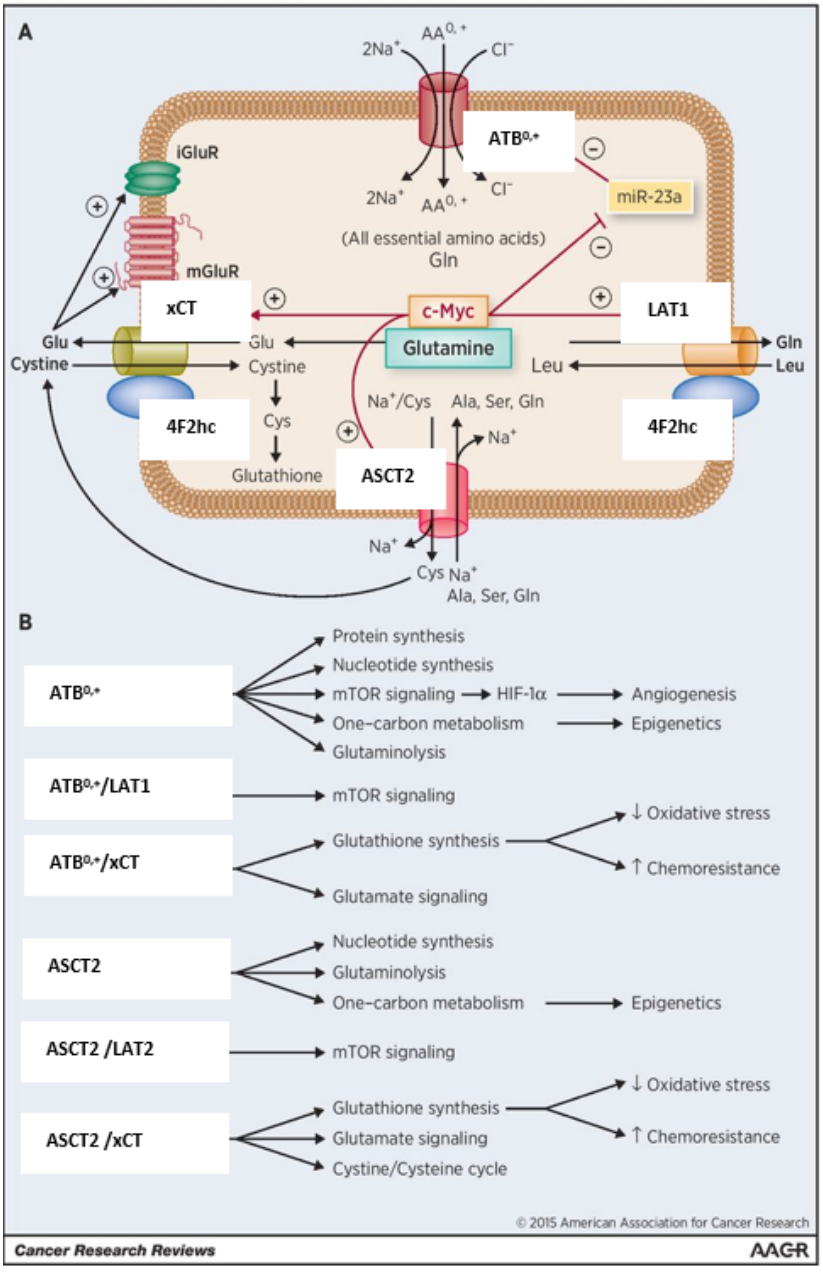

Figure 3: The amino acid transporters that are upregulated in cancer coupling.[14]

1.5 Amino acid transporters in tumour imaging

Increased protein synthesis in tumours results in high demand for amino acids. PET imaging using amino acids and amino acid analogues has shown promise for tumour detection in organ sites with an undesirable FDG-PET background or low FDG uptake. In addition, increased amino acid uptake and upregulation of amino acid transporters is more specific to tumour cells than FDG uptake. As such, amino acid-based tracers are potential alternatives to [^{18}F]-FDG for PET imaging of cancer.[23] If a given amino acid transporter is expressed at a higher density in tumours than in surrounding tissue, ^{18}F labelled substrates of the transporter can be used as a tracer for PET scanning to image the tumour. Several ^{18}F PET probes have been designed and validated for each of the four amino acid transporters (Table 2), but many are yet to be utilised clinically.[12-14]

AAT	Transport mechanism	Substrates	^{18}F-PET probes
ASCT2	Obligatory exchange Na^+/AA exchanged for Na^+/AA Electroneutral	Ala, Ser, Cys, Thr, Gln	FACBC **5**, FMA **6**, FPhPA
LAT1	Obligatory exchange AA exchanged for AA Electroneutral	Large neutral amino acids	FAMT, FET **4**, FPhPA, FACBC **5**
xCT	Obligatory exchange AA exchanged for AA Electroneutral	Cystine, glutamate	FSPG
4F2hc, CD98hc	Chaperone for LAT 1 and xCT	-	-
$ATB^{0,+}$	Unidirectional or $Na^+/Cl^-/AA^{0,+}$ symport Electrogenic	All neutral amino acids, all cationic acids	FET **4**

Table 2: Amino acid transporters that are upregulated in cancer.[14]

Established radiolabelled amino acids for tumour imaging with PET include ^{11}C-methyl-L-methionine (MET) **3** and O-(2-[^{18}F]-fluoroethyl)-L-tyrosine) (FET) **4** (Figure 4). MET **3** is an essential amino acid labelled with ^{11}C (half-life of 20 min) and was developed in the 1980s.[24] The ^{18}F labelled FET **4** was developed in the 1990s as it has a favourable longer half-life of 110 min (Table 4). MET and FET mimic substrates for a class of neutral amino acid transporters via the LAT-1 system (Table 2).[24]

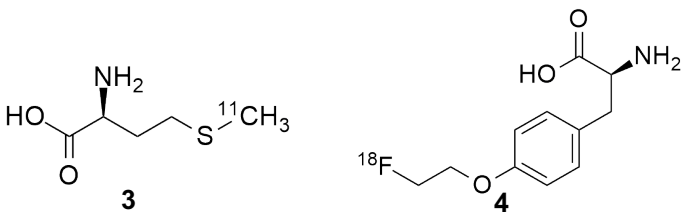

Figure 4: ^{11}C-methyl-L-methionine (MET) and O-(2-[^{18}F]fluoroethyl)-L-tyrosine (FET).

There has been significantly less effort to target the amino acid transporter ASCT2 with fluorinated amino acid analogues (Table 2). However, system Alanine-Serine-Cysteine (ASC) transporters, and in particular, ASCT2, are closely associated with tumour growth and proliferation. ASC has broad substrate selectivity and transports small and neutral amino acids such as alanine, cysteine, serine or threonine.[14] In recent years, a synthetic leucine analogue (*anti*-1-amino-3-^{18}F-fluorocyclobutane-1-carboxylic acid (FACBC) **5**) targeting the functional activity of both ASCT2 and LAT-1 transporter systems has been proposed as a possible radiotracer for prostate cancer (PCa) (Figure 5). PET imaging with ^{11}C- or ^{18}F-choline is currently used in the assessment of prostate cancer relapse to detect the site of disease recurrence even with a very low prostate specific antigen (PSA) level. Unfortunately, choline PET/CT can detect only half of the prostate cancer (PCa) lesions due to slow PCa cell proliferation. Slow PCa cell growth is due to a slow membrane metabolism, and this in turn, results in reduced choline uptake. As FACBC **5**

uptake instead targets the functional activity of amino acid transporters ASCT2 and LAT 1, the distribution of the tracer in the body is more favourable than choline. FACBC **5** PET/CT detection rates are far better than ^{11}C-choline PET/CT (40% compared to 20%).[25]

Several ^{18}F labelled alanine derivatives targeting ASCT2 have also been developed, with 3-(1-[^{18}F]fluoromethyl)-L-alanine (L-[^{18}F]FMA **6**) being the most promising, showing higher uptake than [^{18}F]FDG in a variety of cell lines (Table 2). L-[^{18}F]FMA was metabolically stable and primarily transported via sodium dependent system ASC in *in vitro* and *in vivo* imaging studies, demonstrating fast and clear accumulation in tumours.[26] These promising outcomes suggest that other ASCT2 substrates could be labelled to produce PET imaging agents targeting upregulated ASC amino acid transporters.

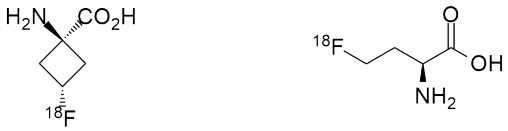

5 **6**

Figure 5: Fluorine-18 labelled FACBC and FMA.

1.6 Overexpressed receptors and their targeting peptides

In addition to overexpression of membrane bound transporters, tumour cells overexpress a range of receptors involved in many primary human cancers.[27]

$\alpha_v\beta_3$ integrin and RGD

Integrins are a subclass of cell adhesion receptors important for cell-to-cell and cell-to-extracellular matrix interactions. They are heterodimeric transmembrane glycoproteins consisting of non-covalently bound α and β-subunits. Integrins are involved in cell migration, differentiation

and survival during angiogenesis.[28] Tumour angiogenesis, or the growth of new blood vessels from pre-existing vasculature, is a well understood mechanism vital to tumour growth and spread.[29]

The $\alpha_v\beta_3$ integrin is highly expressed on activated endothelial cells during angiogenesis. Inhibition of $\alpha_v\beta_3$ mediated cell matrix interactions has been found to induce apoptosis of endothelial cells and $\alpha_v\beta_3$-positive tumour cells. As such, $\alpha_v\beta_3$ antagonists are currently being clinically assessed as potential anti-cancer drugs.[30]

The $\alpha_v\beta_3$ integrin binds to a range of extracellular matrix ligands including fibronectin and victronectin, which contain the common tripeptide binding motif Arg-Gly-Asp (RGD). Peptides that mimic these natural ligands have been developed in search of integrin-targeting pharmaceuticals. One example of an RGD peptide is the anti-angiogenic peptide Cilengitide (**7**, Figure 6) which binds selectively to the $\alpha_v\beta_3$ integrin with subnanomolar IC_{50} values.[31] The structure of Cilengitide was established through a series of ligand orientated design experiments which included the reduction of conformational space by cyclisation, spatial screening of cyclic peptides, and N-methylation. In the cyclic arrangement, the RGD motif forms a kink around glycine, which mimics the RGD conformation of the binding site in fibronectin.[32]

Structure activity relationship studies found that a hydrophobic D-amino acid (e.g. D-Phe) and the proton of the amide bond between residues 3 and 4 (Asp and D-Phe) were essential for activity. Position 5, however, proved to have no effect on biological affinity and was found to be a dispensable residue. N-methylation of amino acids (such as N-methyl valine in **7**) was found to enhance resistance to proteolytic cleavage. The cyclic RGD peptide Cilengitide (Arg-Gly-Asp-D-Phe-N(Me)Val) **7** was found to be the most potent antagonist fitting the aforementioned criteria.[32]

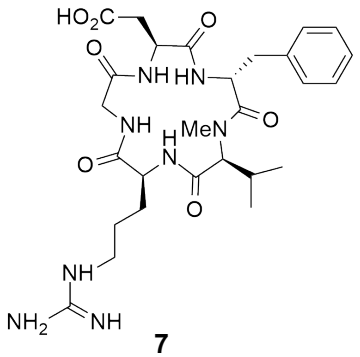

7

Figure 6: Cilengitide

Chemokine receptor 4 (CXCR4) and the targeting peptide FC131

The human chemokine system includes 40 chemokines and 18 chemokine receptors. Chemokine receptors are defined by their ability to induce directional migration of cells toward a gradient of a chemotaxis. CXCR4 is a chemokine receptor that selectively binds the chemokine stromal cell-derived factor 1 (SDF-1). CXCR4-based chemotaxis acts directly on tumour cell migration and invasion towards an SDF-1 gradient.[33] High expression levels of SDF-1 have been found at common sites of breast cancer metastases, including axillary lymph nodes, lungs, liver and bone marrow.[34]

Certain chemokine receptors, such as CXCR4, also play a critical role in enabling HIV-1 entry. Studies of CXCR4 antagonists have therefore been initiated in the search for anti-HIV therapeutics.[35] Anti-HIV compounds derived from self-defence peptides of horseshoe crabs, tachyplesin, and polyphemusin have previously been investigated. T22 ([Tyr^{5,12},Lys^{7}]-polyphemusin, was found to be the most potent anti-HIV peptide (Figure 7, **8**). T22 is an 18-residue peptide amide, which adopts an antiparallel β-sheet structure, incorporating a type-II turn maintained by two intramolecular disulfide bridges. Structure activity relationship studies revealed that T22 could be downsized to the 14-residue analogue T140 (Figure 8, **9**), which contains only

one disulfide bridge, Substitution of Trp-3 for L-3-(2-naphthyl)alanine increased potency and introduction of citrulline at position 9 decreased cytotoxicity. Further, the inhibitory activity of T140 against HIV-1 entry though CXCR4 is far greater than that of T22 (IC_{50} values of 0.43 nM and 5.05 nM respectively) indicating the enhanced ability of T140 to bind to CXCR4.[36-38]

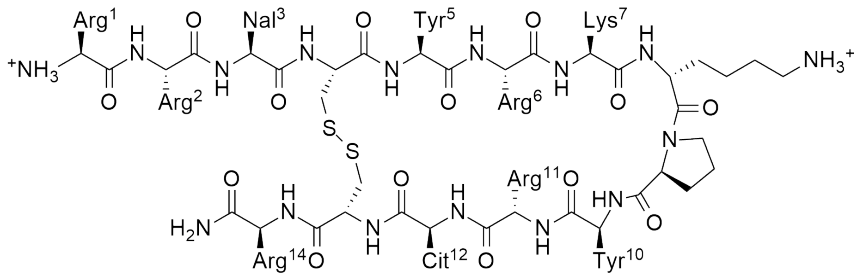

8

Figure 7: T22 ([Tyr^{5,12},Lys^{7}]-polyphemusin

Given CXCR4's role in tumour development and proliferation, analogues of known antagonists such as T140 **9** have been extensively studied towards developing anti-cancer lead compounds. The four pharmacologically most important residues of the T140 **9** for binding to CXCR4 were first confirmed by molecular dynamic modelling and through a series of alanine scans. Indispensible residues were Arg^{2}, Nal^{3}, Tyr^{5} and Arg^{14}. The Arg^{14} residue of T140 was shown to form strong hydrogen bonds with Asp^{171} of CXCR4 while Arg^{2} was shown to be extended near the N-terminus of CXCR4 interacting with Asp^{10} and Asn^{11}. The Tyr^{5} and Nal^{3} residues were shown to form a hydrophobic network of stabilisation with the Phe^{174}, Tyr^{190} and Phe^{201} of the receptor.[39]

Cyclic pentapeptides (previously described by Dechantsreiter *et al.*[32] with RGD peptides) were chosen as a molecular template to orientate these four requisite residues in proximity. In

search of smaller T140 analogues, Fujii *et al.*[39] found that cyclic pentapeptides containing the four pharmacologically most important residues of the T140 peptide (Arg^2, Nal^3, Tyr^5 and Arg^{14}) were similar in potency to T140. The peptide with the highest affinity for CXCR4 was cyclo(Nal^1-Gly^2-D-Tyr^3-Arg^4-Arg^5) and was named FC131 (Figure 8, **10**). The CXCR4-antagonistic activity (IC_{50} value of 4 nM) of **10** was identical to that of T140 despite a significant reduction in structural complexity.[39]

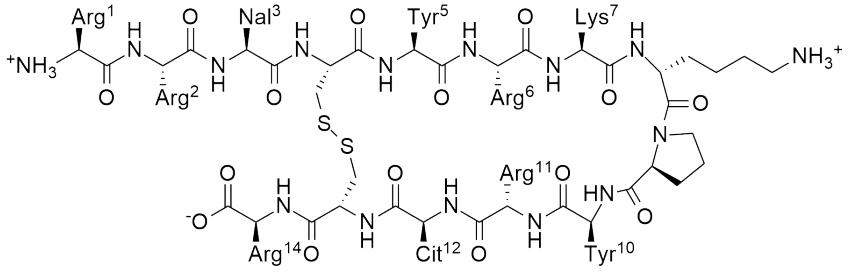

9

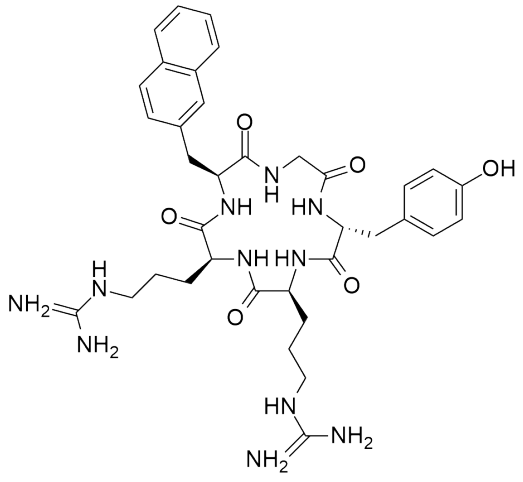

10

Figure 8: T140 ***9*** *and its analogue FC131* ***10****.*

Structure activity relationship studies of FC131 **10** suggest that Arg^5 and hydrophobic 2-Nal^1 bind deep in the receptor main binding crevice, while Arg^5 and D-Tyr^3 experience

conformational flexibility and face the extracellular surface of the receptor. As such, structural modifications of FC131 peptides could be considered at the Arg^4 or D-Tyr^3 positions.[40,41]

1.7 Radiolabelled peptides for PET imaging of cancer

Human cancer cells overexpress many receptors that are potential molecular targets. Radiolabelled peptides that bind with high affinity and specificity to such receptors on tumour cells have great potential for diagnostic imaging and targeted radionuclide therapy. For example, the somatostatin **11** (SST) receptor is overexpressed in some types of neuroendocrine tumours (NETs) and has been targeted effectively with SST peptide analogues in nuclear imaging.[42]

^{111}In-DTPA-octreotide (**12**, Figure 9) was the first US Food and Drug Administration (FDA) approved diagnostic radiopeptide for scintigraphy of patients with NETs. The high expression of SST receptors in various cancers has provided the molecular basis for the success of ^{111}In-DTPA-octreotide **12** as a tumour targeting peptide and opened new avenues for the development of other tumour specific peptides with potential use in nuclear oncology.[43,44]

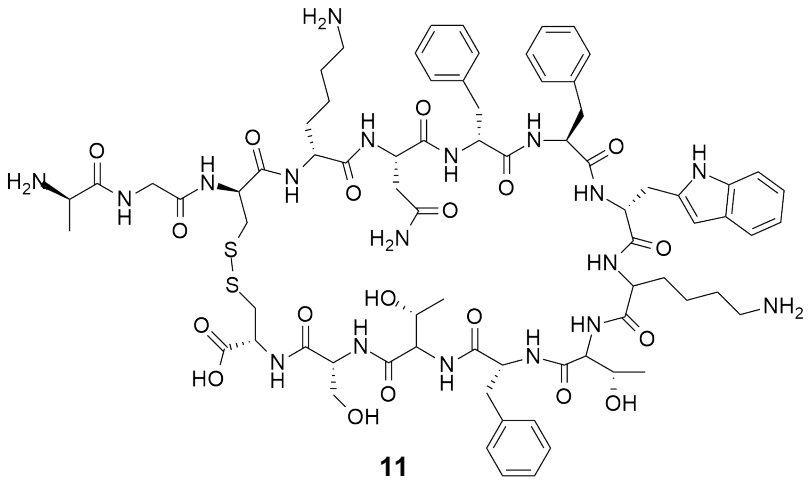

11

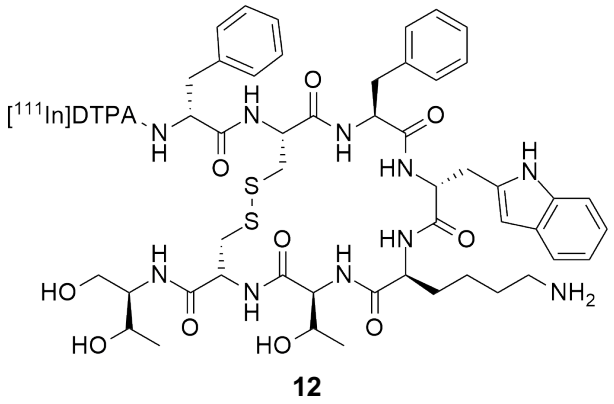

12

Figure 9: Somatostatin and ^{111}In-DTPA-octreotide

Many peptides exhibit extremely high affinities (nano- or sub-nanomolar range) for cell surface receptors. The successful development of new radiolabelled peptides for imaging of cancer is dependent on molecular modifications of a given peptide while preserving the binding affinity for target receptors.[45]

1.8 Synthesis of radiolabelled peptides

There are two distinct methods of incorporating radionuclides onto peptides: indirect and direct. A common direct method of incorporating radiometals onto peptides is pendant labelling, which involves a bifunctional metal chelator that both attaches itself to the peptide and coordinates to a radiometal (Figure 10).[47] A method of indirect labelling is via prosthetic groups, which are bifunctional labelling agents that contain both the radionuclide of interest and a functional group allowing for bioconjugation to peptides. The radionuclide is first installed on the prosthetic group before conjugation to the biologically relevant peptide.[46,47]

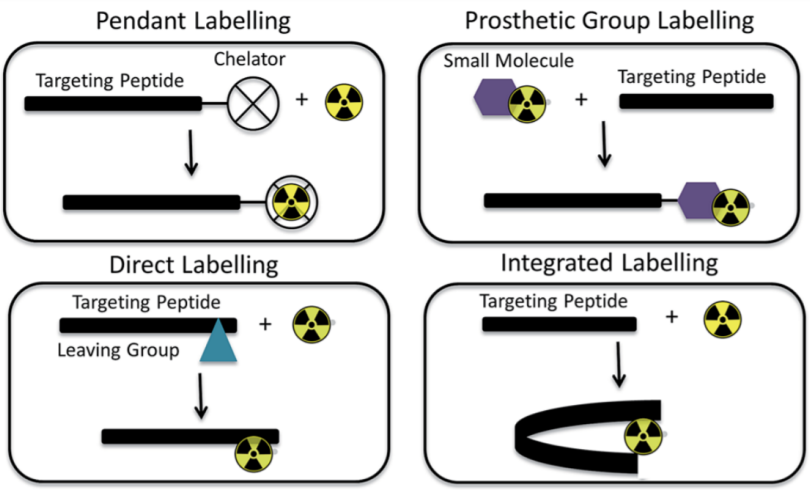

Figure 10: Methods of incorporating radionuclides onto peptides[47]

Automation in radiolabelling

Radiopharmaceuticals can be synthesised routinely and safely if their synthesis is automated. In addition, automation results in higher reproducibility and robustness, Good Manufacturing Practice (GMP) compliance, uniformity of end products and better control on sterility and dissemination.[55] Accordingly, much effort has focused on the development of automated modules to facilitate radiochemical reactions effectively and reproducibly in lead-shielded hot cells. The iPHASE MultiSyn module for example, is an automated multi-synthesis radiosynthesiser that is capable of synthesising radiometal containing theranostic agents (Figure 11).[48,49]

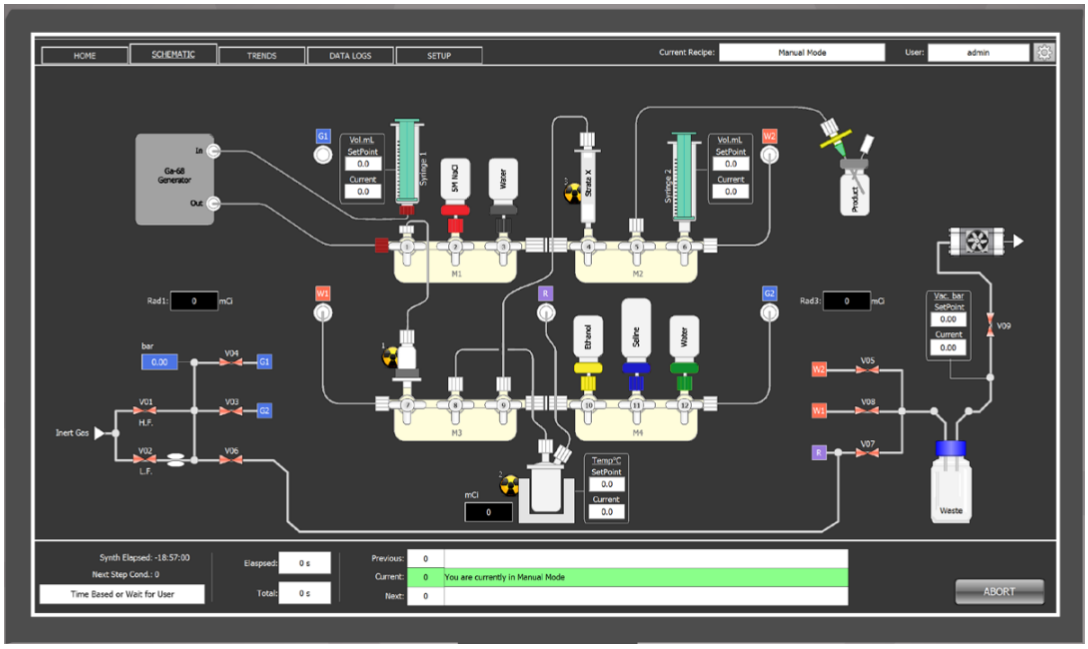

Figure 11: iPHASE MultiSyn module for automated radiosynthesis.[49]

DOTA peptides

Gallium-68 is a positron emitting isotope with a half-life of 67.6 min, which predominantly decays via 1.92 MeV positron emission (89%). The relatively short half-life and charged hydrophilic nature of gallium-68 lead to advantages such as rapid renal clearance and limited harm to the patient due to reduced dose. Furthermore, gallium-68 is conveniently and economically obtained from a ^{68}Ge/^{68}Ga generator.[50] Macrocyclic chelators that contain three or four nitrogen atoms in the ring are typically used to introduce radiometals such as ^{68}Ga. DOTA (1,4,6,10-tetraazacyclododecane-1,4,7,10-tetraaceticacid) remains the most commonly used chelator as it is readily available and has well-understood coordination chemistry.[51] The somatostatin receptor–targeting radiopeptide [^{68}Ga]DOTA-Tyr-Octreotide (^{68} Ga-DOTATOC) (Figure 12, **13**) is used routinely in diagnostic imaging of somatostatin receptor-positive tumours. The same ligand

labelled with high or medium energy beta emitters such as yttrium-90 or lutetium-77 can be used in therapy.[52]

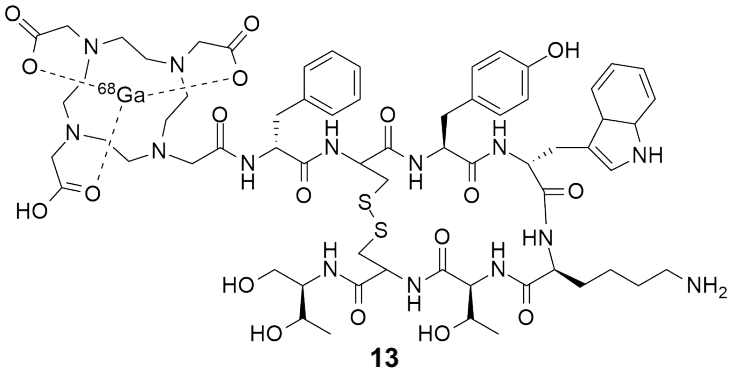

Figure 12: [^{68}Ga]DOTA-Tyr-Octreotide.

Indirect $^{18}F^-$ fluorine labelling of peptides

Introducing fluorine-18 into peptides can be complicated. The harsh conditions required to facilitate direct $^{18}F^-$ fluorination of aromatic and aliphatic precursors are typically not compatible with peptides as the latter may degrade at the high temperatures required.[53] While peptides are typically soluble in water, such conditions are not suitable for nucleophilic substitution with fluoride due to a high degree of solvation, reducing its nucleophilicity. Enhancement of the solubility and nucleophilicity of $^{18}F^-$ in organic solvents is achieved by the addition of a phase transfer catalyst (PTC) such as [2.2.2]cryptand (K_{222}) or by the addition of bulky tetrabutylammonium cation. Enhancement is achieved as PTCs not only solubilise the $^{18}F^-$, but also create sufficient charge separation between the $^{18}F^-$ and the cationic counterion to form reactive 'naked' fluoride. Poorly nucleophilic bases such as carbonate or bicarbonate ions are typically used for radiofluorinations.[54] Indirect fluorination is the most feasible method of incorporating fluorine-18 onto peptides. Indirect fluorination can be carried out by initial radiofluorination of a small organic molecule, known as a prosthetic group. This prosthetic group

is then conjugated to the peptide under mild conditions. Radiolabelled prosthetic groups are bifunctional labelling agents that incorporate both the fluorine-18 radionuclide and a reactive functional group that facilitates ligation to the peptide.[55]

Acylation is a common technique used to ligate radiolabelled prosthetic groups to peptides via amide bond formation. Amide bonds are relatively stable bonds *in-vivo* and are highly abundant in peptides.[56] Acylating precursors are generally activated carboxylic acid derivatives that can be coupled to an amine group in the corresponding peptide. Some of the most common acylating prosthetic groups are N-succinimidyl 4-^{18}F-fluorobenzoate ([^{18}F]SFB) (Scheme 1, **16**) and 4-nitrophenyl 2-^{18}F-fluoropropionate ([^{18}F]NFP) (Scheme 2, **23**) due to their *in-vivo* stability and favourable biological characteristics. In order to synthesise a fluorobenzoylated derivative, a fluorobenzoate active ester must be synthesised, such as [^{18}F]SFB (Scheme 1, **16**).[57] Typically, synthesis of ^{18}F-labelled activated esters used for peptide acylations requires several steps. For example, [^{18}F]SFB **16** is produced by a 3-step process: i) substitution of 4-trimethylammonium ethyl benzoate **14** with $^{18}F^-$; ii) saponification of the ethyl ester; and iii) activation of the carboxylic acid **15** as the NHS ester **16** (Scheme 1). [^{18}F]SFB can then be coupled to a free amine on a peptide or protein **17**. The major limitation associated with incorporation of a $^{18}F^-$ fluorobenzoate moiety is its hydrophobicity, which can negatively affect the biodistribution of the peptide conjugate. The labelling efficacy of [^{18}F]-fluorobenzoate with hindered amines is also problematic.[58]

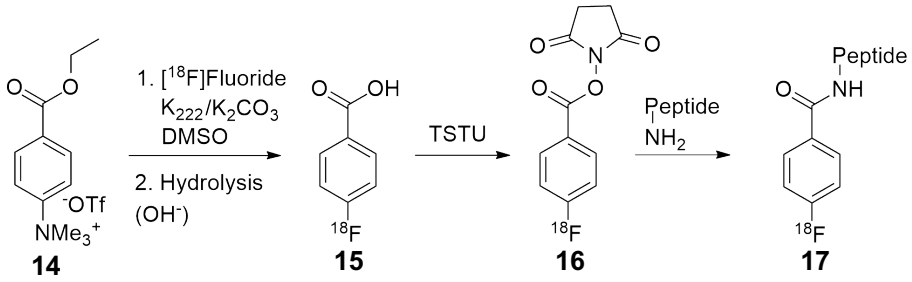

Scheme 1: Synthesis of [^{18}F]-labelled peptide via [^{18}F]SFB.

Another commonly used acylation prosthetic group, which overcomes some of the shortcomings of fluorobenzoate, is 4-nitrophenyl 2-^{18}F-fluoropropionate, [^{18}F]NFP **23**. [^{18}F]NFP **23** possesses good *in-vivo* stability, is readily synthesised, and has favourable biological characteristics. [^{18}F]NFP **23** is a particularly useful acylation agent due to its small size as compared to the fluorobenzoate derivative. As a result, peptides labelled with a $^{18}F^{-}$ fluoropropionoyl group may have similar binding affinity and biological character to the parent peptide and are less hydrophobic.[59]

Initial efforts to synthesise [^{18}F]NFP **23** by Guhlke *et al.*[59] were complex (Scheme 2). Propionate esters are volatile, therefore a bulky ester protecting group was introduced. The bulky bromide ester **20** undergoes bromide–fluoride substitution under nucleophilic radiofluorination conditions. The fluorinated ester **21** is then purified and hydrolysed. The trimethylammonium salt of the fluoropropionate **22** is then treated with dinitrophenyl carbonate to form the desired ester **23**. Liu *et al.*[60] attempted to simplify this procedure by limiting the synthesis to one pot with only a single RP-HPLC purification step (Scheme 3). However, the synthesis of **23** remains relatively complex as **24** requires $^{18}F^{-}$ labelling **25**, hydrolysis **26** and activation of the potassium salt. In addition, the process requires two drying steps.[60]

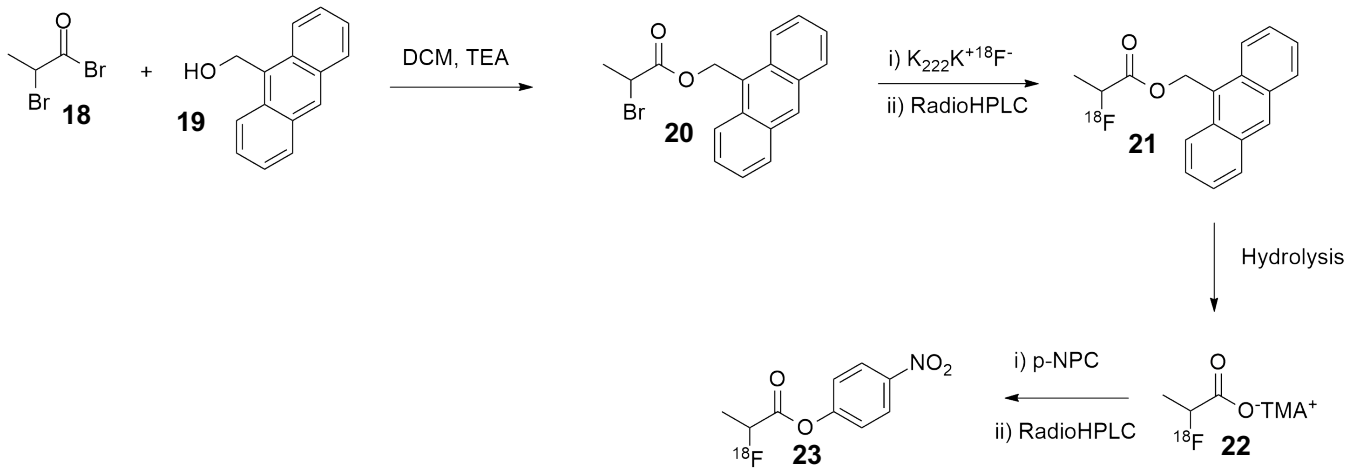

Scheme 2: Guhlke et al. synthesis of [^{18}F]NFP.

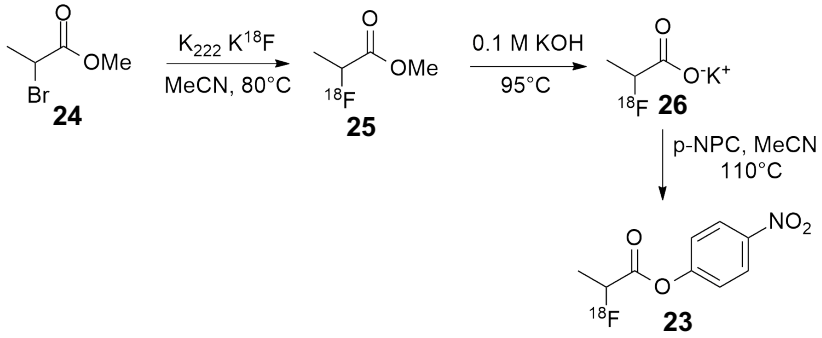

Scheme 3: Chen et al. synthesis of [^{18}F]NFP.

Studies in the Hutton group have since developed an innovative one-step and automated radiochemical synthesis for the preparation of [^{18}F]NFP **23**. In this procedure, the active ester **28** is formed and subsequently radiofluorinated with $^{18}F^-$ in a single step (Scheme 4).[68]

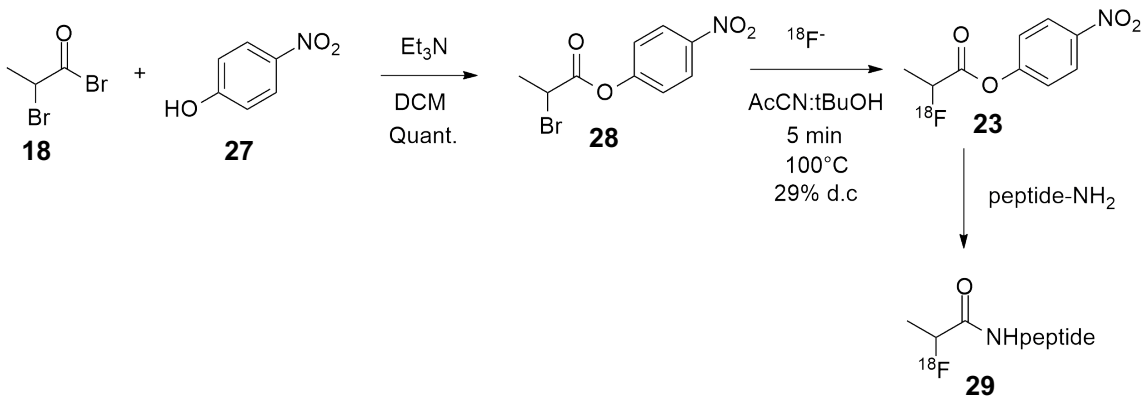

Scheme 4: One-step radiosynthesis of [^{18}F]NFP and acylation of peptide.[59]

Furthermore, simplification of the synthesis of [^{18}F]NFP **23** has enabled straightforward preparation of relevant tracers for PET imaging of $\alpha_v\beta_3$ related tumours such as [^{18}F]GalactoRGD **31** (Scheme 5, **31**).[59]

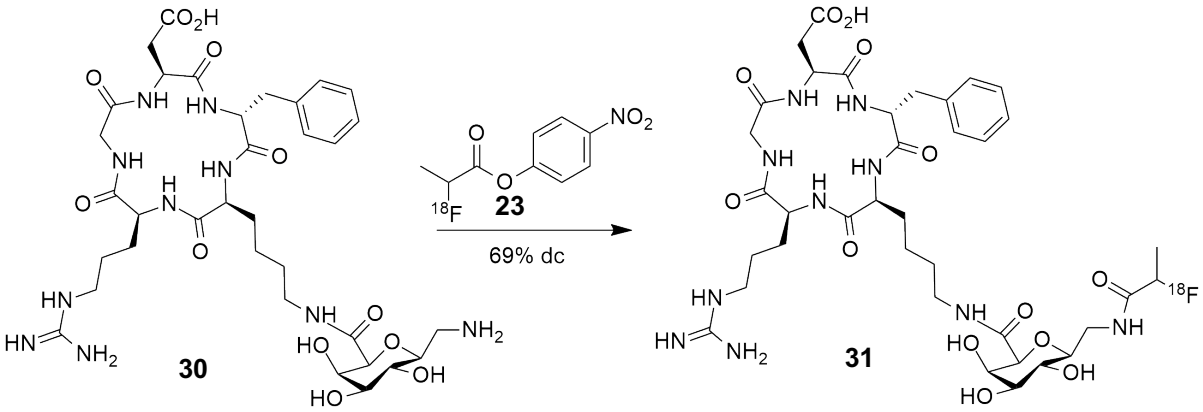

Scheme 5: [^{18}F]FP -Galacto RGD synthesis with [^{18}F]NFP.

The only other example of 1-step radiosynthesis of ^{18}F-labelled acyl prosthetic groups is the preparation of **33** by Olberg *et al.*[61] Olberg showed treatment of the TFP ester of trimethylammonium nicotinamide **32** with $^{18}F^-$ gave **33** (Scheme 6). [^{18}F]Fluoronicotinic esters functionalised with a suitable leaving group at the 2-position are highly activated for nucleophilic

aromatic substitution with [^{18}F]fluoride (Scheme 6). Olberg *et al.* described the synthesis of 2-[^{18}F]fluoropyridine, **33** in high yields of 60–70% with high specific activity. The ^{18}F labelled prosthetic group based on a nicotinic acid tetrafluorophenyl ester did not require any additional electron withdrawing substituent for activation, as is common for nucleophilic homoaromatic substitutions. The active [^{18}F]-fluoronicotinic ester **33** was used to acylate an RGD peptide in phosphate buffer/DMSO/MeCN for 10 min to afford amidated product **34** in 84% yield (Scheme 6, **34**).[61]

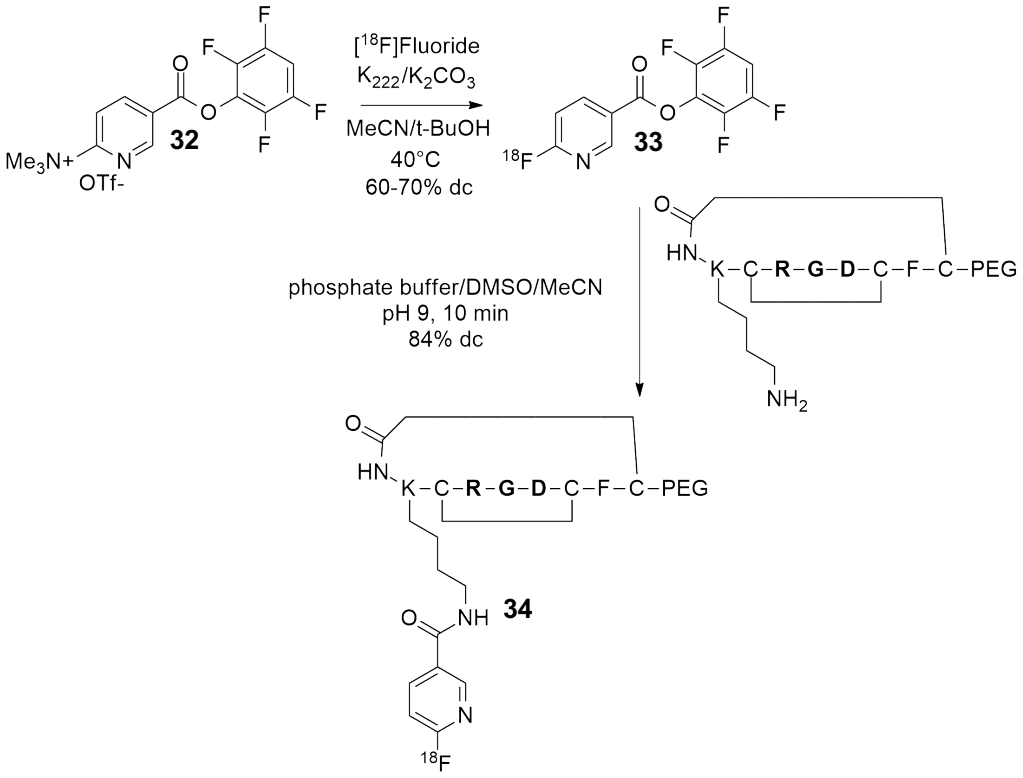

Scheme 6: Radiosynthesis of TFP ligation to RGD peptide.[61]

1.9 Radiolabelled peptides and problems with lipophilicity

The sub-optimal biodistribution of radiolabelled peptides is a common problem in PET imaging, as peptides are often lipophilic. Lipophilicity results in uptake of the peptide in the

hepatic system, which can potentially hamper visualisation of a tumour.[62] In addition, uptake in the hepatic system increases protein binding and reduces the free fraction of peptide in plasma available for binding.[63] FC131 peptides showing high affinity and specificity for the CXCR4-receptor have been developed as radiotracers for the non-invasive imaging of tumours.[64] FC131 **10** has previously been radioiodinated with ^{124}I to generate **35** (Figure 13) (K_D= 0.4 nM). However, the lipophilicity of **35** resulted in poor imaging.[64] A common method to overcome lipophilicity in cyclic pentapeptides is to attach a hydrophilic group such as glucose (as in **31**) which can result in reduced liver uptake, increased tumour uptake and increased renal clearance.[65]

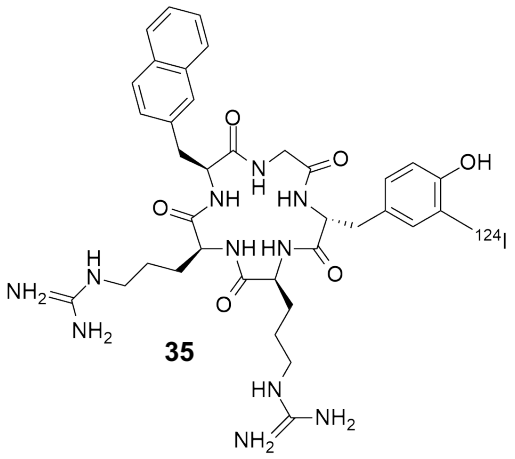

Figure 13: [^{124}I]-FC131

One of the few CXCR4-directed radiolabelling agents in development is FC131 analogue **36**, which incorporates a ^{68}Ga-DOTA moiety (Figure 14). Biodistribution studies showed that the increase in hydrophilicity due to incorporation of the DOTA moiety and $^{68}Ga^{3+}$ was effective in reducing the liver and intestine uptake.[66]

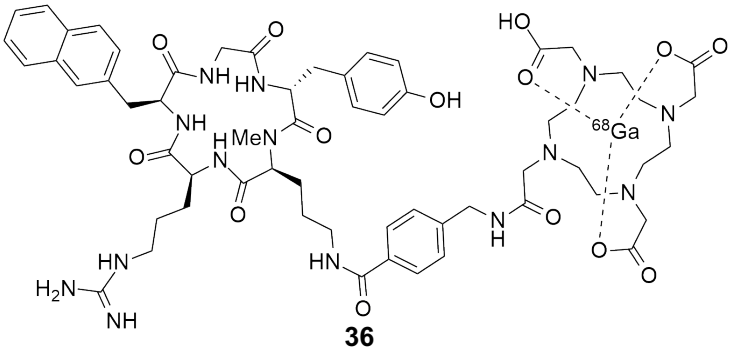

36

Figure 14: [^{68}Ga]-Pentixafor

Increasing hydrophilicity of radiolabelled peptides by sulfonation

Sulfonation of peptides was first proposed by Previero *et al.*[67] as a convenient solution to increase hydrophilicity of tyrosine and tryptophan without introduction of structural complexity. Studies in the Hutton group have shown that late stage sulfonation of tyrosine-containing peptides is a feasible and efficient method to increase hydrophilicity.[68] Sulfonated "RGD" peptide **37** radiolabelled with [^{18}F]NFP **23** had excellent *in-vivo* results with good tumour uptake and low retention in non-target organs in a small animal PET imaging study. The kidney to liver uptake ratio was higher than the labelled non-sulfonated RGD peptide, suggesting increased hydrophilicity of the peptide, as renal clearance was enhanced (Figure 15).[68]

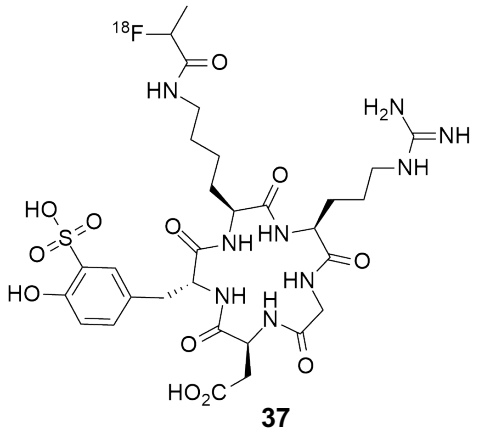

37

Figure 15: [^{18}F]-fluoropropionate sulfonated "RGD" peptide.

1.10 Aims

Aim 1: Apply sulfonation method to CXCR4-targeting peptides

Given the hydrophobic nature of FC131 **10** diminishes its utility as a CXCR4-targeting peptide, our first aim is to investigate sulfonation of FC131 and analogues to improve biodistribution. FC131 analogues will be synthesised by standard SPPS protocols, macrocyclised, globally deprotected, and further reacted under the sulfonation conditions previously described by the Hutton group (chlorosulfonic acid in TFA, Scheme 7) .[68]

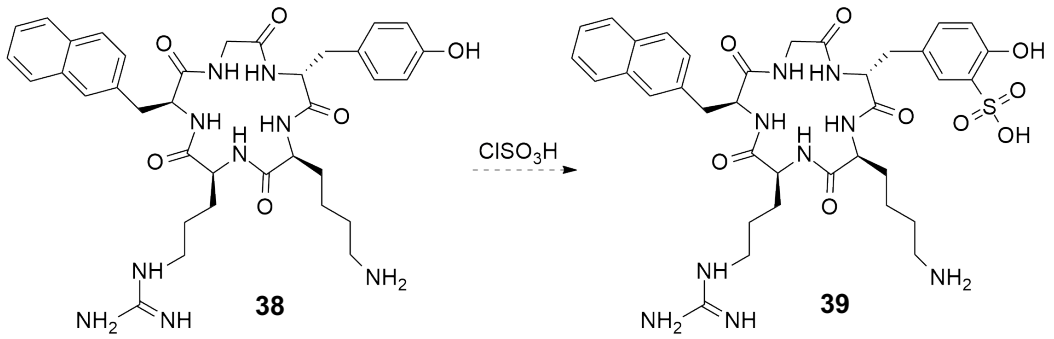

Scheme 7: Sulfonation of FC131 analogue with chlorosulfonic acid.

Aim 2: Expand direct ^{18}F fluorination of nitrophenyl ester prosthetic groups and radiolabelling of CXCR4 targeting-peptides

Previous work by the Hutton group utilised [^{18}F]NFP **23** to radiolabel RGD peptides (Figure 15).[59] Although NFP acylation is well understood, we are interested in further exploring the nitrophenyl activated ester as a method of installing [^{18}F]-fluorobenzamides and [^{18}F]-fluoronicotimamides. With optimised radiolabelling conditions established for ^{18}F-fluorination of nitrophenyl activated esters, these conditions will be applied to FC131 peptides containing a free amine on a side chain (Scheme 8).

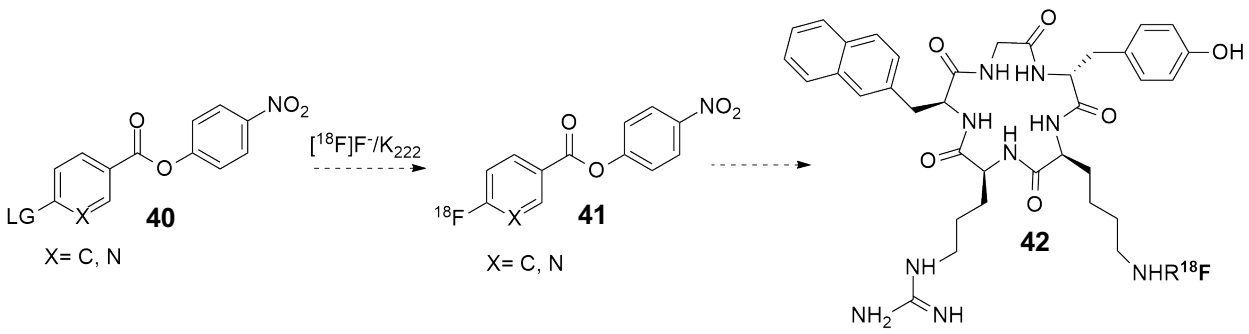

Scheme 8: Radiofluorination of 4-nitrophenyl esters containing appropriate leaving groups.

Aim 3: Investigate synthesis of ^{18}F-labelled threonine

In addition to targeting CXCR4 receptors for cancer imaging, we also aim to target amino acid transporters with ^{18}F-radiolabelled amino acids. We are particularly interested in the ASCT2 amino acid transport system and, as such, we will synthesise radiofluorinated threonine. Two methods are proposed for the radiofluorination of threonine: via ring opening of epoxide **43** via $^{18}F^-$ fluoride, and by isotope exchange (^{19}F–^{18}F) of trifluoroborate threonine analogue **45** (Scheme 9).

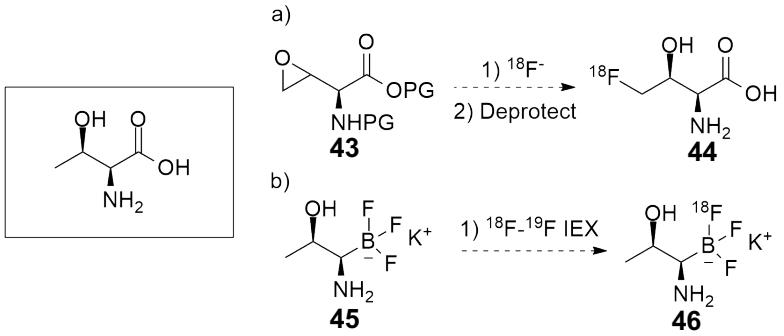

Scheme 9: Methods to achieve radiolabelled "threonine" analogues via an epoxide or trifluoroborate.

RESULTS AND DISCUSSION

CHAPTER 2: SULFONATION OF CXCR4-TARGETING PEPTIDES

2.1 Sulfonation of FC131-type peptides

A variety of methods are available to improve *in vivo* properties of a radiolabelled peptide, including conjugation of hydrophilic groups such as sugars and PEGs. However, incorporation of biodistribution enhancers can be difficult due the limited reactive sites on a given peptide and the protecting group manipulations required for the conjugation of sugars or a PEG group.[69] The simple, one-step, site-specific sulfonation of cyclic RGD pentapeptides has previously been developed within the Hutton group and resulted in dramatic improvement in biodistribution properties (Figure 15).[68] As the sulfonation occurs on the tyrosine residue of the RGD peptide, we decided to implement the same strategy of sulfonation of a tyrosine-containing FC131 peptide. RGD peptides typically contain a lysine residue to allow for acylation of a fluorine-18 containing prosthetic group.[70] Similarly, as the arginine in position 4 of FC131 **10** is exposed to the extracellular environment during binding to CXCR4, a lysine will be substituted at this position.[41] Thus, the initial target was cyclic pentapeptide **39**, containing lysine and sulfonated tyrosine residues. Peptide **39** could be accessed by sulfonation of **38**, which would be available from linear protected peptide **47**. The linear protected peptide would be assembled via a typical solid phase peptide synthesis strategy[71] from **48** (Scheme 10).

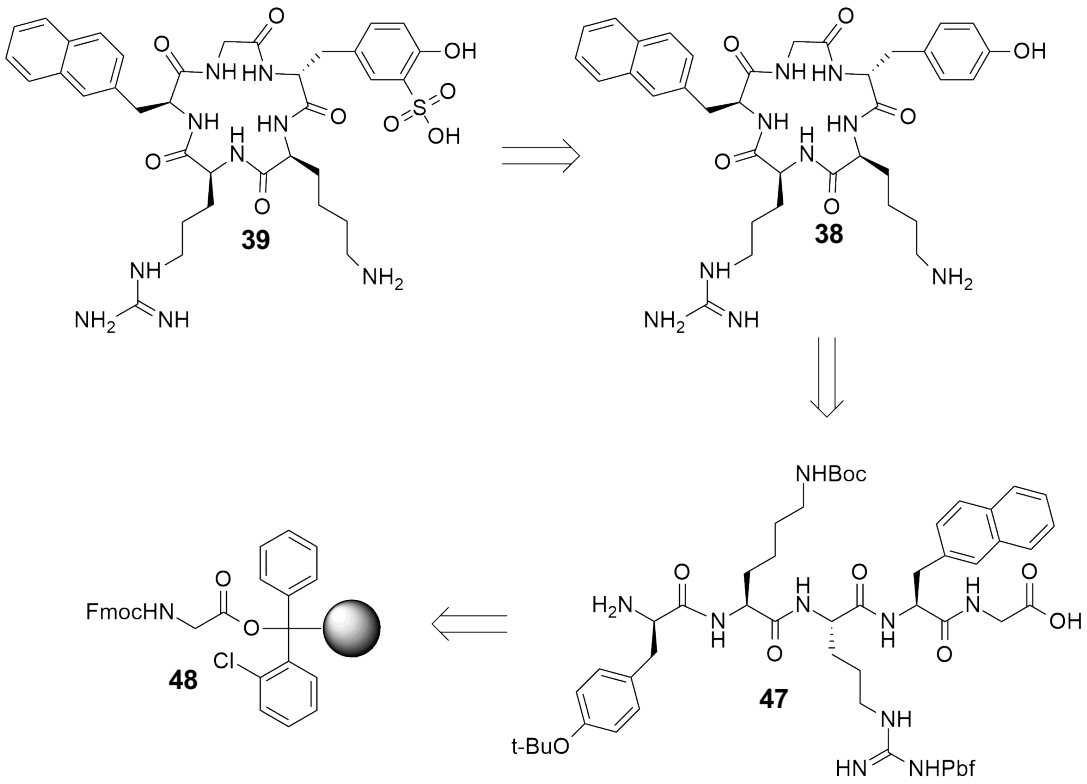

Scheme 10: Proposed retrosynthesis of sulfonated FC131-type peptide.

Synthesis of FC131-type peptide

The synthesis of FC131-type peptide **38** was approached through a standard solid phase peptide synthesis protocol, with late stage sulfonation. First, Fmoc glycine was attached onto 2-chlorotrityl resin **48**. Through an iteration of deprotection and coupling reactions (with HATU/DIPEA) the linear protected peptide was assembled on resin to generate **49** (Scheme 11). The N-terminal Fmoc group was deprotected and the peptide was cleaved from the resin with 1% TFA in DCM. Macrocyclisation of the crude linear peptide **47** was then performed by treatment with HATU/DIPEA under dilute conditions (approx. 1 mg/ml in DCM) to furnish **50**, which was then globally deprotected with 95% TFA. The crude mixture was then purified by RP-HPLC to yield cyclic peptide **38** in 20% overall yield based on initial resin loading. The structure of the cyclic pentapeptide was confirmed by mass spectrometry (ESI-MS), which exhibited a protonated

molecule ion at *m/z* 702.372 $[M+H]^+$ and 351.689 $[M+2H]^{2+}$. In addition, ^{1}H NMR analysis displayed two doublets (2H each) at δ 6.95 and 6.65 ppm, indicative of a tyrosine residue, with seven additional peaks between δ 7.87–7.19 ppm indicative of the napthylalanine residue. The presence of five α-H's between δ 4.4–3.4 ppm further confirmed the structure of **38**.

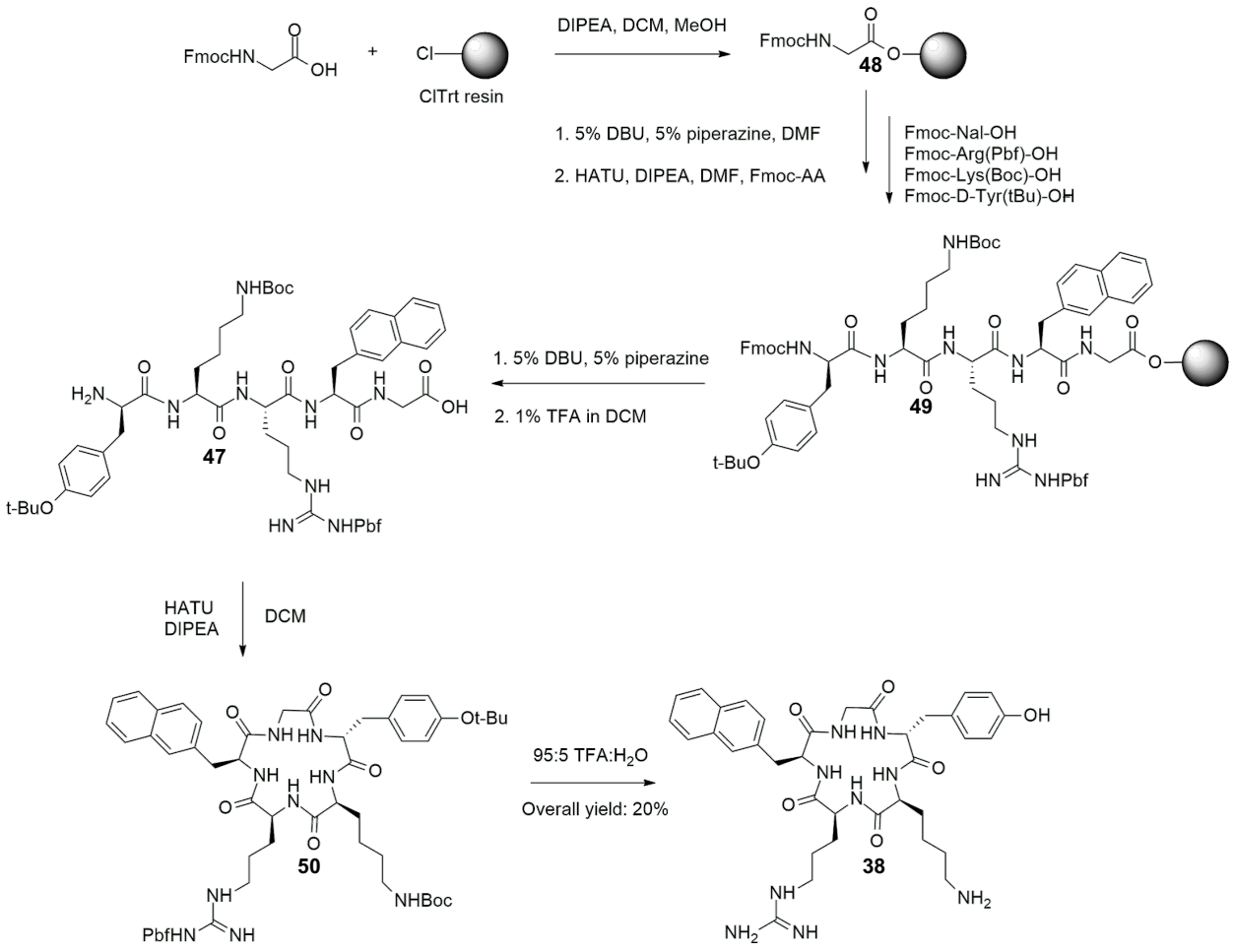

Scheme 11: SPPS, macrocylisation and global deprotection of FC131-type peptide.

With the cyclic pentapeptide **38** in hand, sulfonation of the tyrosine residue was attempted by treatment with chlorosulfonic acid (5% in TFA). Mass spectrometric analysis of the product showed a molecular ion at *m/z* 862.28, which corresponds to a doubly-sulfonated adduct. ^{1}H NMR

spectroscopic analysis displayed three resonances consistent with a trisubstituted aromatic ring at δ 6.98 (d), 7.29 (dd) and 7.61, consistent with a sulfonated tyrosine side chain (Figure 16). In addition, only six other aromatic proton resonances were observed indicating substitution on the napthylalanine ring. A downfield singlet was indicative of the hydrogen ortho to the sulfonic acid with no adjacent H (f, Figure 16). Thus, it was determined that sulfonation of both aromatic groups had occurred to generate product **51** (Scheme 12, Figure 16).

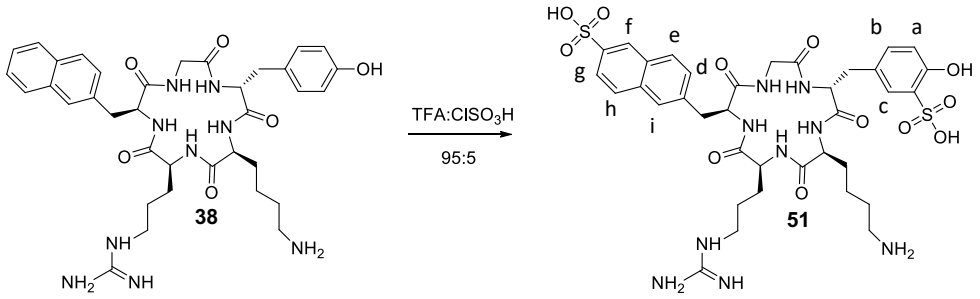

Scheme 12: Sulfonation of FC131 with excess chlorosulfonic acid.

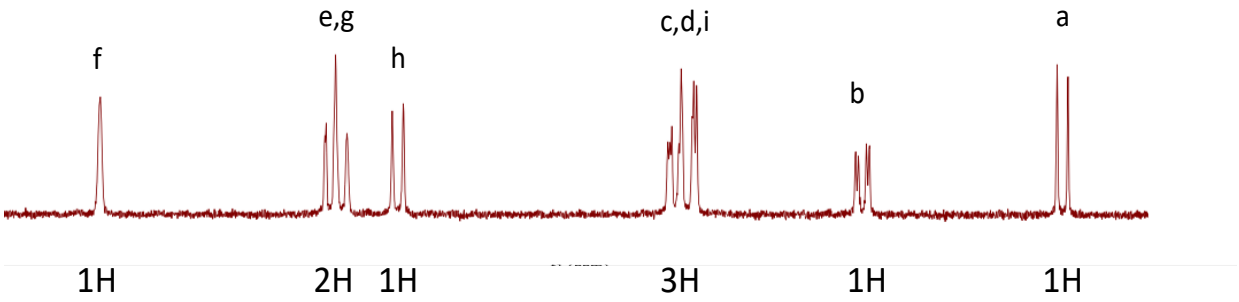

Figure 16: ^{1}H NMR of aromatic region of 51

Though we presume sulfonation occurs at the 6-position of the naphthalene ring,[72] substitution at the 7-position cannot be ruled out at this time. Though, sulfonation of both aromatic rings would presumably increase the hydrophilicity of the resultant peptide to a greater extent than mono-sulfonation, structure activity relationship studies suggest the napthyl group is buried deep

in a hydrophobic pocket when FC131 is bound to CXCR4,[41] and as such sulfonation at this site may be deleterious to binding affinity. Further, Thiele *et al*.[41] performed structure-activity relationship studies of aromatic positions in cyclopeptide CXCR4. Substitution of napthylalanine with the similar aromatic amino acid phenylalanine, resulted in greater than 200-fold loss of potency. Substitution of the D-tyrosine with the structurally dissimilar glycine, however, was found to be only 13-fold less potent. Such findings suggest that sulfonation of the D-tyrosine should have less impact on binding affinity than sulfonation of the napthylalanine.[41,73]

Accordingly, we sought conditions that would generate a mono-sulfonated adduct. Treatment of the peptide **38** with one equivalent of chlorosulfonic acid in TFA afforded a white precipitate. The precipitate was analysed by ESI-MS and displayed a protonated molecular ion at *m/z* 782.33, corresponding to a mono-sulfonated product. ^{1}H NMR analysis displayed two doublets (2H each) indicative of a tyrosine residue, while the remaining six aromatic H's were similar to those observed for **51**, indicative of a sulfonated napthylalanine residue. Thus, it was apparent that mono-sulfonation had occurred selectively on the napthylalanine residue to give **52** (Scheme 13, Figure 17).

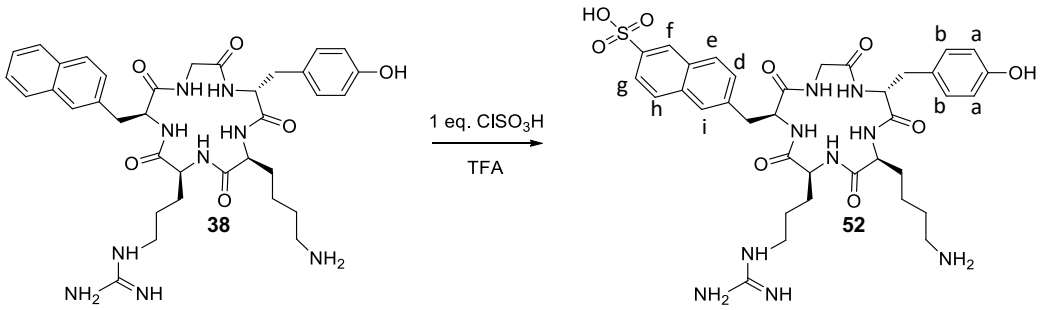

Scheme 13: Sulfonation of FC131 with 1 equiv. chlorosulfonic acid.

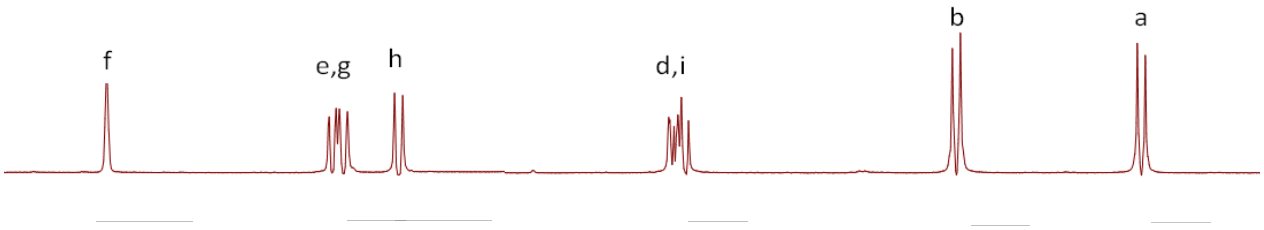

Figure 17: Aromatic region of ^{1}H NMR spectrum of 52.

An alternative route to produce **39**, containing a sulfonated tyrosine, the sulfonated D-tyrosine was therefore necessary. A solid phase peptide synthesis route to incorporate the pre-sulfonated tyrosine residue was envisaged. Firstly, the Fmoc-protected sulfonated tyrosine **54** was required.

Initial attempts to afford Fmoc-protected sulfonated tyrosine **54** were undertaken by treating the commercially available Fmoc tyrosine derivative **53** with one equivalent of chlorosulfonic acid in TFA (Scheme 14). Analysis of the crude product by ESI-MS indicated the formation of mono- and doubly- sulfonated adducts (*m/z* 484.12 and 564.08 respectively) as well as starting material. Thus, the non-selective electrophilic aromatic substitution had resulted in a mixture of products including, presumably, sulfonation of the Fmoc group to give **55**. The acid labile tBu protecting group was expectedly absent in all products.

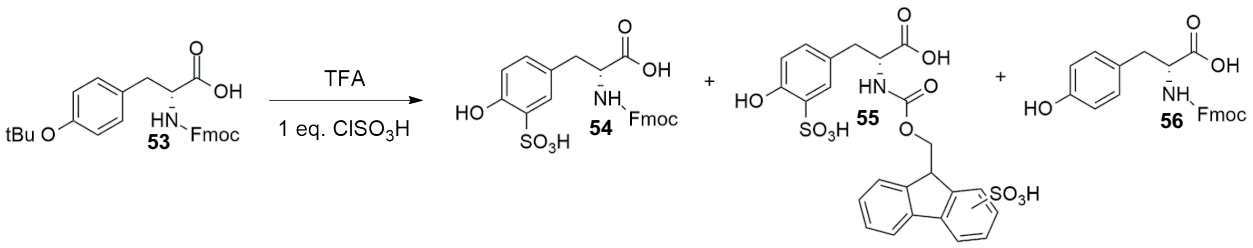

Scheme 14: Sulfonation of Fmoc-D-Tyr(tBu)-OH

As selective sulfonation of the protected tyrosine residue was not successful, sulfonation of free D-tyrosine was performed as described by Previero *et al.* [67] Accordingly, D-tyrosine was treated with chlorosulfonic acid in TFA (Scheme 15). The sulfonated tyrosine **58** was formed as a

white precipitate, which was treated with Fmoc-OSu in the presence of mild base to generate Fmoc-D-Tyr-(SO_3H) **54** in 92% yield over 2 steps. The Fmoc protected sulfonated D-tyrosine **54** in hand, it was next incorporated into a SPPS of the modified FC131-type peptide.

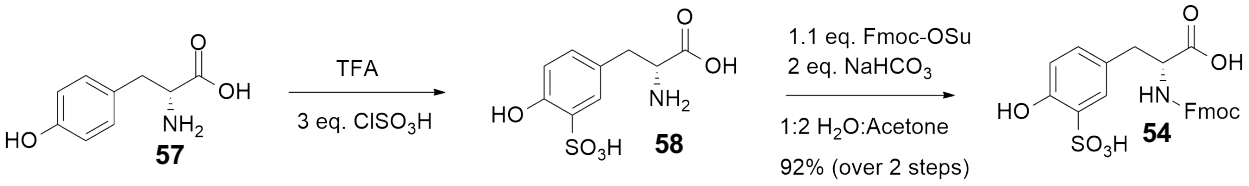

Scheme 15: Sulfonation and Fmoc protection of D-tyrosine.

Standard solid phase peptide synthesis protocols were followed to produce linear protected peptide **59** (Scheme 16). A HATU/DIPEA coupling strategy was utilised for all amino acids with the exception of the sulfonated Fmoc-D-tyrosine **54**, which was coupled with HOBt/DIC as base free conditions were preferable in the presence of a free phenol.[74] After the final Fmoc deprotection, the linear peptide was cleaved from the resin by treatment with 1% TFA in DCM. The linear peptide **60** was then cyclised under dilute conditions (1 mg/ml) with HOBt/DIC and globally deprotected with TFA. The crude cyclic peptide was purified by preparative RP-HPLC to afford the product **39** in 5% overall yield (based on initial resin loading). Confirmation of the cyclic peptide structure was obtained by mass spectrometry (ESI-MS: *m/z* 782.37, corresponding to $[M+H]^+$). The product was also analysed by ^1H NMR spectroscopy: three resonances consistent with a trisubstituted aromatic ring were observed at δ 6.89 (d), 7.20 (dd) and 7.68 (s), consistent with a sulfonated tyrosine side chain.

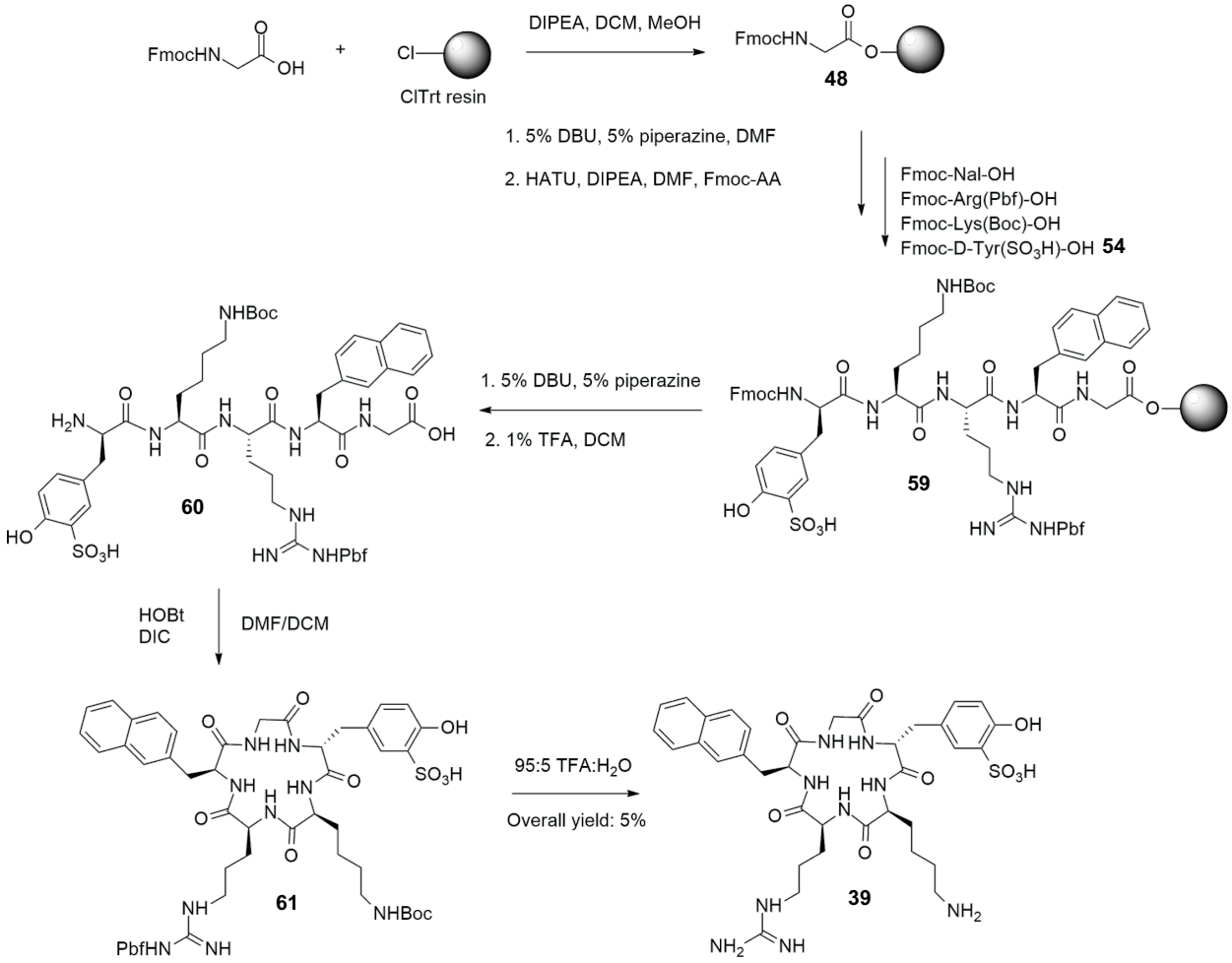

Scheme 16: Synthesis of sulfonated FC131-type peptide.

RP-HPLC analysis of FC131-type sulfonated analogues

The hydrophilic character of FC131-type peptides and their sulfonated analogues was investigated using RP-HPLC retention time as an indicator of hydrophilicity (Figure 18).[75] The early elution time of sulfonated FC131-type peptides **51** and **39** demonstrates that sulfonation significantly increased hydrophilicity. The retention time of doubly sulfonated FC131-type peptide **51** was expectedly less than that of non-sulfonated peptide **38** and mono-sulfonated FC131-type peptide **39** indicative of that peptide **51** was most hydrophilic. Importantly, mono- sulfonated

peptide **39** still had a significantly reduced retention time compared to the non-sulfonated analogue **38**.

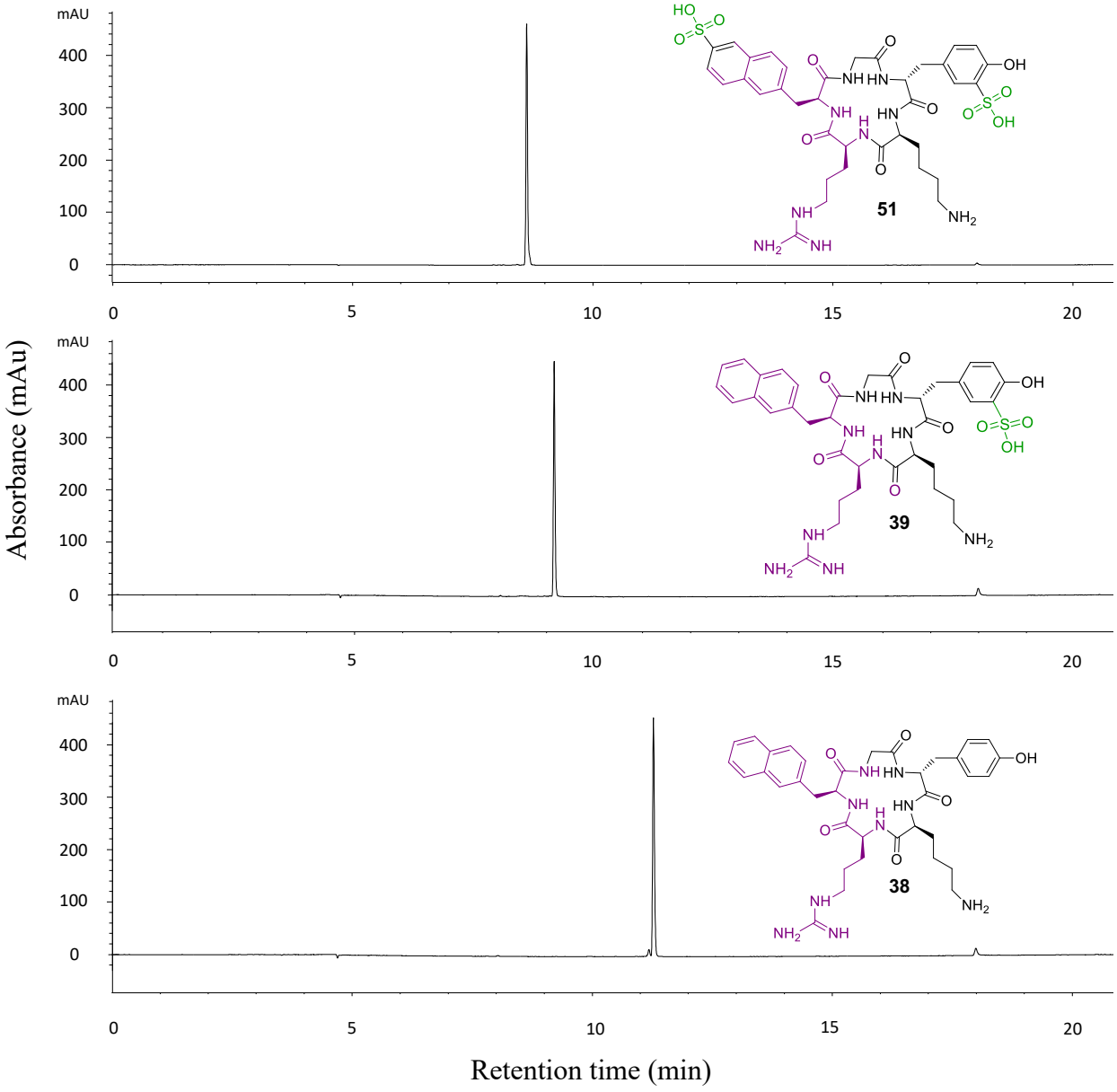

Figure 18: RP-HPLC traces of non-sulfonated and sulfonated FC131-type peptides.

Given the reported requirement of unmodified napthylalanine to maintain high potency to CXCR4, the biodistribution profile of the tyrosine sulfonated FC131-type peptide **39** was of particular interest.[73]

2.2 Radiolabelling and biodistribution of sulfonated FC131-type peptide

The first step towards evaluating the biodistribution profile of **39** was to incorporate a radiolabelled prosthetic group. Fluoropropionate was chosen, and for characterisation purposes the 'cold' ^{19}F-version of the desired radiolabelled peptide was synthesised.[59] Accordingly, fluoropropionic acid **62** was coupled to sulfonated peptide **39** employing base-free DIC/HOBt conditions in order to minimise base-catalysed side products (Scheme 17).[74] The reaction mixture was purified by RP-HPLC to afford a major component as a white powder in 76% yield. The white powder was analysed by ESI-MS and displayed a protonated molecular ion at *m/z* 856.35, corresponding to fluoropropionamide product **63**. The ^{1}H NMR spectrum of peptide **63** closely resembled that of sulfonated peptide **39** but with additional resonances at 5.03 (m, 1H, CH) and 1.55 (m, 3H, CH_3) confirming the formation of **63**. Incorporation of radiolabelled [^{18}F]-fluoropropionate was next investigated.

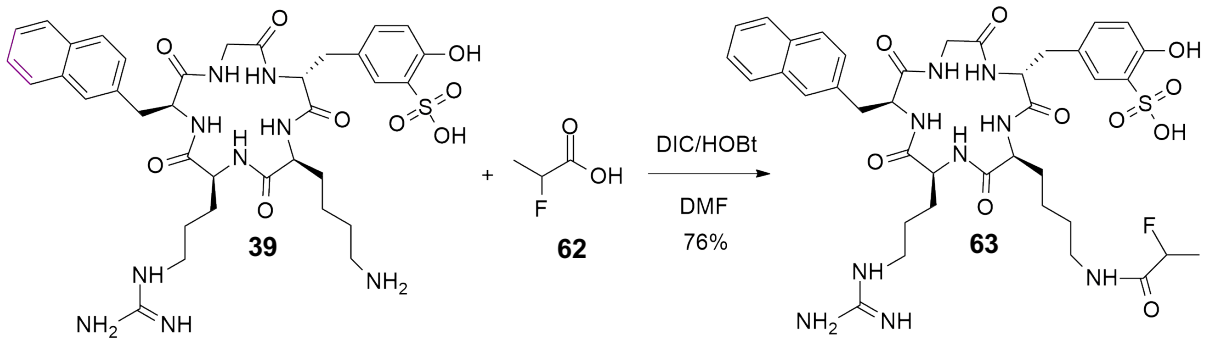

Scheme 17: ^{19}F cold standard synthesis.

Automated radiosynthesis module TRACERlab FXFN

The TRACERlab FXFN is a generic radiosynthesis module that has been utilised in a range of one-pot radiosynthesis procedures, affording great versatility (Figure 19).[76]

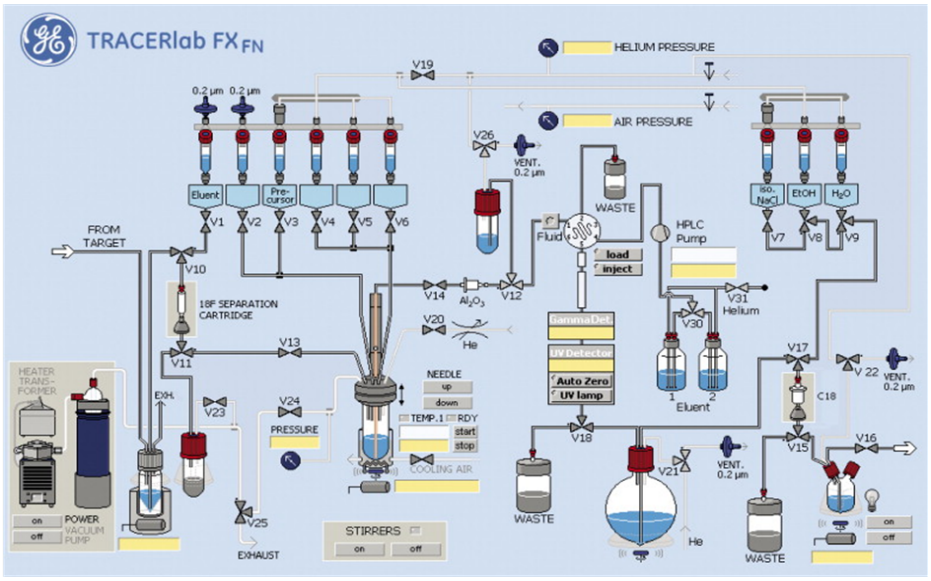

Figure 19: TRACERlab FXFN[76]

This synthesis module enables multiple solid phase extractions, HPLC purification, formulation and multiple reactions which can take place in a single reactor vessel. All fluids and reagents are transferred using vacuum and an inert gas such as nitrogen. Initially $^{18}F^-$ is transferred from a cyclotron into an activity vial and then isolated on an ion-exchange cartridge. The $^{18}F^-$ is typically eluted as the $K_{222}/K^{+18}F^-$ complex and dried in the reactor. Reagents are transferred from a sequence of vials to the reactor to facilitate the reaction and purification. Following HPLC, purified tracers can be isolated on a C18 cartridge or formulated in a sterile solution.[76]

[^{18}F]NFP synthesis and conjugation

The one-pot radiosynthesis of [^{18}F]NFP **23** was carried out as described previously (Scheme 4).[59] 2-bromopropionylbromide **18** was reacted with 4-nitrophenol **27** in the presence of base to afford the ester **28** in 96% yield. Ester **28** was analysed by ^{1}H NMR spectroscopy and two resonances were observed that were consistent with a para-substituted aromatic ring at δ 8.28 (d) and δ 7.31 (d) confirming product identity. To radiolabel brominated ester **28**, [^{18}F]HF was

acquired by cyclotron bombardment of oxygen-18 enriched water and introduced into the automated radiosynthesis module, TRACERlab FXFN (Figure 19). The fluoride was then trapped with a QMA (quaternary methyl ammonium) anion exchange cartridge and eluted with cryptand, kryptofix 2.2.2 and aqueous $KHCO_3$. The cryptand and the fluoride were eluted into a reactor containing the brominated precursor **28**. The reaction mixture was heated at 100°C for 15 min to generate [^{18}F]NFP **23**. The reaction mixture was then eluted though an alumina cartridge (which traps the excess fluoride) and then purified by preparative HPLC, with the radiolabelled ester **23** collected at ~ 20 min in 18% n.d.c yield. (Figure 20).

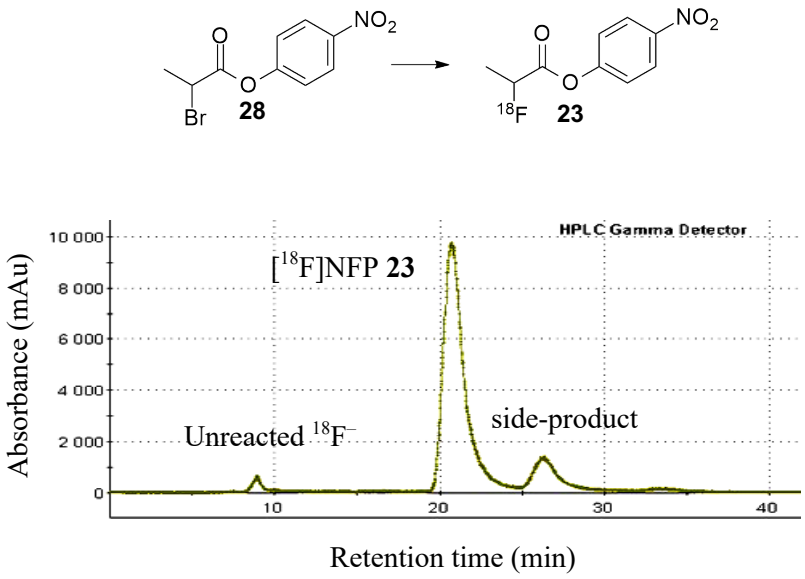

Figure 20: RP-HPLC radiotrace of [^{18}F]NFP.

Radiosynthesis of the ^{18}F-labeled FC131-type peptide **64** was performed by treatment of peptide **39** with labelled active ester **23** (Scheme 18). The reaction mixture was diluted in water and directly purified by RP-HPLC. Coinjection with the previously prepared cold standard **63** showed coincident peaks with a retention time of 21.3 min, indicating that the peptide had been

radiolabelled to afford the ^{18}F-fluorinated peptide **64** (Figure 21). The product was manually collected and trapped on a C18 SPE cartridge in preparation for *in vivo* evaluation.

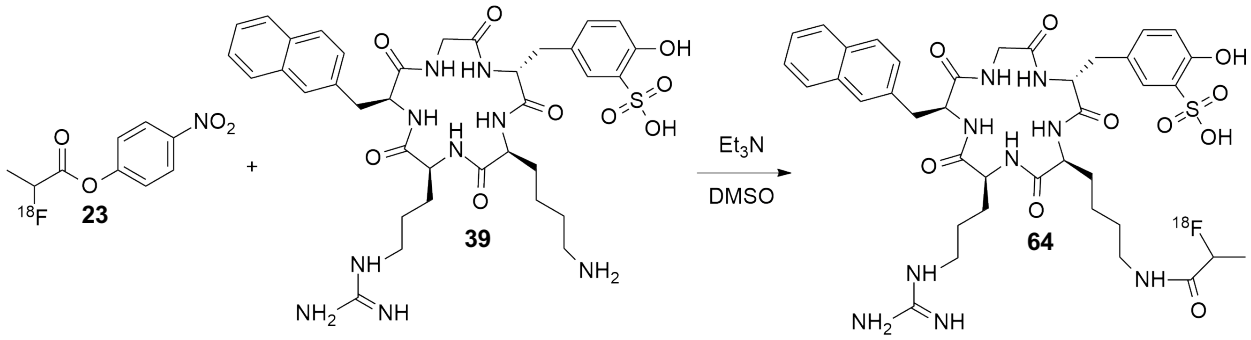

Scheme 18: Synthesis of ^{18}F radiolabelled FC131-type peptide.

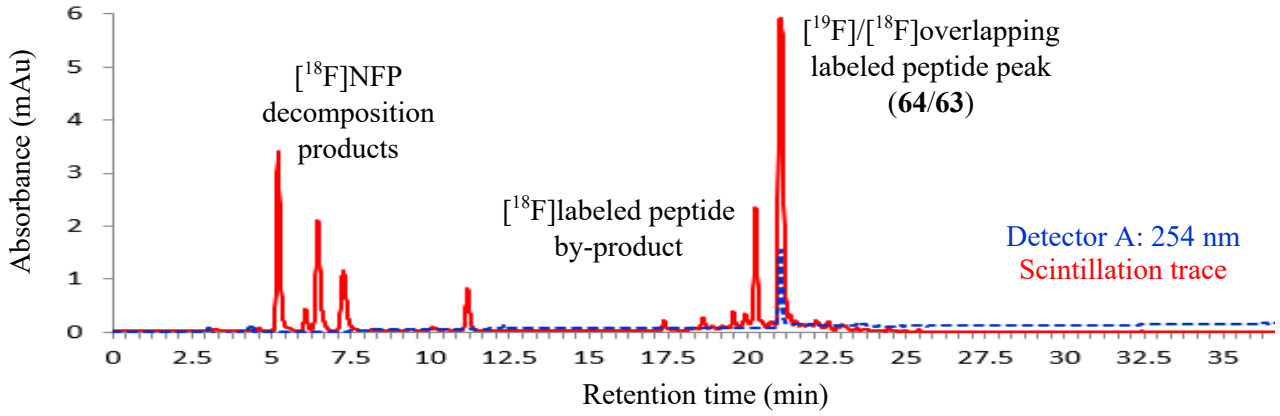

Figure 21: RP-HPLC trace of cold standard **63** *(blue) (UV=254 nm) and radiotrace of reaction mixture containing product* **64** *(red).*

Biological evaluation of [^{18}F]FP sulfonated FC131-type peptide

The *in vivo* properties of [^{18}F]FP labelled sulfonated FC131-type peptide **64** were investigated by small animal PET imaging in mice. Subcutaneous tumours that constitutively express high levels of CXCR4 were employed. Two different cell lines were tested; MV4-11 (a

human acute myeloid leukaemia cell line) and Z138 (a human mantle cell lymphoma cell line). Tail vein injection of ~10 MBq of ^{18}F-radiolabelled peptide **64** was administered to three mice and after 1 h the biodistribution of the tracer was assessed. Figure 22 shows three different PET projections of the biodistribution in a mouse. A CT image of the mouse superimposed on the PET scan is shown on the panel furthest to the left. Biodistribution of **64** was shown to be predominately in the bladder, liver, gut and gall bladder, but no tumour uptake was observed. Regardless, the uptake conveys some valuable information about the metabolism of our agent. Curiously, the uptake in the gut and liver is significant despite evidence of decreased lipophilicity. Furthermore, determination of the logP of this agent is problematic as sulfonates tend to act as surfactants.[77] The complete lack of tumour uptake suggests that modification to the tyrosine residue may not as well tolerated as the literature suggests.[41,73] Additionally, specific activity of **64** was relatively low (0.45 MBq/μg). However, specific activities as low as 0.20 MBq/μg have been reported for CXCR4 SPECT peptide ^{III}In-DTPA-Ac-TZ14011 where tumour visualisation was still possible.[40] The second cell line tested was Z138, a human mantle cell lymphoma. The biodistribution of this cell line mirrored that of the MV4-11 cell line.

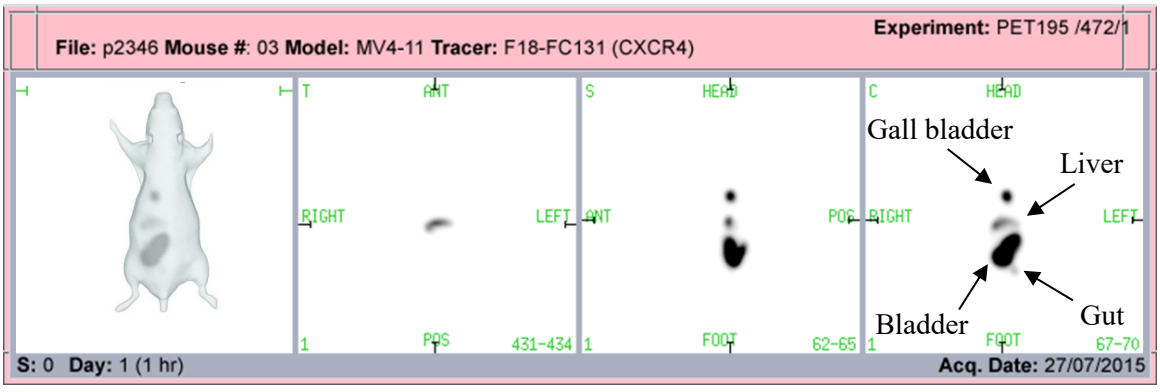

*Figure 22: Micro PET typical biodistribution of sulfonated FC131-type peptide **64** in an MV4-11 cell line.*

2.3 Small library of CXCR4 targeting cyclic pentapeptides

As a result of the poor of biodistribution of ^{18}F-radiolabelled peptide **64**, further investigations of CXCR4 targeting cyclic pentapeptides were essential. As such, we opted to synthesise a small library of cyclic pentapeptide analogues. We proposed to vary our CXCR4 targeting peptide scaffold though: 1) sulfonation of the tyrosine residue, 2) replacement of lysine with N-methylated D-ornithine (as demonstrated in Pentixafor **36**)[78] and 3) installation of various fluorinated prosthetic groups on the side chain amine of N-methylated D-ornithine (Figure 23).

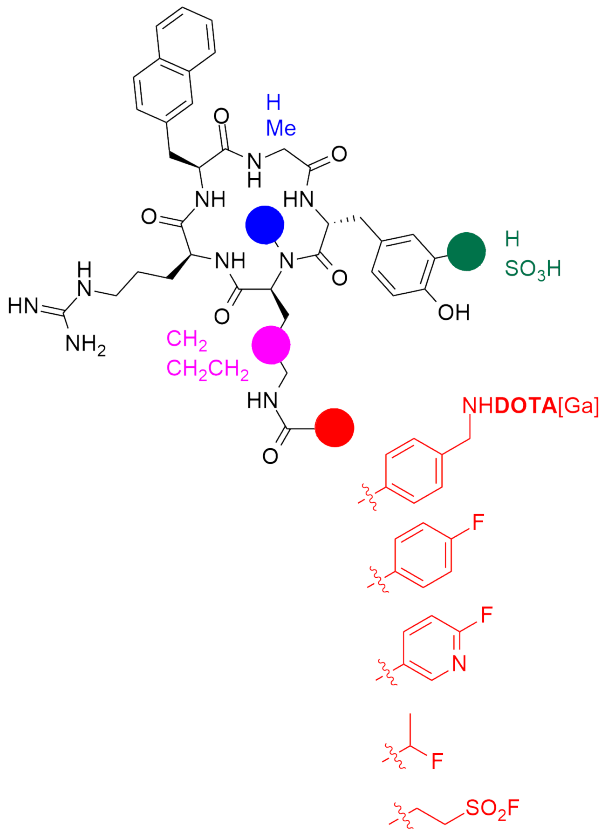

Figure 23: Proposed CXCR4-targeting peptide analogues.

General SPPS pathway for CXCR4-targeting peptide analogues before side chain modification

The synthesis of all proposed analogues began with Fmoc-glycine loaded on chlorotrityl resin **48** which underwent a standard SPPS protocol to afford a tetrapeptide on resin **65** (Scheme 19). An on-resin N-methylation protocol was performed as described by Miller and Scanlan.[79] The free amine of D-ornithine was nosylated with o-NBSCl to afford **66**, which underwent on-resin methylation under Mitsunobu conditions with use of methanol as an alkylation source **67**, and denosylated with thiolate nucleophile to achieve the free N-methylated sequence on resin **68**. Fmoc tyrosine, or its sulfonated equivalent **54,** was then coupled on resin resulting in pentapeptides on resin **69**/**70**. To allow for further modification, the side chain alloc group of D-ornithine was deprotected with $Pd(PPh_3)_4$ to afford **71**/**72** (Scheme 19).

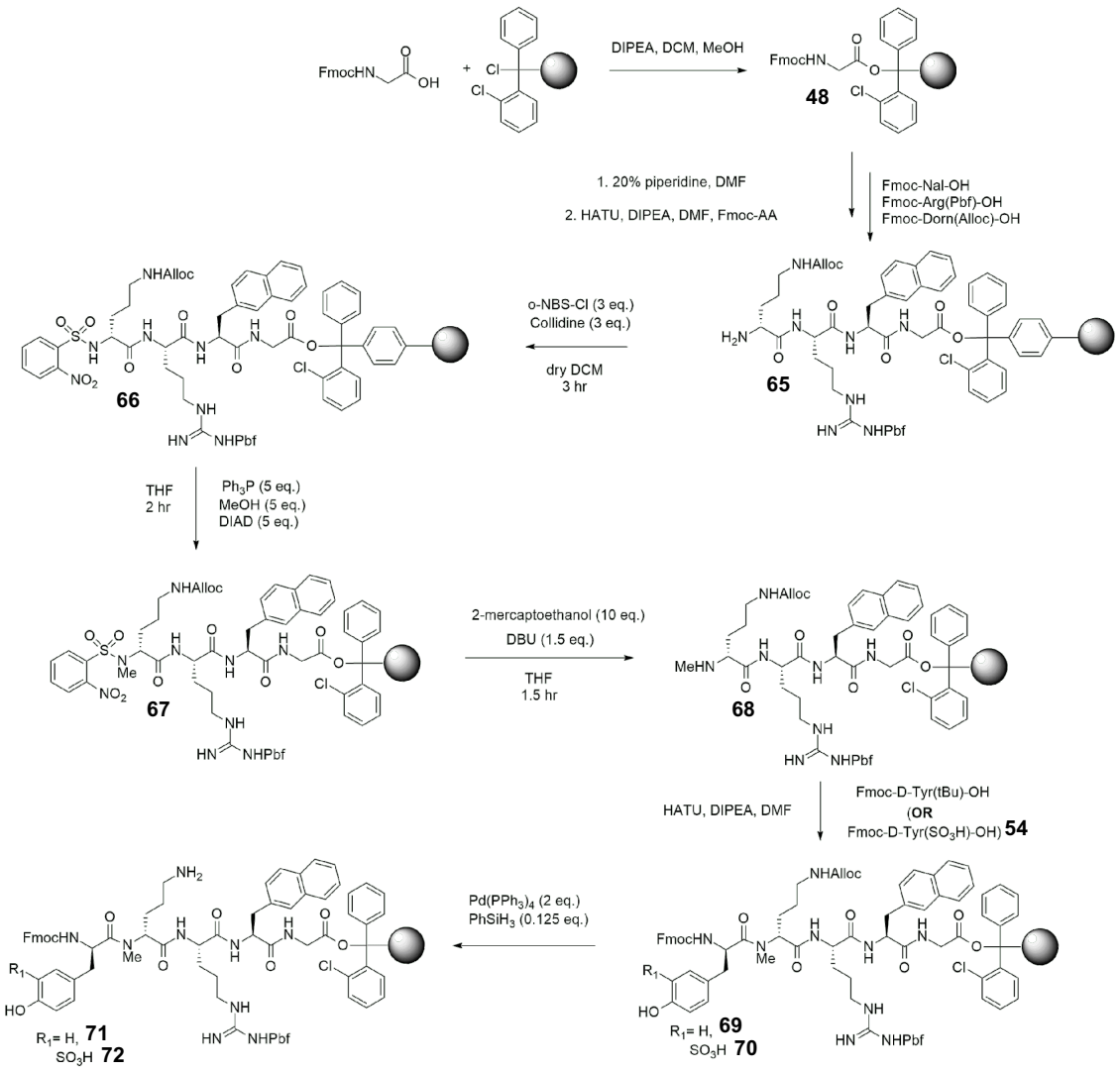

Scheme 19: General SPPS pathway for CXCR4 targeting peptides before side chain modification.

Synthesis of CXCR4 targeting peptide pentixafor and sulfonated analogue

The first analogues that we chose to prepare and evaluate were 'Pentixafor' **80** and its sulfonated equivalent **81**. From peptides **71**/**72**, N-alloc-aminomethylbenzoic **73** was coupled onto the lysine side chain with HATU/DIPEA and then the alloc group deprotected with $Pd(PPh_3)_4$ to afford **74**/**75** (Scheme 20). Coupling of protected DOTA proceeded with HATU/DIPEA, the final N-terminal Fmoc group was removed with 20% piperidine and the peptide was cleaved from resin

with 1% TFA to afford linear peptides **76**/**77**. Linear peptides **76**/**77** were then macrocyclised under dilute conditions, then globally deprotected with 95% TFA to furnish cyclic pentapeptides **78**/**79**. The DOTA containing peptides **78**/**79** were treated with gallium nitrate at pH 3 and then purified by preparative RP-HPLC to afford peptides **80** and **81** in 0.4% and 0.7% overall yield (based on initial resin loading). The cyclic peptide structure was confirmed by mass spectrometry (ESI-MS: *m/z* 1287.507/644.257/429.840 and 1366.457/684.235/456.492 corresponding to $[M+H^+]/[M+2H]^+/[M+3H]^{3+}$ for non-sulfonated **80** and sulfonated peptide **81**, respectively.)

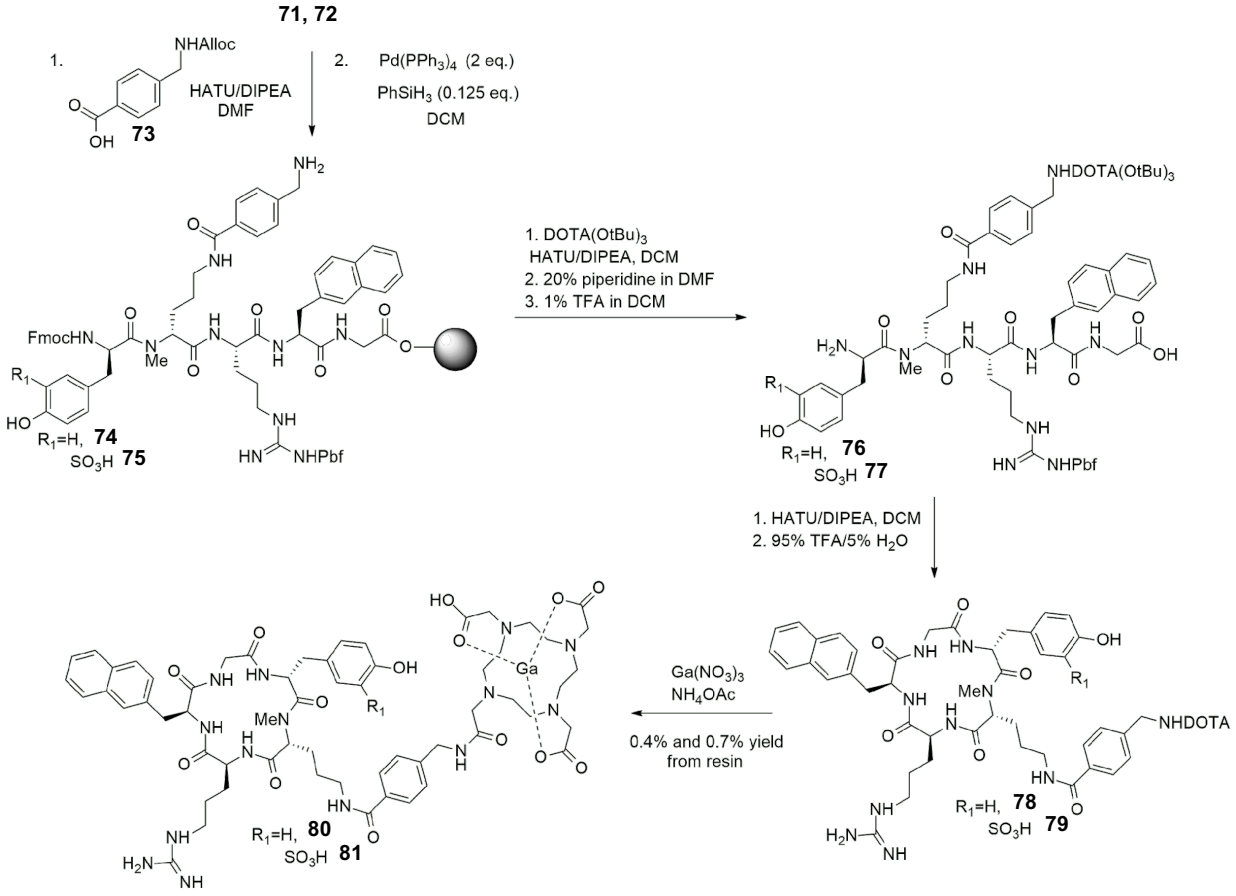

Scheme 20: Synthesis of pentixafor and sulfonated pentixafor.

Synthesis of CXCR4-targeting peptide cyclo(D-Tyr(SO_3H)-N(Me)-D-Orn(FB)-Arg-Nal-Gly)

Fluorobenzoylated peptide **88** has been shown to have excellent CXCR4 binding affinity (IC_{50}= 9 ± 1 nM).[66] As such, we were interested in evaluating the effect of sulfonation of the tyrosine residue on its binding affinity and biodistribution. From peptides **71**/**72**, fluorobenzoic acid was coupled with HATU/DIPEA to afford **82**/**83** on resin (Scheme 21). The N-terminal Fmoc group was removed with 20% piperidine and then the peptide was cleaved from resin with 1% TFA to afford linear peptides **84**/**85**. Linear peptides **84**/**85** were macrocyclised under dilute conditions to achieve protected cyclic peptides **86**/**87**. Global deprotection was achieved by treatment with 95% TFA and then the peptides were purified by preparative RP-HPLC to afford products in **88** and **89** in 2.0% and 3.0% overall yield, respectively (based on initial resin loading). The cyclic peptide structures were confirmed by mass spectrometry (ESI-MS: *m/z* 825.384/413.195 and 905.341/453.174 corresponding to $[M+H^+]/[M+2H]^+$ for non-sulfonated **88** and sulfonated peptide **89**, respectively).

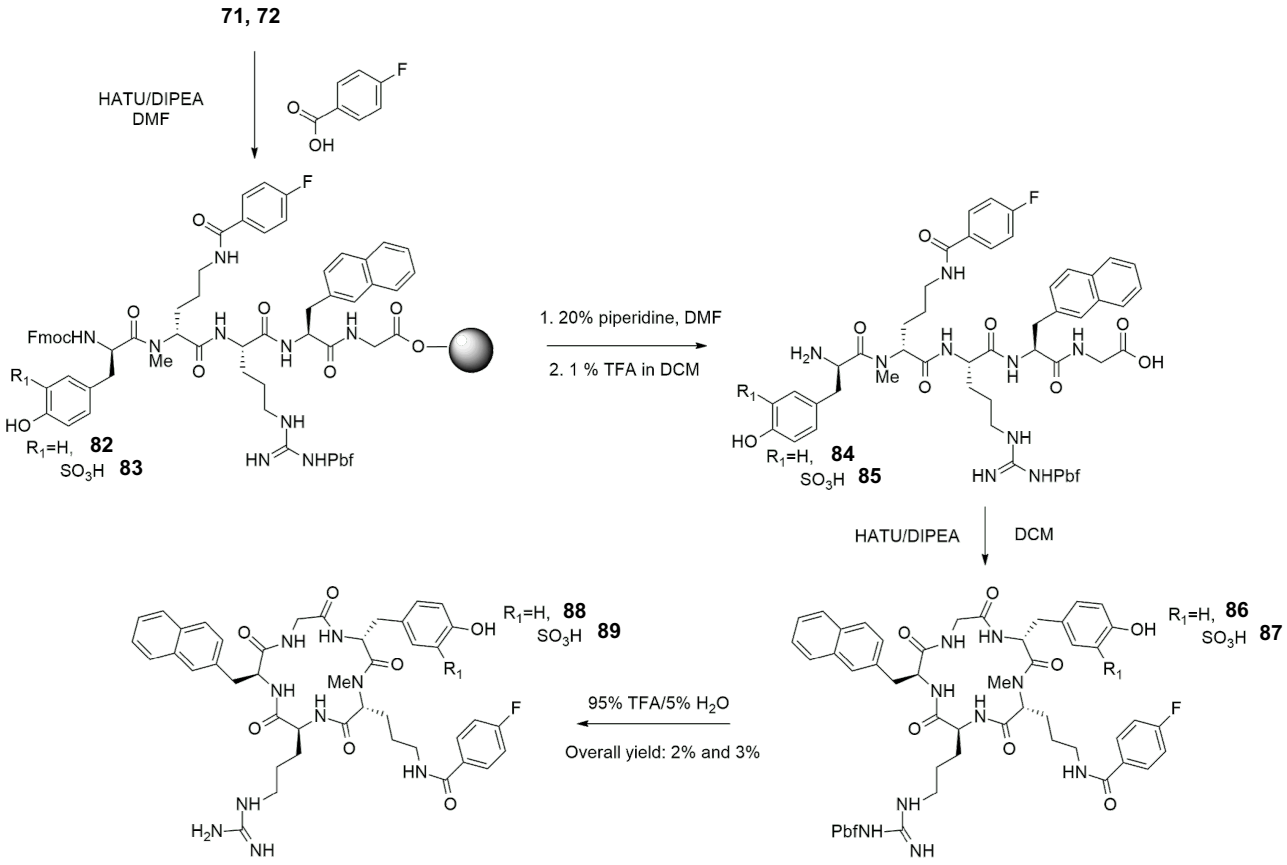

Scheme 21: Synthesis of CXCR4 targeting peptide containing fluorobenzamide.

Synthesis of CXCR4-targeting peptide cyclo(D-Tyr(SO_3H)-N(Me)-D-Orn(FPy)-Arg-Nal-Gly)

Given the successful synthesis of **88**/**89** we next investigated the synthesis of the structurally similar compound cyclo(D-Tyr(SO_3H)-N(Me)-D-Orn(FPy)-Arg-Nal-Gly) **96** and its sulfonated equivalent **97**, which contain a fluoronicotinate prosthetic group. Fluoronicotinic acid was coupled to **71**/**72** with HATU/DIPEA to afford **90**/**91** on resin (Scheme 22). The N-terminal Fmoc group was removed with 20% piperidine and then the peptide was cleaved from resin with 1% TFA to afford linear peptides **92**/**93**. Linear peptides **92**/**93** were macrocyclised under dilute conditions (1 mg/ml) to furnish protected cyclic peptides **94**/**95**. Global deprotection was achieved

with 95% TFA and the peptides were purified by preparative RP-HPLC by preparative RP-HPLC to afford products in **96** and **97** in 2.0% and 2.0% overall yield, respectively (based on initial resin loading). The cyclic peptide structures were confirmed by mass spectrometry (ESI-MS: *m/z* 825.384/413.195 and 905.341/453.174 corresponding to $[M+H^+]/[M+2H]^+$ for non-sulfonated **96** and sulfonated peptide **97**, respectively).

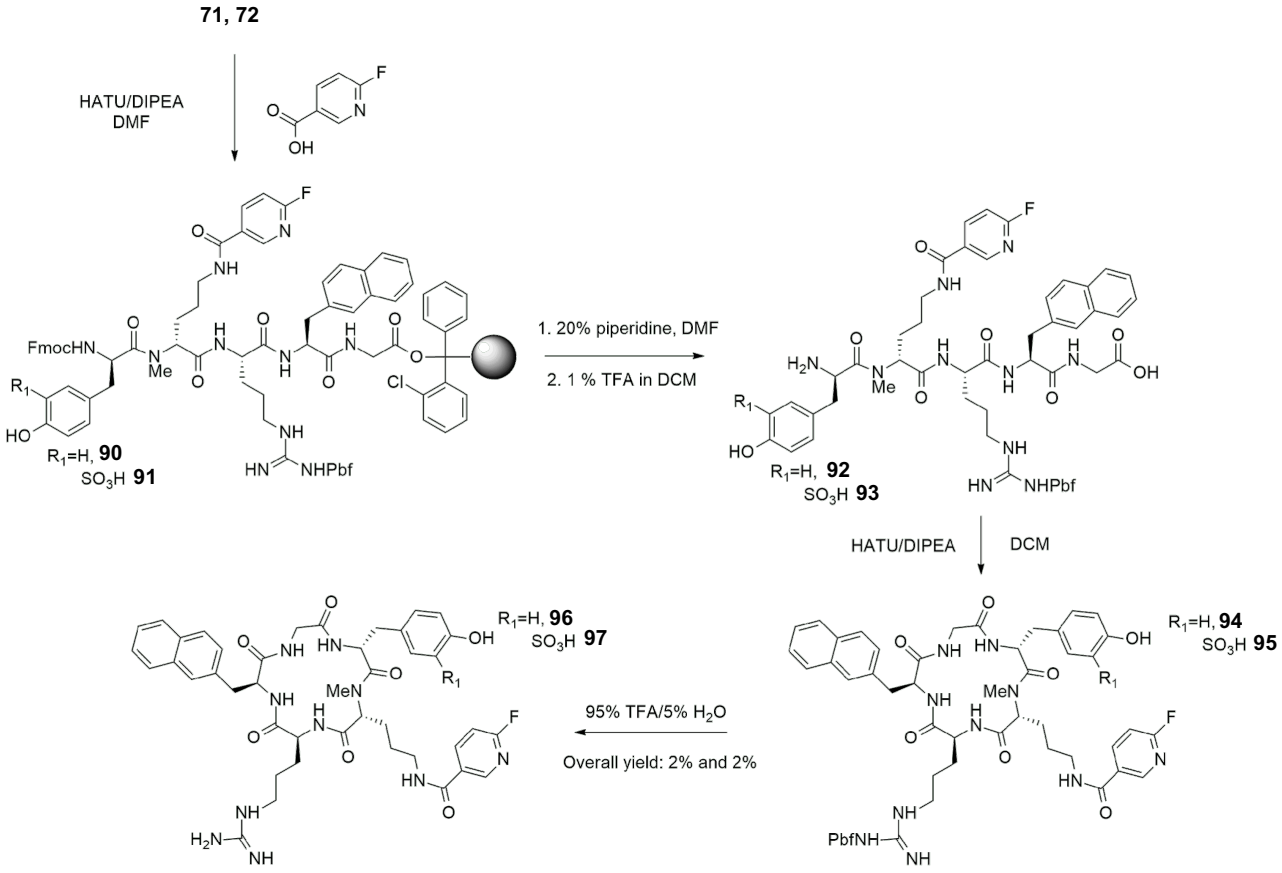

Scheme 22: Synthesis of CXCR4 targeting peptide containing fluoronicotinamide.

Synthesis of CXCR4-targeting peptide cyclo(D-Tyr(SO_3H)-N(Me)-D-Orn(ESF)-Arg-Nal-Gly)

While the fluorobenzoylated analogue **104** is structurally dissimilar to previous analogues synthesized (**88**/**89** and **96**/**97**), we believed that this analogue could have superior biodistribution

as sulfonyl fluorides are highly polar and hydrophilic. In addition, ethane sulfonyl fluoride is a minimalist prosthetic group that is reportedly stable *in vivo*. We were also interested in evaluating the effect of sulfonation of the tyrosine residue on its binding affinity and biodistribution. Ethene sulfonyl fluoride is a strong Michael acceptor so was easily coupled to the 'soft' nucleophilic group on the D-ornithine of **71**/**72** in DMF to afford **98**/**99** on resin (Scheme 23).[80] The N-terminal Fmoc group was removed with 20% piperidine and the peptide was cleaved from resin with 1% TFA to afford linear peptides **100**/**101**. Linear peptides **100**/**101** were macrocyclised under dilute conditions to furnish protected cyclic peptides **102**/**103**, which were globally deprotected with 95% TFA and purified by preparative RP-HPLC to afford products **104** and **105** in 0.5% and 1.0% overall yield, respectively (based on initial resin loading). The cyclic peptide structure was confirmed by mass spectrometry (ESI-MS: *m/z* 825.384/413.195 and 905.341/453.174 corresponding to $[M+H^+]/[M+2H]^+$ for non-sulfonated **104** and sulfonated peptide **105** respectively).

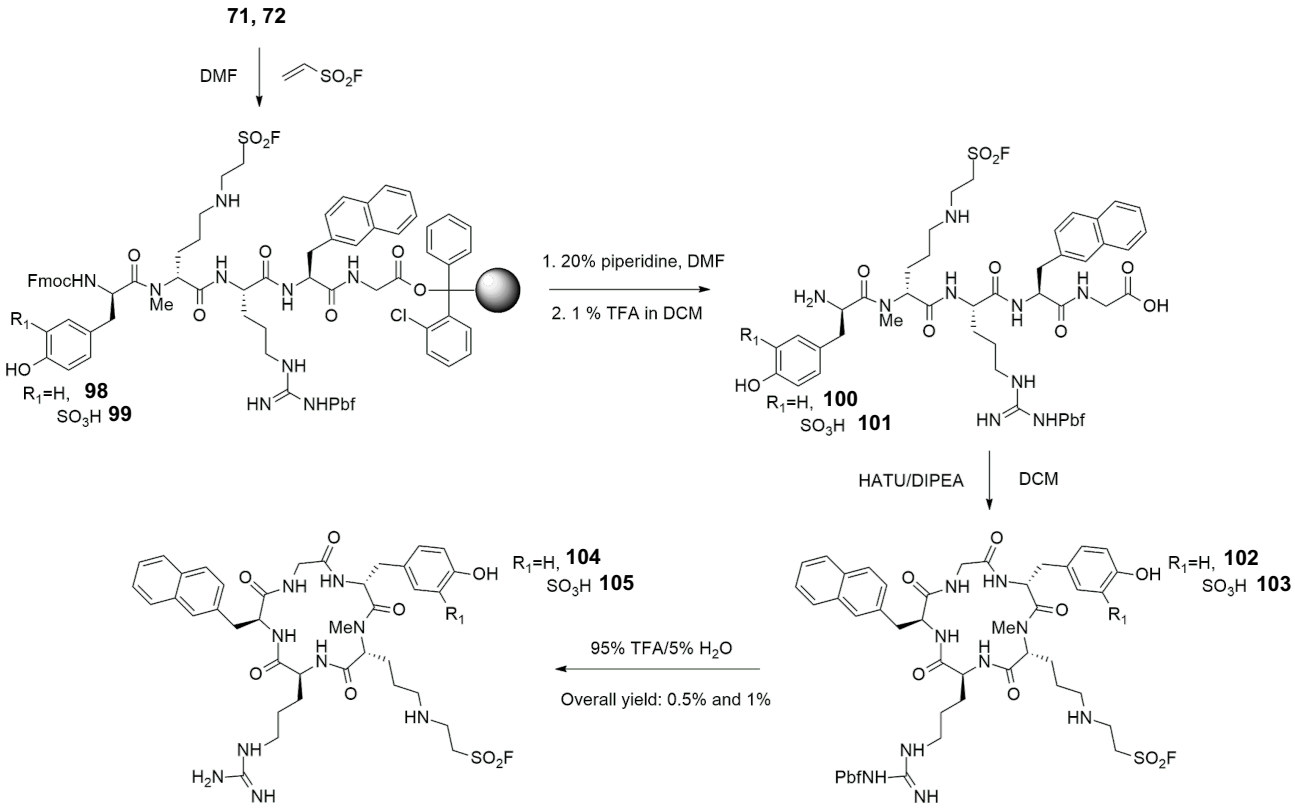

Scheme 23: Synthesis of CXCR4 targeting peptide containing ethane sulfonyl fluoride.

Alternative synthetic strategy

Through SPPS routes outlined in Schemes 20–23, peptides containing various fluorinated prosthetic groups, with/without sulfonation of the tyrosine residue, were successfully prepared. However, in all cases overall yields were low (~ 1%). Accordingly, we sought to investigate alternative routes that would furnish these peptides in increased yields. In a bid to improve the yields and number of synthetic steps to our analogues, a divergent strategy was proposed in which cyclic peptides **106**/**107** would be generated as common, late stage intermediates, with subsequent coupling of various prosthetic groups generating the library of peptides: **80**/**81**, **88**/**89**, **96**/**97** and **104**/**105**. Cyclic pentapeptides **106**/**107** which would be available from linear protected peptides **108**/**109**, assembled from a solid phase synthesis protocol. As side chain modification will instead

be performed in solution instead of on resin, orthogonal protection on resin is no longer required. Instead, side chain protection of D-ornithine with N-Boc was chosen over N-Alloc as it can easily be removed under acidic conditions (Scheme 24).

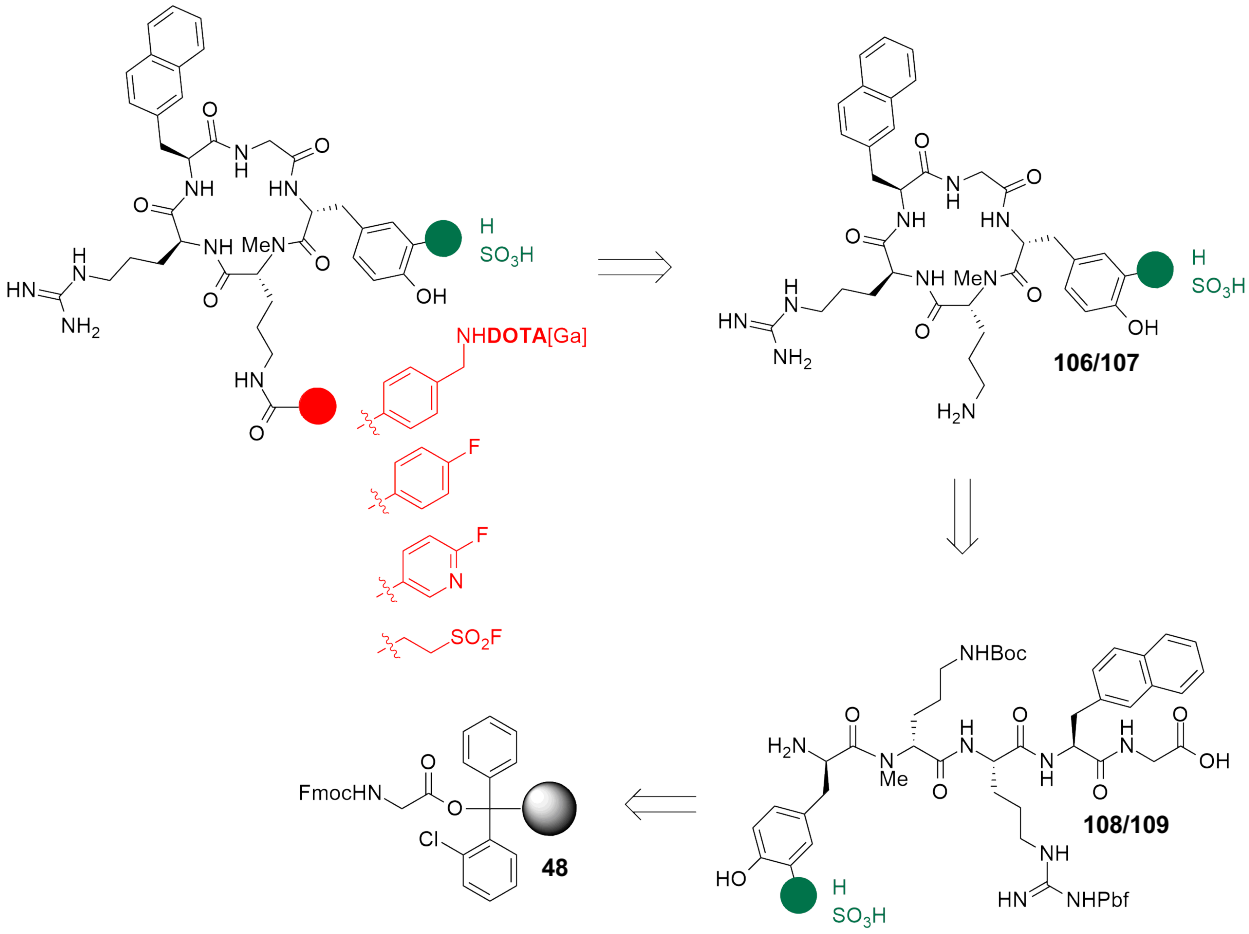

Scheme 24: Proposed retrosynthesis of CXCR4 targeting peptides.

Synthesis of CXCR4-targeting peptides prior to solution phase side chain modification

The synthesis of cyclic peptides **106** and **107** began with Fmoc-glycine loaded on chlorotrityl resin **48**, which was reacted under standard SPPS protocols to afford the tetrapeptide on resin **110** (Scheme 25). An on-resin N-methylation protocol was performed as described

previously.[76] The free amine of D-ornithine was nosylated with o-NBSCl to afford **111**, treated under Mitsunobu reaction conditions in the presence of methanol to generate N-methylated peptide **112** as before, then denosylated with 2-mercaptoethanol to achieve the free N-methylated sequence on resin **113**. Fmoc-tyrosine or its sulfonated equivalent **54** was coupled on resin resulting in pentapeptides **114**/**115**. The N-terminal Fmoc group was removed with 20% piperidine and the peptide was cleaved from resin with 1% TFA to form linear peptides **108**/**109**. The linear peptides **108**/**109** were macrocyclised under dilute conditions to form **116**/**117**. Global deprotection was achieved with 95% TFA, then the peptides were purified by preparative RP-HPLC to afford the non-sulfonated **106** and sulfonated analogue **107** in 8.0% and 10%, respectively (based on initial resin loading). The cyclic peptide structures were confirmed by mass spectrometry (ESI-MS: *m/z* 702.372/351.689 and 782.329/391.668 corresponding to $[M+H^+]/[M+2H]^+$ for non-sulfonated **106** and sulfonated peptide **107** respectively).

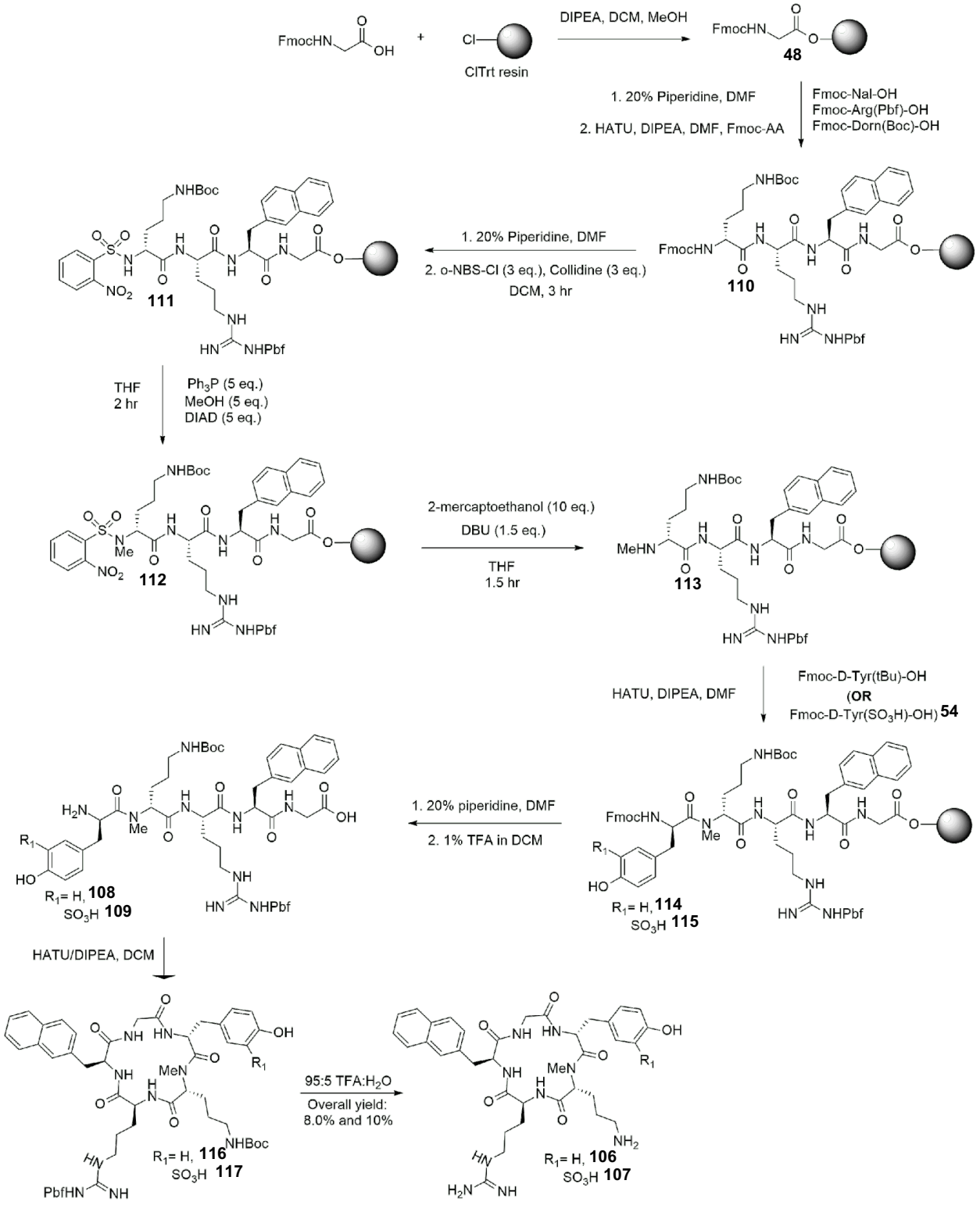

Scheme 25: Synthesis of cyclo(DTyr[1]-NMe-DOrn[2]-Arg[3]-Nal[4]-Gly[5]) and sulfonated analogue.

With peptides **106**/**107** in hand, a new synthetic strategy toward **80**/**81**, **88**/**89**, **96**/**97** and **104**/**105** could be investigated (Scheme 26). Coupling of ethene sulfonyl fluoride to **106**/**107** afforded **104**/**105** analogues in in 4.0% and 3.0% overall yields (based on initial resin loading). Similarly, coupling fluorobenzoic acid or fluoronicotinic acid to peptides **106**/**107** with HATU/DIPEA resulted in 8.0% and 7.0% overall yields (based on initial resin loading) of **88** and **89**, respectively and 7.0% and 10% overall yields (based on initial resin loading) of **96** and **97**, respectively. To obtain DOTA peptides **80/81**, N-Boc aminomethylbenzoic acid **118** was coupled to peptide precursors **106**/**107** with HATU/DIPEA to afford **119**/**120**. The Boc group was removed with 30% TFA then peptide was treated with DOTA NHS ester to obtain **78** and **79** in 8.0% and 10% overall yield (based on initial resin loading), respectively. Chelation to gallium proceeded in identical fashion to that described previously to afford peptides **80**/**81** in an overall yield of 6.0% and 8.0% yields (based on initial resin loading). The divergent approach showed significant improvement of yields over the previous linear synthetic routes (Table 3). Analytical data of all peptides matched the previous method.

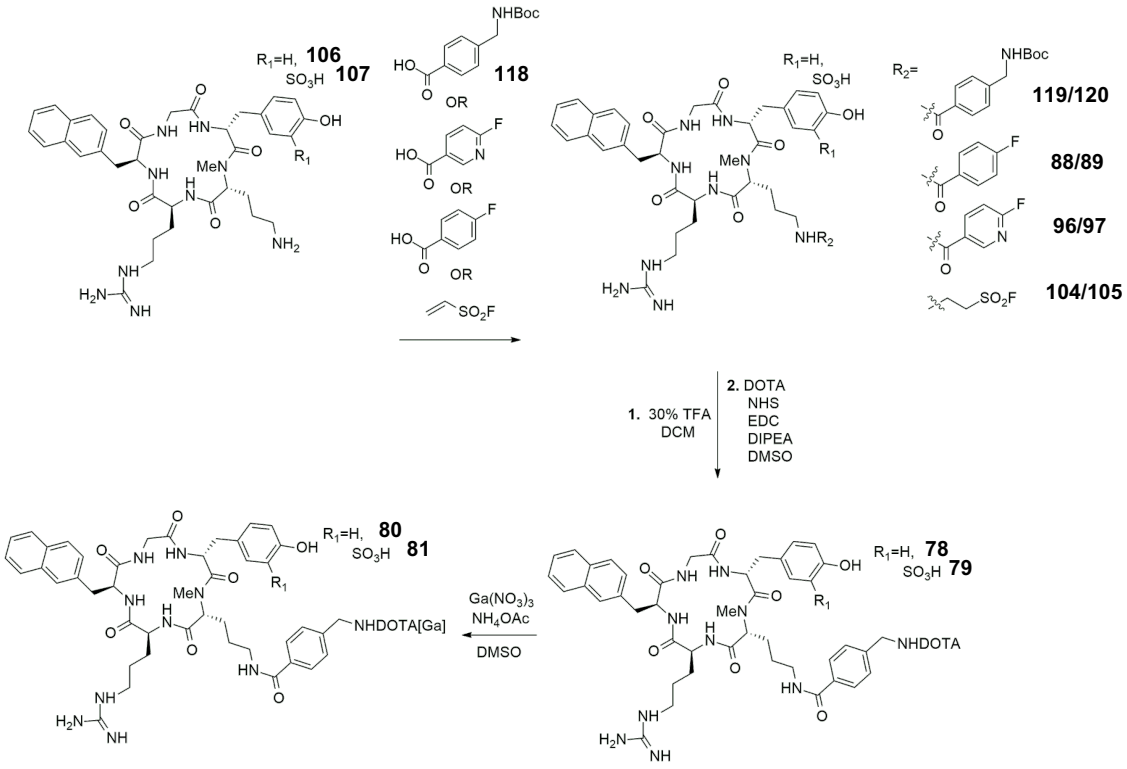

Scheme 26: Alternative synthesis of CXCR4 targeting peptides.

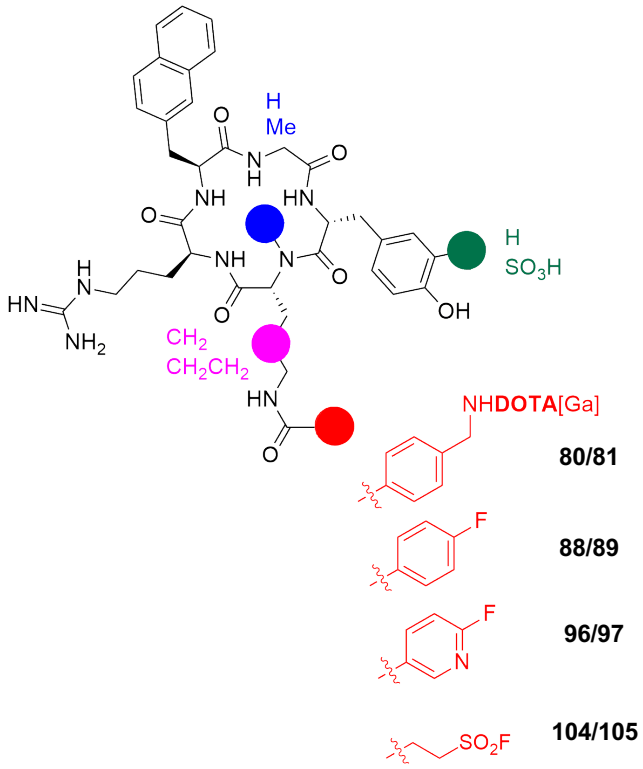

Peptides	Previous strategy (% overall yield)	Divergent strategy (% overall yield)
80/81	0.5% / 1.0%	6.0% / 8.0%
88/89	2.0% / 3.0%	8.0% / 7.0%
96/97	2.0% / 2.0%	7.0% / 10%
104/105	0.4% /0.7%	4.0% / 3.0%

Table 3: Comparison of overall yields.

2.4 Competitive binding assays on CXCR4- targeting peptide analogues

Competitive binding assays were performed at Cancer Research Laboratories/Victoria Research Laboratories London Regional Cancer Centre London, Ontario. CXCR4 affinities were determined through competitive binding assays using U87.CD4.CXCR4 cells with [^{125}I]-SDF-1 as the radioligand. T140 **9** and FC131 **10** were used as a reference to ensure validity of results. A suspension of U87.CD4.CXCR4 was added to each Eppendorf tube, which were subsequently incubated. The tubes were centrifuged and the supernatant removed, and the amount of [^{125}I]-SDF-1 bound to the cells was measured using a gamma counter. A lower reading corresponded to CXCR4-targeting peptide preferentially binding to the cells. Initial IC_{50}s obtained under normal assay conditions (i.e. with use of Eppendorf tubes for incubation, followed by centrifugation) showed little or no binding of any peptide including for FC131 **10**. A "high throughput" approach was then investigated at 10^{-5} M (a higher concentration than normal for a typical assay) and 10^{-8} M of peptide. As total bindings exceeded 100% in many cases, there was clearly a flaw in the assay (Table 4). While this data should be interpreted cautiously, it is interesting to note that the sulfonated version **97** seems to produce better results at 10^{-5} M than the non-sulfonated version **96**. Some analogues are not shown due to limited peptide quantity or peptide consumption while troubleshooting (Table 4).

Peptide	Amino acid sequence or modification				% total binding of ^{125}I SDF-1	
					10^{-5} M	10^{-8} M
T140, **9**	14 amino acid peptide				42%	82%
FC131, **10**	cyclo[Nal^1-Gly^2-D-Tyr^3-Arg^4-Arg^5]				69%	89%
81	SO_3H	Me	CH_2	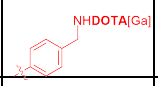	102%	107%
79	SO_3H	Me	CH_2	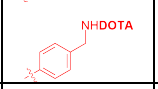	87%	109%
88	H	Me	CH_2	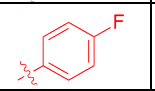	113%	184%
89	SO_3H	Me	CH_2	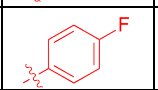	-	-
96	H	Me	CH_2	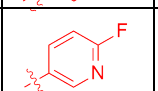	108%	109%
97	SO_3H	Me	CH_2	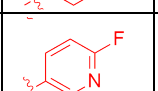	72%	108%

Table 4: Comparison of binding affinities of CXCR4 targeting peptide analogues at 10^{-5} M and 10^{-8} M concentrations.

Further investigations of these results suggested that normal assay conditions are not suitable for FC131 analogues, and that this may account for the higher than expected readings.[81] It was hypothesised that for small cyclic pentapeptides, % total binding values greater than 100% could be attributed to [^{125}I]-SDF-1 binding to the sides of the Eppendorf tubes. A new method was developed using 96 well filter plates to combat the issue of [^{125}I]-SDF-1 binding to the vials. Preliminary binding assay results for FC131 **10** using this new method are more reasonable, and an IC_{50} of 20 nM was obtained – comparable to Fujii's value of 4 nM (Figure 24).[40] Efforts are now underway to further optimise this binding assay in order to re-analyse our peptides **80**/**81**, **88**/**89**, **96**/**97** and **104**/**105**.

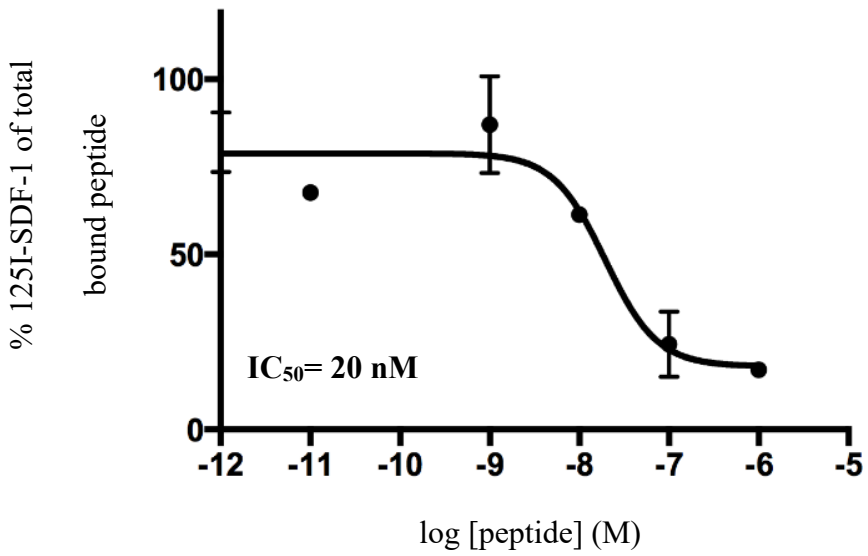

Figure 24: IC_{50} plot of FC131 with 96 well plate method.

CHAPTER 3: DIRECT ^{18}F-FLUORINATION OF NITROPHENYL ESTER PROSTHETIC GROUPS AND RADIOLABELLING OF CXCR4 TARGETING-PEPTIDES

3.1 Synthesis of [^{18}F]-fluoronicotinic esters

Recent work in the Hutton group has demonstrated an innovative approach to preparing 4-nitrophenyl-2-[^{18}F]fluoropropionate **23** in a single step.[68] Another useful preactivated acylation agent is 2,3,5,6-tetrafluorophenyl-6-[^{18}F]fluoronicotinate **33** (Scheme 27). Pyridine-based acylating agents such as **32** are particularly favourable as the electron deficient ring enables facile ^{18}F-fluorination under mild conditions.[61] Despite the similarities between **23** and **33**, a direct comparison of the two in terms of their stability under harsh radiofluorination conditions and their acylation rates has not yet been investigated.

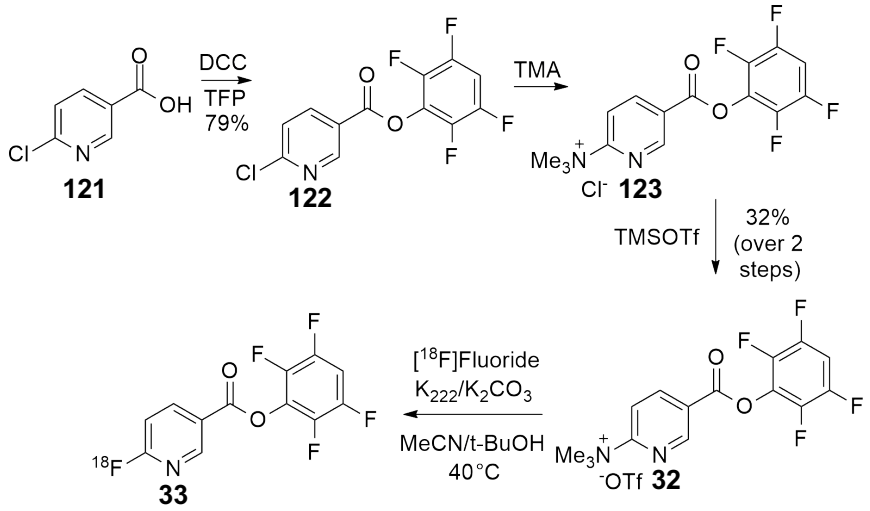

Scheme 27: Olberg et al. method of synthesis of [^{18}F]TFP active ester.

We began our investigations by synthesising 2,3,5,6-tetrafluorophenyl-6-[^{18}F]fluoronicotinate **33**. 6-Bromonicotinic acid **124** was treated with 2,3,5,6-tetrafluorophenol in the presence of EDC to form ester **125** in 75% yield (Scheme 28). The bromo substituent in **125** is

highly activated towards nucleophilic aromatic substitution.[82] Such activation allowed for the synthesis of the 2-trimethylammonium bromide salt upon treatment with trimethylamine (TMA) in THF to afford **126** in 72% yield. Olberg *et al.* found that the chloride salt **123** had poor solubility in acetonitrile required for radiofluorination, so the counterion was exchanged with methyl triflate.[61] However, we found the bromide salt **126** was sufficiently soluble in tAmOH:DMSO (2:3) solvent mixture required for radiofluorination and thus anion substitution was not necessary.

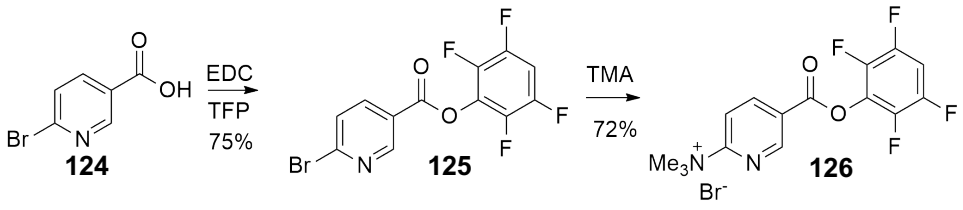

Scheme 28: Synthesis of bromide salt.

As the preparation of most ^{18}F-labelled tracers requires more than one radiochemical reaction or HPLC purification, the use of an improved automated system, the dual reactor iPHASE FlexLAB has been recently developed.[59] The iPHASE FlexLAB is a new automated radiosynthesis module that contains two reactor vessels and two HPLC modules (Figure 25). In the preparation of radiolabelled peptides, the labelling prosthetic group can be synthesised in the first reactor in a similar fashion to the TRACERlab FXFN module. After isolation of the radiolabelled prosthetic group by HPLC purification, it can be conjugation to the peptide in the second reactor vessel.[59]

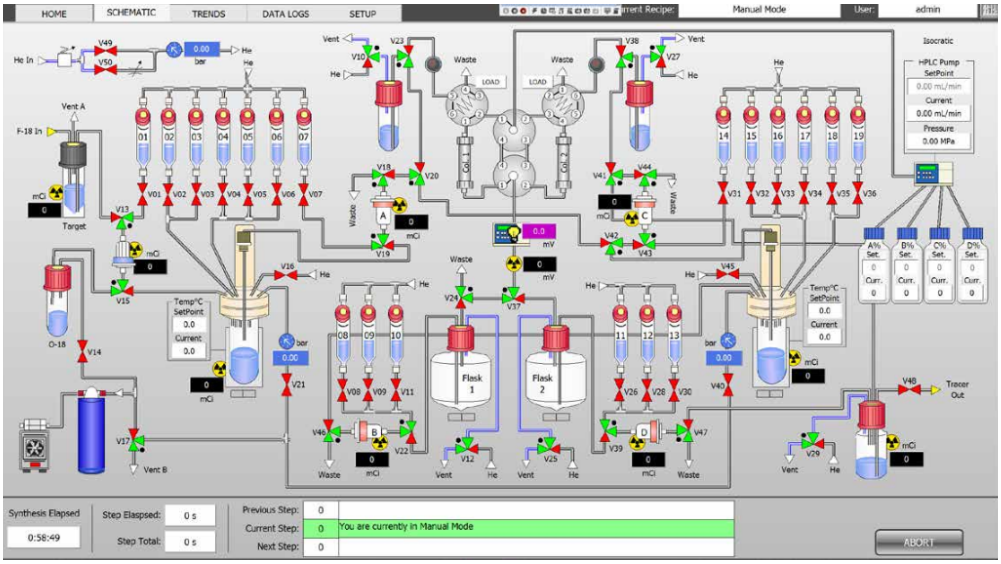

Figure 25: iPHASE FlexLAB module.[59]

Accordingly, the iPHASE Flexlab module was utilised to label **126**. ^{18}F-fluoride was isolated on a Waters QMA anion exchange cartridge and eluted with a mixture of Kryptofix and $KHCO_3$ followed by azeotropic drying to afford the reactive $K_{222}.K^{+18}F^-$ complex in the reactor vial. Ester **126** in DMSO:tAmOH (2:3) was dispensed into the reactor vial and the mixture was heated to 100°C for 5 min. The reaction mixture remained colourless although a white precipitate was observed. The mixture was diluted with 0.1% TFA in 60:40 H_2O:MeCN and the diluted reaction mixture was purified by RP-HPLC, to furnish [^{18}F]-fluoronicotinic ester **33** in variable yield (33–75% n=3, non-decay corrected). Reproducibility of this radiofluorination was particularly problematic. QC analysis of the isolated product showed several decomposition products indicating the instability of the product **33** (Scheme 29).

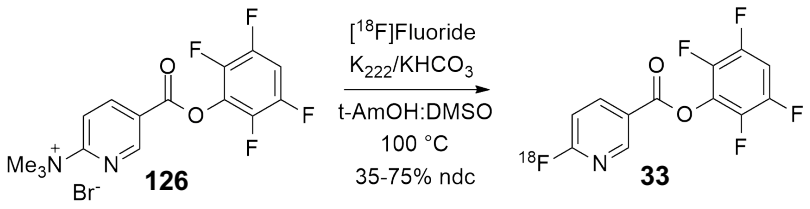

Scheme 29: The synthesis of TFP [^{18}F]-fluoronicotinic ester.

For synthesis of the 4-nitrophenyl ester equivalent of **33**, a similar synthetic strategy was investigated. 6-Bromonicotinic acid **124** and 4-nitrophenol **27** were added in the presence of EDC to afford ester **127** in 80% yield. Treatment of the bromo ester **127** with excess TMA furnished the trimethylammonium bromide salt **128** as a precipitate, which was isolated in 70% yield (Scheme 30).

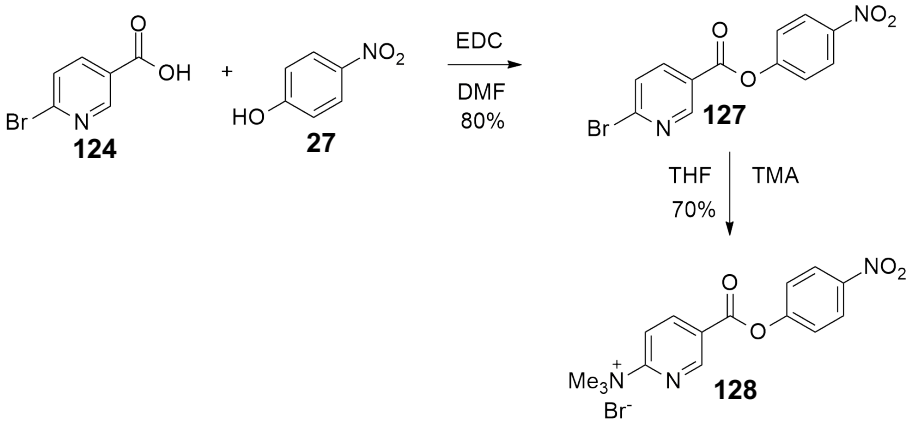

Scheme 30: Synthesis of trimethyl ammonium nicotinic 4-nitrophenyl ester.

To radiolabel **128**, the ester was treated with $K_{222}.K^{+18}F^-$ in a similar manner to the procedure employed for conversion of **126** to **33**. The reaction mixture was purified by preparative RP-HPLC to generate [^{18}F]-fluoronicotinic ester **129** in 95% yield (n=3, 58% isolated yield decay corrected to SOS) and >99% purity (Scheme 31). The radiolabelling of **128** was far more effective and reproducible than its TFP equivalent **126**.

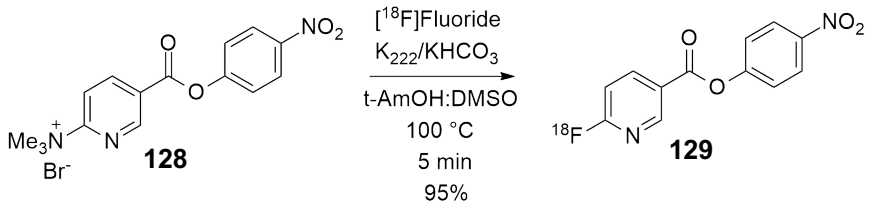

Scheme 31: Radiolabelling of fluoronicotinic 4-nitrophenyl ester.

3.2 Synthesis of [^{18}F]-fluorobenzoates

Typically, a multistep synthesis is required to produce [^{18}F]-fluorobenzamides.[57] For example, the synthesis of [^{18}F]SFB **16** (Scheme 1) involves an initial radiolabelling step followed by saponification of the ethyl ester and activation of the carboxylic acid.[57] The advantage of [^{18}F]NFP **23** and [^{18}F]F-Py-TFP **33** is that pre-activated ester is radiolabelled in a single step.[61,68] We decided to investigate the synthesis and radiolabelling of benzoate ester **130**, which incorporates both a TMA leaving group and an activated PNP ester (Figure 26).

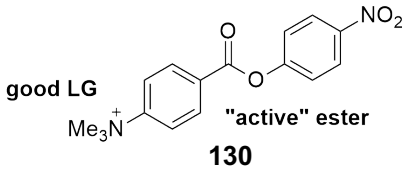

Figure 26: Proposed design of precursor

To begin the synthesis of **130**, dimethyl amino benzoic acid **131** and 4-nitrophenol **27** were reacted in the presence of EDC to afford the desired ester **132** in 75% yield. Ester **132** was then methylated upon addition of methyl triflate in dry DCM to afford the trimethyl ammonium triflate salt **130** in 92% yield (Scheme 32).

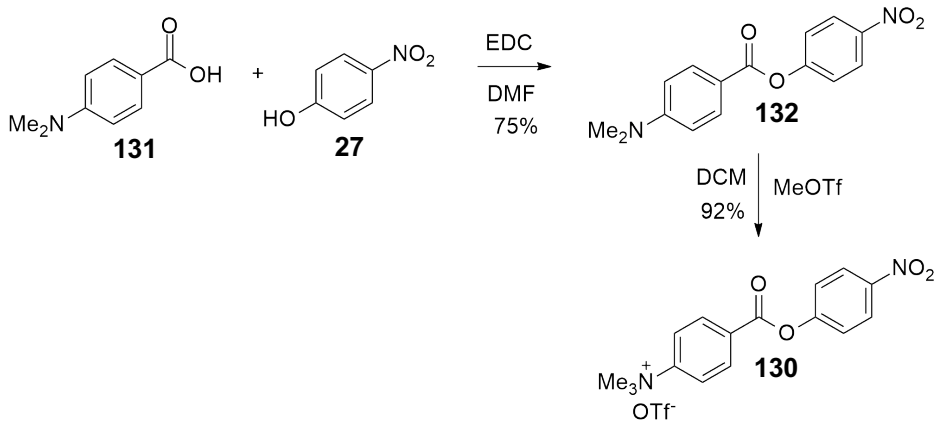

Scheme 32: Synthesis of trimethyl ammonium benzoic acid 4-nitrophenyl ester.

Radiolabelling of **130** was attempted with the $K_{222}.K^{+18}F^-$ complex similar to the preparation of **33** and **129**. Unfortunately, $^{18}F^-$ substitution was not successful and no product **133** could be detected (Scheme 33). It is not clear why this substitution did not proceed.

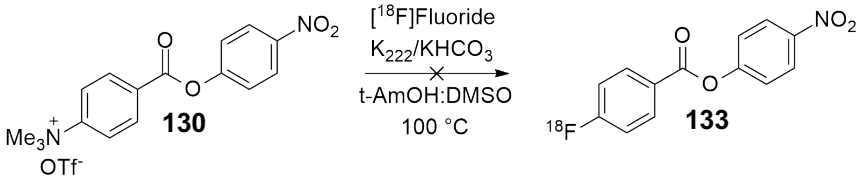

Scheme 33: Unsuccessful radiolabelling of ester.

Accordingly, we decided to explore aromatic labelling via a hypervalent iodine (III) species. These species are known to be "super" leaving groups which are suitable for both electron rich and electron poor aromatic systems.[83] The synthesis began with condensation of 4-iodobenzoyl chloride **134** and 4-nitrophenol **27** in the presence of TEA to form the ester **135** in 85% yield (Scheme 34). Ester **135** was then oxidised with mCPBA in pTsOH to form an intermediate [hydroxy(tosyloxy)iodo]arene in situ, as described by Chun and Pike.[84] Anisole, an electron rich arene, was then added to form the diaryliodonium salt as the tosylate species **136** in 90% yield.

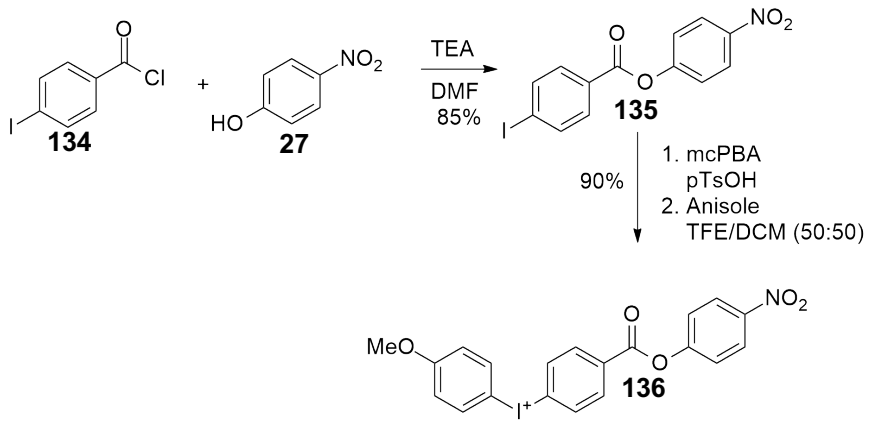

Scheme 34: Synthesis of diaryliodonium salt PNP ester.

In the unsymmetrical iodonium species **136**, the electron rich aryl ring serves as a "spectator ring", while the benzoate ring serves as a target for radiofluorinaton.[85] Treatment of **136** with reactive $K_{222}.K^{+18}F^-$ complex, with use of slightly milder potassium oxalate over potassium bicarbonate as base, generated [^{18}F]-fluorobenzoic ester **133** within 5 min in 68% yield (non-decay corrected) (Scheme 35) Interestingly, it was discovered that the amount of precursor is critical to optimise labelling of **136** precursor. The reaction proceeded in highest yields with 20 mg of precursor **136** to achieve radiofluorinated product **133** in 88% yield (n=3, 42% isolated yield decay corrected to SOS). Curiously, no such correlation was observed with **129** and **33**.

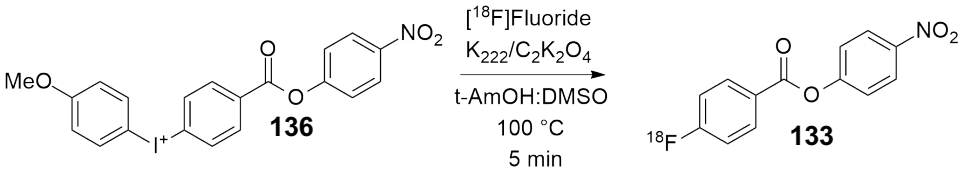

Amount of precursor	% yield
5 mg	not observed
10 mg	68%
20 mg	88%

Scheme 35: Manual optimization of [^{18}F]-fluorobenzoic ester via iodonium salt.

Given the success of radiolabelling **136** to afford **133**, we decided to the explore the synthesis and radiolabelling of the TFP iodonium salt **139**. The synthesis of **139** proceeded in an analogous fashion to the procedure described in Scheme 36 but with 2,3,5,6-tetrafluorophenol **137** in place of **27** to afford iodonium tosylate **139** in 88% yield (Scheme 36).

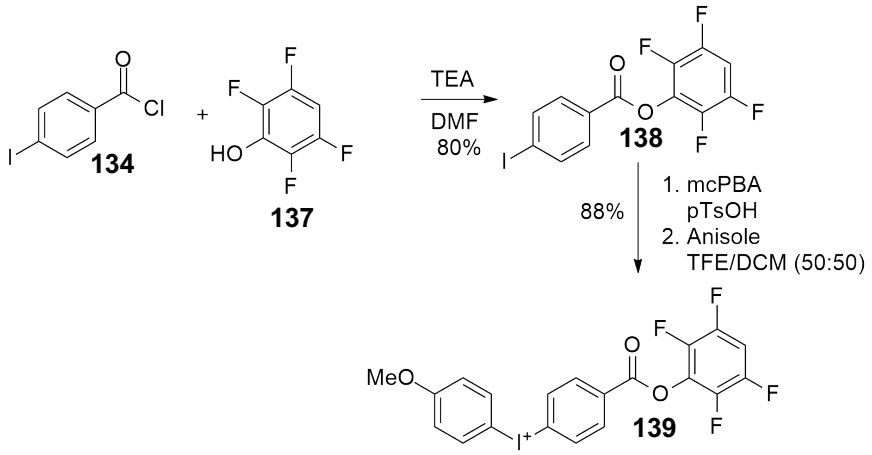

Scheme 36: Synthesis of TFP iodonium salt.

Interestingly, the ^{18}F-fluorination of the TFP ester **139** resulted in radiochemical yields of only 1% yield of **140** (n=3, non-decay corrected) (Scheme 37) in a stark contrast to the high yields obtained for PNP ester **133**. It appears that the 4-nitrophenyl ester enables better radiolabelling than TFP esters.

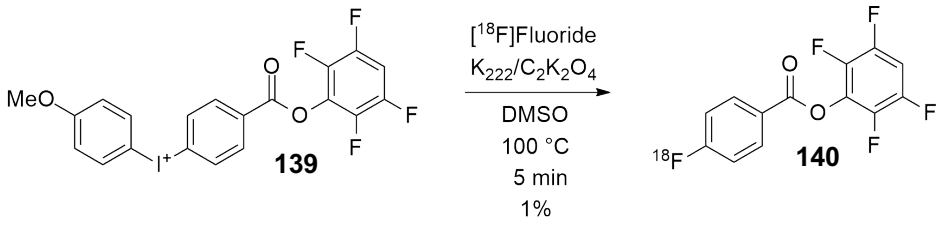

Scheme 37: Synthesis of TFP [^{18}F]-fluorobenzoate.

The stability of the [^{18}F]-fluoronicotinic PNP **129**, [^{18}F]-fluorobenzoate PNP **133** and [^{18}F]-fluoronicotinic TFP **33** in DMSO were assessed. PNP esters **129** and **133** were remarkably stable for over 9 h in DMSO. However, TFP ester **33** underwent complete hydrolysis in DMSO in less than 1 h.

3.3 Relative efficiencies of acylation: PNP versus TFP ester

We were interested in a direct comparison of acylation efficiencies of [^{18}F]-fluoronicotinic TFP **33**, [^{18}F]-fluoronicotinic PNP **129** and [^{18}F]-fluorobenzoate PNP **133** (Scheme 38, Figure 27). The efficiency of acylation was assessed by treating the acyl donors with benzyl amine [0.07–9.17 μM] for 10 min. Yields of acylated products were based on ^{18}F activity and radioHPLC integration. PNP esters [^{18}F]-fluoronicotinate **129** and [^{18}F]-fluorobenzoate **133** showed improved acylation efficiencies, affording 93–100% yield of amidated product **141** and **142** respectively at the highest concentration of benzylamine (9.17 μM) compared to 73 ± 1% yield when acylating with TFP ester **33**. Yields of acylation dropped as the concentration of benzylamine decreased below ~5 μM, for all esters. In addition, the acylation rates of TFP ester **33** were found to be less consistent than

the acylation rates of PNP esters **129** and **133**. The higher and consistent acylation rates of the PNP esters can be attributed to their higher stability in solution.

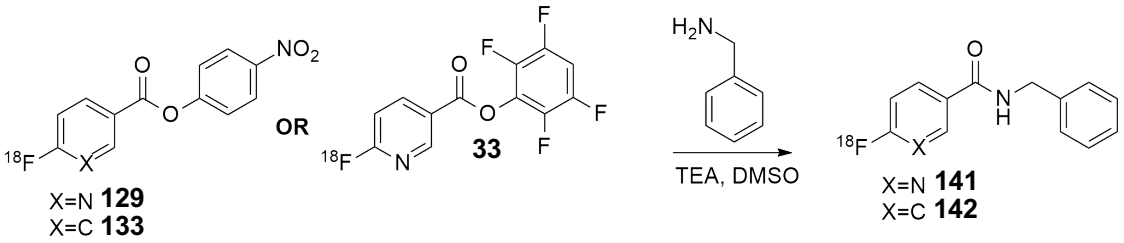

Scheme 38: Relative efficiencies of acylation of TFP versus PNP with benzylamine as a substrate.

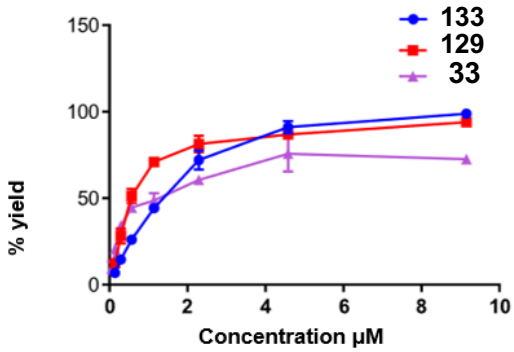

Figure 27: Acylation of esters with benzyl amine to afford amidated products. Yield calculated as an average over 3 runs.

3.4 Automated radiolabelling of CXCR4 peptide with [^{18}F]4-nitrophenyl 4-fluorobenzoate

The major disadvantage of ^{18}F fluorination of biomolecules is the laborious and time-consuming preparation of ^{18}F labelling prosthetic groups.[86] In addition, biomolecules are often costly and larger quantities than desirable are required to label efficiently.[87] The formation of ester **133** demonstrated, to our knowledge, the first one-step synthesis of an activated ester of [^{18}F]-

fluorobenzoate in a high and reproducible yield. In addition, the acylation of amines with **133** was shown to be very efficient even at concentrations as low as ~1 μM (Scheme 38, Figure 27). As such, we were interested in radiolabelling our previously synthesised CXCR4-targeting peptides **106** and **107** at a similar concentration. The ester **133** was prepared according to optimised methods (Scheme 35). Isolated [^{18}F]-fluorobenzoate ester **133** was eluted from a solid phase extraction cartridge (SPE) into the second reactor vessel using a mixture of 1.0 mg peptide **106** or **107** in DMSO:MeCN:TEA and reacted for 5 min. The mixture was then purified by preparative radioRP-HPLC. Coinjection with authentic reference samples **88**/**89** confirmed that both CXCR4 targeting peptides had been labelled in good yield (60% and 62% yield respectively, decay corrected to SOS) with sufficient specific activity (0.86–0.93 MBq/μg) (Scheme 39). For the first time, to our knowledge, a [^{18}F]-fluorobenzamide was formed on the side chain of a peptide in good yields in just two-steps. In addition, the successful labelling of **143** and **144** puts us in good stead to evaluate these CXCR4-targeting peptides *in vivo*.

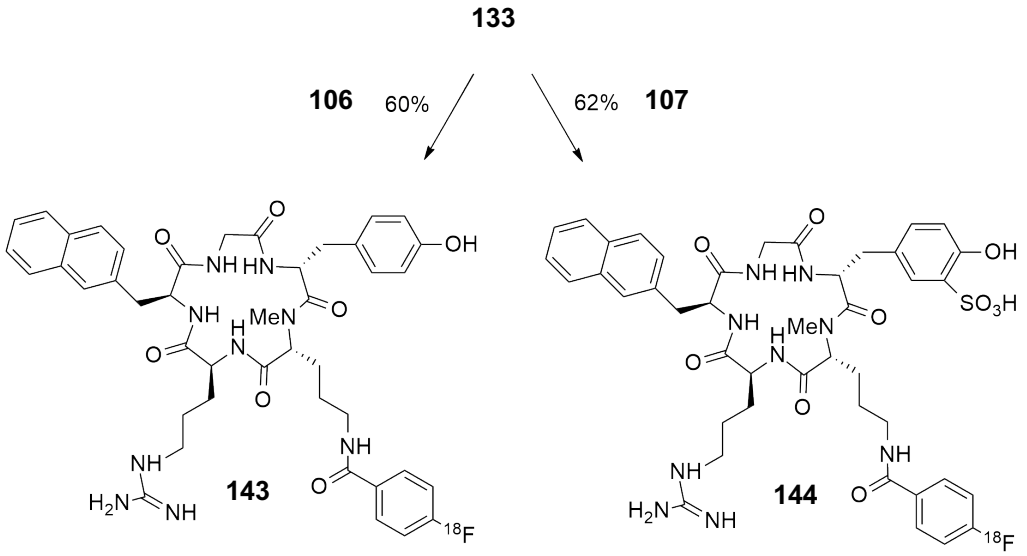

Scheme 39: Fully automated synthesis of CXCR4-targting peptides with [^{18}F]-fluorobenzoate 4-nitrophenyl ester

3.5 Radiolabelling of sulfonated pentixafor precursor with [^{68}Ga]

With the prosthetic group labelling of CXCR4-targeting peptides optimised, the radiolabelling of DOTA-linked peptides with $^{68}Ga^{3+}$ was investigated.[88] Considering the clinical success of 'Pentixafor' **36**, we were interested in radiolabelling the sulfonated equivalent **79** and ultimately evaluating its biodistribution.[66] Radiolabelling of sulfonated 'Pentixafor' **79** was performed on the iPHASE MultiSyn module (Figure 11). A standard [^{68}Ga]DOTATATE protocol was followed whereby **79** was radiolabelled with $^{68}Ga^{3+}$ at pH 3.[89] Both radioTLC (Figure 28) and coinjection of authentic sample **81** on radioHPLC, confirmed product **145** in 80% d.c yield (Scheme 40) with sufficient specific activity (1.1 MBq/μg). Pending binding assay results, sulfonated pentixafor **145** will be evaluated *in vivo*.

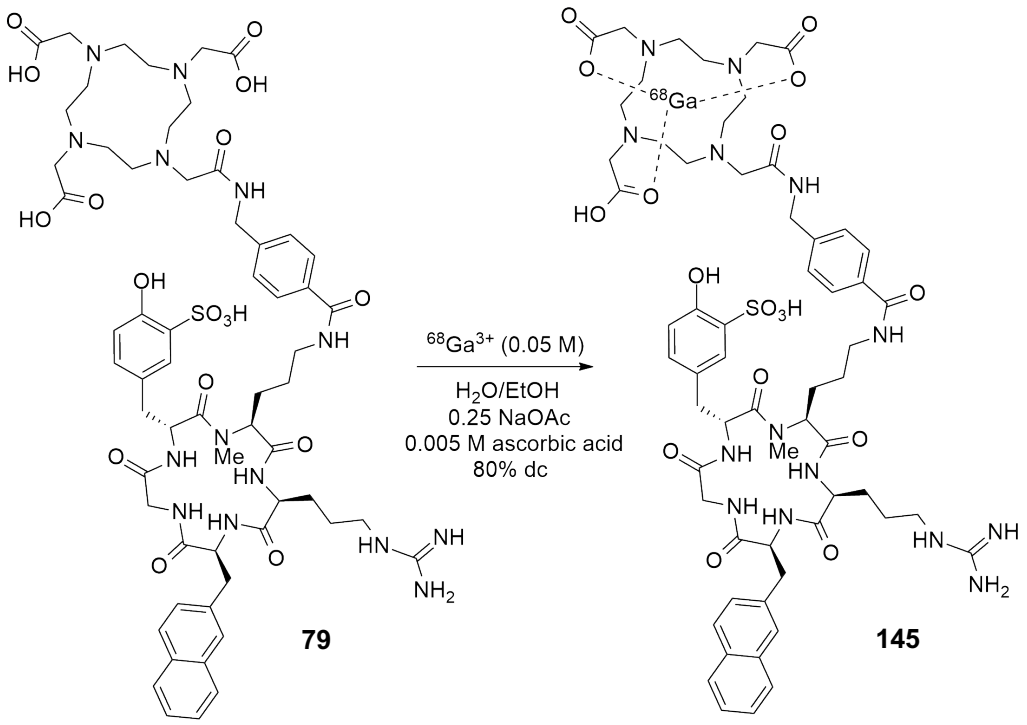

Scheme 40: Radiolabelling of sulfonated pentixafor with $^{68}Ga^{3+}$.

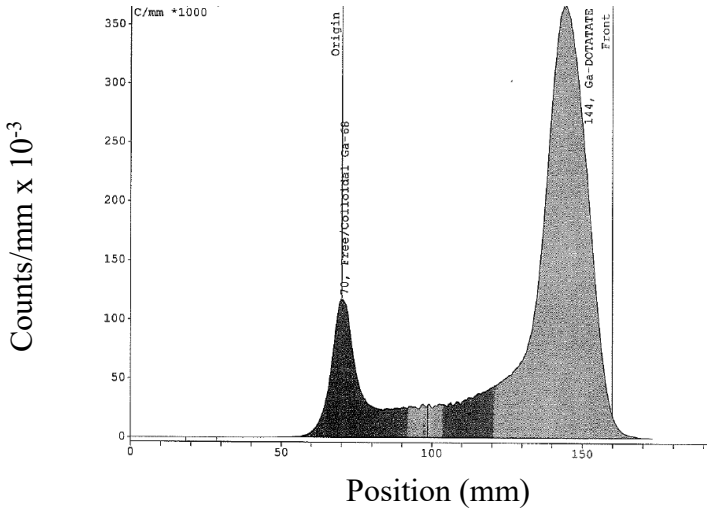

Figure 28: RadioTLC showing "free" $^{68}Ga^{3+}$ (left) and chelated $^{68}Ga^{3+}$ (right).

CHAPTER 4: SYNTHESIS OF ^{18}F-LABELLED THREONINE ANALOGUES

4.1 Fluorine-18 labelling of amino acids

Radiolabelled amino acids in PET imaging target the increased level of amino acid transport by tumour cells. Radiolabelling of amino acids with fluorine-18 is favourable as the half-life of fluorine-18 matches the time scale of amino acid transport and protein synthesis.[90] In addition, the half-life of fluorine-18 allows for shipping of radiolabelled amino acids to hospitals without access to a cyclotron or radiochemistry laboratory.[90] Introduction of ^{18}F through nucleophilic substitution reactions is the most common approach to radiofluorinated amino acids.[91] For example, [^{18}F]FET **4** can be synthesised from nucleophilic substitution of tosylate precursor **146** followed by deprotection of **147** (Scheme 41).[92] Similarly, *anti*-3[^{18}F]FACBC **5** can be produced from nucleophilic substitution of triflate precursor **148** followed by deprotection of **149** (Scheme 42).[93]

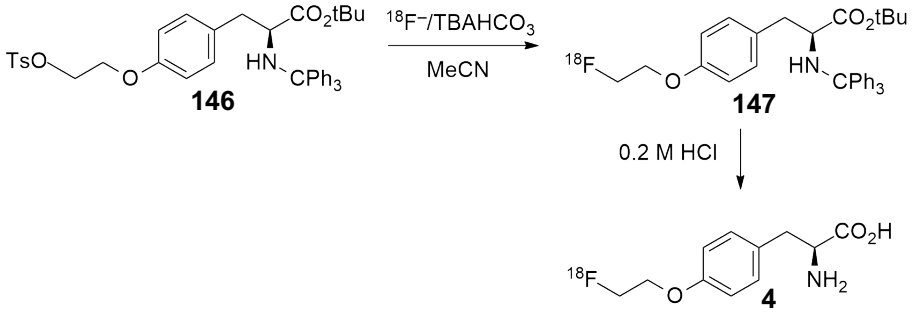

Scheme 41:[^{18}F]-FET radiofluorination described by Siddiq et al.[92]

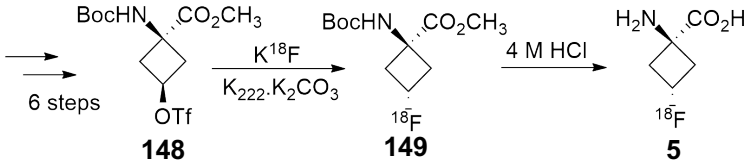

Scheme 42:[^{18}F]-FACBC radiofluorination as described by McConathy.[93]

Our interest in targeting ASCT-2 facilitated amino acid transport led to consideration of a radiolabelled threonine analogue such as **44**. Graham *et al.*[94] have demonstrated that fully protected [^{18}F]-4-fluorothreonine **151** could be prepared from a 4:1 mixture of diastereomers of epoxide precursor **149**, in the presence of the dimeric cobalt(III)salen catalyst **150** (Scheme 43).[94] However, N-Cbz and methyl ester groups of **151** are not easily removed without forcing conditions. To our knowledge, biodistribution of radiolabelled and deprotected **151** has not yet been explored.

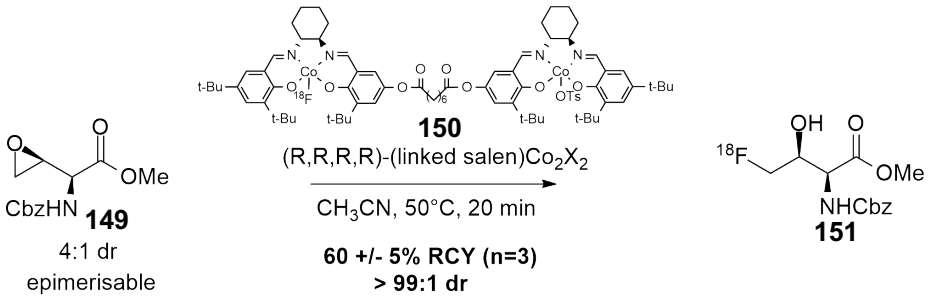

Scheme 43: [^{18}F]-L-fluorothreonine synthesis via cobalt mediated epoxide ring opening.[94]

4.2 [^{18}F]-fluorothreonine via cobalt mediated epoxide ring opening

Initial investigations to synthesise a ^{18}F-radiolabelled threonine analogue followed a similar approach to Graham *et al* via a vinyl glycine precursor.[94] However, we proposed that a protecting group switch to TFA-labile protecting groups was necessary for ease of deprotection as required for radiosynthesis.[95] The epoxide should be available from a vinyl glycine precursor. Accordingly, **156** was synthesised via methods described by Afzali-Ardanki and Rapoport (Scheme 44).[96] L-methionine **152** was esterified in quantitative yield to furnish **153**, followed by Cbz protection to afford **154** in similarly excellent yield. Oxidation of methionine derivative **154** to the corresponding sulfoxide **155** with sodium periodate also proceeded in quantitative yield. The sulfoxide **155** then underwent thermal dehydrosulfenylation at low pressure. Using a Kugelrohr instrument, a pressure of 8 mmHg was achieved but the reaction was not efficient at

temperatures lower than 200°C. Under these conditions, the desired protected L-vinylglycine product **156** was isolated in a moderate 57% yield together with significant amounts of E,Z isomers of the α,β-unsaturated analogue. Protected L-vinylglycine **156** was then deprotected with 6M HCl to afford L-vinylglycine **157** in 85% yield. Boc protection followed by formation of the PMB ester were performed in good yields to furnish protected L-vinylglycine **159**. Treatment of **159** with mCPBA afforded epoxide **160** as a 3:1 mixture of diastereomers (Scheme 44).[94]

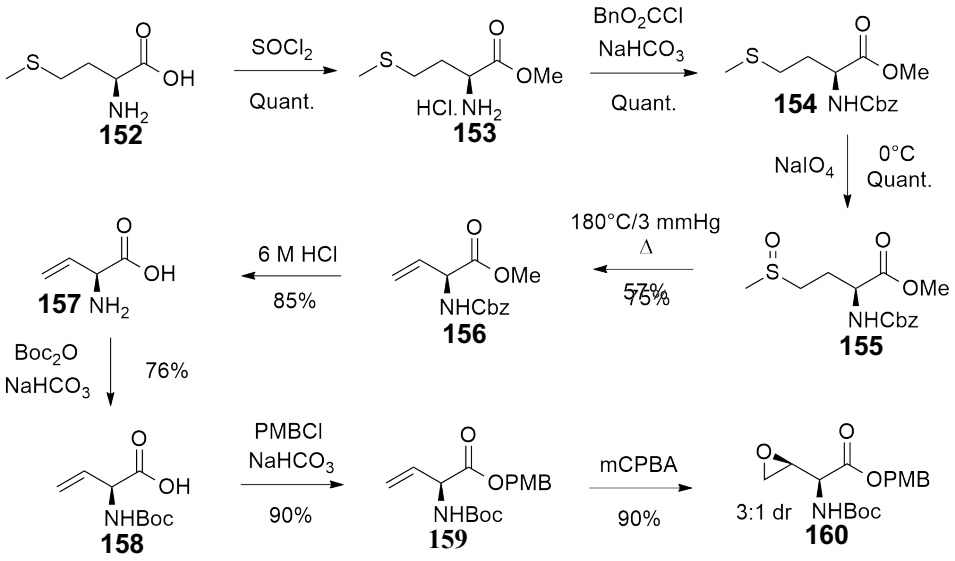

Scheme 44: Synthesis of protected epoxide precursor.

The epoxide **160** was then treated under a range of fluorination conditions. Co-salen complexes with a variety of fluoride sources failed to generate the fluorothreonine product (Table 5, entries 1–5). The use of Co(III)salenOTs, in combination with 70% HF-pyr (Table 5, entry 3) gave trace amounts (5%) of **161**. These observations were consistent with Kalow and Doyle's previous observations of cobalt-mediated hydrofluorination of epoxides.[97] Kalow and Doyle observed that chiral Lewis acid mediated reactions of epoxides with HF-pyridine complex suffered from low enantioselectivity and catalyst degradation. Instead, Doyle and Kalow utilised a combination of benzoyl fluoride (PhCOF) and hexafluoroisopropanol (HFIP) in the presence of

amine co-catalyst to provide a mild release of fluoride, resulting in the formation of a fluorohydrin product with excellent enantiocontrol.[97] Kalow and Doyle hypothesised that the mechanism is likely via amine catalysed in situ slow formation of HF, which in turn could generate the active (salen)Co(III)fluorine complex.[97] As such, epoxide **160** was treated with Co(II)salen, PhCOF and HFIP and amine co-catalyst 1,5-diazabicyclo(4.3.0)non-5-ene (DBN) to furnish protected (2S,RS)-fluorothreonine **161** in good yield.[97]

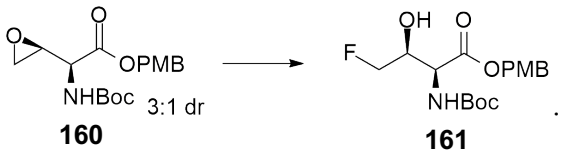

160 **161**

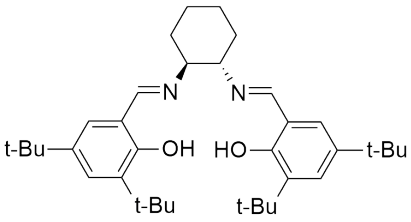

162

*"Salen" ligand

Entry	Fluoride source	*Catalyst	Base	Solvent	Yield
1	KHF_2/18-crown-6	(S,S)Cr(III)salenCl **163**	-	DMF	0%
2	KF/18-crown-6	(S,S)Co(III)salenOTs **164**	-	MeOH	0%
3	70% HF-pyr	(S,S)Co(III)salenOTs **164**	-	MTBE	5%
4	KF/18-crown-6	(S,S)Co(II)salen **165**	-	MTBE	0%
5	70% HF-pyr	(S,S)Co(II)salen **165**	-	MTBE	0%
6	TBAF	(S,S)Co(II)salen **165**	-	Toluene	0%
7	HFIP/PhCOF	(S,S)Co(II)salen **165**	DBN	MTBE	60%

Table 5: Lewis acid promoted fluorination of epoxide with a range of catalysts/fluoride sources

Though the use of HFIP/PhCOF enabled preparation of fluorothreonine in good yield, we were concerned about difficulties in elaboration of this procedure to incorporate ^{18}F. Radiofluorination would require prior preparation of $PhCO^{18}F$, or indirect preparation of the Co-

^{18}F-salen complex (Scheme 45). We were also interested in applying a more general methodology that could potentially be applied to all amino acids.

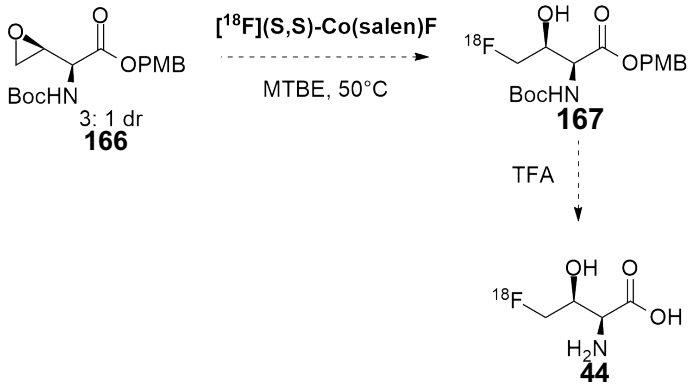

Scheme 45: [^{18}F]-fluorination and deprotection of epoxide precursor.

4.3 Organotrifluoroborates for ^{18}F-labeling

Organotrifluoroborates were first utilised for ^{18}F-labelling by Liu *et al.*[99] whereby a zwitterionic organotrifluoroborate was appended to several target molecules via an azidoethyl-alkylammoniomethyltrifluoroborate (azidoethyl-AMBF$_3$) prosthetic group **169** (Scheme 46).[99]

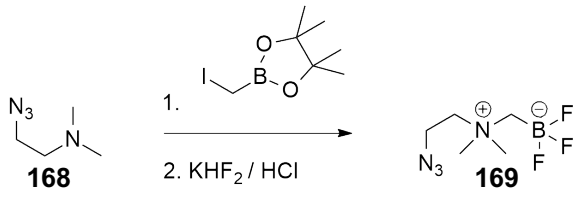

Scheme 46: Synthesis of azidoethyl-AMBF$_3$

AMBF$_3$ radioprosthetic groups can be appended to peptides or small molecules such as rhodamine B derivative **170** (Scheme 47) through click chemistry. To radiolabel AMBF$_3$-rhodamine B conjugate **171** facile ^{18}F-^{19}F isotope exchange (IEX) was employed to furnish ^{18}F-labelled isotopomer **172** in good yield and high purity (>98%).[99]

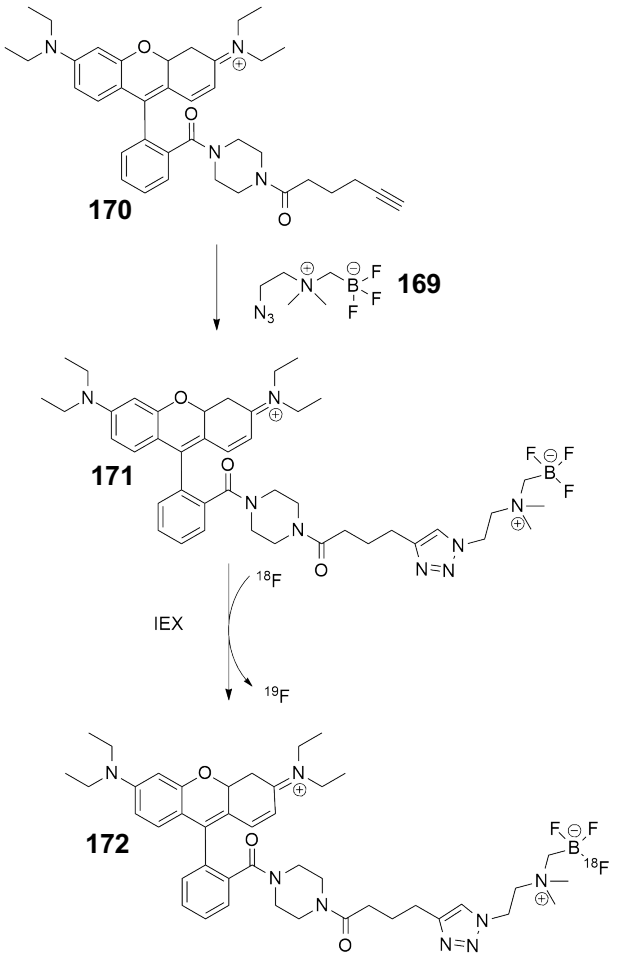

Scheme 47: Facile labelling of rhodamine B by ^{18}F-^{19}F isotope exchange (IEX).

Boramino acid as a marker for amino acid transporters

Building on earlier work, Liu *et al.*[100] investigated boramino acids as amino acid mimics. The structures of boramino acids (BAAs) **174** are similar to those of the corresponding natural amino acids **173** (Figure 29). The carboxylate, $–CO_2^–$, however, is replaced with a trifluoroborate $–BF_3^–$, which is not metabolised *in vivo* and can be readily labelled with ^{18}F-fluoride through ^{18}F-^{19}F isotope exchange (IEX). Furthermore, Liu *et al.* demonstrated that the *in vivo* stability of the trifluoroborate moiety (which is generally poor) is substantially increased by the adjacent positively charged ammonium group (Figure 29).[100]

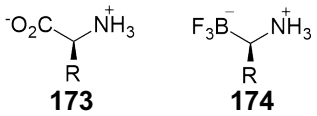

Figure 29: Amino acid and boramino acid.

Substitution of the carboxylate group of amino acids by a boronic acid ($B(OH)_2$) has been studied previously due to its structural similarity to a carboxylate (CO_2^-) (Figure 30). While both boronic acids and carboxylates are planar, the boronic acid is a neutral moiety, whereas a carboxylate possesses a negative charge.[100,101] The trifluoroborate group, however, possesses a negative charge. Density functional theory (DFT) prediction shows the charge distribution of Phe-$B(OH)_2$ **176** is visibly different from that of natural Phe **175**, whereas Phe-BF_3 **177** exhibits nearly identical charge distribution with natural Phe **175** (Figure 30). Thus, DFT studies suggest that BAAs might bind to amino acid transporters in a similar manner to natural amino acid ligands. A docking study with Phe-BF_3 to the large neutral amino acid transporter LAT-1 predicted a binding constant of Phe-BF_3 (K_i = 60.33 μM), similar to that of the natural amino acid Phe (41.49 μM), further supporting the idea that BAAs are ideal amino acid mimics.[100]

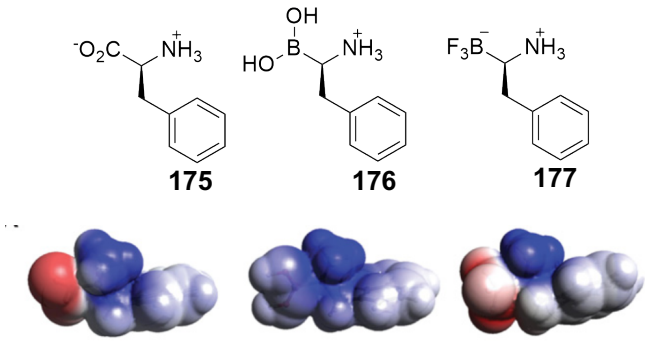

Figure 30: Phenylalanine, boronic acid and trifluoroborate analogues and their molecular electrostatic potential (MEP) prediction.[100]

Furthermore, Liu *et al.*[100] showed that boramino acids could be radiolabelled with the IEX process previously described (Scheme 48).[99]

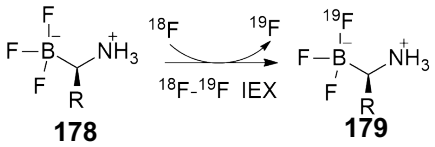

178 **179**

Scheme 48: ^{18}F-BAAs radiosynthesised via one-step ^{18}F-^{19}F isotope exchange reaction.

Liu *et al.*[100] prepared the ^{18}F BAAs ^{18}F-Phe-BF_3, ^{18}F-Leu-BF_3, ^{18}F-Ala-BF_3 and ^{18}F-Pro-BF_3 and showed they exhibited high AAT-mediated tumour uptake and rapid clearance from normal organs and tissues. Most notably, compared to ^{18}F-FDG **2** (the standard PET imaging agent for cancer diagnosis), ^{18}F-BAAs exhibited substantially lower background uptake, particularly in brain tissue and regions of inflammation. Such high tumour specificity is highly desirable in PET imaging.[100] However, synthesis of ^{18}F-BAAs is complex, particularly with amino acids with branched or functionalised side chains, such as threonine. To synthesise an α-amino boronic ester **184** in high enantiopurity, a homologation reaction of an alkyl boronic ester (containing appropropriate pinanediol) **182** is required to introduce a C–C bond as described Matteson *et al.*[101] Further, nucleophilic displacement of chloride on **183** is required with lithium bis(trimethylsilyl)amide, which is then hydrolysed to give desired α-amino boronate **184**. The desired trifluoroborate **185** can then be accessed from **184** with KF/HCl in quantitative yield (Scheme 49).

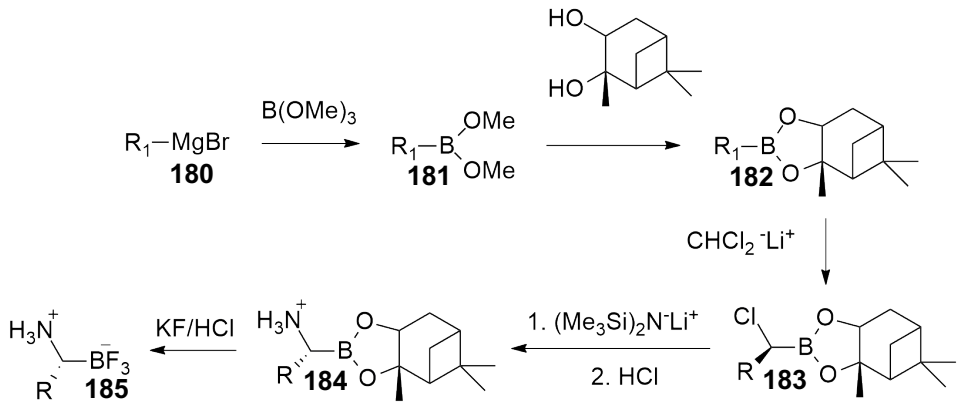

Scheme 49: General synthetic routes of α-amino trifluoroborates

Shortly after Liu et al.[100] reported the synthesis of amino trifluoroborates, Li *et al.*[102] reported the synthesis of α-amino boronates **188** from an N-Boc protected amino acid, **186**, via a decarboxylative borylation (Scheme 50).[102-104]

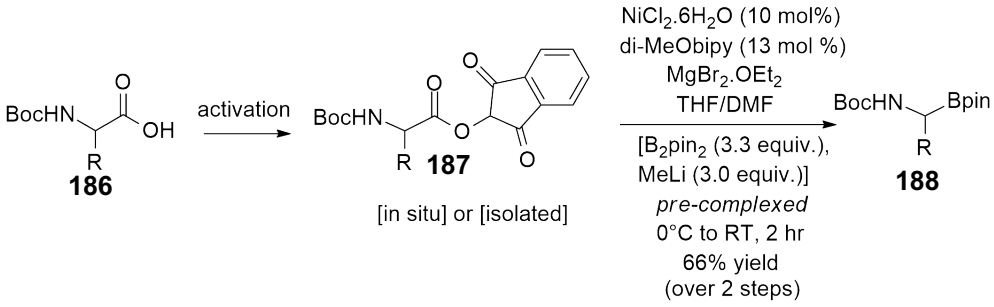

Scheme 50: Nickel catalysed decarboxylative borylation of amino acid.

Li *et al*.'s method provides a mild, scalable and general access to α-amino boronates via NHPI esters. Li *et al*. described that the boronate ester **191** could easily be hydrolysed into corresponding boronic acid.[105] However, we envisaged that this methodology could be used to transform amino acids **189** into α-amino trifluoroborates **192**, through treatment of the pinacol boronate **191** with KHF_2 (Scheme 51).[100] The main disadvantage of this method is that decarboxylative borylation proceeds via a radical intermediate and this results in loss of

stereochemical integrity at the α-carbon. However, reduction in synthetic complexity significantly outweighs this generation of racemic product.

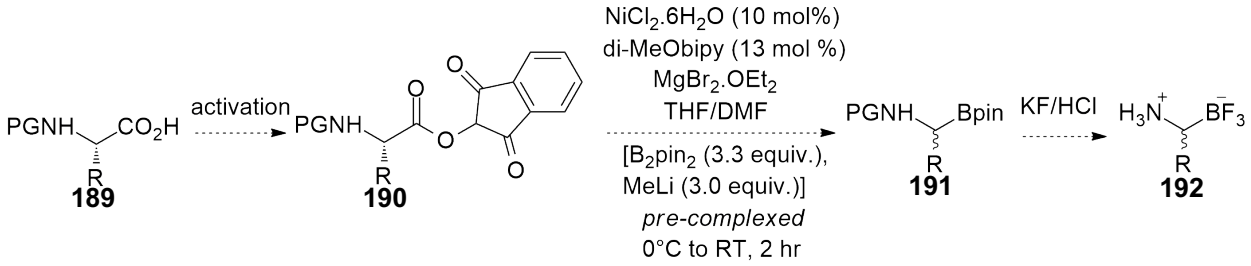

Scheme 51: Proposed synthesis of α amino trifluoroborates via nickel catalysed decarboxylation.

Accordingly, towards the synthesis of the threonine derived BAA, N-Boc-Thr(OtBu)-OH **193**, was activated with NHPI to form redox ester **194** which was converted to boronate **195** under Liu's conditions (Scheme 52). As the pinacol ester **195** was unstable to chromatography, the crude product **195** was first evaporated before being treated with 3M KF and 4M HCl to form the desired potassium trifluoroborate salt **196**. Purification by RP HPLC gave product **196** in 75% overall yield (Scheme 52).

Similarly, conversion of protected tyrosine **197** to the NHPI redox active ester **198** was followed by treatment with decarboxylative borylation conditions to produce the α-amino boronate **199**, which was further converted to the desired trifluoroborate **200** in 72% overall yield (Scheme 53). Protected aspartic acid **201** was converted to trifluoroborate **204** in 70% overall yield with the same protocol (Scheme 54).

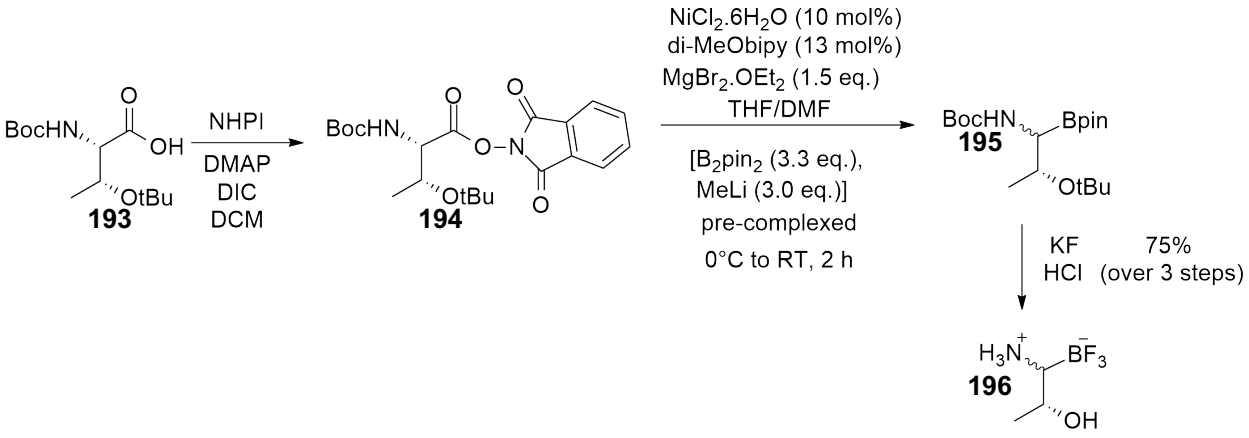

Scheme 52: Nickel catalysed decarboxylation, borylation and trifluoroborate synthesis from N-Boc-L-Thr-OtBu-OH.

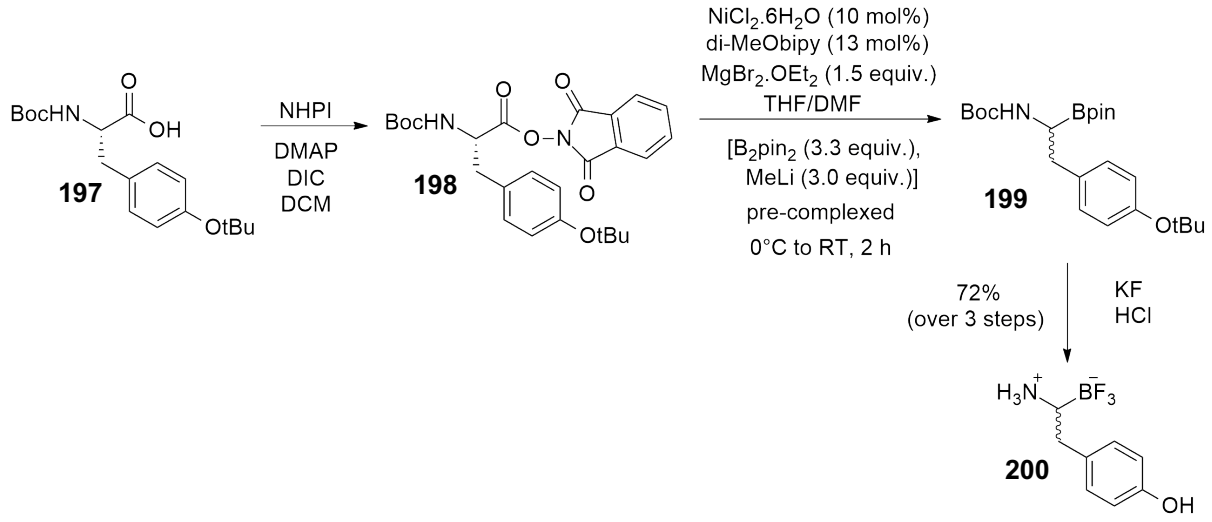

Scheme 53: Nickel catalysed decarboxylation, borylation and trifluoroborate synthesis from N-Boc- L-Tyr-OtBu-OH.

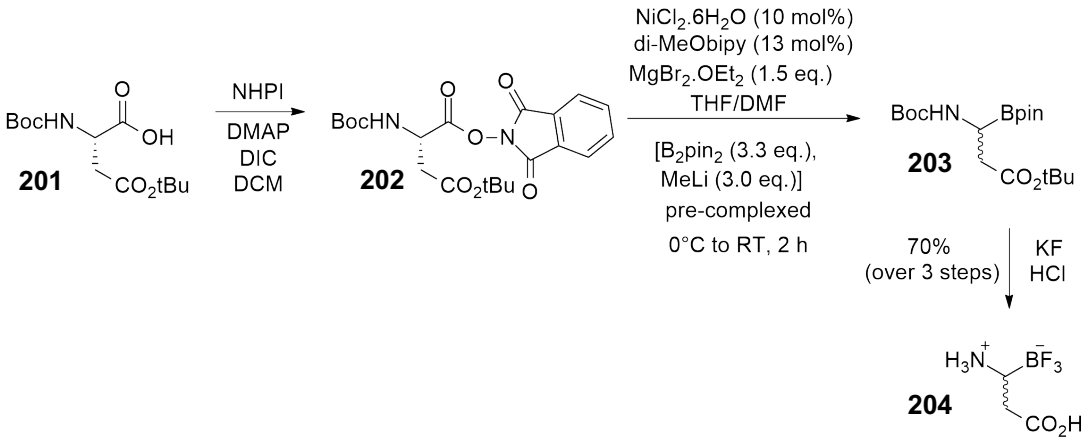

Scheme 54: Nickel catalysed decarboxylation, borylation and trifluoroborate synthesis from N-Boc-L-Asp-OtBu-OH.

Radiolabelling of threonine trifluoroborate

Efforts to radiolabel threonine trifluoroborate through IEX of **196** were first explored.[100] The reaction of IEX of **196** to **205** proceeded to a limited extent at 80°C for 15 min (Scheme 55). Shown below is a radioTLC plate demonstrating some conversion: the major peak at R_f=0.4 represents ^{18}F-fluoride while the peak at R_f=0.7 is presumably product **205** indicating a yield of 6% n.d.c yield (Figure 31). Further work needs to be done to optimise radiolabelling and conduct biological evaluation. Once radiolabelling of Thr-BF_3 **196** has been optimised, radiolabelling of Tyr-BF_3 **200** and Asp-BF_3 **204** will be investigated.

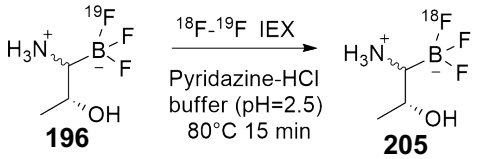

Scheme 55: Radiolabelling of Thr-BF_3 via IEX.

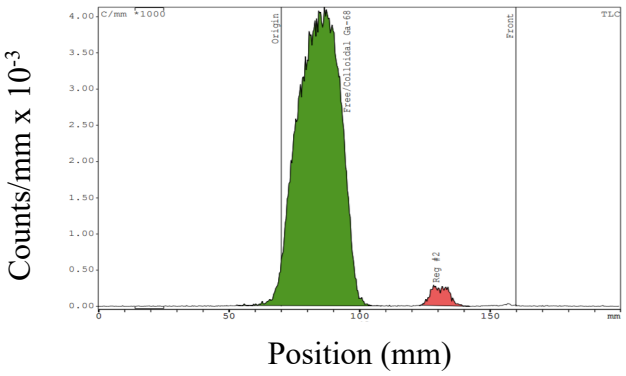

Figure 31: RadioTLC plate of $^{19}F/^{18}F$ IEX of Thr-BF_3

CONCLUSIONS AND FUTURE WORK

A general methodology to afford amino acid trifluoroborate analogues via decarboxylative borylation has been successfully developed (Scheme 56). The radiolabelling of ASCT2-targeting threonine trifluoroborate analogue **196** by ^{19}F–^{18}F IEX requires further optimisation before biological evaluation *in vivo* (Scheme 55). Once optimised, tyrosine and aspartic acid trifluoroborate analogues will be similarly radiolabelled and biologically evaluated.

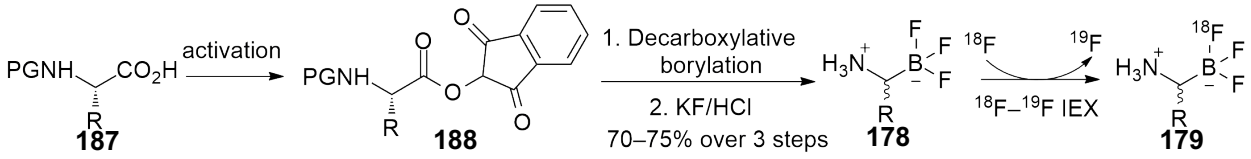

Scheme 56: Synthesis of amino acid trifluoroborates from protected amino acids.

Direct ^{18}F fluorination of 4-nitrophenyl ester prosthetic groups has been expanded to the radiofluorination of 4-nitrophenyl nicotinates and benzoates (Figure 32). Our studies demonstrated that 4-nitrophenyl esters are uniquely stable under radiofluorination conditions yet reactive enough to acylate amine containing precursors at concentrations as low as ~1 μM, in high radiochemical yields. Further, the stability of 4-nitrophenyl esters appear superior to known acylating 2,3,5,6-tetrafluorophenyl esters.

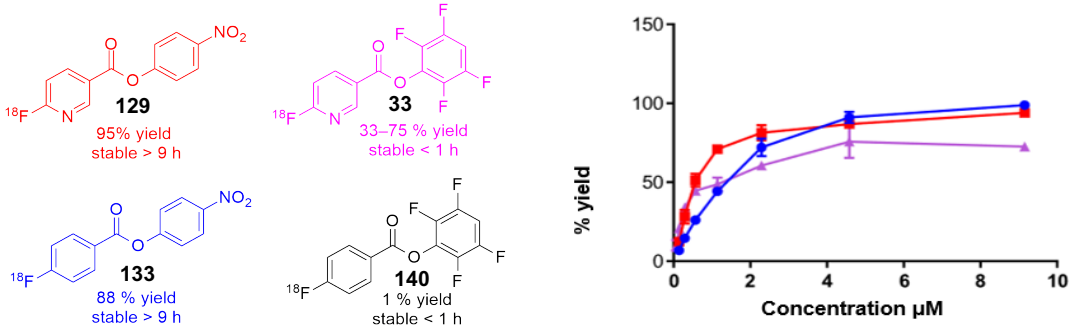

Figure 32: Yields, stability and reactvity of PNP's vs TFP nicotinates and benzoates.

Sulfonation of CXCR4-targeting peptides was achieved through sulfonation of the tyrosine residue **54** with chlorosulfonic acid prior to SPPS (Scheme 58). The earlier elution times of sulfonated CXCR4-targeting peptides on analytical RP-HPLC traces compared to their non-sulfonated analogues suggests that sulfonated peptides have decreased lipophilicity (Figure 18). Pending optimisation of the CXCR4 competitive binding assay, through use of vessels that do not interfere with binding of the radiolabelled competitor, the sulfonated CXCR4-targeting peptide with the best binding will be radiolabelled with already optimised methods and biologically evaluated *in vivo*.

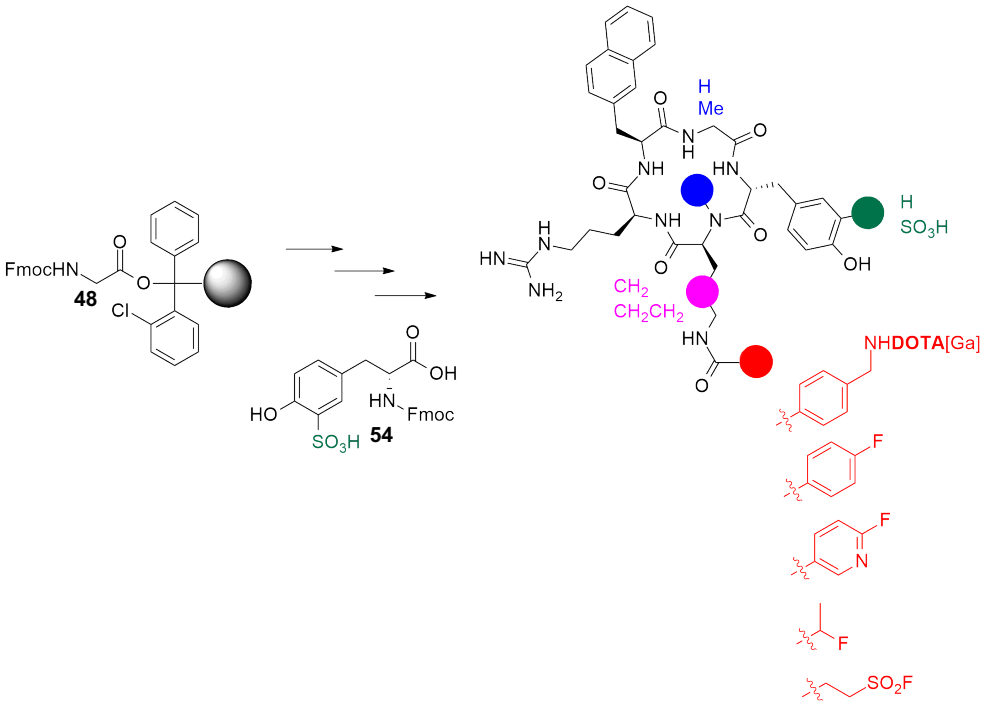

Scheme 57: Synthetic strategy to afford library of sulfonated CXCR4-targeting peptides.

CHAPTER 5: EXPERIMENTAL

Materials

Anhydrous THF, DCM and diethyl ether were obtained by passage though columns of neutral alumina using a solvent dispensing system (Glass Contour). DMSO and DMF were dried by storing over 4 Å molecular sieves under argon for three days prior to use. Chromatographic silica (40–63 micron) was used for flash chromatography. Flash chromatography was performed using silica gel (230-400 mesh). Automated chromatography was performed on a Reveleris PREP purification system. Analytical thin layer chromatography was performed with silica gel 60 F254 (0.2 mm) and inspection was achieved by short-wave UV light. NMR spectra were recorded on an Agilent MR400, Varian Inova 500 spectrometer, Bruker 600 or Bruker 700 spectrometer. Data obtained were analysed using TopSpin 3.5 or Mestrenova 6.0.2-547. Chemical shifts were calibrated to the residual peak of the corresponding deuterated solvent. $CDCl_3$ (7.26 ppm), D_2O (4.56 ppm), d_6 DMSO (2.5 ppm) and CD_3OD (4.8 and 3.3 ppm). Mass spectra were recorded on an Agilent ESI-TOF or OrbiTRAP infusion mass spectrometer. Preparative reverse phase HPLC (RP-HPLC) was performed using an Agilent 1200 series LC system. Analytical RP-HPLC was performed on an Agilent 1100 series LC system. The mobile phase typically utilised solvent A (0.1% TFA in H_2O) and solvent B (0.1% TFA in MeCN) with a flow rate of 1 ml/min for analytical RP-HPLC, and 8 ml/min for preparative RP-HPLC. Columns used for HPLC purification and analysis were the following:

Column A: Amide Polaris C18 Amide, 180 Å, 3 µm, 250 × 2.0 mm.

Column B: Varian long Agilent Varian pursuit XRs 5 C18, 100 Å, 10 µm, 150 × 21.2 mm.

Column C: Phenomenex Synergi Hydro-RP, 80 Å, 10 µm, 250 × 10 mm.

Column D: Phenomenex Kinetex C18 AXIA, 100 Å, 5µm, 150 × 21.2 mm.

Column E: Hypersil BDS C18, 130 Å, 5µm, 150 mm × 4.6 mm.

^{18}F-radiolabelled compounds were purified and analysed on a Shimadzu LC-10 HPLC system equipped with an LC-10 VP system controller (HPLC 3). Columns used were the following:

Column F: Luna C18, 180 Å, 5µm, 250 x 10.00 mm

Column G: Phenomenex Luna C18, 100 Å, 5µm, 250 x 21mm.

Column H: Jupiter Proteo, 90 Å, 4 µm, 250 x 4.5 mm (QC analysis of ^{18}F-radiolabelled peptides).

General Solid Phase Peptide Synthesis Protocols

The syntheses of linear protected pentapeptides was accomplished using standard Fmoc solid phase peptide synthesis (SPPS). 2-Chlorotrityl chloride polystyrene resin was used as the solid support. The synthesis of the peptides was accomplished manually using polypropylene syringes with sintered discs (Torviq).

General protocol for amino acid loading onto 2-chlorotrityl chloride resin

Fmoc amino acid (5 eq.) was dissolved in DIPEA (4 eq.) and dry DCM (10 ml/g of resin) containing if necessary, a small amount of dry DMF (to facilitate dissolution of the acid). This solution was added to 2-chlorotrityl chloride resin (1 mmol/g, 1 eq.) and agitated for 120 min. The resin was washed with DCM/MeOH/DIPEA (17:2:1, 3 × 10 ml), DCM (3 × 10 ml), DMF (3 × 10 ml) and DCM (3 × 10 ml).

General resin loading determination protocol

Dry Fmoc amino acid loaded resin (3 × 7 mg) was weighed accurately. A solution of 2% DBU in DMF (2 ml) was added to all samples. The solutions were agitated for 30 min and then diluted to 10 ml with MeCN in 10 ml volumetric flasks. These solutions were further diluted by taking 2 ml of each and diluting to 25 ml with MeCN in a 25 ml volumetric flask. A reference solution was prepared without the addition of the resin. Three quartz cuvettes were prepared with 3 ml of test solution, while one cuvette was prepared with 3 ml of reference solution. The cells were placed in a spectrophotometer and the absorbance was recorded at 304 nm. An estimate of loading of the first residue attachment was ascertained from the equation below:

Fmoc loading (mmol/g)= $(Abs_{sample} - Abs_{reference}) \times 16.4$/mg of resin.[106]

TNBS test for confirmation of coupling/deprotection reaction on resin

A qualitative test was carried out for each coupling/deprotection step using the TNBS test. A small fraction of the resin (approx. 20 beads) were placed into an Eppendorf tube. 1% 2,4,6-trinitrobenzenesulfonic acid in DMF (10 µl) of 5% DIPEA in DMF (10 µl) were added and the mixture was agitated for 2 min. The presence of a free amine results in a red bead, whereas colourless beads indicate the Fmoc protected amine.[107]

General Fmoc deprotection protocol

Method A*:* The resin-bound peptide was treated with a solution of 5% DBU/20% piperidine in DMF or 5% DBU/5% piperazine in DMF for 10 min, drained and then repeated. The resin was then washed with DMF (5 × 10 ml) and DCM (2 × 10 ml). A TNSB test was then performed to ensure complete deprotection.

***Method B*:** The resin bound peptide was treated with a solution of 20% piperidine in DMF or 5% piperazine in DMF (10 ml/g) for 10 min, drained and then repeated. The resin was then washed with DMF (5 × 10 ml) and DCM (2 × 10 ml).

General Fmoc-amino acid coupling protocol

Method A: The Fmoc-protected amino acid (1 eq. 0.1 mmol) was dissolved in a solution of HATU (19 mg, 0.1 mmol, 1 eq.) in DMF (2 ml). Additional DMF (2 ml) may be required to dissolve the acid. DIPEA (70 µl, 0.4 mmol, 4 eq.) was then added and the amino acid was activated for 2 min. The activated amino acid solution was added to the resin and agitated for 1 h. The resin was then drained and then washed with DMF (3 × 10 ml) and DCM (2 × 10 ml). A TNSB resin test was performed to confirm coupling.

Method B*:* The Fmoc protected amino acid (1 eq. 0.1 mmol) was dissolved in a solution of HOBt (27 mg, 0.2 mmol, 2 eq.) in DMF (2 ml). Additional DMF (2 ml) may be required to dissolve the acid. DIC (61 µl, 0.4 mmol, 4 eq.) was then added and left for 2 min. The coupling solution was added to the resin and agitated for 20 min. The resin was then drained and then washed with DMF (3 × 10 ml) and DCM (2 × 10 ml). A TNSB resin test was performed to confirm coupling.

General protocol for methylation on resin

Resin (0.05 mmol) was treated with a solution of o-nitrobenzenesulfonyl chloride (33.3 mg, 0.15 mmol) and 2,4,6 collidine (33 µl, 0.25 mmol) in DCM (0.5 ml) for 2 h at rt. After draining the solvent, the resin was washed with DCM (3 × 10 ml), DMF (3 × 10 ml), and THF (3 × 10 ml). To a suspension of the *N*-Ns protected resin in anhydrous THF (0.5 ml) was added MeOH (10 µl, 0.25 mmol), PPh_3 (65.5 mg, 0.25 mmol), and diethyldiazodiaarboxylate (114 µl, 0.25 mmol)

at 0 ℃. The mixture was shaken for 2 h at rt, the solvent was drained, and the resin was washed with THF (3 × 10 ml) and $CHCl_3$ (3 × 10 ml). The N-methylated resin was treated with DBU (33 µl, 0.5 mmol) and 2-mercaptoethanol (35 µl, 0.5 mmol) for 1.5 h at rt to effect removal of the N-Ns group. Finally, the resin was drained and then washed with DCM (3 × 10 ml), DMF (3 × 10 ml) and DCM (3 × 10 ml).[78]

General on resin alloc deprotection protocol

$Pd(PPh_3)_4$ (7.00 mg,, 6.25 µmol, 0.125 eq.,) in DCM (0.5 ml) was added to the resin bound peptide (0.05 mmol scale) followed by addition of phenyl silane (12 µl, 0.1 mmol, 2 eq.) in 0.5 ml DCM. The mixture was then agitated for 30 min. After that time, the resin was drained and then washed with DMF (3 × 10 ml) and DCM (3 × 10 ml).[78]

General coupling protocol for coupling carboxylic acid on resin

To a solution of peptide on resin (0.1 mmol scale) in DMF, carboxylic acid (2 eq., 0.2 mmol) in DMF, HATU (0.2 mmol, 38 mg, 2 eq.,) and DIPEA (70 µl, 0.4 mmol, 4 eq.) were added and the mixture was agitated for 1 h. The resin bound peptide was then drained and then washed with DMF (3 × 10 ml) and DCM (3 × 10 ml).

General coupling of ethene sulfonyl fluoride on resin

To a solution of peptide on resin (0.1 mmol scale) in DMF (5 ml), ethene sulfonyl fluoride (7.45 µl, 0.09 mmol, 0.9 eq.) was added and then agitated for 30 min in order to afford mono substituted analogue. Doubly substituted analogue could be achieved with a solution of peptide on resin on resin (0.1 mmol scale) in DMF (5 ml), ethene sulfonyl fluoride (40.9 µl, 0.49 mmol, 5 eq.), which was agitated for 30 min. After coupling, resin bound peptide was drained and then washed with DMF (3 × 10 ml) and DCM (3 × 10 ml).[80]

General resin cleavage protocol

The resin was washed with DMF (3 × 10 ml), DCM (3 × 10 ml), and diethyl ether (3 × 10 ml) and dried under vacuum for 15–20 min and then transferred to a polypropylene tube. A solution of 1% TFA in DCM (10–20 ml/g of resin) was added and the resin was agitated at rt for 1 h, after which time the resin turned dark brown/purple. The resin was then filtered and washed with DCM. Successful cleavage was indicated by a change of colour of the resin from brown/purple to green. The combined filtrate was concentrated in vacuo and the residue was reconstituted in 0.1% TFA MeCN/H_2O (2:3) and lyophilised.

General pentapeptide cyclisation protocol

Linear protected peptide (0.1 mmol scale) was dissolved in DCM (1 mM) followed by addition of HATU (76 mg, 0.2 mmol, 2 eq.), DIPEA (70 µl ,0.4 mmol, 4 eq.) and the reaction mixture was stirred for 4 h. DCM was then evaporated and the crude material was reconstituted in 0.1% TFA MeCN/H_2O (2:3) and lyophilised.

General protocol for deprotection of cyclic pentapeptides

Lyophilised crude cyclised peptide was reacted with 95% TFA/2.5% H_2O and 2.5% TIPS (5 ml) and left stirring for 2 h. The TFA was then removed via a stream of N_2. The crude material was reconstituted in MeCN/H_2O (2:3) containing 0.1% TFA and lyophilised. The lyophilised material was then purified using preparative RP-HPLC.

General coupling protocol for coupling carboxylic acid to peptide in solution

To a solution peptide (1.0 µmol, 1 eq.) in DMF (10 mM) was added was carboxylic acid (2.0 µmol, 2 eq.) in DMF, followed by HATU (0.76 mg, 2.0 µmol, 2 eq.) and DIPEA (0.70 µl, 4.0

μmol, 4 eq.). The mixture was then diluted with water (4 ml) and then purified by preparative RP-HPLC.

General coupling of ethene sulfonyl fluoride in solution

To a solution of peptide (1.0 μmol, 1 eq.) in DMF (10 mM), ethene sulfonyl fluoride (0.07 μl, 0.9 μmol, 0.9 eq.) was added and then stirred for 30 min in order to afford mono substituted analogue. Doubly substituted analogue could be achieved (0.10 mmol, 1 eq.) in DMF (5 ml), ethene sulfonyl fluoride (0.39 μl, 5.0 μmol, 5 eq.), which was agitated for 30 min. After 30 min, the reaction was diluted with water (4 ml) then purified by preparative RP-HPLC.[78]

General N-Boc deprotection of peptide in solution

The peptide (0.1 mmol) was dissolved in 30% TFA in DCM (5 ml) and stirred for 2 h. The volatiles were evaporated under N_2 and the crude mixture was reconstituted in 0.1% TFA MeCN/H_2O (2:3) and lyophilised.

General coupling protocol for coupling DOTA to peptide in solution

To a solution of peptide (5.00 μmol) in dry DMSO (100 μl) was added DOTA (10.1 mg, 25.0 μmol, 5 eq.), NHS (2.88 mg, 25.0 μmol, 5 eq.) and EDC (2.33 mg, 15.0 μmol, 3 eq.). The mixture was sonicated for 30 min at 40 °C. The solution was diluted with H_2O and purified by preparative RP HPLC.[108]

General protocols for radiochemistry

Radiosynthesis was performed either using a GE TRACERlab FXFN, iPHASE FLEXLab or iPHASE MultiSyn housed in a COMECER lead box. [^{18}F]Fluoride was purchased from Cyclotek Aus. Pty. Ltd., prepared using a PETtrace 16.5MeV cyclotron incorporating a high

pressure niobium target for the production of [^{18}F]Fluoride (GE Healthcare). All anhydrous solvents were obtained as 100 ml bottles from Sigma Aldrich. Solvents for formulation and HPLC were obtained from Merck. BAXTER water was used for all formulations and HPLC solvents. QMA and alumina cartridges were purchased from Waters. C18 SPE cartridges were Phenomenex Strata-X 33µ polymeric reversed phase (30mg/ml). RadioTLC was performed on a TLC scanner (Bioscan, BF-C1000).

TRACERlab FXFN and iPHASE dual reactor purification

Semi-preparative high performance liquid chromatography (HPLC) was performed in the GE TRACERlab FXFN using a S1021 solvent delivery system equipped with a UV and scintillation detectors. HPLC was performed in the dual reactor using a KNAUER pump (1050), UV detector (2500) and a manager (5050). Radiation was detected using a KNAUER solid state photodiode scintillator in a TO-5 case.

General protocol for [$^{18}F^{-}$] loading onto QMA cartridge, subsequent elution and formation of anhydrous $K_{222}/K^{+18}F^{-}$ complex

The [^{18}F]fluoride isolated onto the preconditioned QMA cartridge was drained into the reactor using a solution of $KHCO_3$ or $C_2K_2O_4$ (2–4 mg) and kryptofix 2.2.2 (10–12 mg) in H_2O:MeCN (40:60, 1 ml). The solution of $K_{222}/K^{+18}F^{-}$ drained into the reactor was heated (85–100°C) under vacuum and a stream of helium for 7 min then it was further dried for another 10 min at 120 °C under vacuum.

Yield and chemical reaction time determination

The reaction time was measured from the beginning of [^{18}F]fluoride drying to the end of formulation of the final product. The activity in the reactor is the most accurate representation of

[^{18}F]fluoride available for reaction. Thus, the radiochemical yields were calculated from the beginning of the drying step.

General protocol for the formulation of radiolabelled peptides for animal studies

The fraction containing the peptide was collected from the HPLC and diluted with H_2O (20–40 ml). The peptide was isolated from the HPLC mobile phase on a C18 SPE cartridge, which was subsequently washed with PBS (10 ml). The ^{18}F-labelled peptide was then eluted with ethanol (0.3 ml) and diluted with PBS (3 ml).

General protocol for small animal PET imaging

5×10^6 MV4-11 (human acute myeloid leukaemia) cells were implanted subcutaneously in 50 % Matrigel on the right flank of NOD/SCID/Interleukin 2 receptor gamma chain null mice (otherwise known as NSG mice). Tumours were measured using callipers and tumour volume determined according to the equation: $0.5 \times \text{length} \times (\text{width})^2$. On the day of imaging tumour volumes were between 150 and 600 mm^3. 8×10^6 Z138 (human mantle cell lymphoma) cells implanted in 50 % Matrigel into the right flank of Balb/c nudes. Mice were injected with 200 μCi–300 μCi of radiolabelled peptide. Mice were anaesthetized and then scanned for 10 min using Mosaic small animal PET scanner (Philips Medical Systems, Ohio, USA; resolution 2.7 mm at the centre of the FOV) at the desired time point post injection. The Energy window utilised during imaging was within 450–700 keV and a 6ns coincidence-timing window was employed. PET images were acquired in 3D mode and the collated data was corrected for [^{18}F]fluorine decay and random disintegrations. 3D RAMLA algorithm was utilised to reconstruct the images. In addition, the uptake of tracer in different regions of the body was determined using the region of interest

(ROI) software on the Mosaic workstation by drawing ROIs around tumours as well as background regions.

General IC_{50} protocol

CXCR4 affinities were determined through competitive binding assays using U87.CD4.CXCR4 cells with [^{125}I]-SDF-1 as the radioligand. The peptide of interest (at concentrations ranging from 10^{-12} to 10^{-6} M) and [^{125}I]-SDF-1 (20 pM) were mixed with the binding buffer (20 mM HEPES, 0.5% BSA in PBS, pH 7) in 1.5 ml Eppendorf Protein LoBind vials. A suspension of U87.CD4.CXCR4 cells (50,000 cells) was added to each vial to give a final volume of 300 µl. The vials were shaken at 550 rpm for 20 minutes at 37 °C. Immediately after the incubation, the vials were centrifuged at 13,000 rpm for 5 minutes and the supernatant removed. The cell pellet was washed with 500 µl of 50 mM Tris buffer (pH 7) and centrifuged again. The amount of [^{125}I]-SDF-1 bound to the cells was measured using a gamma counter (PerkinElmer).[109]

** This is the protocol used for the IC_{50} "scan" that resulted in undesirable numbers. We believe that assays involving peptides that are not derived from T140 cause [^{125}I]-SDF-1 to stick to the Eppendorf tubes and this is causes the higher than expected values.

Modified IC_{50} protocol

CXCR4 affinities were determined though competitive binding assays using U87.CD4.CXCR4 cells with [^{125}I]-SDF-1 as the radioligand. The peptide of interest (at concentrations ranging from 10^{-12} to 10^{-6} M) and [^{125}I]-SDF-1 (20 pM) were mixed with the binding buffer (20 mM HEPES, 0.5% BSA in PBS, pH 7) in 1.5 ml Eppendorf Protein LoBind vials. A suspension of U87.CD4.CXCR4 cells (50,000 cells) was added to each vial to give a final

volume of 300 µl. The vials were shaken at 550 rpm for 20 minutes at 37 °C. Immediately after the incubation, the solution was passed though a Multiscreen HTS 96-well HV filter plate (Millipore). Each well was washed with binding buffer (200 µl × 2). The filters were punched out of the plate and placed in scintillation tubes. The amount of [^{125}I]-SDF-1 bound to the cells was measured using a gamma counter (PerkinElmer).

cyclo(D-Tyr-Arg-Arg-Nal-Gly) "FC131" (10)

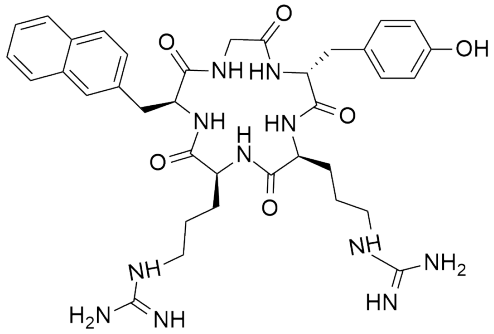

Linear protected D-Tyr(OtBu)-Arg(Pbf)-Arg(Pbf)-Nal-Gly was prepared from glycine-loaded chlorotrityl resin according to general coupling and cleavage protocols. To a solution of linear protected D-Tyr(OtBu)-Arg(Pbf)-Arg(Pbf)-Nal-Gly (115 mg, 0.1 mmol) in DCM (115 ml) was added HATU (38.7 mg, 0.1 mmol) and DIPEA (68 µl, 1.4 mmol) and the reaction mixture was stirred for 4 h. The mixture was concentrated in vacuo to afford crude product, which was dissolved in TFA:H_2O (95:5, 20 ml) and stirred for 2 h. TFA was evaporated by a stream of N_2. Diethyl ether (50 ml/g) was added to precipitate the peptide and the supernatant was decanted. The crude precipitate was then dissolved in H_2O/MeCN (3:2, 50 ml) and lyophilised. Lyophilised material was purified by preparative RP-HPLC (0.1% TFA in 10–50% MeCN:H_2O over 60 min, column D) to afford **10** as a white powder (365 mg, 12% yield). ESI-MS $[M+H]^+$ ($C_{36}H_{48}N_{11}O_6^+$): *m/z* 730.378 (calculated), 730.378 (observed). Analytical data consistent with literature data.[39]

4-Nitrophenyl 2-[^{18}F]fluoropropionate ([^{18}F]NFP) (23)

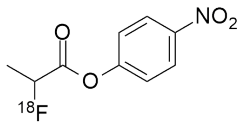

A solution of K_{222} (12–14 mg), $KHCO_3$ (3–7 mg) in MeCN:H_2O (1 ml, 3:2, vial 1, see Table 6) was eluted though the QMA cartridge containing nucleophilic $^{18}F^-$ into the reaction vessel. To the anhydrous $K_{222}{\cdot}K^+$ $^{18}F^-$ complex (1.10 GBq), compound **28** (20.0 mg, 0.07 mmol) in tBuOH:MeCN (2 ml, 4:1, vial 3) was added. After 5 min of heating at 100°C, the reaction solvent was concentrated (~0.5 ml) at 65°C and diluted with 0.1% TFA MeCN:H_2O (3:2, 1.5 ml, vial 4). The reaction mixture was then transferred into the loop vial. The reaction vial was washed with additional 0.05% TFA MeCN:H_2O (3:2, 1.5 ml, vial 6) and transferred to the HPLC loop vial. The reaction mixture was then purified by preparative RP-HPLC (0.05% TFA in 10–50% MeCN:H_2O over 60 min, column F) to afford title compound **23** (196 MBq, 18% yield n.d.c) as a clear solution. Retention time of the analytical sample matched that of an authentic sample. Automation details are illustrated in Table 6.

Position	Reagents or Materials
V 10 – V 11	Sep-Pack Light QMA
V 1	12–14 mg Kryptofix in 700 µl MeCN
V 1	3–7 mg $KHCO_3$ in 300 µl H_2O
V 3	20 mg ester **28** in tBuOH: MeCN (4:1, 2 ml)
V 4	0.05 % TFA MeCN:H_2O (0.9:0.6, 1.5 ml)
V 6	0.05 % TFA MeCN:H_2O (0.9: 0.6, 1.5 ml)
V 9	H_2O (5 ml)
V 14 – V 12	Alumina Cartridge
V 17 – V 15	C18 SPE Cartridge

Table 6: Automation details of [^{18}F]NFP

4-Nitrophenyl 2-bromopropionate (28)

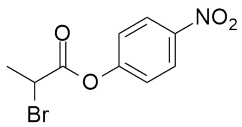

To a solution of (±)-2-bromopropionylbromide **18** (0.48 ml, 4.64 mmol) in DCM (10 ml), 4-nitrophenol **27** (0.66 g, 4.64 mmol) was added. Triethylamine (0.64 ml, 4.64 mmol) was added dropwise at 0°C, and the mixture was stirred for 2 h. The precipitate was removed by filtration and washed with DCM. The filtrate was concentrated under reduced pressure and the residue purified by flash chromatography (1:2 petroleum spirits:ethyl acetate) to afford the purified product **28** (1.07 g, 96% yield) as a white solid. ^{1}H NMR (500 MHz, $CDCl_3$) δ 8.28 (d, 2H, *J*=9.1 Hz), 7.31 (d, *J*=9.1 Hz, 2H), 4.60 (q, 1H, *J*=6.8 Hz), 1.94 (d, 3H, *J*=6.8 Hz). ^{13}C NMR (125 MHz, $CDCl_3$)

δ 167.8, 154.9, 125.2, 122.0, 38.9, 21.1. (lit. m.p. 37–39 °C).[42] Analytical data consistent with literature data.[68]

4-Nitrophenyl 2-fluoropropionate

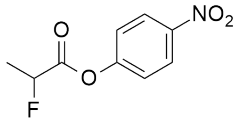

To a suspension of 2-fluoropropionic acid **62** (22.0 mg, 0.24 mmol) in THF (2 ml), DCC (49.3 mg, 0.24 mmol) and 4-nitrophenol **27** (33.3 mg, 0.24 mmol) were added. The reaction was stirred overnight and the solvent was evaporated under reduced pressure. The residue was purified by RP-HPLC (0.1 % TFA in 20–100 % MeCN:H_2O over 80 min, Column B) to afford the title compound as a white solid after lyophilisation (15.3 mg, 30% yield) ^{1}H NMR (500 MHz, $CDCl_3$) δ 8.30 (d, 2H, *J*=9.0 Hz), 7.34 (d, 2H, *J*=9.0 Hz), 5.28 (dq, 1H, *J*=48.2, 6.9 Hz), 1.76 (dd, 3H, *J*=23.4, 6.9 Hz). ^{13}C NMR (125 MHz, $CDCl_3$) δ 167.9, 154.5, 145.7, 125.3, 122.1, 85.2, 18.1. ^{19}F NMR (470 MHz, $CDCl_3$) δ –129.8. (lit. m.p. 78–79 °C). Analytical data consistent with literature data.[68]

2,3,5,6-Tetrafluorophenyl 4-[^{18}F]fluoronicotinate ([^{18}F]TFN) (33)

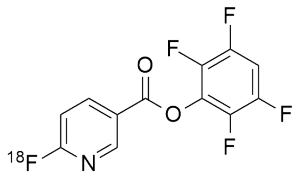

[^{18}F]Fluoride in [^{18}O] water was transferred to the iPHASE FlexLAB radiosynthesis module and passed through a pre-conditioned QMA cartridge. Trapped [^{18}F]fluoride (2.15–6.26 GBq) was eluted into the reaction vessel with a solution containing $KHCO_3$ (2–3 mg, 20–30 μmol) and Kryptofix 2.2.2 (10–12 mg, 27–32 μmol) in 300 μl H_2O/700 μl MeCN. The solution was

evaporated at 65°C under nitrogen flow and vacuum for 13 min, followed by heating at 120°C under nitrogen then vacuum for a further 7 min. To the anhydrous [^{18}F]KF/K_{222}/$KHCO_3$ residue, precursor **126** (10 mg, 3.0 μmol) in DMSO:tAmOH (0.4:0.6, 1 ml) was added. After 5 min at 100 °C, the solvent was evaporated to half volume, and the residue was diluted with 0.05% TFA in H_2O/MeCN (1.3:0.2, 1.5 ml). The mixture was transferred to the loop injection vial. The reaction vial was washed with 0.05% TFA in H_2O/MeCN (1.3:0.2, 1.5 ml). and transferred to the loop injection vial. Purification by preparative HPLC (0.05% TFA in 15–80% MeCN:H_2O over 40 min, column F) afforded the title compound **33** (356–854 MBq, 35–75% yield (n=3) decay corrected to SOS). The total reaction time was 40 min. Automation details are illustrated in Table 7.

2,3,5,6-Tetrafluorophenyl 6-fluoronicotinate

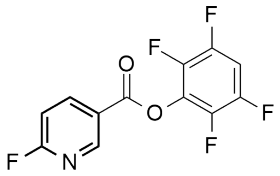

To fluoronicotinic acid (1.00 g, 7.14 mmol, 1 eq.) tetrafluorophenol **134** (0.986 g, 7.14 mmol, 1 eq.) and EDC.HCl (1.35 g, 7.14 mmol, 1 eq.) was added DMF (~ 5 ml) and stirred for 4 h. H_2O (5 ml) was added and the product was then extracted into DCM (3 × 50 ml), washed with H_2O (3 × 50 ml) and 0.1M HCl (3 × 50 ml). The residue was recrystallised from DCM to afford product as yellow crystals (1.64 g, 79% yield). ^{1}H NMR (500 MHz, $CDCl_3$): δ 9.10 (dt, *J*=2.5, 0.5 Hz, 1H), 8.57 (ddd, *J*=8.6, 7.4, 2.5 Hz, 1H), 7.13 (ddd, *J*=8.6, 3.0, 0.5 Hz, 1H), 7.09 (tt, *J*=9.9, 7.2 Hz, 1H). ^{13}C NMR (101 MHz, $CDCl_3$) δ 166.6 (d, *J* = 245.3 Hz), 160.6, 151.2, 148.1–148.3 (m), 147.1–147.4 (m), 145.3–145.8 (m), 142.6–142.9 (m), 126.1, 111.3 (d, *J*=37.9 Hz), 105.1–105.9 (m). ^{19}F NMR (470 MHz, $CDCl_3$): δ –58.3 (dd, *J*=2.5, 7.4 Hz), –138.8–140.1 (m), –152.9–

153.8 (m). ESI-MS $[M+H]^+$ ($C_{12}H_5F_5NO_2^+$): *m/z* 290.023 (calculated), 290.023 (observed). Analytical data consistent with literature data.[62]

cyclo(D-Tyr-Lys-Arg-Nal-Gly) (38)

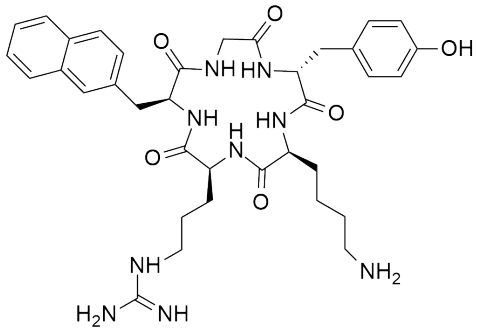

Linear protected D-Tyr(OtBu)-Lys(Boc)-Arg(Pbf)-Nal-Gly **47** was prepared from glycine-loaded chlorotrityl resin according to general coupling and cleavage protocols. To a solution of linear protected D-Tyr(OtBu)-Lys(Boc)-Arg(Pbf)-Nal-Gly **47** (113 mg, 0.1 mmol) in DCM (113 ml) was added HATU (38.7 mg, 0.1 mmol) and DIPEA (68 µl, 0.1 mmol) and the reaction mixture was stirred for 4 h. The mixture was concentrated in vacuo to afford crude product, which was dissolved in TFA:H_2O (95:5, 20 ml) and stirred for 2 h. TFA was evaporated by a stream of N_2. Diethyl ether (50 ml/g) was added to precipitate the peptide and the supernatant was decanted. The crude precipitate was then dissolved in H_2O/MeCN (3:2, 50 ml) and lyophilised. Purification was achieved by preparative RP-HPLC (0.1% TFA in 10–25% MeCN:H_2O over 50 min, column C) to afford the product **38** (47.2 mg, 20% based on initial resin loading) as a white powder. ESI-MS $[M+H]^+$ ($C_{36}H_{48}N_9O^+$): *m/z* 702.372 (calculated), 702.372 (observed). ^{1}H NMR (700 MHz, d_6-DMSO) δ 8.39 (d, *J*=7.1 Hz, 1H), 8.20 (d, *J*= 6.6 Hz, 1H), 7.87 (d, *J*=7.7 Hz, 1H), 7.83 (d, *J*=4.5 Hz, 1H), 7.68 (s, 1H), 7.47–7.41 (m, 3H), 7.37 (d, *J*=8.3 Hz, 1H), 6.95 (d, *J*=8.4 Hz, 2H), 6.65 (d, *J*=8.3 Hz, 2H), 4.12 (dd, *J*=16.0, 7.0 Hz, 1H), 3.88–3.81 (m, 1H), 3.77 (dd, *J*=15.5 Hz, 7.0 Hz, 1H), 3.21–3.15 (m, 3H), 3.14 (dd, *J*=13.1, 7.7 Hz, 2H), 2.77–2.68 (m, 5H), 2.69–2.62 (m, 3H),

1.57–1.52 (m, 3H), 1.46–1.35 (m, 4H), 1.27–1.12 (m, 5H), 1.15 (d, *J*=7.5 Hz, 2H), 0.94 (d, *J*=7.4 Hz, 1H), 0.85–0.72 (m, 2H), 0.79–0.71 (m, 2H).

cyclo(D-Tyr(SO$_3$H)-Lys-Arg-Nal-Gly) (39)

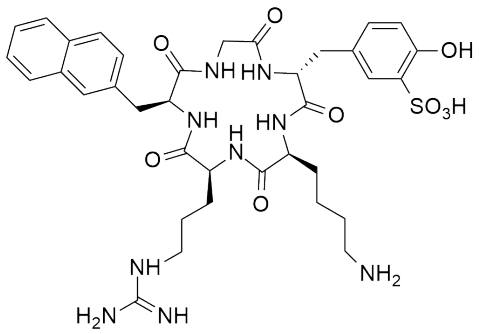

Linear protected D-Tyr(OtBu)-Lys(Boc)-Arg(Pbf)-Nal-Gly **60** was prepared from glycine-loaded chlorotrityl resin and solid phase peptide synthesis protocols. To a solution of linear protected D-Tyr(OtBu)-Lys(Boc)-Arg(Pbf)-Nal-Gly **60** (78.1 mg, 0.448 mmol) in DMF (1 ml) and DCM (80 ml) was added HOBt (22.8 mg, 0.150 mmol) and DIC (47 µl, 0.3 mmol) and the reaction was stirred for 4 h. The mixture was concentrated in vacuo to afford crude product, which was dissolved in TFA:H_2O (95:5, 20 ml) and stirred for 2 h. TFA was evaporated by a stream of N_2. Diethyl ether (50 ml/g) was added to precipitate the peptide and the supernatant was decanted. The crude precipitate was then dissolved in H_2O/MeCN (3:2, 50 ml) and lyophilised. Purification was achieved by preparative RP-HPLC (0.1% TFA in 10–25% MeCN:H_2O over 50 min, column C) to afford the product **39** as a white powder (10 mg, 5% based on initial resin loading). ESI-MS $[M+H]^+$($C_{36}H_{47}N_9O_9S^+$): *m/z* 782.373 (calculated), 782.373 (observed). δ ^{1}H NMR (700 MHz, D_2O) δ 7.85–7.79 (m, 3H), 7.80 (d, *J*=7.8 Hz, 1H), 7.68 (s, 1H), 7.47–7.41 (m, 2H), 7.39 (dd, *J*=8.8, 1.5 Hz, 1H), 7.20 (dd, *J*=8.7, 2.3 Hz, 1H), 6.89 (d, *J*=8.7 Hz, 1H), 4.08 (m, 1H), 3.98 (t, *J*=7.9 Hz, 1H), 3.66–3.78 (m, 3H), 3.30 (dd, *J*=12.3, 6.0 Hz, 3H), 3.08–3.01 (m, 2H), 2.81–2.64 (m, 5H), 2.61–2.52 (m, 3H), 1.57–1.51 (m, 3H),

1.44–1.40 (m, 4H), 1.35–1.27 (m, 4H), 1.23 (td, *J*=14.7, 6.1 Hz, 1H), 1.12 (ddd, *J*=19.6, 10.9, 6.5 Hz, 2H), 0.93 (dt, *J*=14.9, 8.9 Hz, 1H), 0.80–0.73 (m, 2H), 0.69–0.65 (m, 2H).

cyclo(D-Tyr-(SO$_3$H)-Lys-Arg-Nal(SO$_3$H)-Gly) (51)

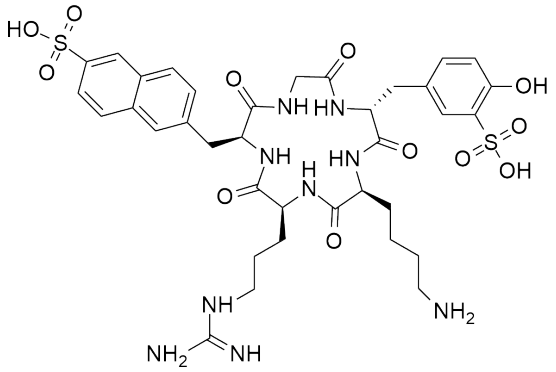

To a solution of c(D-Tyr-Lys-Arg-Nal-Gly) **38** (4.0 mg, 5.7 μmol) in TFA (0.30 ml), chlorosulfonic acid (20 μl, 0.30 mmol) was added and a white precipitate was formed instantaneously. The peptide was left to stand for 30 min, after which H_2O (1 ml) was added and the reaction mixture was concentrated by a stream of nitrogen to about 0.5 ml. The residue was diluted with H_2O (2 ml) and directly purified by preparative RP-HPLC (0.1% TFA in 0–40% MeCN:H_2O over 50 min, column C) to afford the product **51** (3.0 mg, 75% yield) as a white powder. ESI-MS $[M+H]^+$ ($C_{36}H_{48}N_9O_{12}S_2^+$): *m/z* 862.286 (calculated), 862.286 (observed). ^{1}H NMR (500 MHz, D_2O) δ 8.48 (s, 1H), 8.11 (t, *J*=8.1 Hz, 2H), 8.01 (d, *J*=8.5 Hz, 1H), 7.58–7.52 (m, 3H), 7.29 (dd, *J*=8.5, 2.3 Hz, 1H), 6.98 (d, *J*= 8.4 Hz, 1H), 4.45 (m, 1H), 4.15 (m, 1H), 4.04 (m, 1H), 3.80 (m, 1H), 3.43–3.37 (m, 3H), 3.15–3.02 (m, 5H), 2.88–2.62 (m, 5H), 2.63 (dd, *J*=13.8, 5.3 Hz, 1H), 2.51–2.42 (m, 2H), 1.65–1.57 (m, 3H), 1.45–1.37 (m, 4H), 1.34–1.29 (m, 4H), 1.25 (m, 1H), 1.18–1.12 (m, 2H), 0.90 (m, 1H), 0.76–0.71 (m, 2H), 0.54–0.48 (m, 2H).

cyclo(D-Tyr-Lys-Arg-Nal(SO$_3$H)-Gly) (52)

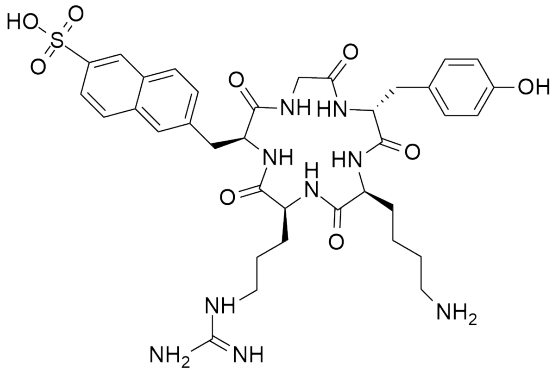

To a solution of c(D-Tyr-Lys-Arg-Nal-Gly) **38** (4.0 mg, 5.70 μmol) in TFA (0.30 ml), chlorosulfonic acid (0.40 μl, 5.70 μmol) was added. The peptide was left to stand for 30 min, after which H_2O (1 ml) was added and the reaction mixture was concentrated by a stream of nitrogen (~0.5 ml). The concentrated mixture was then further diluted by H_2O (2 ml) and purified by preparative RP-HPLC (0.1% TFA in 0–30% MeCN:H_2O over 100 min, column C) to afford the product **52** as a white powder (2.0 mg, 50% yield). ESI-MS $[M+H]^+$: ($C_{36}H_{48}N_9O_9S^+$) *m/z* 782.329 (calculated), 782.329 (observed). ^{1}H NMR (700 MHz, D_2O) δ 8.39 (s, 1H), 8.02–7.98 (m, 2H), 7.93 (m, 1H), 7.48–7.41 (m, 2H), 7.06 (d, *J*=8.8 Hz, 2H), 6.78–6.71 (m, 2H), 4.37 (dd, *J*=11.1, 6.0 Hz, 1H), 4.04 (m, 1H), 3.94 (dd, *J*=10.6, 5.6 Hz, 1H), 3.37–3.35 (m, 2H), 3.33–3.22 (m, 4H), 3.00 (m, 1H), 2.80–2.58 (m, 6H), 2.54 (m, 1H), 2.38 (m, 1H), 1.59–1.49 (m, 3H), 1.45–1.41 (m, 4H), 1.39–1.24 (m, 6H), 1.11–1.08 (m, 2H), 0.82–0.75 (m, 4H).

N-(9H-fluoren-9-yl)methoxy)carbonyl)amino)-D-tyrosine-3-sulfonate (54)

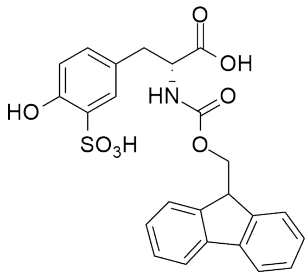

To a solution of D-tyrosine **57** (500 mg, 2.76 mmol) in TFA (2.00 ml), chlorosulfonic acid (928 µl, 14.0 mmol) was added. The reaction was left for 30 min, then H_2O was added (1 ml) and the reaction mixture was concentrated by a stream of nitrogen (~0.5 ml). Diethyl ether (50 ml) was added and the supernatant was decanted to afford sulfonated tyrosine **58** as white powder. The precipitate was dissolved in H_2O:dioxane (1:2, 150 ml) and the pH was adjusted to 7 with the addition of 10% $NaHCO_3$ (10 ml). To this mixture, Fmoc-OSu (1.05 g, 3.1 mmol) and $NaHCO_3$ (471 mg, 5.61 mmol) were added and the solution was stirred for 4 h. The volatiles were evaporated under reduced pressure and washed with diethyl ether (3 × 100 ml) to remove unreacted Fmoc-OSu. The aqueous layer was then acidified to pH 3 with concentrated HCl and extracted into ethyl acetate (3 × 300 ml). The combined organic layers were dried over magnesium sulfate and concentrated under reduced pressure. The crude material was then purified by preparative RP-HPLC (0.1% TFA in 0–60% MeCN:H_2O over 60 min, column D) to afford product **54** as a white powder (1.21 g, 92% yield) ESI-MS $[M+H]^+$ ($C_{24}H_{21}NO_8S^+$) *m/z* 484.101 (calculated), 484.101 (observed). ^{1}H NMR (500 MHz, D_2O) δ 8.31 (s, 1H), 7.73–7.70 (m, 2H), 7.45–7.40 (m, 3H), 7.21–7.15 (m, 3H), 6.98 (dd, *J*=8.1, 1.1 Hz, 1H), 6.74 (d, *J*=8.0 Hz, 1H), 4.41 (dd, *J*=10.5 Hz, 6.2 Hz, 1H), 4.13 (m, 1H). 3.98 (t, J=5.6 Hz, 1H), 3.01 (dd, *J*=13.9, 4.4 Hz, 1H), 2.73 (dd, *J*=11.1, 6.4 Hz, 1H), 2.54 (d, *J*=13.5 Hz, 1H), 2.09 (s, 1H), 1.37 (m, 1H), 1.25 (dd, *J*=16.1, 8.9 Hz, 1H). ^{13}C NMR (125 MHz, D_2O) δ 176.6, 151.6, 151.4, 150, 148.5, 133.8, 133.0, 129.1, 127.8, 127.3, 126.1, 124.8, 120.6, 117.2, 68.8, 57.1, 46.8, 36.7.

cyclo(D-Tyr(SO$_3$H)-Lys(FP)-Arg-Gly) (63)

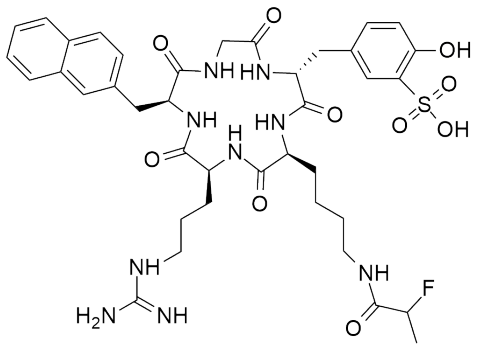

To a suspension of 2-fluoropropionic acid **62** (0.40 µl, 5.0 µmol), HOBt (0.40 mg, 2.0 µmol), DIC (0.80 µl, 5.0 µmol) in DMF (0.5 ml), c(D-Tyr(SO$_3$H)-Lys-Arg-Gly) **39** (1.0 mg, 2.0 µmol) was added. After 4 h, the reaction was diluted with water and then purified by preparative RP-HPLC (0.1 % TFA in 0–10 % MeCN:H_2O over 100 min, column A) to afford the product **63** as a white powder (1.3 mg, 76% yield). ESI-MS $[M+H]^+$ ($C_{39}H_{50}FN_9O_{10}S^+$) *m/z* 856.351 (calculated), 856.351 (observed). ^{1}H NMR (700 MHz, D_2O) δ 7.82–7.72 (m, 4H), 7.68 (s, 1H), 7.47–7.41 (m, 3H), 7.40–7.37 (m, 2H), 7.18 (d, *J*=11.0 Hz, 1H), 6.88 (d, *J*=8.6 Hz, 1H), 4.37 (d, *J*=16.9 Hz, 1H), 4.02–3.90 (m, 4H), 3.81–3.77 (m, 2H), 3.68–3.62 (m, 2H), 3.50 (dd, *J*=14.6, 7.4 Hz, 1H), 3.35 (m, 1H), 3.27–3.19 (m, 3H), 3.07–2.95 (m, 5H), 2.79–2.73 (m, 2H), 2.65–2.58 (m, 3H), 2.37–2.33 (m, 2H), 2.18 (m, 1H), 1.60 (m, 1H), 1.44–1.39 (m, 5H), 1.33–1.28 (m, 2H), 0.80–0.71 (m, 2H).

cyclo(D-Tyr-Lys(FP)-Arg-Nal-Gly)

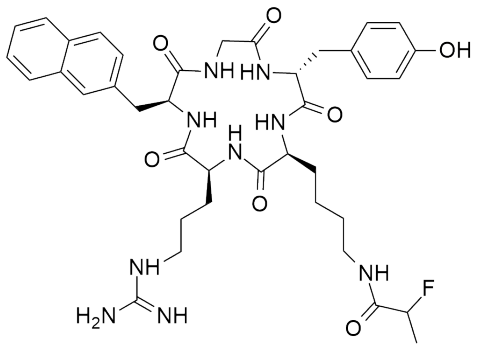

To a suspension of 2-fluoropropionic acid **62** (0.40 µl, 5.0 µmol), HOBt (0.40 mg, 2.0 µmol), DIC (0.80 ul, 5.0 µmol) in DMF (0.5 ml), c(D-Tyr-Lys-Arg-Nal-Gly) **38** (1.0 mg, 2.0 µmol) was added. After 4 h, the reaction was diluted with H_2O purified by preparative RP-HPLC (0.1 % TFA in 0–10 % MeCN:H_2O over 100 min, column A) to afford the title peptide as a white powder (1.1 mg, 71% yield). ESI-MS $[M+H]^+$ ($C_{39}H_{50}FN_9O_7^+$) *m/z* 776.362 (calculated), 776.362 (observed).

cyclo(D-Tyr-Lys(FP)-Arg-Nal(SO$_3$H)-Gly)

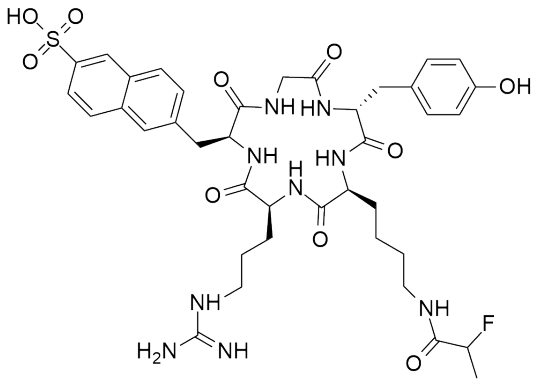

To a suspension of 2-fluoropropionic acid **62** (0.40 µl, 5.0 µmol), HOBt (0.40 mg, 2.0 µmol), DIC (0.80 ul, 5.0 µmol) in DMF (0.5 ml), c(D-Tyr-Lys-Arg-Nal(SO_3H)-Gly) **52** (1.0 mg, 2.0 µmol) was added. After 4 h, the reaction was diluted with water and then purified by

preparative RP-HPLC (0.1% TFA in 0–10 % MeCN:H_2O over 100 min, column A) to afford title peptide as a white powder (1.4 mg, 82% yield) ESI-MS $[M+H]^+$ ($C_{39}H_{50}FN_9O_{10}S^+$) *m/z* 856.351 (calculated), 856.351 (observed).

cyclo(D-Tyr(SO$_3$H)-Lys(FP)-Arg-Nal(SO$_3$H)-Gly)

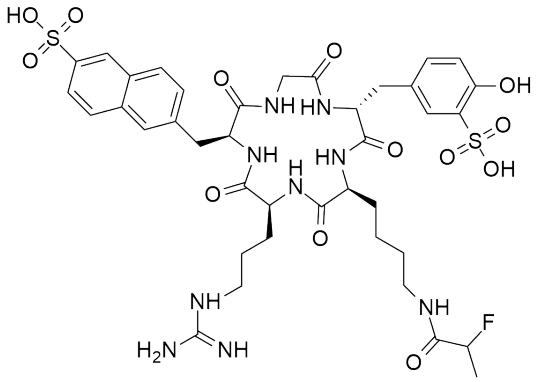

To a suspension of 2-fluoropropionic acid **62** (0.40 µl, 5.0 µmol), HOBt (0.40 mg, 2.0 µmol), DIC (0.80 ul, 5.0 µmol) in DMF (0.5 ml), c(D-Tyr(SO_3H)-Lys-Arg-Nal(SO_3H)-Gly) **51** (1.0 mg, 2.0 µmol) was added. After 4 h, the reaction was diluted with water and then purified by preparative RP-HPLC (0.1 % TFA in 0–10 % MeCN:H_2O over 100 min, column A) to afford title peptide as a white powder (1.5 mg, 79% yield). ESI-MS $[M+H]^+$ ($C_{39}H_{51}FN_9O_{13}S_2^+$): *m/z* 936.302 (calculated), 936.302 (observed).

cyclo(D-Tyr(SO$_3$H)-Lys([^{18}F]FP)-Arg-Nal-Gly) (64)

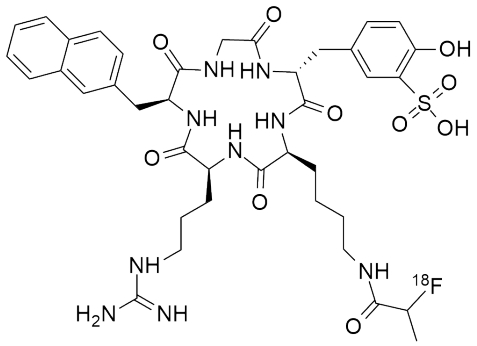

The [^{18}F]NFP **23** (178 MBq) isolated on a C18 SPE cartridge was eluted by DMSO (0.3 ml) into a vial charged with c(D-Tyr(SO_3H)-Lys-Arg-Nal-Gly) **39** (0.5 mg, 0.58 μmol) and a solution of TEA: DMSO (1:20, 10 μl) was subsequently added. After 1 h, the material (59.2 MBq) was analysed by RP-HPLC (0.05 % TFA in 0–80 % MeCN:H_2O over 40 min column G) to afford product **64** in 58% d.c yield (specific activity: 0.45 MBq/μg). The analytical trace of the radiolabelled material **64** matched that of the fully characterised cold material **63**.

Fmoc-D-Orn(Alloc)-OH

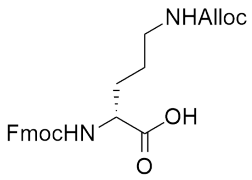

Fmoc-D-Orn(Boc)-OH (600 mg, 1.3 mmol, 1 eq.) was dissolved in a solution of 30% TFA in DCM (5 ml) and the reaction was stirred for 1 h. The TFA was evaporated under reduced pressure and then further dried under high vacuum. The mixture was dissolved in H_2O (12.5 ml) and Na_2CO_3 (551 mg, 5.2 mmol). Allyl chloroformate (138 μl, 1.3 mmol) dissolved in THF (12.5 ml) was added to the reaction dropwise. The reaction was stirred for 4 h and THF was evaporated under reduced pressure. The aqueous layer was washed with diethyl ether (1 × 25 ml), acidified with conc. HCl to pH 1 and the product extracted with ethyl acetate (3 × 25 ml). The combined organic layers were dried over Na_2SO_4 and concentrated under reduced pressure to give the product as a colourless syrup (0.51g, 90% yield). ^{1}H NMR (400 MHz, d_6-DMSO) δ 12.55 (s, 1H), 7.86 (dd, *J*=11.2, 7.2 Hz, 2H), 7.71 (d, *J*=7.4 Hz, 2H), 7.63 (d, *J*=8.0 Hz, 1H), 7.40 (t, *J*=7.4 Hz, 2H), 7.30 (dd, *J*=12.9, 5.8 Hz, 2H), 7.19 (t, *J*=5.2 Hz, 1H), 5.88 (ddd, *J*=22.4, 10.5, 5.3 Hz, 1H), 5.24 (d, *J*=17.3 Hz, 1H), 5.14 (d, *J*=10.4 Hz, 1H), 4.44 (d, *J*=5.1 Hz, 2H), 4.22–4.18 (m, 3H), 3.91 (dt, *J*=8.7, 4.6 Hz, 1H), 2.97–2.93 (m, 2H), 1.70 (m, 1H), 1.45–1.39 (m, 3H). ^{13}C NMR (101 MHz, d_6-

DMSO) δ 174.3, 163.2, 156.5, 143.5, 141.3, 141.2, 133.1, 128.1, 127.5, 125.7, 123.0, 120.6, 99.8, 66.0, 54.0, 47.1, 39.0, 31.4, 31.1, 30.7, 30.6, 29.6, 26.9, 25.5. ESI-MS $[M+H]^+$ ($C_{24}H_{27}N_2O_6^+$): *m/z* 439.186 (calculated), 429.186 (observed). Analytical data consistent with literature data.[110]

4-((Allyloxycarbonyl)aminomethyl)benzoic acid (73)

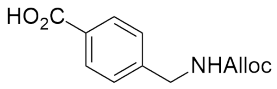

A solution of 4-(aminomethyl))benzoic acid (100 mg, 0.66 mmol) and 10% $NaHCO_3$ (2 ml) in dioxane (1.0 ml) was cooled to 0°C. The mixture was treated with a solution of allyl chloroformate (70 µl, 0.66 mmol) warmed to rt and stirred for 12 h. The dioxane was evaporated under reduced pressure and the aqueous layer washed with diethyl ether (1 × 6 ml), acidified with conc. HCl (~1 ml) to pH 1 and the product extracted with ethyl acetate (3 × 6 ml). The combined organic layers were dried over Na_2SO_4 and concentrated under vacuum to give title compound **73** as a colourless syrup (150 mg, 95% yield). ^{1}H NMR (400 MHz, d_6-DMSO) δ 12.02, (bs, 1H), 7.88 (d, *J*=8.0 Hz, 2H), 7.34 (d, *J*=8.0 Hz, 2H), 5.88 (m, 1H), 5.27 (d, *J*=17.1 Hz, 1H), 5.16 (d, *J*=10.6 Hz, 1H), 4.49 (t, *J*=7.5 Hz, 2H), 4.23 (m, *J*=8.9 Hz, 2H).^{13}C NMR (101 MHz, d_6-DMSO) δ 170.8, 129.8, 127.4, 117.5, 101.7, 66.8, 64.7, 60.2, 53.3, 43.9. ESI-MS $[M+H]^+$ ($C_{12}H_{14}NO_4^+$): *m/z* 236.091 (calculated), 236.091 (observed). Analytical data consistent with literature data.[66]

cyclo(D-Tyr-N(Me)-D-Orn(Amba, DOTA)-Arg-Nal-Gly) (78)

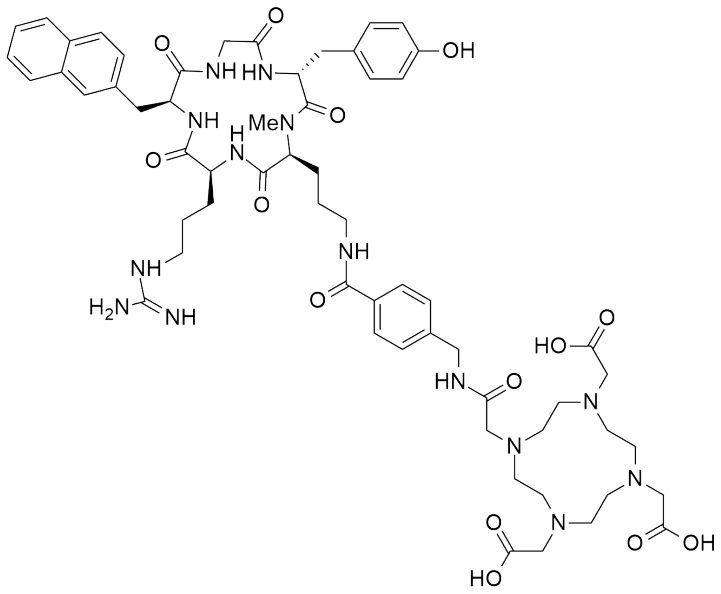

Method A: Linear protected D-Tyr(OtBu)-N(Me)-D-Orn(Amba, DOTA(OtBu)$_3$)-Arg(Pbf)-Nal-Gly **76** was prepared from glycine-loaded chlorotrityl resin according to general coupling, cleavage, methylation, alloc deprotection and coupling of carboxylic acids on resin protocols. To a solution of linear protected D-Tyr(OtBu)-N(Me)-D-Orn(Amba, DOTA(OtBu)$_3$)-Arg(Pbf)-Nal-Gly **76** (171 mg, 0.1 mmol) in DCM (171 ml) was added HATU (38.7 mg, 0.1 mmol) and DIPEA (68 µl, 0.4 mmol) and the reaction was stirred for 12 h. The mixture was concentrated under reduced pressure and globally deprotected with a solution of 95% TFA, 2.5% H_2O and 2.5% TIPS (5 ml). The crude material was purified by preparative RP-HPLC (0.1% TFA 0–30% MeCN:H_2O over 10 min, 30–35% over 30 min, 35%–95% over 10 min, Column D) to afford product **78** as a white powder (0.6 mg, 0.5 % yield overall yield based on initial resin loading). ESI-MS $[M+H]^+$ ($C_{60}H_{81}N_{14}O_{14}^+$) *m/z* 1221.605 (calculated), 1221.605 (observed). Analytical data consistent with literature data.[66]

Method B: To a solution of c(D-Tyr-N(Me)-D-Orn-Arg-Nal-Gly) **106** (5.00 mg, 7.12 μmol, 1 eq.), HATU (5.40 mg, 14.2 μmol, 2 eq.) in DMF (100 μl), N-Boc amino methyl benzoic acid **118** (3.56 mg, 14.2 μmol, 2 eq.) and DIPEA (4.95 ul, 28.5 μmol, 4 eq.) were added and the reaction was stirred for 1 h to afford **119**. Boc deprotection was then performed with 95% TFA in DCM (30 ml) for 1 h and the TFA removed under N_2 for 20 min. The crude reaction mixture was then reacted with DOTA (14.4 mg, 35.6 μmol, 5 eq.), NHS (4.09 mg, 35.6 μmol, 5 eq.), EDC (3.32 mg, 21.4 μmol, 3 eq.), DIPEA (4.95 μl, 28.5 μmol, 4 eq) in DMSO (100 μl) and sonicated for 30 min. The mixture was diluted with H_2O (4 ml) and then purified with preparative RP-HPLC (0.1% TFA 0–30% MeCN:H_2O over 10 min, 30–35% over 30 min, 35%–95% over 10 min, column D) to afford product **78** as a white powder (9.8 mg, 8.0% overall yield based on initial resin loading) ESI-MS $[M+H]^+$ ($C_{60}H_{81}N_{14}O_{14}^+$): *m/z* 1221.605 (calculated), 1221.605 (observed). Analytical data consistent with literature data.[66]

cyclo(D-Tyr(SO$_3$H)-N(Me)-D-Orn(Amba, DOTA)-Arg-Nal-Gly) (79)

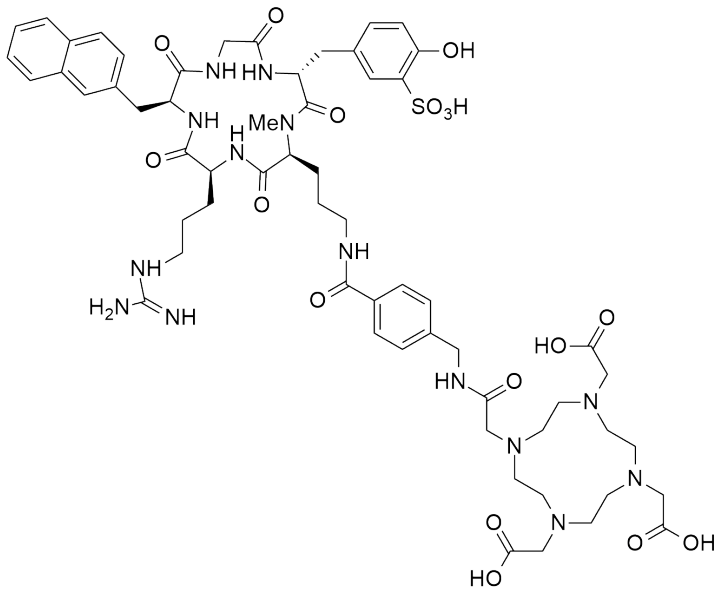

***Method A**:* Linear protected D-Tyr(SO$_3$H)-N(Me)-D-Orn(Amba, DOTA(OtBu)$_3$)-Arg(Pbf)-Nal-Gly **77** was prepared from glycine-loaded chlorotrityl resin according to general coupling, cleavage, methylation, alloc deprotection and coupling of carboxylic acids on resin protocols. To a solution of linear D-Tyr(SO$_3$H)-N(Me)-D-Orn(Amba, DOTA(OtBu)$_3$)-Arg(Pbf)-Nal-Gly **77** (174 mg, 0.1 mmol) in DCM (174 ml) was added HATU (38.7 mg, 0.1 mmol) and DIPEA (68 µl, 1.24 mmol) and the reaction was stirred for 12 h. The mixture was concentrated under reduced pressure and then globally deprotected with a solution of 95% TFA, 2.5% H_2O and 2.5% TIPS (5 ml). The crude material was purified by preparative RP-HPLC (0.1% TFA 0–30% MeCN:H_2O over 10 min, 30–35% over 30 min, 35%–95% over 10 min, Column D) to afford product **79** as a white powder (1.0 mg, 0.8% overall yield based on initial resin loading). ESI-MS $[M+H]^+$ ($C_{60}H_{81}N_{14}O_{17}S^+$): *m/z* 1301.561 (calculated), 1301.561 observed).

Method B: To a solution of c(D-Tyr(SO$_3$H)-N(Me)-D-Orn-Arg-Nal-Gly-OH) **107** (5.00 mg, 6.39 µmol, 1 eq.), HATU (4.86 mg, 12.8 µmol, 2 eq.) in DMF (100 µl), N-Boc amino methyl

benzoic acid **118** (3.21 mg, 12.8 µmol, 2 eq.) and DIPEA (4.44 µl, 25.6 µmol, 4 eq.) were added and the reaction was stirred for 1 h. Global deprotection was then performed with 95% TFA in DCM (30 ml) for 1 h and TFA was removed under N_2 for 20 min. The crude reaction mixture was then reacted with DOTA (12.9 mg, 31.9 µmol, 5 eq.), NHS (3.67 mg, 31.9 µmol, 5 eq.), EDC (3.67 mg, 19.2 µmol, 3 eq.), DIPEA (4.44 µl, 28.5 µmol, 4 eq) in DMSO (100 µl) and sonicated for 30 min. The mixture was diluted with H_2O (4 ml) and then purified with preparative RP-HPLC (0.1% TFA 0–30% MeCN:H_2O over 10 min, 30–35% over 30 min, 35%–95% over 10 min, column D) to afford product **79** as a white powder (13.0 mg, 10% yield based on initial resin loading) ESI-MS $[M+H]^+$ ($C_{60}H_{81}N_{14}O_{17}S^+$): *m/z* 1301.561 (calculated), 1301.561 observed).

cyclo(D-Tyr-N(Me)-D-Orn(Amba, DOTA, Ga)-Arg-Nal-Gly) (80)

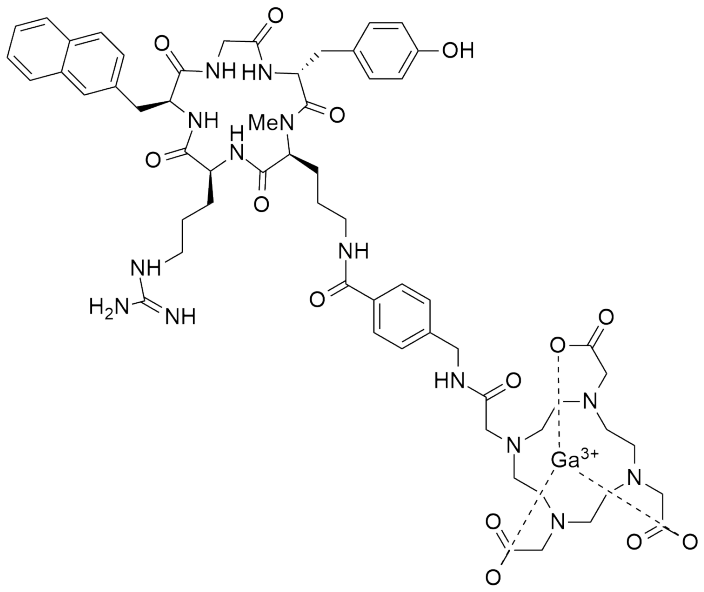

To c(D-Tyr-N(Me)-D-Orn(Amba, DOTA)-Arg-Nal-Gly) **78** (1.0 mg, 0.82 µmol, 1.0 eq.), ammonium acetate (0.5 ml, 0.01 M) was added and the reaction was treated with gallium nitrate (2.0 mg, 8.19 µmol, 10 eq.) After 24 h of stirring at rt, the solution was purified by preparative RP-HPLC (0.1% TFA 0–30% MeCN:H_2O over 10 min, 30–35% over 30 min, 35%–95% over 10 min,

column D) to afford product **80** as a white powder (0.8 mg, 75% yield). ESI-MS $[M+H]^+$ ($C_{60}H_{78}GaN_{14}O_{14}^+$): *m/z* 1287.507 (calculated), 1287.507 (observed). Analytical data consistent with literature data.[66]

cyclo(D-Tyr(SO$_3$H)-N(Me)-D-Orn(Amba, DOTA, Ga)-Arg-Nal-Gly) (81)

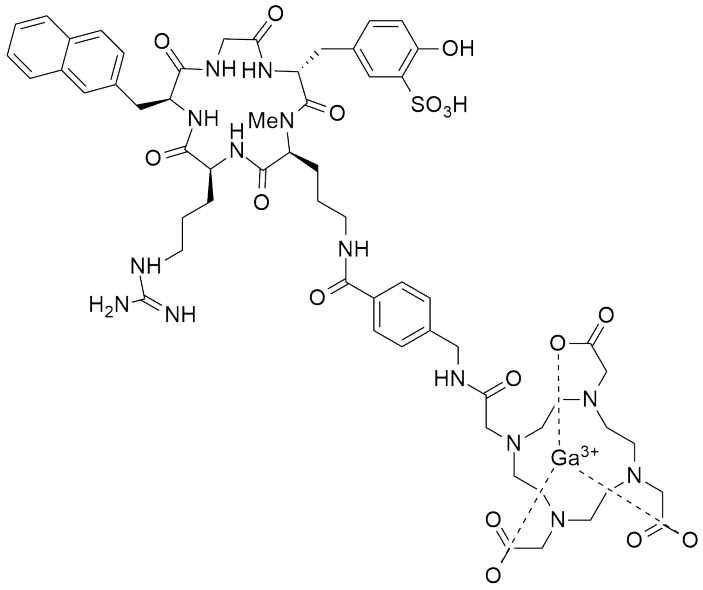

To c(D-Tyr(SO$_3$H)-N(Me)-D-Orn(Amba, DOTA)-Arg-Nal-Gly) **79** (1.0 mg, 0.82 μmol, 1.0 eq.), ammonium acetate (0.5 ml, 0.01M) was added and the reaction was treated with gallium nitrate (2.0 mg, 8.19 μmol, 10 eq.) After 24 h of stirring at rt, the solution was purified by preparative RP-HPLC (0.1% TFA 0–30% MeCN:H_2O over 10 min, 30–35% over 30 min, 35%–95% over 10 min, column D) to afford product **81** as a white powder (0.9 mg, 80% yield). ESI-MS $[M+H]^+$ ($C_{60}H_{78}GaN_{14}O_{17}S^+$): *m/z* 1367.464 (calculated), 1367.464 observed.

cyclo(D-Tyr-N(Me)-D-Orn(FB)-Arg-Nal-Gly) (88)

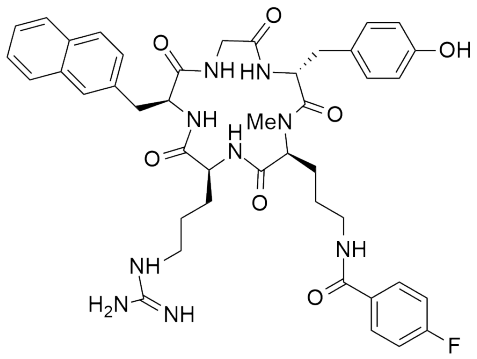

***Method A*:** Linear protected D-Tyr(OtBu)-N(Me)-D-Orn(FB)-Arg(Pbf)-Nal-Gly **84** was prepared from glycine-loaded chlorotrityl resin according to general coupling, cleavage and methylation on resin protocols. To a solution of linear protected D-Tyr(OtBu)-N(Me)-D-Orn(FB)-Arg-Nal-Gly **84** (115 mg, 0.1 mmol) in DCM (115 ml) was added HATU (38.7 mg, 0.1 mmol) and DIPEA (68 µl, 0.4 mmol) and the reaction was stirred for 4 h. The mixture was concentrated under reduced pressure and globally deprotected with a solution of 95% TFA, 2.5% H_2O and 2.5% TIPS (5 ml). The crude material was purified by preparative RP-HPLC (0.1% TFA 0–30% MeCN:H_2O over 10 min, 30–35% over 30 min, 35%–95% over 10 min, Column D) to afford product **88** as a white powder (1.65 mg, 2.0% overall yield based on initial resin loading). ^{1}H NMR (600 MHz, D_2O) δ 7.75–7.68 (m, 3H), 7.62–7.57 (m, 3H), 7.39–7.33 (m, 2H), 7.31 (dd, *J*=17.8, 7.1 Hz, 1H), 7.10–7.05 (m, 2H), 7.03–7.00 (m, 2H), 6.65 (d, *J*=8.7 Hz, 1H), 6.59 (d, *J*=8.7 Hz, 1H), 4.22 (dd, *J*=20.6, 12.9 Hz, 1H), 4.00 (t, *J* = 8.1 Hz, 1H), 3.85 (m, 1H), 3.60 (dt, *J*=13.4, 9.3 Hz, 2H), 3.51 (dd, *J*=11.9, 4.2 Hz, 2H), 3.42 (dd, *J* = 11.7, 6.9 Hz, 1H), 3.33 (m, 1H), 3.19–3.13 (m, 2H), 3.03–2.99 (m, 2H), 2.89–2.83 (m, 3H), 2.83 (s, 1H), 2.74 (dd, *J* = 15.1, 5.0 Hz, 1H), 2.65 (m, 1H), 2.52 (s, 1H), 2.46 (m, 1H), 2.33 (m, 1H), 2.03 (m, 1H), 1.84 (m, 1H), 1.68 (m, 1H), 1.62 (m, 1H), 1.49 (m, 1H), 1.28 (m, 1H), 1.21 (d, *J* = 6.9 Hz, 3H), 1.10 (m, 1H), 0.84–0.78 (m,

2H), 0.53–0.48 (m, 2H). ESI-MS $[M+H]^+$ ($C_{43}H_{51}FN_9O_7^+$): *m/z* 824.389 (calculated), 824.389 (observed). Analytical data consistent with literature data.[66]

***Method B*:** To a solution of c(D-Tyr-N(Me)-D-Orn-Arg-Nal-Gly) **106** (5.00 mg, 7.12 µmol, 1 eq.), HATU (5.41 mg, 14.2 µmol, 2 eq.) in DMF (100 µl), fluorobenzoic acid (14.2 µmol, 1.99 mg, 2 eq.) and DIPEA (5 µl , 28.4 µmol, 4 eq.) were added and the reaction was stirred for 1 h. H_2O (4 ml) was added and then the diluted mixture was purified by preparative RP-HPLC (0.1% TFA 0–30% MeCN:H_2O over 10 min, 30–35% over 30 min, 35%–95% over 10 min, column D) to afford product **88** as a white powder (6.6 mg, 8.0% overall yield based on initial resin loading). ESI-MS $[M+H]^+$ ($C_{43}H_{51}FN_9O_7^+$): *m/z* 824.389 (calculated), 824.389 (observed). Analytical data consistent with literature data.[66]

cyclo(D-Tyr(SO$_3$H)-N(Me)-D-Orn(FB)-Arg-Nal-Gly) (89)

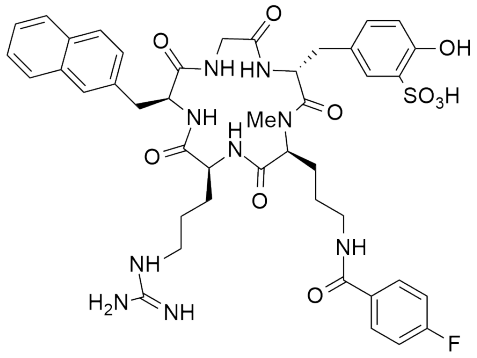

***Method A*:** Linear protected D-Tyr(SO_3H)-N(Me)-D-Orn(FB)-Arg(Pbf)-Nal-Gly-OH **85** was prepared from glycine-loaded chlorotrityl resin according to general coupling, cleavage and methylation on resin protocols. To a solution of linear D-Tyr(SO_3H)-N(Me)-D-Orn(FB)-Arg(Pbf)-Nal-Gly **85** (117 mg, 0.1 mmol) in DCM (117 ml) was added HATU (38.7 mg, 0.1 mmol) and DIPEA (67 µl, 0.4 mmol) were added and the reaction was stirred for 4 h. The mixture was concentrated under reduced pressure and globally deprotected with 95% TFA, 2.5% H_2O and 2.5%

TIPS (5 ml). The crude material was purified by preparative RP-HPLC (0.1% TFA 0–30% MeCN:H_2O over 10 min, 30–35% over 30 min, 35%–95% over 10 min, Column D) to afford product **89** as a white powder (2.7 mg, 3% overall yield based on initial resin loading). ESI-MS $[M+H]^+$ ($C_{43}H_{51}FN_9O_{10}S^+$): *m/z* 904.345 (calculated), 904.345 (observed). ^1H NMR (600 MHz, H_2O+D_2O) δ 8.72 (d, *J*=8.0 Hz, 1H), 8.50 (s, 1H), 8.42 (d, *J*=8.8 Hz, 1H), 8.22 (dd, *J*=11.9, 5.7 Hz, 1H), 7.81 (ddd, *J*=21.6, 18.0, 10.3 Hz, 3H), 7.78–7.72 (m, 2H), 7.64 (d, *J*=7.9 Hz, 1H), 7.42–7.30 (m, 4H), 7.16– 7.18 (m, 3H), 6.81 (d, *J*=8.7 Hz, 1H), 6.76 (d, *J*=8.7 Hz, 1H), 6.51 (s, 1H), 6.37 (s, 1H), 4.27 (dd, *J*=15.2, 9.8 Hz, 1H), 4.05 (q, *J*=7.3 Hz, 1H), 3.89 (d, *J*=20.9 Hz, 1H), 3.66 (m, 1H), 3.56 (dt, *J*=9.3, 4.8 Hz, 1H), 3.40 (m, 1H), 3.15–3.07 (m, 4H), 2.96–2.88 (m, 2H), 2.84 (dd, *J*=13.7, 4.7 Hz, 1H), 2.74 (m, 1H), 2.45 (m, 1H), 2.38 (m, 1H), 1.98 (d, *J*=7.5 Hz, 1H), 1.77 (m, 1H), 1.70 (m, 1H), 1.62 (m, 1H), 1.38–1.32 (m, 2H), 1.26–1.19 (m, 2H), 1.14 (s, 2H), 0.99 (dd, *J* = 18.3, 5.4 Hz, 1H), 0.83 (m, 1H), 0.63–0.58 (m, 2H).

***Method B*:** To a solution of c(D-Tyr(SO_3H)-N(Me)-D-Orn-Arg-Nal-Gly) **107** (5.00 mg, 6.39 μmol, 1 eq.), HATU (4.86 mg, 2 eq.) in DMF (100 μl), fluorobenzoic acid (1.79 mg, 12.8 μmol, 2 eq.) and DIPEA (25.6 μmol, 4.45 μl, 4 eq.) were added and the reaction was stirred for 1 h. H_2O (4 ml) was added and solution was purified by preparative RP-HPLC (0.1% TFA 0–30% MeCN:H_2O over 10 min, 30–35% over 30 min, 35%–95% over 10 min, column D) to afford product **89** as a white powder (6.3 mg, 7.0% overall yield based on initial resin loading). ESI-MS $[M+H]^+$ ($C_{43}H_{51}FN_9O_{10}S^+$): *m/z* 904.345 (calculated), 904.345 (observed).

cyclo(D-Tyr-N(Me)-D-Orn(FPy)-Arg-Nal-Gly) (96)

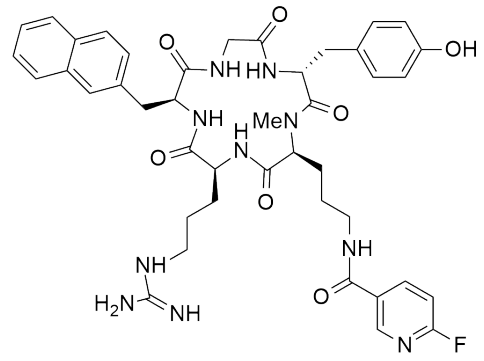

Method A: Linear protected D-Tyr-(OtBu)-N(Me)-D-Orn(FPy)-Arg(Pbf)-Nal-Gly **92** was prepared from glycine-loaded chlorotrityl resin according to general coupling, cleavage and methylation on resin protocols. To a solution of linear D-Tyr(OtBu)-N(Me)-D-Orn(FPy)-Arg(Pbf)-Nal-Gly **93** (115 mg, 0.1 mmol) in DCM (115 ml) was added HATU (38.7 mg, 0.1 mmol) and DIPEA (68 µl, 0.4 mmol were added and the reaction was stirred for 4 h. The mixture was concentrated under reduced pressure and globally deprotected with a solution of 95% TFA, 2.5% H_2O and 2.5% TIPS (5 ml). The crude material was purified by preparative RP-HPLC (0.1% TFA 0–30% MeCN:H_2O over 10 min, 30–35% over 30 min, 35%–95% over 10 min, Column D) to afford product **96** as a white powder (1.7 mg, 2.0% overall yield). ESI-MS $[M+H]^+$ ($C_{42}H_{50}FN_{10}O_7^+$): *m/z* 825.384 (calculated), 825.384 (observed).

Method B: To a solution of c(D-Tyr-N(Me)-D-Orn-Arg-Nal-Gly) **106** (5.00 mg, 7.12 µmol, 1 eq.), HATU (5.41 mg, 14.2 µmol, 2 eq.) in DMF (100 µl), fluoronicotinic acid (14.2 µmol, 2.00 mg, 2 eq.) and DIPEA (5 µl , 28.4 µmol, 4 eq.) were added and the reaction was stirred for 1 h. H_2O (4 ml) was added and solution was purified by preparative RP-HPLC (0.1% TFA 0–30% MeCN:H_2O over 10 min, 30–35% over 30 min, 35%–95% over 10 min, column D) to afford

product **96** as a white powder (5.8 mg, 7.0% overall yield). ESI-MS $[M+H]^+$ ($C_{42}H_{50}FN_{10}O_7^+$): *m/z* 825.384 (calculated), 825.384 (observed).

cyclo(D-Tyr(SO$_3$H)-N(Me)-D-Orn(FPy)-Arg-Nal-Gly) (97)

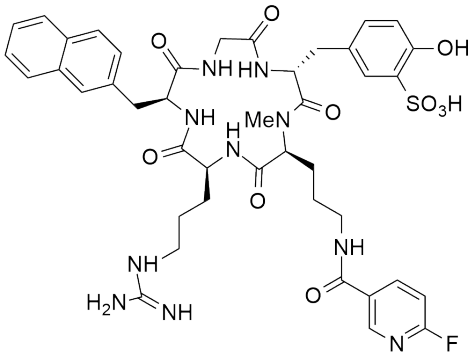

***Method A*:** Linear protected D-Tyr(SO_3H)-N(Me)-D-Orn(FPy)-Arg(Pbf)-Nal-Gly **93** was prepared from glycine-loaded chlorotrityl resin according to general coupling, cleavage and methylation on resin protocols. To a solution of linear D-Tyr(SO_3H)-N(Me)-D-Orn(FPy)-Arg(Pbf)-Nal-Gly **93** (117 mg, 0.1 mmol) in DCM (117 ml) was added HATU (38.7 mg, 0.1 mmol) and DIPEA (68 µl, 0.4 mmol) and the reaction was stirred for 4 h. The mixture was concentrated under reduced pressure and then globally deprotected with a solution of 95% TFA, 2.5% H_2O and 2.5% TIPS (5 ml). The crude material was purified by preparative RP-HPLC (0.1% TFA 0–30% MeCN:H_2O over 10 min, 30–35% over 30 min, 35%–95% over 10 min, Column D) to afford product **97** as a white powder (1.8 mg, 2.0% overall yield based on initial resin loading). ESI-MS $[M+H]^+$ ($C_{42}H_{50}FN_{10}O_{10}S^+$): *m/z* 905.341 (calculated), 905.341 (observed).

Method B: To a solution of c(D-Tyr(SO_3H)-N(Me)-D-Orn-Arg-Nal-Gly) **107** (5.00 mg, 6.39 µmol, 1 eq.), HATU (4.86 mg, 2 eq.) in DMF (100 µl), fluoronicotinic acid (1.80 mg, 12.8 µmol, 2 eq.) and DIPEA (25.6 µmol, 4.45 ul, 4 eq.) were added and the reaction was stirred for 1 h. H_2O (4 ml) was added and solution was purified by preparative RP-HPLC (0.1% TFA 0–30%

MeCN:H_2O over 10 min, 30–35% over 30 min, 35%–95% over 10 min, column D) to afford product **97** white powder (9.1 mg, 10% overall yield based on initial resin loading) ESI-MS $[M+H]^+$ ($C_{42}H_{50}FN_{10}O_{10}S^+$): *m/z* 905.341 (calculated), 905.341 (observed).

cyclo(D-Tyr-N(Me)-D-Orn(ESF)-Arg-Nal-Gly) (104)

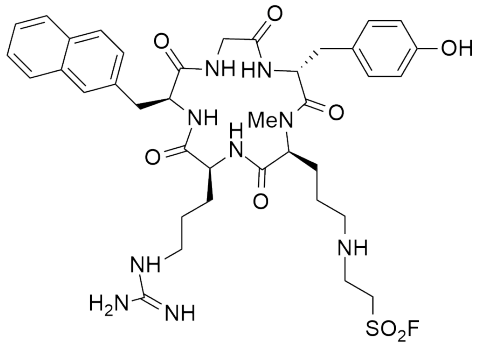

***Method A*:** Linear protected D-Tyr(OtBu)-N(Me)-D-Orn(ESF)-Arg(Pbf)-Nal-Gly **100** was prepared from glycine-loaded chlorotrityl resin according to general coupling, cleavage, methylation and coupling of ethene sulfonyl fluoride on resin protocols. To a solution of D-Tyr(OtBu)-N(Me)-D-Orn(ESF)-Arg(Pbf)-Nal-Gly **100** (114 mg, 0.1 mmol) in DCM (114 ml) was added HATU (38.7 mg, 0.1 mmol) and DIPEA (68 µl, 0.4 mmol) and the reaction was stirred for 4 h. The mixture was concentrated under reduced pressure and globally deprotected with a solution of 95% TFA, 2.5% H_2O and 2.5% TIPS (5 ml). The crude material was purified by preparative RP-HPLC (0.1% TFA 0–30% MeCN:H_2O over 10 min, 30–35% over 30 min, 35%–95% over 10 min, Column D) to afford product **104** as a white powder (0.4 mg, 0.5% overall yield based on initial resin loading). ESI-MS $[M+H]^+$ ($C_{38}H_{51}FN_9O_8S^+$): *m/z* 812.355 (calculated), 812.355 (observed).

***Method B*:** To a solution c(D-Tyr-N(Me)-D-Orn-Arg-Nal-Gly) **106** (5.00 mg, 7.12 µmol, 1 eq.), ethene sulfonyl fluoride (0.53 µl, 6.41 µmol, 0.9 eq.) in DMF (100 µl) was stirred for 1 h.

H_2O (4 ml) was added and the solution was purified by preparative RP-HPLC (0.1% TFA 0–30% MeCN:H_2O over 10 min, 30-35% over 30 min, 35%-95% over 10 min, column D) to afford product **104** as a white powder (3.2 mg, 4.0% overall yield based on initial resin loading). ESI-MS $[M+H]^+$ ($C_{38}H_{51}FN_9O_8S^+$): *m/z* 812.355 (calculated), 812.355 (observed).

cyclo(D-Tyr-N(Me)-D-Orn(ESF)$_2$-Arg-Nal-Gly)

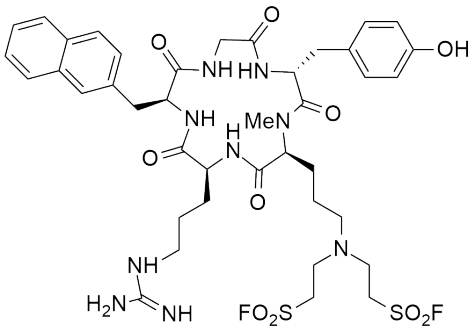

Method A: Linear protected D-Tyr(OtBu)-N(Me)-D-Orn(ESF)$_2$-Arg(Pbf)-Nal-Gly was prepared from glycine-loaded chlorotrityl resin according to general coupling, cleavage, methylation and coupling of ethene sulfonyl fluoride (in excess) on resin protocols. To a solution of D-Tyr(OtBu)-N(Me)-D-Orn(ESF)$_2$-Arg(Pbf)-Nal-Gly-OH (87.4 mg, 0.1 mmol) in DCM (87 ml) was added HATU (38.7 mg, 0.1 mmol) and DIPEA (67 µl, 0.4 mmol) were added and the reaction was stirred for 4 h. The mixture was concentrated under reduced pressure and globally deprotected with a solution of 95% TFA, 2.5% H_2O and 2.5% TIPS (5 ml). The crude material was purified by preparative RP-HPLC (0.1% TFA 0–30% MeCN:H_2O over 10 min, 30–35% over 30 min, 35%–95% over 10 min, Column D) to afford title compound as a white powder (0.7 mg, 0.7% overall yield based on initial resin loading). ESI-MS $[M+H]^+$ ($C_{40}H_{54}F_2N_9O_{10}S_2^+$) *m/z* 922.339 (calculated), 922.339 (observed).

Method B: To a solution of c(D-Tyr-N(Me)-D-Orn-Arg-Nal-Gly) **106** (5.00 mg, 7.12 μmol, 1 eq.), ethene sulfonyl fluoride (2.94 μl, 35.6 μmol, 5.0 eq.) in DMF (100 μl) was stirred for 1 h. H_2O (4 ml) was added and solution was purified by preparative RP-HPLC (0.1% TFA 0–30% MeCN:H_2O over 10 min, 30–35% over 30 min, 35%–95% over 10 min, column D) to afford title compound as a white powder (2.8 mg, 3.0% overall yield based on initial resin loading). ESI-MS $[M+H]^+$ ($C_{40}H_{54}F_2N_9O_{10}S_2^+$) 922.339 (calculated), $[M+H]^+$ 922.339 (observed).

cyclo(D-Tyr(SO$_3$H)-N(Me)-D-Orn(ESF)-Arg-Nal-Gly) (105)

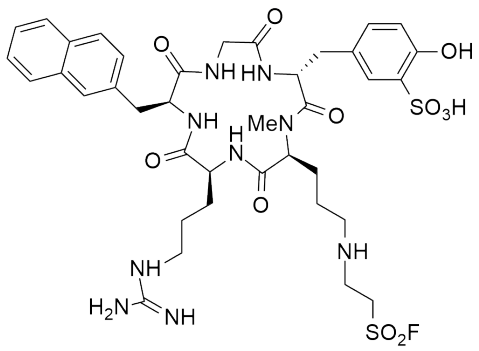

***Method A*:** Linear protected D-Tyr(SO_3H)-N(Me)-D-Orn(ESF)-Arg(Pbf)-Nal-Gly **101** was prepared from glycine-loaded chlorotrityl resin according to general coupling, cleavage, methylation and coupling of ethane sulfonyl fluoride on resin protocols. To a solution of D-Tyr(SO_3H)-N(Me)-D-Orn(ESF)-Arg(Pbf)-Nal-Gly-OH **101** (116 mg, 0.1 mmol) in DCM (116 ml) was added HATU (38.7 mg, 0.1 mmol) and DIPEA (68 μl, 1.24 mmol) and the reaction was stirred for 4 h. The mixture was concentrated under reduced pressure and globally deprotected with a solution of 95% TFA, 2.5% H_2O and 2.5% TIPS (5 ml). The crude material was purified by preparative RP-HPLC (0.1% TFA 0–30% MeCN:H_2O over 10 min, 30–35% over 30 min, 35%–95% over 10 min, Column D) to afford product **105** a white powder (0.9 mg, 1.0% overall yield

based on initial resin loading). ESI-MS $[M+H]^+$ ($C_{38}H_{51}FN_9O_{11}S_2^+$) *m/z* 892.312 (calculated), 892.312 (observed).

***Method B*:** To a solution of c(D-Tyr(SO_3H)-N(Me)-D-Orn-Arg-Nal-Gly-OH) **107** (5 mg, 6.39 μmol, 1 eq.), ethene sulfonyl fluoride (0.48 μl, 5.75 μmol, 0.9 eq.) in DMF (100 μl) was stirred for 1 h. H_2O (4 ml) was added and solution was purified by preparative RP-HPLC (0.1% TFA 0-30% MeCN:H_2O over 10 min, 30-35% over 30 min, 35%-95% over 10 min, column D) to afford product **105** as a white powder (2.68 mg, 3.0% overall yield based on initial resin loading). ESI-MS $[M+H]^+$ ($C_{38}H_{51}FN_9O_{11}S_2^+$): *m/z* 892.312 (calculated), $[M+H]^+$ 892.312 (observed).

cyclo(D-Tyr(SO$_3$H)-N(Me)-D-Orn(ESF)$_2$-Arg-Nal-Gly)

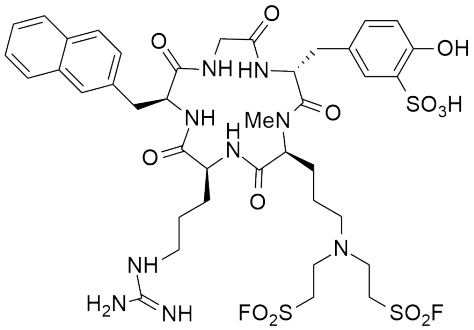

Method A: Linear protected D-Tyr(SO_3H)-N(Me)-D-Orn(ESF)$_2$-Arg-Nal-Gly was prepared from glycine-loaded chlorotrityl resin according to general coupling, cleavage, methylation and coupling of ethane sulfonyl fluoride (in excess) on resin protocols. To a solution of D-Tyr(SO_3H)-N(Me)-D-Orn(ESF)$_2$-Arg-Nal-Gly (116 mg, 0.1 mmol) in DCM (116 ml) was added HATU (38.7 mg, 0.1 mmol) and DIPEA (68 μl, 0.4 mmol) and the reaction was stirred for 4 h. The mixture was concentrated under reduced pressure and globally deprotected with solution of 95% TFA, 2.5% H_2O and 2.5% TIPS (5 ml). The crude material was purified by preparative

RP-HPLC (0.1% TFA 0–30% MeCN:H_2O over 10 min, 30–35% over 30 min, 35%–95% over 10 min, Column D) to afford title compound as a white powder (1.1 mg, 1.1% overall yield based on initial resin loading). ESI-MS $[M+H]^+$ ($C_{40}H_{54}F_2N_9O_{13}S_3^+$) *m/z* 1002.296 (calculated), 1002.296 (observed).

Method B: To a solution of c(D-Tyr(SO_3H)-N(Me)-D-Orn-Arg-Nal-Gly) **107** (5 mg, 6.39 µmol, 1 eq.), ethene sulfonyl fluoride (2.64 µl, 31.9 µmol, 5 eq.) in DMF (100 µl) and stirred for 1 h. H_2O (4 ml) was added and solution was purified by preparative RP-HPLC (0.1% TFA 0–30% MeCN:H_2O over 10 min, 30–35% over 30 min, 35%–95% over 10 min, column D) to afford title compound as a white powder (0.8 mg, 0.8% overall yield based on initial resin loading). ESI-MS $[M+H]^+$ ($C_{40}H_{54}F_2N_9O_{13}S_3^+$) *m/z* 1002.296 (calculated), 1002.296 (observed).

cyclo(D-Tyr-D-Orn-Arg-Nal-Gly) (106)

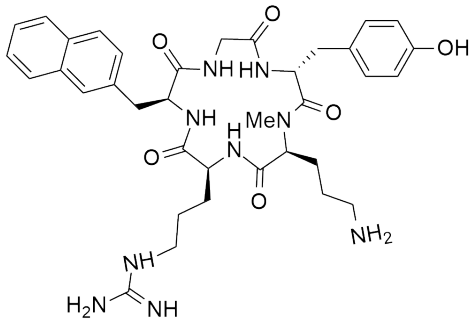

Linear protected D-Tyr(OtBu)-D-Orn(Boc)-Arg(Pbf)-Nal-Gly **108** was prepared from glycine-loaded chlorotrityl resin according to general coupling, cleavage and methylation on resin protocols. To a solution of linear protected D-Tyr(OtBu)-D-Orn(Boc)-Arg(Pbf)-Nal-Gly-OH **108** (113 mg, 0.1 mmol) in DCM (113 ml), HATU (38.7 mg, 0.1 mmol) and DIPEA (68 µl, 0.4 mmol) were added and the reaction was stirred for 4 h. The mixture was concentrated under reduced pressure and globally deprotected with a solution of 95% TFA, 2.5% H_2O and 2.5% TIPS (5 ml).

The crude material was purified by preparative RP-HPLC (0.1% TFA 0–30% MeCN:H_2O over 10 min, 30–35% over 30 min, 35%–95% over 10 min, Column D) to afford compound **106** as a white powder (5.6 mg, 8.0% overall yield based on initial resin loading). ESI-MS $[M+H]^+$ ($C_{36}H_{48}N_9O_6^+$): *m/z* 702.372 (calculated), 702.372 (observed). Analytical data consistent with literature data.[111]

cyclo(D-Tyr(SO$_3$H)-N(Me)-D-Orn-Arg-Nal-Gly) (107)

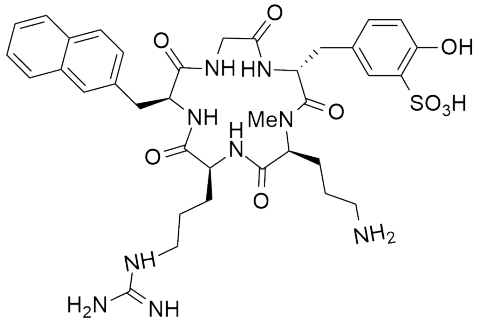

Linear protected D-Tyr(SO_3H)-N(Me)-D-Orn(Boc)-Arg(Pbf)-Nal-Gly **109** was prepared from glycine-loaded chlorotrityl resin according to general coupling, cleavage and methylation on resin protocols. To a solution of linear protected D-Tyr(SO_3H)-N(Me)-D-Orn(Boc)-Arg(Pbf)-Nal-Gly **109** (115 mg, 0.1 mmol) in DCM (115 ml) was added HATU (38.7 mg, 0.1 mmol) and DIPEA (68 µl, 0.4 mmol) and the reaction was stirred for 4 h. The mixture was concentrated under reduced pressure and globally deprotected with a solution of 95% TFA, 2.5% H_2O and 2.5% TIPS (5 ml). The crude material was purified by preparative RP-HPLC (0.1% TFA 0–30% MeCN:H_2O over 10 min, 30–35% over 30 min, 35%–95% over 10 min, Column D) to afford **107** as a white powder (7.8 mg, 10% yield based on initial resin loading). ESI-MS $[M+H]^+$ ($C_{36}H_{48}N_9O_9S^+$): *m/z* 782.329 (calculated), 782.329 (observed).

4-((tert-Butoxycarbonylaminomethyl)benzoic acid (118)

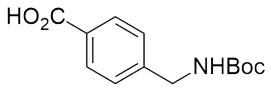

A solution of 4-(aminomethyl))benzoic acid (100 mg, 0.66 mmol) and $NaHCO_3$ (10% in water, 2.0 ml) in dioxane (1.0 ml) was cooled to 0°C. The mixture was treated with a solution of Boc anhydride (70 µl, 0.66 mmol) and stirred at rt for 12 h. The dioxane was evaporated under reduced pressure and aqueous layer washed with diethyl ether (1 × 6 ml), acidified with conc. HCl to pH 1 (~ 1 ml) and the product extracted with ethyl acetate (3 × 6 ml). The combined organic layers were dried Na_2SO_4 and concentrated under reduced pressure to give a sufficiently pure crystalline powder **118** (150 mg, 95% yield). ^{1}H NMR (400 MHz, d_6-DMSO) δ 12.78 (s, 1H), 7.86 (d, *J*=7.7 Hz, 2H), 7.31 (d, *J*=7.9 Hz, 2H), 4.15 (t, *J*=8.9 Hz, 2H), 1.32 (s, 9H). ^{13}C NMR (101 MHz, d_6-DMSO) δ 167.6, 156.3, 145.8, 129.8, 129.4, 127.3, 78.5, 43.6, 28.7. ESI-MS $[M+H]^+$ ($C_{13}H_{18}NO_4^+$): *m/z* 252.123 (calculated), 252.123 (observed). (lit. m.p. 164–168 °C). Analytical data consistent with literature data.[112]

2,3,5,6-Tetrafluorophenyl 6-bromonicotinate (125)

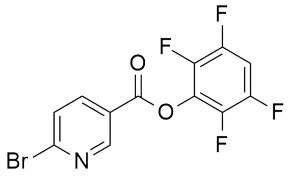

To 6-bromonicotinic acid **124** (100 mg, 0.49 mmol, 1.0 eq.), tetrafluorophenol **137** (82 mg, 0.49 mmol, 1.0 eq.) and EDC.HCl (114 mg, 0.59 mmol, 1.2 eq.) was added DMF (~ 5 ml) and the reaction was stirred for 4 h. H_2O (5 ml) was added and the mixture was extracted with DCM (3 × 50 ml) and the organic phase was washed with H_2O (3 × 50 ml) and 0.1M HCl (3 × 50 ml), dried

and evaporated. The product was recrystallized from hexane. To complete crystallization, the product was stored at 4°C overnight. White needle shaped crystals were isolated and rinsed with ice-cold hexane (3 × 10 ml) to afford product **125** (128 mg, 75% yield). ^{1}H NMR (400 MHz, $CDCl_3$) δ 9.14 (m, 1H), 8.28 (d, *J*=8.3 Hz, 1H), 7.71 (d, *J*=8.3 Hz, 1H), 7.09 (m, 1H). ^{13}C NMR (101 MHz, $CDCl_3$) δ 161.2, 152.4, 151.6, 148.5, 147.3–147.8 (m), 145.1, 146.1 (m), 141.0–141.5 (m), 129.4, 128.7, 103.9 (t, *J*=22.8 Hz). ^{19}F NMR (470 MHz, $CDCl_3$) δ –134.14 (m), –148.38 (dt, *J* = 15.8, 8.4 Hz). ESI-MS $[M+H]^+$ ($C_{12}H_5BrF_4NO_2^+$) *m/z* 349.943 (calculated), 349.943 (observed).

2,3,5,6-Tetrafluorophenyl 6-trimethylammonium bromide nicotinate (126)

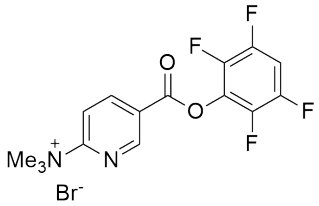

To 6-bromonicotinic tetrafluorophenyl ester **125** (100 mg, 0.287 mmol, 1 eq.) was added TMA (1M in THF) (1.43 ml, 1.43 mmol, 5 eq.) in dry THF (3 ml) and the solution was stirred at rt for 4 h. Et_2O (1 ml) was added and the precipitate was filtered and washed with dry THF to afford **126** as a white powder (68.0 mg, 72 % yield). ^{1}H NMR (500 MHz, d_6-DMSO) δ 9.39 (dd, *J*=2.3, 0.8 Hz 1H), 8.97 (dd, *J*=8.7, 2.3 Hz, 1H), 8.38–8.43 (m, 1H), 8.08 (dq, *J*=11.0, 7.4 Hz, 1H), 3.66 (s, 9H). ^{13}C NMR (126 MHz, d_6-DMSO) δ 161.0, 160.3, 150.8, 149.6–150.3 (m), 147.1–147.7 (m), 143.6, 141.5, 125.3, 117.1, 105.7 (t, *J*=23.6 Hz), 55.2. ^{19}F NMR (470 MHz, d_6-DMSO) δ –138.6–138.2 (m), –152.9 (dt, *J*=16.2, 8.4 Hz). ESI-MS $[M+H]^+$($C_{15}H_{13}F_4N_{22}^+$) *m/z* 329.091 (calculated), 329.091 (observed).

4-Nitrophenyl 6-bromonicotinate (127)

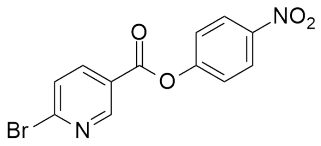

To 6-bromonicotinic acid **124** (2.0 g, 9.90 mmol, 1 eq.), 4-nitrophenol **27** (1.38 g, 9.90 mmol, 1 eq.) and EDC.HCl (2.28 g. 1.47 mmol, 1.2 eq.) was added DMF (~5 ml) and stirred for 4 h. H_2O (5 ml) was added and the mixture was extracted with DCM (3 × 50 ml) and the organic phase was washed with H_2O (3 × 50 ml) and 0.1M HCl (3 × 50 ml), dried and evaporated. The residue was recrystallised from DCM to afford product **127** as transparent needle-shape crystals (2.56 g, 80% yield). ^{1}H NMR (400 MHz, d_6-DMSO) δ 9.06 (d, *J*=2.5 Hz, 1H), 8.36–8.28 (m, 3H), 7.92 (d, *J*=8.3 Hz, 1H), 7.64–7.60 (m, 2H). ^{13}C NMR (101 MHz, d_6-DMSO) δ 162.8, 155.5, 152.1, 147.3, 145.8, 140.9, 129.1, 125.8, 125.1, 123.7. ESI-MS $[M+H]^+$ ($C_{12}H_8BrN_2O_4^+$) *m/z* 322.966 (calculated), 322.966 (observed).

4-Nitrophenyl 6-trimethylammonium bromide nicotinate (128)

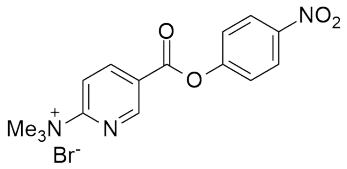

To bromo ester precursor **127** (1.0 g, 9.90 mmol) was added TMA (1.0 M in THF, 32.5 ml, 32.5 mmol. 5 eq.) in dry THF (30 ml) and the solution was stirred at rt for 4 h. Et_2O (10 ml) was added and the precipitate was filtered and washed with dry THF (3 × 10 ml) to afford **128** as white crystals (2.2 g, 70% yield). ^{1}H NMR (400 MHz, $CDCl_3$) δ 9.28 (d, *J*=1.4 Hz, 1H), 9.04 (d, *J*=8.7 Hz, 1H), 8.90 (dd, *J*=8.7, 1.8 Hz, 1H), 8.37 (d, *J*=9.0 Hz, 2H), 7.46 (d, *J*=9.0 Hz, 2H), 4.14 (s,

9H).^{13}C NMR (101 MHz, $CDCl_3$) δ 162.0, 160.3, 155.3, 150.4, 145.9, 143.1, 127.6, 125.9, 123.8, 116.5, 55.0. ESI-MS $[M+H]^+$ ($C_{15}H_{16}N_3O_4^+$) *m/z* 302.113 (calculated), 302.112 (observed).

4-Nitrophenyl 6-[^{18}F]fluoronicotinate ([^{18}F]NFN) (129)

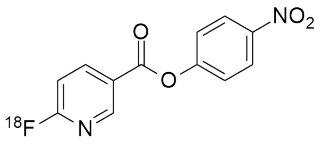

[^{18}F]Fluoride in [^{18}O] water was transferred to the iPHASE FlexLAB radiosynthesis module and passed through a pre-conditioned QMA cartridge. Trapped [^{18}F]fluoride (2.41–7.15 GBq) was eluted into a reaction vessel with a solution containing $KHCO_3$ (2–3 mg, 20–30 μmol) and Kryptofix 2.2.2 (10–12 mg, 27–32 μmol) in 300 μl H_2O/700 μl MeCN. The solution was evaporated at 65°C under nitrogen flow and vacuum for 13 min, followed by heating at 120 °C under nitrogen then vacuum for a further 7 min. To the anhydrous [^{18}F]KF/K_{222}/$KHCO_3$ residue, precursor **128** (10 mg, 33 μmol) in DMSO:tAmOH (0.4:0.6, 1 ml) was added. After 5 min at 100 °C, the solvent was evaporated to half volume, and the residue was diluted with mobile phase (0.05% TFA H_2O/MeCN, 1.3:0.2, 1.5 ml). The mixture was transferred to the loop injection vial. The reaction vial was then washed with mobile phase (0.05% TFA H_2O/MeCN, 1.3:0.2, 1.5 ml). and transferred to the loop injection vial to be then purified by preparative HPLC (0.05% TFA in 15–80% MeCN:H_2O over 40 min, column F) to afford the title compound **129** (555–792 MBq, 95% yield (n=3), 58% isolated yield decay corrected to SOS). The total reaction time was 40 min. Automation details are illustrated in Table 7.

4-Nitrophenyl 6-fluoronicotinate

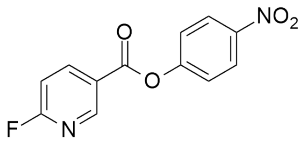

To fluoronicotinic acid (2.0 g, 9.90 mmol, 1 eq.), 4-nitrophenol **27** (1.38 g, 9.90 mmol, 1 eq.) and EDC-HCl (2.28 g. 1.47 mmol, 1.2 eq.) was added DMF (~5 ml) and the reaction was stirred for 4 h. H_2O (10 ml) was added and the mixture was extracted with DCM (3 × 100 ml) and the organic phase was washed with H_2O (3 × 50 ml) and 0.1M HCl (3 × 100 ml), dried and evaporated. Residue was recrystallised from DCM to afford pure product as transparent needle shape crystals (2.2 g, 95% yield). ^{1}H NMR (400 MHz, $CDCl_3$) δ 9.07 (d, *J*=1.9 Hz, 1H), 8.52–8.56 (m, 1H), 8.34 (d, *J*=8.9 Hz, 2H), 7.43 (d, *J*=8.9 Hz, 2H), 7.12 (dd, *J*=8.6, 2.9 Hz, 1H). ^{13}C NMR (101 MHz, $CDCl_3$) δ 166.4 (d, *J*=248.1 Hz), 161.9, 151.2 (d, *J*=17.0 Hz), 145.7, 143.2 (d, *J*=9.7 Hz), 125.4, 123.1 (d, *J*=4.6 Hz), 122.5, 110.1 (d, *J*=37.5 Hz), 109.9. ^{19}F NMR (470 MHz, $CDCl_3$) δ –58.71 (d, *J*=5.6 Hz). ESI-MS $[M+H]^+$ ($C_{12}H_8FN_2O_4^+$) *m/z* 263.046 (calculated), 263.046 (observed).

4-Nitrophenyl 4-trimethylammonium triflate benzoate (130)

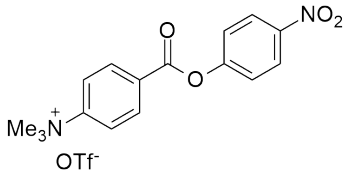

To 4-(dimethylamino)benzoic nitrophenyl ester **132** (0.447 g, 1.56 mmol, 1 eq.) in dry DCM (20 ml), methyl triflate (200 µl, 5.46 mmol, 3.5 eq.) was added at 0°C under argon atmosphere and the reaction was stirred for 12 h. The precipitate was filtered and washed with DCM (3 × 10 ml) to give pure product **130** as a white powder (0.432 g, 92% yield). ^{1}H NMR (400

MHz, d_6-DMSO) δ 8.36–8.25 (m, 4H), 8.20 (d, *J*=8.4 Hz, 2H), 7.65 (d, *J*=8.8 Hz, 2H), 3.66 (s, 9H). ^{13}C NMR (101 MHz, d_6-DMSO) δ 163.1, 155.6, 151.6, 145.8, 132.1, 130.4, 125.8, 123.7, 122.0, 56.9. ^{19}F NMR (470 MHz, d_6-DMSO) δ –77.75. ESI-MS $[M+H]^+$ ($C_{16}H_{17}N_2O_4^+$) *m/z* 301.118 (calculated), 301.118 (observed).

4-Nitrophenyl 4-(dimethylamino)benzoate (132)

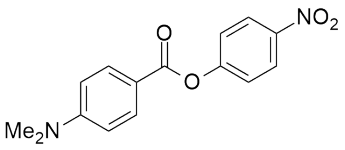

To 4-(dimethylamino)benzoic acid **131** (1.0 g, 6.1 mmol, 1 eq.), 4-nitrophenol **27** (0.842 g, 6.1 mmol, 1 eq.) and EDC.HCl (1.17 g, 7.32 mmol, 1.2 eq.,) was added DMF (~ 5 ml) and the reaction was stirred for 4 h. H_2O (10 ml) was added and the mixture was extracted with DCM (3 × 100 ml) and the organic phase was washed with H_2O (3 × 100 ml) and 0.1M HCl (3 × 100 ml), dried and evaporated. Residue was recrystallised from DCM to afford product **132** as transparent needle shape crystals (1.3 g, 75% yield). ^{1}H NMR (400 MHz, $CDCl_3$) δ 8.30 (d, *J*=8.9 Hz, 2H), 8.04 (d, *J*=8.9 Hz, 2H), 7.39 (d, *J*=8.9 Hz, 2H), 6.70 (d, *J*=8.8 Hz, 2H), 3.10 (s, 6H).^{13}C NMR (101 MHz, $CDCl_3$) δ 164.9, 156.3, 153.6, 148.9, 144.6, 136.7, 132.2, 125.1, 122.7, 40.1. ESI-MS $[M+H]^+$ ($C_{15}H_{15}N_2O_4^+$): *m/z* 287.102 (calculated), 287.102 (observed). (lit. m.p. 158.5–159.5 °C).[112] Analytical data consistent with literature data.[112]

4-Nitrophenyl 4-[^{18}F]fluorobenzoate ([^{18}F]NFB) (133)

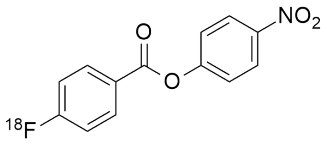

[^{18}F]Fluoride in [^{18}O] water was transferred to the iPHASE FlexLAB radiosynthesis module and passed through a pre-conditioned QMA cartridge. Trapped [^{18}F]fluoride (1.11–7.40 GBq) was eluted into a reaction vessel with a solution containing $C_2K_2O_4$ (2–3mg, 12–18 μmol) and Kryptofix 2.2.2 (10–12 mg, 27–32 μmol) in 300 μl H_2O/700 μl MeCN. The solution was evaporated at 65°C under nitrogen flow and vacuum for 13 min, followed by heating at 120 °C under nitrogen then vacuum for a further 7 min. To the anhydrous [^{18}F]KF/K_{222}/$C_2K_2O_4$ residue, iodonium salt **136** (20 mg, 42 μmol) in DMSO: tAmOH (0.4:0.6, 1 ml) was added. After 5 min at 100 °C, the solvent was evaporated to half volume, and the residue was diluted with mobile phase (0.05% TFA H_2O/MeCN, 1.3:0.2, 1.5 ml). The mixture was transferred to the loop injection vial. The reaction vial was then washed with mobile phase (0.05% TFA H_2O/MeCN, 1.3:0.2, 1.5 ml) and transferred to the loop injection vial to be then purified by preparative HPLC (0.05% TFA in 15–80% MeCN:H_2O over 40 min, column F) to afford the title compound **133** (564–762 MBq, 88% yield (n=3), 42% isolated yield decay corrected to SOS). The total reaction time was 45 min. Automation details are illustrated in Table 7.

4-Nitrophenyl 4-fluorobenzoate

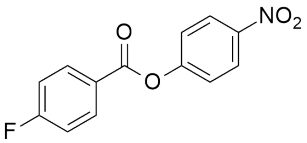

To fluorobenzoic acid (0.71 mmol, 100 mg, 1 eq.), 4-nitrophenol **27** (0.71 mmol, 98.6 mg, 1 eq.) and EDC.HCl (135 mg, 0.71 mmol, 1 eq.) was added DMF (~5 ml) and the reaction was stirred at rt for 4 h. H_2O (5 ml) was added and the mixture was extracted with DCM (3 × 50 ml) and the organic phase was washed with H_2O (3 × 50 ml) and 0.1M HCl (3 × 50 ml), dried and evaporated. Residue was recrystallised from DCM to afford pure product as a white crystal shape (41 mg, 90% yield). ^{1}H NMR (400 MHz, $CDCl_3$) δ 8.60–8.53 (m, 2H), 8.23 (dd, *J*=8.6, 5.5 Hz), 7.43–7.38 (m, 2H), 7.22–7.18 (m, 2H). ^{13}C NMR (400 MHz, $CDCl_3$) 166.2 (d, *J*=253.3 Hz), 164.3, 155.8, 145.6, 133.5 (d, *J*=9.8 Hz), 126.6, 125.8, 123.8 (d, *J*=3.2 Hz), 116.7 (d, *J*=22.3 Hz). ^{19}F NMR (470 MHz, $CDCl_3$) δ –58.72 (d, *J*=5.6 Hz). ESI-MS $[M+H]^+$ ($C_{13}H_9FNO_4^+$): *m/z* 262.051 (calculated), 262.051 (observed). (lit. m.p. 127–128 °C.)[113] Analytical data consistent with literature data.[113]

4-Nitrophenyl 4-iodobenzoate (135)

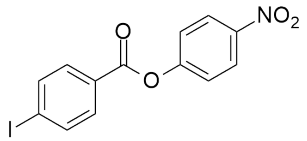

To 4-iodobenzoylchloride **134** (1.91 g, 7.18 mmol, 1 eq.) in dry DCM (~5 ml) was added 4-nitrophenol **27** (1.00 g, 7.18 mmol, 1 eq.,) and TEA (2.00 ml, 14.4 mmol, 2 eq.) and the reaction was stirred at rt for 4 h. H_2O (5 ml) was added and the mixture was extracted with DCM (3 × 50 ml) and the organic phase was washed with H_2O (3 × 50 ml) and 0.1M HCl (3 × 50 ml), dried and

concentrated to ~5 ml and diethyl ether (~ 1 ml) was added. The product **135** crystallised as a slightly yellow crystal shape (2.26 g, 85% yield). ^{1}H NMR (400 MHz, $CDCl_3$) δ ^{1}H NMR (400 MHz, $CDCl_3$) δ 8.33 (d, *J*=9.0 Hz, 1H), 7.96–7.84 (m, 2H), 7.41 (d, *J*=8.9 Hz, 1H). ^{13}C NMR (101 MHz, $CDCl_3$) δ 163.8, 155.4, 145.5, 138.2, 131.6, 127.9, 125.3, 122.5, 102.5. ESI-MS $[M+H]^+$ ($C_{13}H_9INO_4^+$) *m/z* 369.957 (calculated), *m/z* 369.957 (observed). (lit. m.p. 170–171 °C.)[114] Analytical data consistent with literature data.[114]

4-Methoxyphenyl 4-(4-nitrophenoxycarbonyl)phenyliodonium tosylate (136)

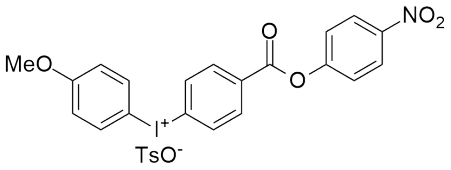

To 4-nitrophenyl 4-iodobenzoate **135** (0.14 g, 0.27 mmol, 1 eq.) mCPBA (0.20 g, 0.98 mmol, 2.8 eq.) and pTsOH (0.10 g, 0.57 mmol, 1.6 eq.) was added anisole (0.071 ml, 0.66 mmol, 2.4 eq.) in 50% TFE/DCM (~ 5 ml). The reaction was stirred at rt for 4 h. Et_2O (1 ml) was added and the mixture was stirred for 1 h. The precipitate was filtered off and recrystallised from DCM to afford pure product **136** as a white powder (0.31 g, 90% yield). ^{1}H NMR (400 MHz, d_6-DMSO) δ 8.36 (dd, *J*=12.6, 8.7 Hz, 4H), 8.19 (dd, *J*=8.5, 4.5 Hz, 4H), 7.60 (d, *J*=9.0 Hz, 2H), 7.45 (d, *J*=7.9 Hz, 2H), 7.08 (dd, *J*=8.2, 4.1 Hz, 4H), 3.79 (s, 3H), 2.29 (s, 3H). ^{13}C NMR (101 MHz, d_6-DMSO) δ 163.4, 162.6, 155.6, 146.2, 145.8, 138.0, 137.9, 135.7, 133.0, 131.8, 128.5, 125.9, 125.8, 123.7, 123.3, 118.0, 106.1, 56.2, 21.2. ESI-MS $[M+H]^+$ ($C_{20}H_{15}INO_5^+$): *m/z* 475.998 (calculated), 475.998 (observed).

2,3,5,6-Tetrafluorophenyl 4-iodobenzoate (138)

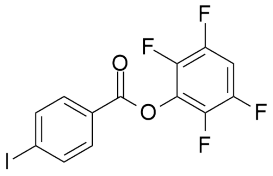

To 4-iodobenzoyl chloride **134** (1.91 g, 7.18 mmol, 1 eq.), tetrafluorophenol **137** (1.20 g, 7.18 mmol, 1 eq.) in dry DCM (~ 5 ml) was added TEA (2 ml, 14.4 mmol, 2 eq.) and the reaction was stirred at rt for 4 h. H_2O (5 ml) was added and the mixture was extracted with DCM (3 × 50 ml) and the organic phase was washed with H_2O (3 × 50 ml) and 0.1M HCl (3 × 50 ml), dried and concentrated to ~5 ml and diethyl ether (~ 1 ml) was added. The product **138** crystallised as white crystal shape (2.27 g, 80% yield). ^{1}H NMR (500 MHz, d6-DMSO) δ 8.04 (d, *J*=8.3 Hz, 2H), 7.86–7.83 (m, 2H), 7.72 (dd, *J*=61.6, 8.3 Hz, 1H). ^{13}C NMR (126 MHz, $CDCl_3$) δ 162.2, 146.1 (dtd, *J*=248.9, 11.9, 4.1 Hz), 140.7 (dd, *J*=248.8, 13.2 Hz), 138.2, 138.0 (m), 131.9, 126.6, 103.5 (t, *J*=22.8 Hz), 103.0. ^{19}F NMR (470 MHz, d6-DMSO) δ –138.89–137.78 (m), –153.43 (dt, *J*=16.8, 8.8 Hz). ESI-MS $[M+H]^+$ ($C_{13}H_6F_4IO_2^+$) *m/z* 395.927 (calculated), 395.927. (lit. m.p.168.9–169.5 °C). [115] Analytical data consistent with literature data.[115]

4-Methoxyphenyl 4-(2,3,5,6-tetrafluorophenoxycarbonyl)phenyliodonium tosylate (139)

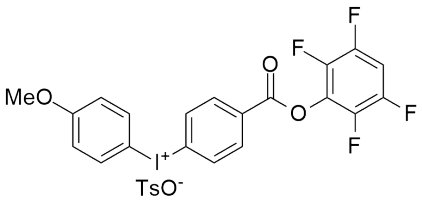

To 2,3,5,6-tetrafluorophenyl 4-iodobenzoate **138** (0.14 g, 0.27 mmol, 1 eq.) mCPBA (0.20 g, 0.98 mmol, 2.8 eq.) and pTsOH (0.10 g, 0.57 mmol, 1.6 eq.) was added anisole (0.071 ml, 0.66 mmol, 2.4 eq.) in 50% TFE/DCM (~ 5 ml). The reaction was stirred at rt for 4 h. Et_2O (1 ml) was

added and the mixture was stirred for 1 h. The precipitate was filtered off and recrystallised from DCM to afford pure product **139** as a white solid (0.12 g, 88% yield). ^{1}H NMR (500 MHz, d_6-DMSO) δ 8.20 (d, *J*=9.0 Hz, 2H), 8.00–8.06 (m, 4H), 7.47 (d. *J*=9.0 Hz, 2H), 7.08–7.05 (m, 1H), 7.00–6.92 (m, 2H), 6.87–6.82 (m, 2H), 3.80 (s, 3H), 2.27 (s, 3H). ^{13}C NMR (101 MHz, d_6-DMSO) δ 161.9, 161.6, 147.2 (dt, *J*=16.2, 4.3 Hz), 144.1 (dt, *J*=15.1, 3.7 Hz), 141.8, 139.4, 141.8, 137.9, 137.1, 135.1, 132.4, 128.6, 128.1, 124.8, 122.7, 117.6, 105.7, 105.4 (t, *J*=23.6 Hz), 56.1, 23.1. ^{19}F NMR (470 MHz, d_6-DMSO) δ –138.82–139.02 (m), –153.27 (dt, *J*=16.7, 8.7 Hz). ESI-MS $[M+H]^+$ ($C_{20}H_{12}F_4IO_3^+$) *m/z* 502.976 (calculated), 502.976 (observed). (lit. m.p. 191.2–192.5 °C).[115] Analytical data consistent with literature data.[115]

2,3,5,6-Tetrafluorophenyl 6-[^{18}F]fluorobenzoate ([^{18}F]TFB) (140)

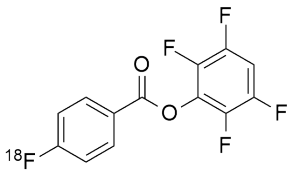

[^{18}F]Fluoride in [^{18}O] water was transferred to the iPHASE FlexLAB radiosynthesis module and passed through a pre-conditioned QMA cartridge. Trapped [^{18}F]fluoride (10.8–8.92 GBq) was eluted into the reaction vessel with a solution containing $C_2K_2O_4$ (2–3 mg, 12–18 μmol) and Kryptofix 2.2.2 (10–12 mg, 27–32 μmol) in 300 μl H_2O/700 μl MeCN. The solution was evaporated at 65°C under nitrogen flow and vacuum for 13 min, followed by heating at 120°C under nitrogen then vacuum for a further 7 min. To the anhydrous [^{18}F]KF/K_{222}/$C_2K_2O_4$ residue, iodonium salt **139** (20 mg, 42 μmol) in DMSO:tAmOH (0.4:0.6, 1 ml) was added. After 5 min at 100 °C, the solvent was evaporated to half volume, and the residue was diluted with mobile phase (0.05% TFA H_2O/MeCN, 1.3:0.2, 1.5 ml). The mixture was transferred to the loop injection vial. The reaction vial was then washed with mobile phase (0.05% TFA H_2O/MeCN, 1.3:0.2, 1.5 ml)

and transferred to the loop injection vial. Purification by preparative HPLC (0.05% TFA in 15–80% MeCN:H_2O over 40 min, column G) afforded the title compound **140** (262–462 MBq, 1.0% yield (n=3) decay corrected to SOS). The total reaction time was 45 min. Automation details are illustrated in Table 7.

2,3,5,6-Tetrafluorophenyl 4-fluorobenzoate

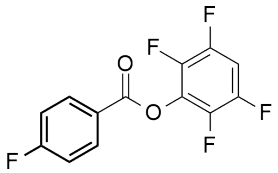

To fluorobenzoic acid (1.0 g, 7.14 mmol, 1 eq.), tetrafluorophenol **137** (0.99 mg, 7.14 mmol, 1 eq.) and EDC.HCl (1.35 g, 7.14 mmol, 1 eq) was added DMF (~ 5 ml) and the reaction was stirred at rt for 4 h. H_2O (10 ml) was added and the mixture was extracted with DCM (3 × 100 ml) and the organic phase was washed with H_2O (3 × 100 ml) and 0.1M HCl (3 × 50 ml), dried and evaporated. Residue was recrystallised from n-hexane to afford product (85% yield, 1.75 g). ^{1}H NMR (500 MHz, d_6-DMSO) δ 8.23–8.18 (m, 2H), 7.99 (qd, *J*=10.7, 7.3 Hz, 1H), 7.48 (dd, *J*=12.3, 5.1 Hz, 2H). ^{13}C NMR (101 MHz, d_6-DMSO) δ 166.7 (d, *J*=254.9 Hz), 161.7, 146.0 (dtd, *J*=24.1, 12.4, 3.7 Hz), 140.6 (dd, *J*=246.3, 15.8 Hz), 134.0 (d, *J*=10.1 Hz), 129.2 (d, *J*=13.9 Hz), 123.1 (d, *J*=2.5 Hz), 117.19 (d, *J*=22.5 Hz), 105.2 (t, *J*=23.7 Hz). ^{19}F NMR (470 MHz, d_6-DMSO) δ –102.20 (dd, *J*=8.3, 5.1 Hz), –139.00–138.15 (m), –153.57 (dt, *J*=15.6, 8.1 Hz). ESI-MS $[M+H]^+$ ($C_{13}H_6F_5O_2^+$) *m/z* 289.028 (calculated), 289.028 (observed). (lit. m.p. 73–74°C).[115] Analytical data consistent with literature data.[115]

Position	Reagents or Materials
V 1	H_2O:MeCN (0.3:0.7, 1 ml) $KHCO_3$ (2 mg) (or $C_2K_2O_4$) and K_{222} (10 mg)
V 2	MeCN (1 ml)
V 3	10–20 mg precursor
V 6	0.05 % TFA H_2O:MeCN (2.6:0.4, 3 ml)
V 9	DMSO (1.5 ml)
V 10	H_2O (5 ml)
HPLC 1 RB	H_2O (30 ml)

Table 7: Automation details of [^{18}F]NFB, [^{18}F]NFN, [^{18}F]TFN or [^{18}F]TFB.

N-Benzyl 6-[^{18}F]fluoronicotinamide (141)

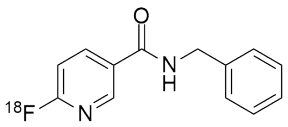

The radioHPLC fraction containing [^{18}F]NFN **129** or [^{18}F]TFN **33** was trapped on a Strata X reversed phase SPE cartridge. [^{18}F]NFN **129** or [^{18}F]TFN **33** (356–1052 MBq) isolated on the Strata X cartridge was eluted with DMSO (1.5 ml) into a vial. For the concentration efficiency experiments, 40 µl of pure eluted [^{18}F]NFN **129** or [^{18}F]TFN **33** was dispensed into vials each containing 100 µl of DMSO and 5 µl TEA. Vials were labelled A H and contained the following concentrations of benzyl amine: A= 9.17 µM; B= 4.56 µM; C=2.29 µM; D=1.15 µM; E= 0.57 µM; F=0.29 µM; G=0.14 µM; and H=0.07 µM. A control was also prepared with 0 µM benzyl amine. After 10 mins, reactions were quenched with 100 µl of H_2O and then~1 MBq of solution from each vial was injected into radioHPLC (0.05% TFA in 15–80% MeCN:H_2O over 15 min, column

H) and % yield of **141** was calculated by radioHPLC integration. Coinjection with authentic sample confirmed product identity. Experiments were performed in triplicates.

N-Benzyl 6-fluoronicotinamide

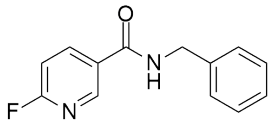

To a solution of fluoronicotinic acid (101 mg, 0.714 mmol, 1 eq.) in DMF (0.5 ml), benzyl amine (117 µl, 1.07 mmol, 1.5 eq.), HATU (298 mg, 0.785 mmol, 1.1 eq.) and DIPEA (372 µl, 2.14 mmol, 3 eq.) were added and the reaction mixture was stirred for 12 h. The solvent was then removed under reduced pressure and partitioned between ethyl acetate (20 ml) and water (20 ml). The organic layer was separated, and the aqueous layer extracted with ethyl acetate (3 × 50 ml). The combined organic layer was washed with 2.0 M aqueous hydrochloric acid (25 ml), saturated sodium carbonate (25 ml) and brine (25 ml). The organic layers were dried over $MgSO_4$, filtered and solvent removed under reduced pressure. The residue was purified by silica chromatography (40% ethyl acetate in hexane) to give the desired product as a white crystal (92 mg, 79% yield). ^{1}H NMR (400 MHz, $CDCl_3$) δ 8.60 (d, *J*=2.0 Hz, 1H), 8.25 (td, *J*=8.0, 2.4 Hz, 1H), 7.38–7.28 (m, 4H), 6.99 (dd, *J*=8.5, 2.9 Hz, 1H), 6.51 (bs, 1H), 4.63 (d, *J*=5.6 Hz, 2H). ^{13}C NMR (101 MHz, $CDCl_3$) δ 165.0 (d, *J*=244.7 Hz), 164.3, 146.6 (d, *J*=15.9 Hz), 140.9 (d, *J*=8.9 Hz), 137.5, 128.9, 128.4. 128.3, 127.9 (d, *J*=7.2 Hz), 109.8 (d, *J*=37.4 Hz), 44.29. ^{19}F NMR (470 MHz, $CDCl_3$) δ –63.29 (d, *J*=5.7 Hz). ESI-MS $[M+H]^+$ ($C_{13}H_{12}FN_2O^+$) : *m/z* 231.092 (calculated), 231.092 (observed).

N-Benzyl 4-[^{18}F]fluorobenzamide (142)

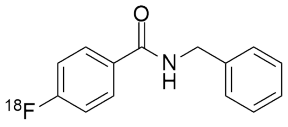

The radioHPLC fraction containing [^{18}F]NFB **133** was trapped on a Strata X reversed phase SPE cartridge. [^{18}F]NFB **133** (341–999 MBq) isolated on the Strata X cartridge was eluted with DMSO (1.5 ml) into a vial. For the concentration efficiency experiments, 40 µl of pure eluted [^{18}F]NFB **133** was dispensed into vials each containing 100 µl of DMSO and 5 µl TEA. Vials were labelled A H and contained the following concentrations of benzyl amine: A= 9.17 µM; B= 4.56 µM; C=2.29 µM; D= 1.15 µM; E= 0.57 µM; F=0.29 µM; G=0.14 µM; and H= 0.07 µM. A control was also prepared with 0 µM benzyl amine. After 10 mins, reactions were quenched with 100 µl of H_2O and then ~ 1 MBq of solution from each vial was injected into radioHPLC (0.05% TFA in 15–80% MeCN:H_2O over 15 min, column H) and % yield of **142** was calculated by radioHPLC integration. Coinjection with authentic sample confirmed product identity. Experiments were performed in triplicates.

N-benzyl-4-fluorobenzamide

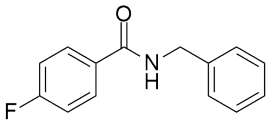

To a solution of fluorobenzoic acid (100 mg, 0.714 mmol, 1 eq.) in DMF (0.5 ml), benzyl amine (117 µl, 1.07 mmol, 1.5 eq.), HATU (298 mg, 0.785 mmol, 1.1 eq.) and DIPEA (372 µl, 2.14 mmol, 3 eq.) were added and the reaction mixture was stirred at rt for 12 h. The solvent was then removed under reduced pressure and partitioned between ethyl acetate (20 ml) and water (20 ml). The organic layer was separated, and the aqueous layer extracted with ethyl acetate (3 × 50

ml). The combined organic layer was washed with 2.0 M aqueous hydrochloric acid (25 ml), saturated sodium carbonate (25 ml) and brine (25 ml). The organic layers were dried over $MgSO_4$, filtered and solvent removed under reduced pressure. The crude was then purified by silica chromatography (40% ethyl acetate in n-hexane) to give the desired product as a white crystal shape (100 mg, 85% yield) ^{1}H NMR (400 MHz, $CDCl_3$) δ 7.79 (dd, *J*=8.7, 5.4 Hz, 2H), 7.38–7.24 (m, 5H), 7.12–7.06 (m, 2H), 6.47 (bs, 1H), 4.62 (d, *J*=5.6 Hz, 2H). ^{13}C NMR (101 MHz, $CDCl_3$) δ 166.0, 164.9 (d, *J*=282 Hz), 138.0, 130.5 (d, *J*=3.0 Hz), 129.3 (d, *J*=8.9 Hz), 128.8, 127.9, 127.7, 115.6 (d, *J*=21.8 Hz), 44.2. ^{19}F NMR (470 MHz, $CDCl_3$) δ –103.9 –102.68 (m). ESI-MS $[M+H]^+$ ($C_{14}H_{13}FNO^+$): *m/z* 230.097 (calculated), 230.097 (observed). (lit. m.p. 134.3–135.6 °C).[116] Analytical data consistent with literature data.[116]

cyclo(D-Tyr-N(Me)-D-Orn([^{18}F]FB)-Arg-Nal-Gly) (143)

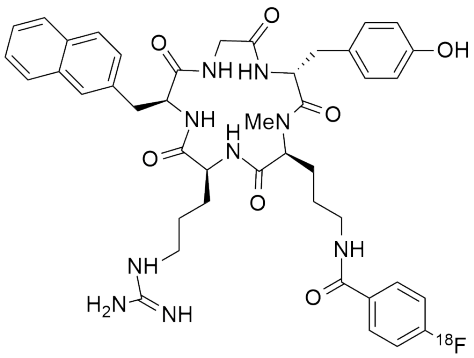

[^{18}F]NFB **133** (2000 MBq) trapped on a on a Strata X reversed phase SPE cartridge was eluted with DMSO:MeCN (0.3:0.4, 0.7 ml, V9) into a vial containing c(D-Tyr-N(Me)-D-Orn-Arg-Nal-Gly) **106** (1.0 mg, 1.4 μmol) and TEA:DMSO (1:20, 20 μl). The mixture was transferred into a reaction vessel. The reaction was heated to 35°C and MeCN was evaporated for 5 min. The reaction mixture was diluted (0.05% TFA H_2O:MeCN, 1.3:0.2, 1.5 ml, V6) and transferred to loop vial 2. The crude reaction mixture was purified by HPLC 2 (0.1 % TFA in 0–80 % MeCN:H_2O

over 40 min, Column E). The HPLC fraction containing the product was diluted with sterile H_2O (30 ml, round bottom flask 2) and isolated on C18 SPE cartridge 2. The peptide **143** was then eluted with DMSO (0.6 ml, vial 12) via a sodium sulfate cartridge into a sterile vial, to obtain fully sterile product **143** (1200 MBq, 60% d.c yield, specific activity:0.86 MBq/µg). Automation details are illustrated in Table 8.

cyclo(D-Tyr(SO$_3$H)-N(Me)-D-Orn([^{18}F]FB)-Arg-Nal-Gly) (144)

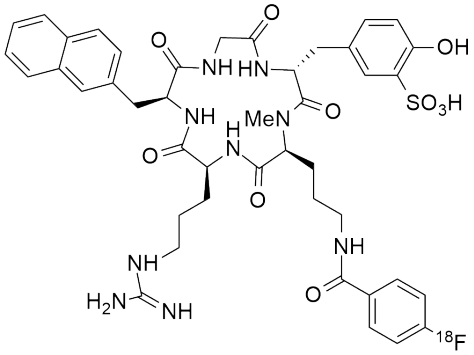

[^{18}F]NFB **133** (2100 MBq) trapped on a on a Strata X reversed phase SPE cartridge was eluted with DMSO:MeCN (0.3:0.4, 0.7 ml, V9) into a vial containing c(D-Tyr(SO$_3$H)-N(Me)-D-Orn-Arg-Nal-Gly) **106** (1.0 mg, 1.4 µmol) and TEA:DMSO (1:20, 20 µl). The mixture was transferred into a reaction vessel. The reaction was heated to 35°C and MeCN was evaporated for 5 min. The reaction mixture was diluted (0.05% TFA H_2O:MeCN, 1.3:0.2, 1.5 ml, V6) and transferred to loop vial 2. The crude reaction mixture was purified by HPLC 2 (0.1 % TFA in 0–80% MeCN:H_2O over 40 min, Column E). The HPLC fraction containing the product was diluted with sterile water (30 ml, round bottom flask 2) and isolated on C18 SPE cartridge 2. The peptide **144** was then eluted with DMSO (0.6 ml, vial 12) via a sodium sulfate cartridge into a sterile vial, to obtain fully sterile product **144** (1302 MBq, 62% d.c yield, specific activity: 0.93 MBq/µg). Automation details are illustrated in Table 8.

Position	Reagents or Materials
V 13–V 15	Sep Pak Light QMA
V 1	H_2O:MeCN (0.3:0.7, 1.0 ml) $C_2K_2O_4$ (2 mg) and K_{222} (10 mg)
V 2	MeCN (1 ml)
V 3	**136** (20 mg) tAmOH:DMSO (0.4:0.6, 1 ml)
V 6	0.05% TFA in H_2O:MeCN (1.3:0.2, 1.5 ml)
V 8	DMSO (1.5 ml)
V 9	H_2O (5 ml)
V 18	**106**/**107** (1.0 mg) DMSO:MeCN (0.3:0.4, 0.7 ml) and 1 µl TEA
V 15	0.05% TFA in H_2O:MeCN (1.3:0.2, 1.5 ml)
V 12	EtOH
HPLC 1 RB	H_2O (30 ml)
HPLC 2 RB	H_2O (30 ml)
V 46–Reactor 2	Na_2SO_4 cartridge
V 46–V 22	C18 SPE cartridge
V 39–V 47	C18 SPE cartridge

Table 8: Automation details for labelling CXCR4 peptides with [^{18}F]NFB on iPHASE Flexlab.

cyclo(D-Tyr(SO$_3$H)-N(Me)-D-Orn(Amba, DOTA, ^{68}Ga)-Arg-Nal-Gly) (145)

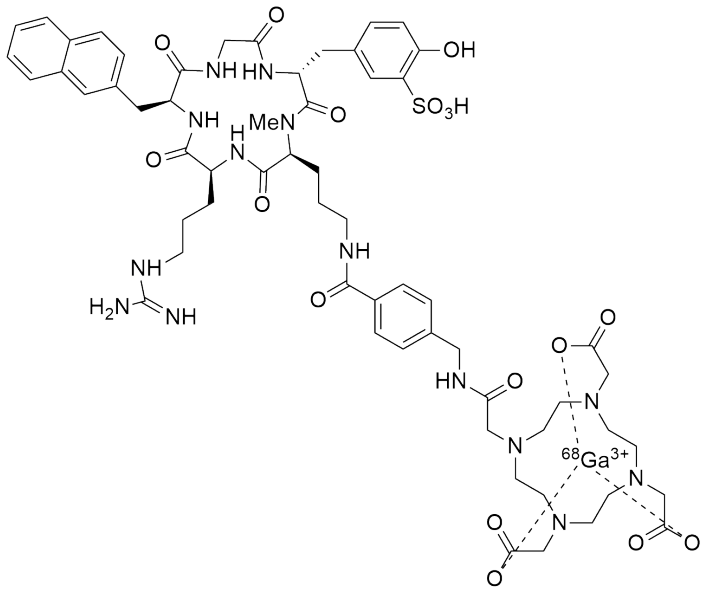

Radiolabelling of **79** was performed on the MultiSyn automated radiosynthesis module (Figure 11). Gallium-68 was eluted from a commercially available Ge-68/Ga-68 generator (ITG) with diluted HCl (0.05 M). Sulfonated peptide precursor c(D-Tyr(SO$_3$H)-N(Me)-D-Orn(Amba, DOTA)-Arg-Nal-Gly) **79** (1.0 mg, 0.77 μmol) was dissolved in H_2O (0.1 ml) and NaOAc (0.25 M, 0.8 ml). To the precursor mixture was added ethanol (200 μl) and ascorbic acid (0.005 M, 200 μl). The precursor solution and eluted gallium-68 was transferred into a reaction vessel for 5 min at 95°C. Radiolabelled material was isolated by S.P.E. purification (Strata X, 30 mg), eluted with DMSO (0.5 ml), diluted with H_2O and analysed by RP-HPLC (0.05% TFA 15–80% MeCN:H_2O over 40 min, column H) and radioTLC. Coinjection of authentic product **81** on RP-HPLC confirmed **145** product formation. Starting activities of 2.1 GBq yielded product **145** in 80% radiochemical yield (based on initial ^{68}Ga activity, decay corrected) in >91% radiochemical purity (specific activity: 1.1 MBq/μg).

Methyl (2S)-amino-4-(methylthio)butanoate hydrochloride (153)

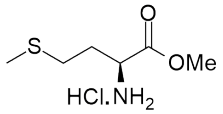

L-Methionine **152** (10.0 g, 0.067 mol) was suspended in MeOH (500 ml) and stirred while thionyl chloride (9.72 ml, 0.134 mol) was added dropwise to the solution at 0 °C. The solution was then heated at reflux for 16 h. The reaction mixture was then evaporated under reduced pressure to yield a pale yellow solid. The solid was triturated with hot diethyl ether and the supernatant discarded to leave the title compound as a white solid which was further dried under vacuum to give **153** (13.6 g, quant. yield) ^{1}H NMR (400 MHz, $CDCl_3$ δ 4.33 (t, *J*=6.4 Hz, 1H), 3.88 (s, 3H), 2.71 (t, *J*=7.0 Hz, 2H), 2.33 (m, 1H), 2.23 (m, 1H), 2.14 (s, 3H).^{13}C NMR (126 MHz, $CDCl_3$) δ 170.4, 53.5, 51.6, 28.6, 28.3, 13.7. ESI-MS $[M+H]^+$ ($C_6H_{14}NO_2SNa^+$) *m/z* 164.074 (calculated), 164.074 (observed). (lit. m.p. 147–150 °C).[96] Analytical data consistent with literature data.[96]

Methyl (2S)-(benzyloxycarbonylamino)-4-(methylthio)butanoate (154)

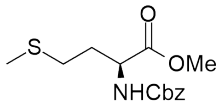

To **153** (14.0 g, 0.070 mol) was added $KHCO_3$ (40.0 g) in H_2O:EtOAc (1:1, 500 ml). Benzyl chloroformate (17.6 ml, 0.11 mol) was added dropwise over a period of 0.5 h. After the mixture was stirred for 4 h, the organic layer was separated, washed with 0.1M HCl (3 × 500 ml), H_2O (3 × 500 ml), dried over Na_2SO_4 and evaporated under reduced pressure to provide **154** as a colourless oily residue (20.9 g, quant.). ^{1}H NMR (400 MHz, $CDCl_3$) δ 7.35–7.28 (m, 5H), 5.41 (d, *J*=7.4 Hz, 1H), 5.11 (s, 2H), 4.51 (dd, *J*=12.7, 7.6 Hz, 1H), 3.75 (s, 3H), 2.53 (t, *J*=7.3 Hz, 2H), 2.16 (dt, *J*=12.9, 7.3 Hz, 1H), 2.08 (s, 3H), 1.96 (dt, *J*=14.6, 7.2 Hz, 1H). ^{13}C NMR (126 MHz,

$CDCl_3$) δ 172.7, 151.0, 128.5, 128.2, 127.2, 67.1, 53.1, 52.5, 31.9, 29.8, 15.4. ESI-MS $[M+H]^+$ ($C_{14}H_{20}NO_4S^+$) *m/z* 298.110 (calculated), 298.110 (observed). (lit. m.p. 42–43 °C).[96] $[\alpha]^{20}_D$+16.9° (c 4, $CHCl_3$). Analytical data consistent with literature data.[96]

Methyl (2S)-(benzyloxycarbonylamino)-4-(methylsulfinyl)butanoate (155)

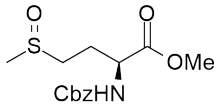

A solution of sodium metaperiodate (300 mg, 1.40 mmol) in H_2O (1.6 ml) was added dropwise to a vigorously stirred solution of sulfide **154** (400 mg, 1.34 mmol) in MeOH (4 ml) at 0°C. The reaction mixture was stirred for an additional 4 h. The precipitated iodate was filtered off and washed with MeOH (3 × 20 ml), and the combined filtrates were concentrated to ~1.5 ml under reduced pressure and then extracted with $CHCl_3$ (3 × 20 ml). The combined organic extracts were washed with H_2O (3 × 50 ml), dried over Na_2SO_4 and evaporated under reduced pressure to give sulfoxide **155** as a yellow oil (440 mg, quant.). ^{1}H NMR (400 MHz, $CDCl_3$) δ 7.52–7.34 (m, 5H), 5.61 (m, 1H), 5.11 (s, 2H), 4.44 (m, 1H), 3.77 (s, 3H), 2.71–2.67 (m, 2H), 2.55 (s, 3H), 2.40 (dt, *J*=14.1, 7.4 Hz, 1H), 2.17 (m, 1H).^{13}C NMR (126 MHz, $CDCl_3$) δ 171.6, 152.9, 136.1, 128.6, 128.3, 128.0, 67.2, 53.1, 52.8, 50.2, 38.6, 26.3. ESI-MS $[M+H]^+$ ($C_{14}H_{20}NO_5S^+$) *m/z* 314.105 (calculated), 314.105 (observed). (lit. m.p. 200–201°C).[96] Analytical data consistent with literature data.[96]

Methyl (2S)-(benzyloxycarbonylamino)but-3-enoate (156)

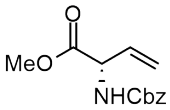

Sulfoxide **155** (3.10 g, 10 mmol) was distilled at 200 °C (8 mmHg) in a Kugelrohr apparatus. The yellowish oily distillate was purified by chromatography on silica (40% ethyl acetate in n-hexane) to give **156** as a yellow oil (1.15 g, 57% yield). ^{1}H NMR (400 MHz, $CDCl_3$) δ 7.43–7.28 (m, 5H), 5.91 (m, 1H), 5.45 (bd, *J*=6.6 Hz, 1H), 5.37 (dd, *J*=17.1, 1.6 Hz, 1H), 5.29 (dd, *J*=10.3, 1.7 Hz, 1H), 5.15 (s, 2H), 4.95 (t, *J*=6.3 Hz, 1H), 3.78 (s, 3H). ^{13}C NMR (101 MHz, $CDCl_3$) δ 170.4, 157.3, 133.8, 130.7, 128.6, 128.3, 128.1, 117.4, 66.6, 62.3, 57.3. ESI-MS $[M+H]^+$ ($C_{13}H_{16}NO_4^+$) *m/z* 202.107 (calculated), 202.107 (observed). $[\alpha]^{20}_D$ –11.8° (c 1.8, CH_3OH). (lit. m.p. 35–36 °C).[96]Analytical data consistent with literature data.[96]

(S)-2-Aminobut-3-enoic acid hydrochloride (157)

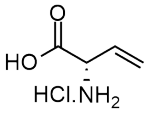

A suspension of **156** (2.50 g, 10 mmol) in hydrochloric acid (6 M, 50 ml) was heated at reflux for 1 h. The solution was cooled, washed with chloroform (2 × 20 ml) and evaporated under reduced pressure. Crystallisation of the residue was achieved by heating in acetone (50 ml) to afford **157** as a white solid (0.867 g, 85% yield). ^{1}H NMR (400 MHz, D_2O) δ 5.92–5.84 (m 1H), 5.47 (ddd, *J*=14.3, 3.5, 1.3 Hz, 2H), 5.43 (d, *J*=7.4 Hz, 1H), 4.51 (d, *J*=7.3 Hz, 1H). ^{13}C NMR (101 MHz, D_2O) δ 171.0, 128.4, 122.5, 55.5. ESI-MS $[M+H]^+$ ($C_4H_8NO_2^+$) *m/z* 102.055 (calculated), 102.055 (observed). (lit. m.p. 175–177 °C).[96] $[\alpha]^{20}_D$ +78.5° (c 1.9, H_2O). Analytical data consistent with literature data.[96]

(S)-2-((tert-Butoxycarbonyl)amino)but-3-enoic acid (158)

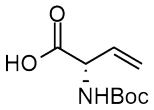

A solution of **157** (275 mg, 2 mmol), Boc_2O (575 mg, 2.1 mmol), and $NaHCO_3$ (335 mg, 4 mmol) in dioxane:H_2O (1:1, 25 ml) was heated at reflux for 2 h. The dioxane was evaporated under reduced pressure, and the aqueous solution was acidified with dilute HCl to pH 3 and extracted with $CHCl_3$ (3 × 15 ml). The combined organic extracts were washed with saturated $NaHCO_3$ (3 × 15 ml) then H_2O (3 × 15 ml), dried over Na_2SO_4, and evaporated under reduced pressure to give **158** as a yellow oil (340 mg, 76% yield). ^{1}H NMR (500 MHz, D_2O) δ 6.10 (d, *J*=6.5 Hz, 1H), 5.29 (d, *J*=17.2 Hz, 1H), 5.23 (d, *J*=10.4 Hz, 1H), 4.59 (d, *J*=3.9 Hz, 1H), 1.58 (s, 9H).^{13}C NMR (101 MHz, D_2O) δ 171.3, 157.4, 134.5, 116.4, 81.6, 58.8, 27.8. ESI-MS $[M+H]^+$ ($C_9H_{15}NNaO_4^+$) *m/z* 224.089 (calculated), $[M+H]^+$: 224.089 (observed). $[\alpha]^{20}_D$ +2.8° (c 4, CH_3OH). Analytical data consistent with literature data.[96]

4-Methoxybenzyl (2S)-((tert-butoxycarbonyl)amino)but-3-enoate (159)

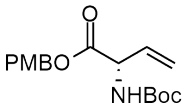

To a stirred solution of **158** (0.36 g, 1.8 mmol) and $NaHCO_3$ (0.16 g, 1.8 mmol) in dry DMF (15 ml), p-methoxybenzyl chloride (0.24 ml, 1.8 mmol) was added under inert atmosphere. The reaction was stirred overnight, then diluted with water (30 ml) and extracted with ethyl acetate (3 × 30 ml). The combined organic layer was concentrated and then purified by column chromatography to give the product **159** as a colourless oil (0.52 g, 90% yield). ^{1}H NMR (500 MHz, $CDCl_3$) δ 7.29 (d, *J*=8.6 Hz, 2H), 6.89 (d, *J*=8.6 Hz, 2H), 5.95–5.84 (m, 1H), 5.33 (dd,

J=17.2, 1.4 Hz, 1H), 5.24 (dd, *J*=10.5, 0.9 Hz, 1H), 5.12 (d, *J*=5.9 Hz, 2H), 4.93–4.87 (m, 1H), 3.81 (s, 3H), 1.45 (s, 9H). ^{13}C NMR (125 MHz, $CDCl_3$) δ 171.1, 164.3, 154.7, 136.0, 130.1, 128.8, 117.3, 113.9, 79.8, 67.2, 62.8, 55.3, 28.3. ESI-MS $[M+H]^+$ ($C_{17}H_{24}NO_5^+$) *m/z* 322.165 (calculated), 322.165 (observed).

4-Methoxybenzyl (2S,3S)-((tert-butoxycarbonyl)amino)-2-(oxiran-2-yl)acetate (160)

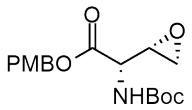

To a stirred solution of **159** (0.20 g, 0.60 mmol) in DCM (160 ml), mCPBA (0.54 g, 3.1 mmol) was added and the mixture stirred for 10 days. The organic phase was cooled to 0°C and then washed with saturated sodium sulfite (3 × 10 ml), saturated $NaHCO_3$ (3 × 10 ml) and brine (3 × 10 ml). The organic phase was then dried over Na_2SO_4 and evaporated under reduced pressure. The residue was then purified by column chromatography (30% ethyl acetate in n-hexane) to give the epoxide **160** as pale yellow oil (0.18 g, 90% yield) as a 3:1 ratio of diastereomers. (syn isomer, major) ^{1}H NMR (400 MHz, $CDCl_3$) δ 7.28 (d, *J*=8.4 Hz, 2H), 6.86 (d, *J*=8.4 Hz, 2H), 5.14–5.10 (m, 2H), 5.00 (d, *J*=8.0 Hz, 1H), 4.65 (d, *J*=8.5 Hz), 3.80 (s,3H,), 3.43 (m, 1H,), 2.75–2.69 (m, 2H), 1.44 (s, 9H). ^{13}C NMR δ 175.6, 159.8, 157.3, 130.2, 128.3, 114.0, 79.6, 67.7, 58.5, 55.3, 51.3, 43.8, 28.2. ESI-MS $[M+H]^+$ ($C_{17}H_{24}NO_6^+$) *m/z* 338.159 (calculated), 338.159 (observed). (anti isomer, minor) ^{1}H NMR (400 MHz, $CDCl_3$) δ 7.30 (d, *J*=8.6 Hz, 2H), 6.89 (d, *J*=8.6 Hz, 2H), 5.17–5.12 (m, 2H), 5.20 (d, *J*=8.2 Hz, 1H), 4.57 (d, *J*=8.5 Hz, 1H), 3.81 (s, 3H), 3.20 (dd, *J*=7.2, 4.1 Hz, 1H), 2.75 (dd, *J*=8.6, 4.3 Hz, 1H), 2.73 (m, 1H), 1.44 (s, 9H). ^{13}C NMR δ 175.3, 159.7, 157.1, 130.9, 129.1, 115.1, 79.2, 67.9, 57.2, 55.5, 51.9, 43.5, 28.1. ESI-MS $[M+H]^+$ ($C_{17}H_{24}NO_6^+$) *m/z* 338.159 (calculated), 338.159 (observed).

(1S,2S)-(+)-1,2-Cyclohexanediamino-N,N'-bis(3,5-di-t-butylsalicylidene)chromium(III) chloride (163)

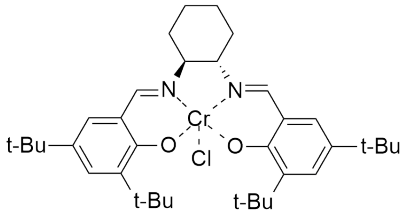

Salen ligand **162** (50 mg, 0.091 mmol) and $CrCl_2$ (10.8 mg, 0.098 mmol) were dissolved in dry THF (1 ml) and stirred under inert conditions at rt for 12 h. The reaction mixture was poured into diethyl ether, organic layer was washed with saturated NH_4Cl solution (3 × 100 ml), brine (3 × 100 ml) and dried over Na_2SO_4. The solvent was evaporated under reduced pressure to give **163** as reddish-brown powder (45 mg, 81% yield). ESI-MS $[M+H]^+$ $(C_{36}H_{52}CrN_2O_2)^+$ *m/z* 596.343 (calculated), 596.343 (observed). Analytical data consistent with literature data.[98]

(1S,2S)-(+)-1,2-Cyclohexanediamino-N,N'-bis(3,5-di-t-butylsalicylidene)cobalt(III) p-toluenesulfonate monohydrate) (164)

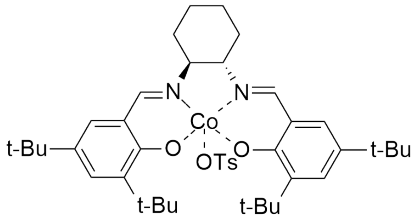

A solution of cobalt(II)salen **165** (35 mg, 0.058 mmol) and p-TsOH (25 mg, 0.13 mmol) in dichloromethane (2 ml) was sonicated for 10 min. The mixture was filtered to remove any insoluble material and the solvent was removed under reduced pressure. The resulting solid was suspended in pentane and filtered to give **164** as a green solid (46 mg, 80% yield). ESI-MS $[M+H]^+$

$(C_{36}H_{52}CoN_2O_2)^+$ *m/z* 603.336 (calculated), 603.336 (observed). Analytical data consistent with literature data.[94]

4-Methoxybenzyl (2S,3S)-((tert-butoxycarbonyl)amino)-4-fluoro-3-hydroxybutanoate (161)

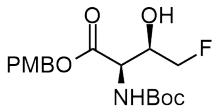

To a mixture of Co(III)salen tosylate **164** (16 mg, 2.6 μmol) and DBN (0.26 μl, 2.1 μmol), HFIP (11 μl, 100 μmol) was added and diluted with diethyl ether (0.13 ml). Epoxide **160** was then added (8.7 mg, 26 μmol), followed by benzoyl fluoride (5.6 μl, 52 μmol) and the mixture was stirred for 12 h. The reaction mixture was purified by column chromatography (30% ethyl acetate in n-hexane) and then further purified by preparative RP-HPLC (0.1% TFA 0–40% MeCN:H_2O over 40 min, Column D) to give protected fluorothreonine **161** as a white solid (8.4 mg, 60% yield). ^{1}H NMR (400 MHz, $CDCl_3$) δ: 7.30–7.27 (m, 2H), 6.90 (d, *J*=8.6 Hz, 2H), 5.28 (bs, 1H), 5.21–5.18 (m, 2H), 4.65 (m, 1H), 4.39 (ddd, *J*=47.2, 9.8, 3.8 Hz, 2H), 4.35 (d, *J*=5.9 Hz, 1H), 3.82 (s, 3H), 1.45 (s, 9H) ^{13}C NMR (400 MHz, $CDCl_3$) δ: 171.2, 168.2, 157.3, 135.6, 130.4, 114.1, 82.9 (d, *J*=162.6 Hz), 79.6, 70.3 (d, *J*=19.1), 68.1, 58.1, 57.7, 28.8. ^{19}F NMR (470 MHz, $CDCl_3$) δ –232.72 (td, J=46.5, 19.6 Hz). ESI-MS $[M+H]^+$ ($C_{17}H_{25}FNO_6^+$) *m/z* 358.166 (calculated), 358.166 (observed).

$NiCl_2.6H_2O$/di-MeObipy catalyst

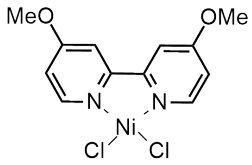

$NiCl_2.6H_2O$ (142.8 mg, 0.60 mmol) was added to di-MeObipy (168.6 mg, 0.77 mmol) and the flask was evacuated and backfilled with argon three times. Dry THF (24 ml, [$NiCl_2.6H_2O$] = 0.025M) was added and the resulting mixture was stirred at rt for 36 h (until no granular $NiCl_2.H_2O$ was observed after sonication) to afford a blue/green suspension.[102]

[B_2pin_2Me]Li complex

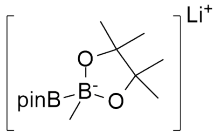

A flask containing B_2pin_2 (1.30 g, 5.13 mmol) was evacuated and backfilled with argon three times. Dry THF (4.67 ml, [[B_2pin_2Me]Li]= 1.1M) was added. MeLi (2.95, 1.6 M in Et_2O) was added at 0 °C dropwise. The reaction mixture was warmed to rt and stirred for 1 h to afford a clear solution.[102]

N-Boc-Thr(OtBu) N'-hydroxyphthalimidyl ester (194)

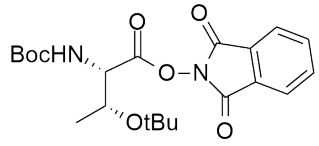

N-Boc-Thr(OtBu)-OH **193** (1.50 g, 5.44 mmol), *N*-hydroxyphthalimide (888 mg, 5.44 mmol) and DMAP (66.6 mg, 0.54 mmol) were dissolved in DCM (24 ml, 0.2M). DIC (0.940 ml,

5.85 mmol) was added and the mixture was stirred for 2 h. The mixture was filtered, and the solid residue rinsed with DCM. The filtrate was concentrated, dissolved in n-hexane and filtered. The filtrate was concentrated to afford the corresponding ester **194** as a light yellow powder (2.27 g, 80% yield). ^{1}H NMR (400 MHz, $CDCl_3$) δ 7.87 (4H, s), 5.40 (d, *J*=9.5 Hz, 1H), 4.60 (d, *J*=8.5, 1H), 4.37 (m, 1H), 1.47 (s, 9H), 1.30 (d, *J*=6.1 Hz, 3H), 1.22 (s, 9H).^{13}C NMR (101 MHz, $CDCl_3$) δ 175.3, 160.8, 156.7, 131.3, 131.1, 125.6, 80.3, 80.1, 74.5, 60.2, 29.8, 29.7, 19.1. ESI-MS ($C_{21}H_{29}N_2O_7^+$) *m/z* 421.196 (calculated), 421.196 (observed). Analytical data consistent with literature data.[117]

tert-Butyl (1RS, 2R)-2-(tert-butoxy)-1-(4,4,5,5-tetramethyl-1,3,2-dioxaborolan-2 yl)propyl)carbamate (195)

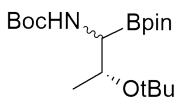

A flask containing phthalimide ester **194** (2.30 g, 5.47 mmol) and $MgBr_2.OEt_2$ (2.11 mg, 8.20 mmol) was evacuated and backfilled with argon three times. $NiCl_2.6H_2O$/di-MeObipy catalyst solution (0.025M, 21.90 ml,) was added and the resulting mixture was stirred vigorously and sonicated until no visible solid was observed. The mixture was then cooled to 0 °C before a suspension of [B_2pin_2Me]Li complex in THF (1.1M, 27.8 ml) was added in one portion. After stirring for 1 h at 0 °C, the reaction was warmed to rt and stirred for another 1h. The reaction mixture was filtered through a pad of Celite and purified by column chromatography (20% ethyl acetate in n-hexane) to afford product **195** as a yellow oil (1.63 g, 83% yield). ^{1}H NMR (400 MHz, $CDCl_3$) δ 5.54 (d, *J*=9.5 Hz, 1H), 3.9 (m, 1H), 3.6 (m, 1H), 1.45 (s, 9H), 1.23 (s, 12H), 1.21 (s,

9H), 1.13 (d, *J*=6.4 Hz, 3H). ^{13}C NMR (101 MHz, $CDCl_3$) δ 157.2, 88.3, 79.7, 79.6, 64.1, 62.4, 28.7, 28.3, 25.8, 21.6. ESI-MS ($C_{18}H_{36}BNO_5^+$) *m/z* 358.276 (calculated), 358.276 (observed).

(1RS, 2R)-1-Ammonio-2-hydroxypropyltrifluoroborate (196)

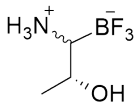

Ester **195** (214 mg, 0.598 mmol) was treated with KF (3M in H_2O, 1.0 ml), HCl (4M in H_2O, 1.0 ml) and MeCN (3.0 ml). The mixture was stirred at rt for 24 h. The solution was lyophilised and then purified by RP-HPLC (0–20% MeCN:H_2O over 50 min, Column D) to afford product **196** as a white solid (84.7 mg, 75% over 3 steps yield) ^{1}H NMR (400 MHz, D_2O) δ 3.90 (m, 1H), 3.63 (td, *J*=11.3, 6.4 Hz, 1H), 1.11 (d, *J*=6.4 Hz, 3H). ^{13}C NMR (101 MHz, D_2O) δ 71.9, 62.4, 19.5. ^{19}F NMR (500 MHz, D_2O): δ –150.49. ESI-MS $[M-H]^-$ ($C_7H_{17}BF_3NO^-$) *m/z* 142.066 (calculated), 142.066 (observed).

N-Boc-Tyr(OtBu) N'-hydroxyphthalimidyl ester (198)

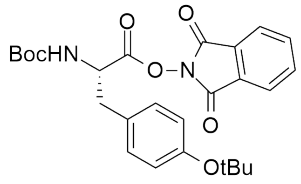

To a solution of N-Boc-Tyr(OtBu)-OH **197** (1.00 g, 2.96 mmol), *N*-hydroxyphthalimide (484 mg, 2.96 mmol) and DMAP (39.2 mg, 0.27 mmol) in DCM (0.2M, 15 ml) was added. DIC (0.51 ml, 3.26 mmol). The mixture was stirred for 2 h. The resulting mixture was filtered, and the solid residue rinsed with DCM. The filtrate was concentrated, dissolved in n-hexane/ethyl acetate (1:1) and filtered. The filtrate was concentrated to afford the corresponding ester **198** as a light

orange powder (1.27 g, 89% yield). ^{1}H NMR (400 MHz, $CDCl_3$,) δ 7.36 (s, 4H), 7.24 (d, *J*=8.5 Hz, 2H), 6.95 (d, *J*=8.5 Hz, 2H), 4.93 (m, 1H), 3.28–2.24 (m, 2H), 1.39 (s, 9H), 1.43 (s, 9H). ^{13}C NMR (101 MHz, $CDCl_3$) δ 177.6, 162.3, 156,9, 157.2, 133.3, 129.5, 128.8, 125.6, 124.4, 86.2, 79.6, 57.5, 37.8, 28.6, 26.7. ESI-MS $[M+H]^+$ $(C_{26}H_{31}N_2O_7)^+$ *m/z* 483.212 (calculated), $[M+H]^+$: 483.212 (observed). Analytical data consistent with literature data.[117]

tert-Butyl (2-(4-(tert-butoxy)phenyl)-1-(4,4,5,5-tetramethyl-1,3,2-dioxaborolan-2-yl)ethyl)carbamate (199)

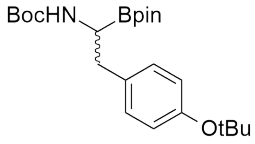

A flask containing ester **198** (750 mg, 1.55 mmol) and $MgBr_2.OEt_2$ (600 mg, 2.33 mmol) was evacuated and backfilled with argon three times. $NiCl_2.6H_2O$/di-MeObipy catalyst solution (6.22 ml, 0.025 M) was added and the resulting mixture was stirred vigorously and sonicated until no visible solid was observed. The mixture was then cooled to 0 °C before a suspension of $[B_2pin_2Me]Li$ complex in THF (1.1M, 7.5 ml) was added in one portion. After stirring for 1 h at 0°C the reaction was warmed to rt and stirred for an additional 1 h. The reaction mixture was then quenched with saturated aq. NH_4Cl until pH = 7. The organic layer was decanted, dried with $MgSO_4$ and concentrated under vacuum to afford product **199** as a yellow oil (540 mg, 83% yield). ^{1}H NMR (400 MHz, $CDCl_3$) δ 7.22 (d, *J*=8.5 Hz, 2H), 6.95 (d, *J*=8.5 Hz, 2H), 4.91 (m, 1H), 3.30–3.25 (m, 2H), 1.39 (s, 9H), 1.43 (s, 9H), 1.10 (s, 12H).^{13}C NMR (101 MHz, $CDCl_3$) δ 158.2, 154.3, 132.6, 128.8, 123.7, 87.6, 86.2, 79.5, 58.9, 30.1, 26.3, 25.1, 23.2. ESI-MS $[M+H]^+$ $(C_{23}H_{39}BNO_5^+)$ *m/z* 420.291 (calculated), 420.291 (observed).

1-Ammonio-2-(4-hydroxyphenyl)ethyltrifluoroborate (200)

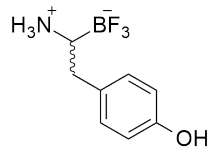

The crude ester **199** (652 mg, 1.55 mmol) was treated with KF (3M in H_2O, 1.0 ml), HCl (4M in H_2O, 1.0 ml) and MeCN (3.0 ml). The mixture was stirred at rt for 72 h, then lyophilised and purified by RP-HPLC (0–20% MeCN:H_2O over 50 min, column D) to afford product **200** as a white solid (309 mg, 72% over 3 steps yield). ^{1}H NMR (500 MHz, D_2O) δ 7.04 (d, *J*=8.5 Hz, 2H), 6.72 (d, *J*=8.5 Hz, 2H), 2.88 (t, *J*=9.8 Hz, 1H), 2.79 (dd, *J*=14.4, 4.5 Hz, 1H), 2.46 (dd, *J*=14.6, 10.9 Hz, 1H).^{13}C NMR (101 MHz, D_2O) δ 157.2, 131.0, 130.2, 115.3, 53.7, 35.0. ^{19}F NMR (500 MHz, D_2O) δ –150.58. ESI-MS $[M-H]^-$ ($C_8H_{10}BF_3NO^-$) *m/z* 204.081 (calculated), 204.081 (observed).

N-Boc-Asp(OtBu) N'-hydroxyphthalimidyl ester (202)

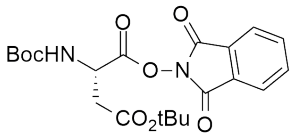

To a solution of N-Boc-Asp(OtBu)OH **201** (0.17 g, 0.60 mmol), NHPI (98 mg, 0.60 mmol) and DMAP (7.0 mg, 0.06 mmol) in dry DCM (3 ml) was added DIC (93 µl, 0.60 mmol). The mixture was stirred for 2 h, filtered and the solid residue rinsed with DCM. The filtrate was concentrated, dissolved in hexane:EtOAc (16:7) and filtered. The filtrate was concentrated to afford the corresponding RAE **202** as a light orange powder (0.232 g, 89%). ^{1}H NMR (400 MHz, $CDCl_3$) δ 7.84 (s, 4H), 6.50 (bs, 1H), 5.48 (d, *J*=8.5 Hz, 1H). 4.58–4.49 (m, 1H), 2.94 (dd, *J*=16.6, 4.4 Hz, 1H), 1.44 (s, 9H), 1.45 (s, 9H) ^{13}C NMR (101 MHz, $CDCl_3$) δ 176.6, 174.0, 161.3, 157.5,

131.3, 131.1, 123.5, 81.1, 79.4, 50.5, 38.1, 27.6, 27.4. ESI-MS $[M+H]^+$ ($C_{21}H_{27}N_2O_8^+$) *m/z* 435.176 (calculated), 435.176 (observed). Analytical data consistent with literature data.[117]

1-Ammonio-2-carboxyethyltrifluoroborate (204)

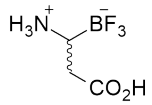

A flask containing pthalimide ester **202** (200 mg, 0.460 mmol) and $MgBr_2.Et_2O$ (170 mg. 0.66 mol) was evacuated and backfilled with argon three times. $NiCl_2.6H_2O$/di-MeObipy catalyst solution (0.025 M, 1.76 ml) was added and the resulting mixture was stirred vigorously and sonicated until no visible solid was observed. The mixture was then cooled to 0°C before a suspension of $[B_2pin_2Me]Li$ complex in THF (1.1M, 2.15 ml) was added in one portion. After stirring for 1 h at 0°C, the reaction was warmed to rt and stirred for an additional 1 h. The reaction was then quenched with saturated aq. NH_4Cl and H_2O (10 ml) was added. The crude mixture was then extracted with ethyl acetate (3 × 30 ml), dried with $MgSO_4$ and then evaporated to dryness under reduced pressure to afford crude pinacol boron **203.** The crude mixture was treated with KF (3M in H_2O, 1.0 ml), HCl (4M in H_2O, 1.0 ml) and MeCN (3.0 ml) and injected straight into RP-HPLC (0-20% acetonitrile over 50 min 0.1% TFA, column D) to afford product **204** as a white solid (70.1 mg, 70% yield over 3 steps). ^{1}H NMR (500 MHz, D_2O) δ 3.92–3.88 (m, 1H), 2.88 (dd, *J*=16.6, 3.9 Hz, 1H), 2.70 (dd, *J*=16.5, 4.2 Hz, 1H). ^{13}C NMR (125 MHz, D_2O) δ 177.1, 49.6, 28.4. ^{19}F NMR (500 MHz, D_2O) δ –150.51. ESI-MS $[M+H]^-$ ($C_3H_6BF_3NO_2^-$) *m/z* 156.044 (calculated), 156.042 (observed).

1-Ammonio-2-carboxyethyl[^{18}F]trifluoroborate (205)

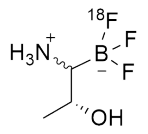

Threonine trifluoroborate **196** (1.5 mg, 0.48 μmol) was dissolved in solution of pyridazine-HCl (pH 2.0–2.5, 1M, 2.0 ml). DMF (2 ml). No carrier added fluoride was trapped on a QMA cartridge and then eluted with saline (7.5 μl, 4.2 MBqs). The mixture was placed on a heat block at 80 °C for 15 minutes. Reaction was quenched by adding NH_4OH (10 μl, 30% v/v). The crude mixture was analysed by radioTLC with NH_4OAc (7.7% w/v)/MeOH (50:50) as mobile phase to confirm product formation to **205** in 6% yield (R_f=0.65).

REFERENCES

(1) Australian Institute of Health and Welfare & Australasian Association of Cancer Registries. *Cancer in Australia: An Overview*; Cancer Series 60; AIHW: Canberra, **2010,** 1-228.

(2) Ruddon, R. W. *Cancer Biology,* 4th ed; Oxford University Press: Oxford, **2007**.

(3) Weissleder, R.; Mahmood, U. *Radiology* **2001**, *219*, 316–333.

(4) Fass, L. *Mol. Oncol.* **2008**, *2*, 115–152.

(5) Vallabhajosula, S. *Molecular Imaging: Radiopharmaceuticals for PET and SPECT*; Springer Science & Business Media: Berlin, Heiderlberg, **2009**.

(6) Dolovich, M. B.; Schuster, D. P. *Proc. Am. Thorac. Soc.* **2007**, *4,* 328–333.

(7) Rahmim, A.; Zaidi, H. *Nucl. Med. Commun*. **2008**, *29*, 193–207.

(8) Boellaard, R.; O'Doherty, M. J.; Weber, W. A.; Mottaghy, F. M.; Lonsdale, M. N.; Stroobants, S. G.; Oyen, W. J. G.; Kotzerke, J.; Hoekstra, O. S.; Pruim, J.; et al. *Eur. J. Nucl. Med. Mol. Imaging* **2010**, *37*, 181–200.

(9) Kilbourn, M. R.; Huizenga, J. R. *Fluorine-18 Labeling of Radiopharmaceuticals*; National Academy Press: Washington, DC, **1990**.

(10) Zhu, A.; Lee, D.; Shim, H. *Semin. Oncol.* **2011**, *38*, 55–69.

(11) Lane, A. N.; Fan, T. W.-M. *Nucleic Acids Res.* **2015**, *43*, 2466–2485.

(12) Wise, D. R.; Thompson, C. B. *Trends Biochem. Sci.* **2010**, *35*, 427–433.

(13) Amelio, I.; Cutruzzolá, F.; Antonov, A.; Agostini, M.; Melino, G. *Trends Biochem. Sci.* **2014**, *39*, 191–198.

(14) Bhutia, Y. D.; Babu, E.; Ramachandran, S.; Ganapathy, V. *Cancer Res.* **2015**, *75*, 1782–1788.

(15) Pouliot, N.; Denoyer, D. *Cancer Forum* **2014**, *38*, 124–128.

(16) Basu, S.; Dhingra, V.; Mahajan, A. *Indian J. Nucl. Med.* **2015**, *25,* 332-341.

(17) Wang, Q.; Hardie, R.-A.; Hoy, A. J.; van Geldermalsen, M.; Gao, D.; Fazli, L.; Sadowski, M. C.; Balaban, S.; Schreuder, M.; Nagarajah, R.; et al. *J. Pathol.* **2015**, *236*, 278–289.

(18) Lin, J.; Raoof, D. A.; Thomas, D. G.; Greenson, J. K.; Giordano, T. J.; Robinson, G. S.; Bourner, M. J.; Bauer, C. T.; Orringer, M. B.; Beer, D. G. *Neoplasia* **2004**, *6,* 74–84.

(19) Kaira, K.; Oriuchi, N.; Sunaga, N.; Ishizuka, T.; Shimizu, K.; Yamamoto, N. *Am. J. Transl. Res.* **2011**, *3*, 383–391.

(20) Rentsch, D.; Schmidt, S.; Tegeder, M. *FEBS Lett.* **2007**, *581*, 2281–2289.

(21) Lynch, C. J. *J. Nutr.* **2001**, *131*, 861S – 865S.

(22) Hensley, C. T.; Wasti, A. T.; DeBerardinis, R. J. *J. Clin. Invest.* **2013**, *123*, 3678–3684.

(23) Challapalli, A.; Aboagye, E. O. *Front. Oncol.* **2016**, *6*, 44.

(24) Juhász, C.; Dwivedi, S.; Kamson, D. O.; Michelhaugh, S. K.; Mittal, S. *Mol. Imaging* **2014**, *13,*1-16.

(25) Nanni, C.; Schiavina, R.; Boschi, S.; Ambrosini, V.; Pettinato, C.; Brunocilla, E.; Martorana, G.; Fanti, S. *Eur. J. Nucl. Med. Mol. Imaging* **2013**, *40* (Suppl 1), 11–17.

(26) Pan, J.; Lau, J.; Mesak, F.; Hundal, N.; Pourghiasian, M.; Liu, Z.; Bénard, F.; Dedhar, S.; Supuran, C. T.; Lin, K.-S. *J. Enzyme Inhib. Med. Chem.* **2014**, *29*, 249–255.

(27) Akhtar, M. J.; Ahamed, M.; Alhadlaq, H. A.; Alrokayan, S. A.; Kumar, S. *Clinica Chimica Acta*. **2014**, *436,* 78–92.

(28) Akiyama, S. K. *Hum. Cell.* **1996**, *9*, 181–186.

(29) Verheul, H. M.; Pinedo, H. M. *Clin. Breast Cancer* **2000**, *1* (Suppl 1), 80–84.

(30) Haubner, R.; Weber, W. A.; Beer, A. J.; Vabuliene, E.; Reim, D.; Sarbia, M.; Becker, K.-F.; Goebel, M.; Hein, R.; Wester, H.-J.; et al. *PLoS Med.* **2005**, *2*, e70.

(31) Schittenhelm, J.; Klein, A.; Tatagiba, M. S.; Meyermann, R.; Fend, F.; Goodman, S. L.; Sipos, B. *Int. J. Clin. Exp. Pathol.* **2013**, *6*, 2719–2732.

(32) Dechantsreiter, M. A.; Planker, E.; Mathä, B.; Lohof, E.; Hölzemann, G.; Jonczyk, A.; Goodman, S. L.; Kessler, H. *J. Med. Chem.* **1999**, *42*, 3033–3040.

(33) Furusato, B.; Mohamed, A.; Uhlén, M.; Rhim, J. S. *Pathol. Int.* **2010**, *60*, 497–505.

(34) Sun, Y.-X.; Wang, J.; Shelburne, C. E.; Lopatin, D. E.; Chinnaiyan, A. M.; Rubin, M. A.; Pienta, K. J.; Taichman, R. S. *J Cell Biochem*. **2003**, *89,* 462–473.

(35) Choi, W.-T.; An, J. *Exp. Biol. Med.* **2011**, *236*, 637–647.

(36) Tamamura, H.; Imai, M.; Ishihara, T.; Masuda, M.; Funakoshi, H.; Oyake, H.; Murakami, T.; Arakaki, R.; Nakashima, H.; Otaka, A.; et al. *Bioorg. Med. Chem.* **1998**, *6,* 1033–1041.

(37) Tamamura, H.; Xu, Y.; Hattori, T.; Zhang, X.; Arakaki, R.; Kanbara, K.; Omagari, A.; Otaka, A.; Ibuka, T.; Yamamoto, N.; et al. *Biochem. Biophys. Res. Commun.* **1998**, *253*, 877–882.

(38) Xu, Y.; Tamamura, H.; Arakaki, R.; Nakashima, H.; Zhang, X.; Fujii, N.; Uchiyama, T.; Hattori, T. *AIDS Res. Hum. Retroviruses* **1999**, *15*, 419–427.

(39) Fujii, N.; Oishi, S.; Hiramatsu, K.; Araki, T. *Angew. Chem. Int. Ed Engl.* **2003**, *42*, 3251-3253.

(40) Kuil, J.; Buckle, T.; van Leeuwen, F. W. B. *Chem. Soc. Rev.* **2012**, *41*, 5239–5261.

(41) Thiele, S.; Mungalpara, J.; Steen, A.; Rosenkilde, M. M.; Våbenø, J. *Br. J. Pharmacol.* **2014**, *171*, 5313–5329.

(42) Cakir, M.; Dworakowska, D.; Grossman, A. *J. Cell. Mol. Med.* **2010**, *14*, 2570–2584.

(43) Lee, S.; Xie, J.; Chen, X. *Biochemistry* **2010**, *49*, 1364–1376.

(44) Thundimadathil, J. *J. Amino Acids.* **2012**, *967347*, 1-13.

(45) Fani, M.; Maecke, H. R.; Okarvi, S. M. *Theranostics* **2012**, *2*, 481–501.

(46) Tolmachev, V. Choice of Radionuclides and Radiolabelling Techniques. In *Targeted Radionuclide Tumor Therapy*; Stigbrand, T., Carlsson, J., Adams, G.P., Eds.; Springer: Dordrecht, Netherlands, **2008**; pp. 145–174.

(47) Charron, C. L.; Hickey, J. L.; Nsiama, T. K.; Cruickshank, D. R.; Turnbull, W. L.; Luyt, L. G. *Nat. Prod. Rep.* **2016**, *33*, 761–800.

(48) Chi, Y.-T.; Chu, P.-C.; Chao, H.-Y.; Shieh, W.-C.; Chen, C. C. *Biomed. Res. Int.* **2014**, 680195.

(49) iPHASE technologies: MultiSyn. http://www.iphase.com.au/multisyn.html (accessed Jun 19, 2018).

(50) Zeng, D.; Desai, A. V.; Ranganathan, D.; Wheeler, T. D.; Kenis, P. J. A.; Reichert, D. E. *Nucl. Med. Biol.* **2013**, *40*, 42–51.

(51) Kilian, K. *Rep. Pract. Oncol. Radiother.* **2014**, *19,* S13–S21.

(52) Gabriel, M.; Decristoforo, C.; Kendler, D.; Dobrozemsky, G.; Heute, D.; Uprimny, C.; Kovacs, P.; Von Guggenberg, E.; Bale, R.; Virgolini, I. J. *J. Nucl. Med.* **2007**, *48*, 508–518.

(53) Brooks, A. F.; Topczewski, J. J.; Ichiishi, N.; Sanford, M. S.; Scott, P. J. H. *Chem. Sci.* **2014**, *5*, 4545–4553.

(54) Lu, S.; Lepore, S. D.; Li, S. Y.; Mondal, D.; Cohn, P. C.; Bhunia, A. K.; Pike, V. W. *J. Org. Chem.* **2009**, *74*, 5290–5296.

(55) Jacobson, O.; Kiesewetter, D. O.; Chen, X. *Bioconjug. Chem.* **2015**, *26*, 1–18.

(56) Chen, K.; Conti, P. S. *Adv. Drug Deliv. Rev.* **2010**, *62*, 1005–1022.

(57) Richter, S.; Wuest, F. *Molecules* **2014**, *19*, 20536–20556.

(58) Tang, G.; Zeng, W.; Yu, M.; Kabalka, G. *J. Labelled. Comp. Radiopharm.* **2008**, *51,* 68–71.

(59) Guhlke, S.; Coenen, H. H.; Stöcklin, G. *Appl. Radiat Isot.* **1994**, *45,* 715–727.

(60) Liu, Z.; Liu, S.; Wang, F.; Liu, S.; Chen, X. *Eur. J. Nucl. Med. Mod. Imaging* **2009**, *36,* 1296–1307.

(61) Olberg, D. E.; Arukwe, J. M.; Grace, D.; Hjelstuen, O. K.; Solbakken, M.; Kindberg, G. M.; Cuthbertson, A. *J. Med. Chem.* **2010**, *53*, 1732–1740.

(62) Chen, X.; Tohme, M.; Park, R.; Hou, Y.; Bading, J. R.; Conti, P. S. *Mol. Imaging* **2004**, *3,* 96–104.

(63) Chen, X.; Park, R.; Hou, Y.; Khankaldyyan, V.; Gonzales-Gomez, I.; Tohme, M.; Bading, J.; Laug, W.; Conti, P. *Eur. J. Nucl. Med. Mol. Imaging* **2004**, *31*, 1081-1089.

(64) Dijkgraaf, I.; Boerman, O. C. *Eur. J. Nucl. Med. Mol. Imaging* **2010**, *37,* 104–113.

(65) Liu, S.; Liu, Z.; Chen, K.; Yan, Y.; Watzlowik, P.; Wester, H.-J.; Chin, F. T.; Chen, X. *Mol. Imaging Biol.* **2010**, *12*, 530–538.

(66) Demmer, O.; Gourni, E.; Schumacher, U.; Kessler, H.; Wester, H.-J. *ChemMedchem* **2011**, *6,* 1789–1791.

(67) Previero, A.; Cavadore, J. C.; Torreilles, J.; Coletti-Previero, M. A. *Biochim. Biophys. Acta* **1979**, *581*, 276–282.

(68) Haskali, M. B.; Denoyer, D.; Noonan, W.; Culinane, C.; Rangger, C.; Pouliot, N.; Haubner, R.; Roselt, P. D.; Hicks, R. J.; Hutton, C. A. *Mol. Pharm.* **2017**, *14*, 1169–1180.

(69) Hausner, S. H.; Abbey, C. K.; Bold, R. J.; Gagnon, M. K.; Marik, J.; Marshall, J. F.; Stanecki, C. E.; Sutcliffe, J. L. *J. Cancer Res*. **2009**, *69,* 5843–5850.

(70) Cai, W.; Zhang, X.; Wu, Y.; Chen, X. *J. Nucl. Med.* **2006**, *47*, 1172–1180.

(71) Palomo, J. M. *RSC Adv.* **2014**, *4*, 32658–32672.

(72) Othmer, D. F.; Jacobs, J. J.; Buschmann, W. J. *Ind. Ed. Chem*. **1943**, *35,* 326–329.

(73) Yoshikawa, Y.; Kobayashi, K.; Oishi, S.; Fujii, N.; Furuya, T. *Bioorg. Med. Chem. Lett.* **2012**, *22*, 2146–2150.

(74) Valeur, E.; Bradley, M. *Chem. Soc. Rev.* **2009**, *38*, 606–631.

(75) Kovacs, J. M.; Mant, C. T.; Hodges, R. S. *Biopolymers* **2006**, *84*, 283–297.

(76) Shao, X.; Hoareau, R.; Hockley, B. G.; Tluczek, L. J. M.; Henderson, B. D.; Padgett, H. C.; Scott, P. J. H. *J. Labelled Comp. Radiopharm*. **2011**, *54*, 292–307.

(77) Short, J.; Roberts, J.; Roberts, D. W.; Hodges, G.; Gutsell, S.; Ward, R. S. *Ecotox. Environ. Safe.* **2010**, *73,* 1484–1489.

(78) Demmer, O.; Dijkgraaf, I.; Schottelius, M.; -J. Wester, H.; Kessler, H. *Org. Let*. **2008**, *10,* 2015–2018.

(79) Miller, S. C.; Scanlan, T. S. *J. Am. Chem. Soc.* **1997**, *119*, 2301–2302.

(80) Zhang, B.; Pascali, G.; Wyatt, N.; Matesic, L.; Klenner, M. A.; Sia, T. R.; Guastella, A. J.; Massi, M.; Robinson, A. J.; Fraser, B. H. *J. Labelled Comp. Radiopharm.* **2018**, *61*, 847–856.

(81) Van Hout, A.; D'huys, T.; Oeyen, M.; Schols, D.; Van Loy, T. *PLoS One* **2017**, *12*, e0176057.

(82) Bunnett, J. F.; Zahler, R. E. *Chem. Rev*. **1951**, *49,* 273–412.

(83) Zhdankin, V.V. *ARKIVOC.* **2009**, *1,* 1-62.

(84) Chun, J.-H.; Pike, V. W. *J. Org. Chem.* **2012**, *77*, 1931–1938.

(85) Pike, V. W. *J. Labelled Comp. Radiopharm.* **2018**, *61*, 196–227.

(86) Block, D.; Coenen, H. H.; Stöcklin, G. *J. Labelled Comp. Radiopharm*. **1988**, *25,* 185–200.

(87) Selivanova, S. V.; Mu, L.; Ungersboeck, J.; Stellfeld, T.; Ametamey, S. M.; Schibli, R.; Wadsak, W. *Org. Biomol. Chem.* **2012**, *10*, 3871–3874.

(88) Breeman, W. A. P.; de Jong, M.; de Blois, E.; Bernard, B. F.; Konijnenberg, M.; Krenning, E. P. *Eur. J. Nucl. Med. Mol. Imaging* **2005**, *32,* 478–485.

(89) Mueller, D.; Breeman, W. A. P.; Klette, I.; Gottschaldt, M.; Odparlik, A.; Baehre, M.; Tworowska, I.; Schultz, M. K. *Nat. Protoc.* **2016**, *11*, 1057–1066.

(90) Wang, M.; Yin, D.; Li, S.; Wang, Y. *Sci. China Ser. B*. **2007**, *50,* 276–283.

(91) Roeda, D.; Dolle, F. *Curr. Radiopharm*. **2010**, *3,* 81–108.

(92) Siddiq, I. S.; Atwa, S. T.; Shama, S. A.; Eltaoudy, M. H.; Omar, W. M. *Appl. Radiat. Isot.* **2018**, *133*, 38–44.

(93) McConathy, J. *J. Nucl. Med.* **2016**, *57*, 1329–1330.

(94) Graham, T. J. A.; Lambert, R. F.; Ploessl, K.; Kung, H. F.; Doyle, A. G. *J. Am. Chem. Soc.* **2014**, *136*, 5291–5294.

(95) Poethko, T.; Schottelius, M.; Thumshirn, G.; Hersel, U.; Herz, M.; Henriksen, G.; Kessler, H.; Schwaiger, M.; Wester, H.-J. *J. Nucl. Med.* **2004**, *45*, 892–902.

(96) Afzali-Ardakani, A.; Rapoport, H. *J. Org. Chem.* **1980**, *45,* 4817–4820.

(97) Kalow, J. A.; Doyle, A. G. *J. Am. Chem. Soc.* **2011**, *133*, 16001–16012.

(98) Bruns, S.; Haufe, G. *J. Fluorine. Chem*. **2000**, *104,* 247–254.

(99) Liu, Z.; Pourghiasian, M.; Radtke, M. A.; Lau, J.; Pan, J.; Dias, G. M.; Yapp, D.; Lin, K.-S.; Bénard, F.; Perrin, D. M. *Angew. Chem. Int. Ed Engl.* **2014**, *53*, 11876–11880.

(100) Liu, Z.; Chen, H.; Chen, K.; Shao, Y.; Kiesewetter, D. O.; Niu, G.; Chen, X. *Sci. Adv*. **2015**, *1,* e1500694.

(101) Matteson. D.S; Ray, R; Rocks, R. R; Tsai, D. J. S. *Organometallics* **1983**, *2*, 1536–1543.

(102) Li, C.; Wang, J.; Barton, L. M.; Yu, S.; Tian, M.; Peters, D. S.; Kumar, M.; Yu, A. W.; Johnson, K. A.; Chatterjee, A. K.; et al. *Science* **2017**, *356,* eaam7355.

(103) Wang, J.; Qin, T.; Chen, T.-G.; Wimmer, L.; Edwards, J. T.; Cornella, J.; Vokits, B.; Shaw, S. A.; Baran, P. S. *Angew. Chem. Int. Ed Engl.* **2016**, *55*, 9676–9679.

(104) Toriyama, F.; Cornella, J.; Wimmer, L.; Chen, T.-G.; Dixon, D. D.; Creech, G.; Baran, P. S. *J. Am. Chem. Soc.* **2016**, *138*, 11132–11135.

(105) Trippier, P.C.; McGuigan, C. *MedchemComm.* **2010**, *1*, 183–198.

(106) Eissler, S.; Kley, M.; Bächle, D.; Loidl, G.; Meier, T.; Samson, D. *J. Pept. Sci.* **2017**, *23*, 757–762.

(107) Hancock, W. S.; Battersby, J. E. *Anal. Biochem.* **1976**, *71*, 260–264.

(108) Tenório-Daussat, C. L.; Hauser-Davis, R. A.; Saint'Pierre, T. D.; Tholey, A.; Schaumlöffel, D. *Microchem. J*. **2015**, *118,* 238–241.

(109) Turnbull, W. L.; Yu, L.; Murrell, E.; Milne, M.; Charron, C. L.; Luyt, L. G. *Org. Biomol. Chem.* **2019**, *17*, 598–608.

(110) Ueda, S.; Oishi, S.; Wang, Z.-X.; Araki, T.; Tamamura, H.; Cluzeau, J.; Ohno, H.; Kusano, S.; Nakashima, H.; Trent, J. O.; et al. *J. Med. Chem.* **2007**, *50*, 192–198.

(111) Li, X.; Liu, N.; Zhang, H.; Knudson, S. E.; Slayden, R. A.; Tonge, P. J. *Bioorg. Med. Chem. Lett*. **2010**, *20,* 6306–6309.

(112) Neuvonen, H.; Neuvonen, K.; Pasanen, P. *J. Org. Chem.* **2004**, *69*, 3794–3800.

(113) Zhang, M.; Zhang, S.; Zhang, G.; Chen, F.; Cheng, J. *Tetrahedron Lett.* **2011**, *52*, 2480–2483.

(114) Zahn, H.; Schade, F. *Chem. Ber*. **1963**, *96,* 1747–1750.

(115) Richarz, R.; Krapf, P.; Zarrad, F.; Urusova, E. A.; Neumaier, B.; Zlatopolskiy, B. D. *Org. Biomol. Chem.* **2014**, *12*, 8094–8099.

(116) Mamat, C.; Flemming, A.; Köckerling, M.; Steinbach, J.; Wuest, F. *Synthesis* **2009**, *19,* 3311-3321.

(117) Jin, Y.; Jiang, M.; Wang, H.; Fu, H. *Sci. Rep*. **2016**, *6,* 20068.